Synergistic Effect of Fluorapatite and Platelet-Rich Plasma on Cell Proliferation and Differentiation: A Novel Strategy to Enhance Dental Implant Osseointegration

Aseel Salman Khazaal Al-Jaboori

Submitted in accordance with the requirements for the degree of
Doctor of Philosophy

The University of Leeds

School of Dentistry

September 2018

The candidate confirms that the work submitted is her own and that appropriate credit has been given where reference has been made to the work of others.

Acknowledgements

I would like first to thank my main supervisor Dr El Mostafa Raif for his precious guidance and suggestions and for giving me the strength, patience and confidence to deal with most of the challenges during the PhD journey and to complete this project.

I would like to express my deepest gratitude to my secondary supervisor Dr Steven Brookes who was always supportive, kind and generous with his valuable advice and comments throughout my work. I would never have been able to finish this work without my supervisors' excellent guidance, constant supervision, useful critiques, and patience.

I would like also to Acknowledge Dr Julie Burke for her great help and support as a secondary supervisor during the first year of my PhD study.

I would like to Acknowledge Mrs Jackie Hudson for her great technical assistance and support with immunohistochemical techniques and with the scanning electron microscopy and confocal microscopy.

A huge thank for my colleagues in Oral Biology Department for their kind help and great support. I would especially like to thank Dr Hanaa Alkharobi for tutoring me ELISA techniques and Dr Aisha Alhodhodi for explaining real time PCR and for being great supportive friends throughout.

I would like to offer my special and warmest thanks to my colleagues and valuable friends Dr Ali Marie, Dr Hasanain Al-Khafaji, Dr Rasha Al-Bannaa, Dr Fahad Al-Dabbagh and Mrs Shabnum Rasheed for their kind support, generous help and advice during my lab work.

I would also like to extend my sincere thanks to my homeland the Republic of Iraq and to the Iraqi Ministry of Higher Education and Scientific Research for granting me a full scholarship and for their generous financial support.

I would like to thank my family; my parents and brothers for their everlasting emotional support. Finally, a big thank you goes to my husband, Dr Muhannad Al-Shaikhali for holding my hand at every step I take and for his endless generous support and great encouragement, therefore I dedicate this thesis to him. My special children Mustafa and Yousif, thank you for being the light of my life, for giving me the power to finish my project and for tolerating all my dark moods throughout the stressful times.

Abstract

This study investigated the synergistic effect of fluorapatite (FA) coatings and platelet-rich plasma (PRP) on cell adhesion, proliferation, differentiation and mineralisation with a view to the use of this combination in enhancing osseointegration of dental implants. Stainless steel (SS) discs tilted at 45° were hydrothermally coated with FA crystals. PRP was extracted from human blood and the release of platelet growth factors (IGF-1 and PDGF-AB) from non-activated and activated PRP loaded on FA coatings into PBS was measured. Cytotoxicity of FA/PRP combinations and their effect on G292 cell proliferation was tested. Osteogenic differentiation of human dental pulp stem cells (hDPSCs) cultured on FA/PRP was investigated using osteogenic marker expression and histochemical stains. The results showed that FA crystals were disorganised on upper disc surfaces and organised on the under surfaces. Organised FA coatings stimulated greater and more sustained release of IGF-1 from non-activated PRP compared to the control (SS/non-activated PRP). The greatest release of PDGF-AB was triggered by thrombin from PRP loaded on organised FA. FA crystals showed good biocompatibility that was enhanced by PRP. Organised FA coatings induced a high cell proliferation when combined with PRP gel compared to the control (SS/FBS). There was a clear PRP donor variability in ALPL and RUNX-2 gene expression by hDPSCs when PRP used in combination with uncoated SS or FA coated surfaces compared to the control (SS/FBS). Organised FA when combined with FBS or PRP didnot enhance OCN expression but increased OPN expression compared to the control. Organised FA induced less ALP activity but high calcium deposition by hDPSCs compared to uncoated SS when both were combined with FBS or PRP, indicative of osteogenic differentiation. Therefore, it can be concluded that PRP in combination with organised FA coating may offer a promising strategy for bone regeneration around the dental implants.

Table of Contents

List of Figures

List of Tables

List of Abbreviations

ALP: Alkaline phosphatase (protein)
ALPL: Alkaline phosphatase (gene)
BMP: Bone morphogenic protein
BMSCs: Bone marrow stem/stromal cells
BSA: Bovine serum albumin
BSE: Black scattered electron
BSP: bone sialoprotein
Ca: Calcium element
Ca^{2+}: Calcium ion
$Ca_3(PO_4)_2$: Calcium phosphate
CD: Cluster of differentiation
cDNA: Complementary DNA
COL1: Type I collagen
dH_2O: distilled water
DMSO: Dimethylsulfoxide
DNA: Deoxy ribonucleic acid
DPSCs: Dental pulp stem/stromal cells
DS: Disorganised
ECM: Extra cellular matrix
EDTA: Etheylenedeiaminetetraacetic acid
EDX: Energy dispersive X-ray spectroscopy
ELISA: Enzyme-linked immunosorbent assay
F: Fluorine
FA: Fuorapatite
FBS: Foetal bovine serum
FGF: Fibroblast growth factor
GFs: Growth factors
HA: Hydroxyapatite
HA/ TCP: Hydroxyapatite/ tricalcium phosphate
hBMSCs: Human bone marrow stem/ stromal cells
hDPSCs: Human dental pulp stromal/stem cells
HRP: Horseradish peroxidase
IGF-1: Insulin-like growth factor-1
LDH: Lactate dehydrogenase enzyme

L-G: L-glutamine

MAPK: Mitogen activated protein kinase

MEM: minimum essential medium

mRNA: Messenger ribonucleic acid

MSCs: Mesenchymal stem cells

NBF: Neutral buffer formalin

OC: Osteocalcin (gene)

OCN: Osteocalcin (protein)

OPN: Osteopontin protein

OR: Organised

P: Phosphorus element

PO_4^{-3}: Phosphate ion

PBS: Phosphate buffered saline

PDGF-AB: Platelet-derived growth factor-AB

Pen/Strep: Penicillin/streptomycin

PPP: Platelet-poor plasma

PRP: Platelet-rich plasma

Pts: Platelets

qRT-PCR: Quantitative real time polymerase chain reaction

RBCs: Red blood cells

RT: Room temperature

RUNX-2: Runt-related transcription factor (gene)

SD: Standard deviation

SE: Secondary electron

SEM: Scanning electron Microscopy

SHED: Stem / stromal cells from exfoliated deciduous teeth

SS: Stainless steel

TE: Tris-EDTA buffer

TGF-β: Transforming growth factor-beta

VEGF: Vascular endothelial growth factor

WBCs: White blood cells

Chapter 1: Literature Review

1.1 General introduction

The use of dental implants for the correction of tooth and tissue loss caused by trauma, disease or genetic disorders has increased exponentially around the world. They have proved to be successful with failure rates of approximately 8 % in the maxilla and 5 % in the mandible (Moy et al., 2004). However, it takes about 4–6 months for dental implants to integrate with the surrounding bone before the functional loading of the dental prosthesis (Adell et al., 1981). Some medical conditions such as osteoporosis and diabetes (Elsubeihi and Zarb, 2002), as well as the need for immediate implant loading to reduce the anxiety of the patient (Gapski et al., 2003), have led to the search for factors that can improve and accelerate dental implant osseointegration.

The capability of the implant surface to stimulate the osteogenic differentiation of cells is a critical factor for osseointegration (Lavenus et al., 2011). A great deal of research has been carried out to modify the physical and chemical properties of the implant surface to better promote this process. One such modification is the coating of implants with fluorapatite (FA). FA coatings are chemically and mechanically stable and offer a high level of biocompatibility. They stimulate hard tissue regeneration with low bio-resorption rate (Bhadang and Gross, 2004; Fathi and Zahrani, 2009). The desirable properties of FA have resulted in many studies focusing on its synthesis. For example, Chen et al. (2006b) described a hydrothermal method to produce aligned FA films with well-organized crystals. However, there is little literature reporting this novel method nor the role of FA coatings on osseointegration of dental implants.

In addition to implant surface quality, growth factors are known to stimulate tissue healing around the implant (Anitua, 1999). However, growth factors, currently delivered as recombinant proteins, are expensive and high doses may be required to achieve any therapeutic effect. And so, an easy and cost-effective way to obtain high concentrations of appropriate growth factors at the implant site has been proposed using platelet-rich plasma (PRP). PRP is a valuable source for many growth factors involved in hard and soft tissue repair (He et al., 2009). Although some authors have reported significant

improvements in tissue healing and bone formation using PRP around the dental implant (Anitua, 2006), others did not observe any improvements (Garcia et al., 2010). Nevertheless, some investigators reported that using PRP in combination with other biomaterials may hold some promise for tissue engineering purposes (Okuda et al., 2005; Yamamiya et al., 2008).

1.2 Dental implants

The dental implant is an inert, alloplastic surgical component used to provide permanent support for a dental prosthesis (crown, fixed bridge or denture) when the bone itself cannot provide sufficient support (Mupparapu and Beideman, 2000). When the implant is surgically placed within the jaw bone by the dentist, the surgical sites should be undisturbed and new bone is allowed to grow around and fuse with the implant for at least 3- 6 months before the artificial prosthesis is attached (Mosby, 2009).

Implant supported prostheses, compared to the traditional removable and fixed restorations exhibit a remarkable capacity to preserve the bone and adjacent teeth which allows the patient to recover normal masticatory function, aesthetics, speech and self- confidence (Misch, 2014).

Dental implants are commonly constructed from commercially pure titanium or titanium alloy because of their excellent biocompatibility, corrosion resistance and desirable physical and mechanical properties. However, materials such as ceramics and other alloys (gold and nickel-chrome-vanadium) are also used for dental implants. These materials are generally selected on the basis of their biocompatibility, strength and corrosion resistance. Nowadays, endosseous dental implants are coated with plasma-sprayed titanium or hydroxyapatite to enhance early bone integration with the implant surface (Mupparapu and Beideman, 2000).

There are three types of dental implants (figure 1) that have been developed:

A. Subperiosteal implants which are metal frameworks that attach on top of the jawbone underneath the gum tissue and the periosteum (a dense layer of vascular connective tissue enveloping the bones).

B. Transosteal implants (mandibular staple) which are either metal pins or U-shaped frames that pass through the jaw bone and the gum tissue into the mouth.

C. Endosteal (endosseous) implants which consist of a distinct, single implant unit (screw- or cylinder-shaped) placed in a drilled hole within the alveolar bone. Endosseous implants are the most commonly used implants due to their long-term clinical success (Searson et al., 2005).

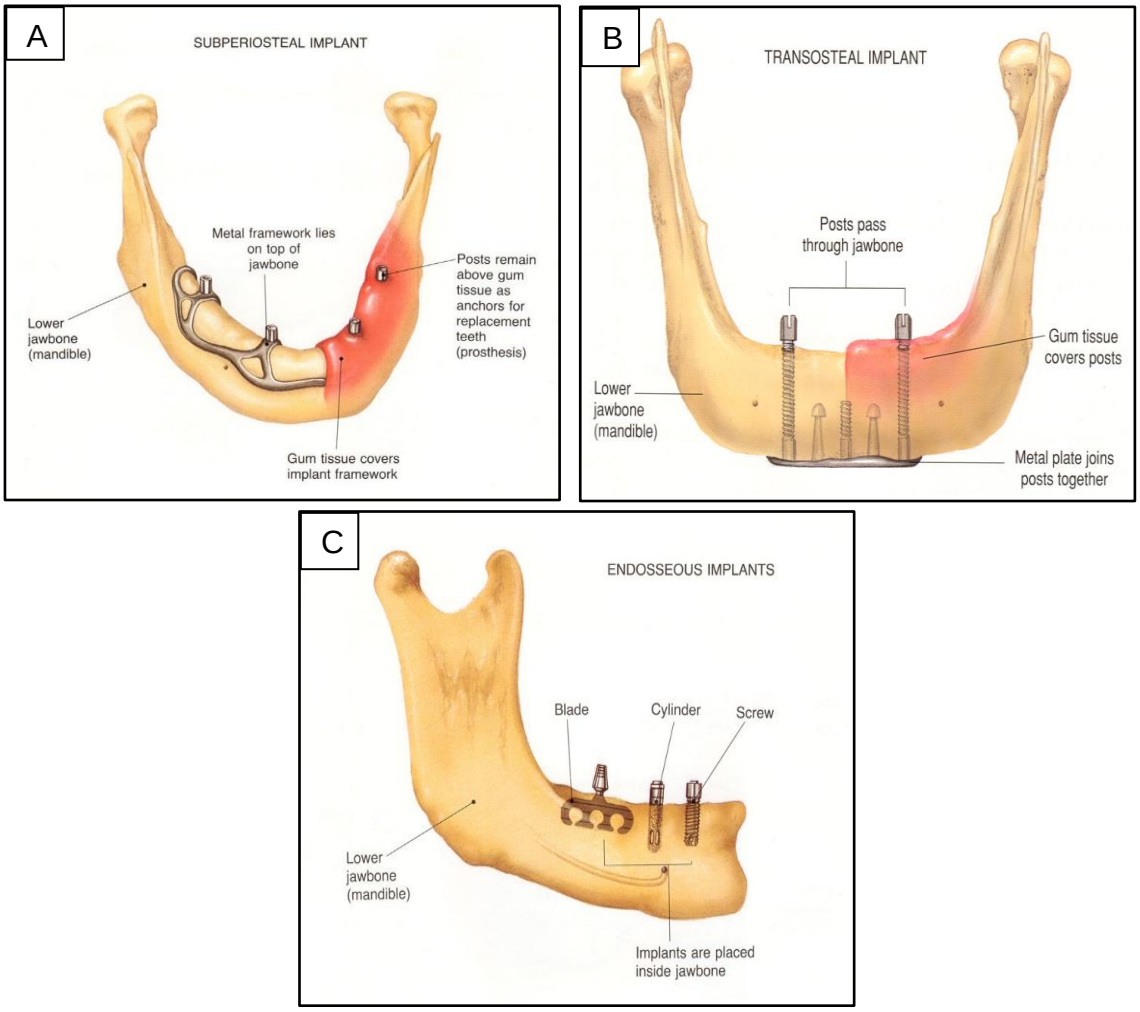

Figure 1: Types of dental implants: A) Subperiosteal implants which are frameworks that attach on top of the jawbone underneath the gum tissue. B) Transosteal implants which are either metal pins or U-shaped frames that pass through the jaw bone into the mouth. C) Endosteal implants which are single implant units that placed in a drilled hole within the alveolar bone (Adapted from http://dentalimplants.uchc. edu/about/ types. html).

Endosseous implants were discovered by Professor Brånemark in the late 1960s when he observed a firm anchorage between a piece of titanium implanted into the bone and the bone itself without any sign of inflammation. He called this new attachment mechanism "Osseointegration" (Brånemark, 1969; Brånemark, 1983). Following the introduction of the Brånemark system of dental implants, the number of endosseous dental implants placed annually worldwide was increased reaching about one million with more than 220 implant brands produced by about 80 manufacturers (Jokstad et al., 2003).
The amount of bone-to-implant contact (BIC) is an important determining factor in osseointegration and the long-term success of endosseous dental implants. Thus, maximizing the BIC and osseointegration has become a key goal of the treatment (Soskolne et al., 2002).

1.3 Osseointegration

Osseointegration is the direct structural and functional contact between ordered, living bone and the surface of a load-carrying implant without the interposition of a fibrous tissue (Brånemark et al., 1969). Osseointegration could also refer to an anchorage mechanism which persists under normal loading conditions and provides a long-term stable prosthesis (Worthington et al., 2003).
Despite the high success rates, implant failure may occur and is defined as the inadequacy of the host tissue to establish or maintain osseointegration. The reported failure rates for Brånemark dental implants were 7.7% over five years (Esposito et al., 1998). Certain criteria have been determined for a successful integration of dental implants such as the lack of implant mobility which is of prime importance, as implant loosening is the most often reported reason for implant removal (Albrektsson et al., 1981).
There are some systemic conditions that are believed to be associated with increased risk of implant failure and may preclude the patient from undergoing implant treatment such as diabetes, osteoporosis, tobacco smoking, radiotherapy, chemotherapy and possibly advanced age. These conditions are generally associated with impaired vascularisation and protein synthesis which seem to compromise soft and hard tissue healing (Searson et al., 2005; Marco et al., 2005; McCracken et al., 2006).

In addition to the systemic factors, six local factors have been suggested to influence the osseointegration including; implant material, implant design, surface conditions, bone quality, surgical technique and implant loading conditions (Albrektsson et al.,1981). There are some controversies in the literature concerning early implant loading with prosthesis. Some studies suggest that loading should be applied 4-6 months after implant placement to avoid fibrous capsule formation around the implant caused by functional forces impacting at the implant-bone interface during wound healing (Adell et al., 1981). Conversely, others advocated immediate or early loading (within 6 weeks of implant placement) as long as the implant is of a roughened (plasma or hydroxyapatite coated implant), threaded design and inserted in good quality bone with good force management (e.g. cross-arch stability) (Salama et al., 1995; Bijlani and Lozada, 1996; Piattelli et al., 1997).
The long-term clinical success of endosseous implants depends mainly on rapid healing with safe integration into the bone. Therefore, the biology of the bone and its healing response to the implant surface has been widely studied.

1.4 Bone structure

Bone is a viable, cellular, highly mineralised connective tissue that maintains some degree of elasticity due to its structure and composition. Bone matrix is comprised of 70 % inorganic component, 20 % organic component and 10% water. The inorganic (mineral) component of bone is composed of carbonated calcium phosphate mineral in the form of hydroxyapatite crystals that are 3 to 29 nm length and 2-3 nm width laid down in the organic matrix (Weiner and Traub, 1992, Rey et al., 2009). The organic part is composed mainly of collagen fibres which form approximately 95 % of the total protein in bone while the rest is non-collagenous proteins including, proteoglycans and glycoproteins (alkaline phosphatase, osteocalcin, osteonectin and bone sialoprotein) (Rodan, 1992). The repetitive nature of the amino acid sequences of the collagen fibres allows the protein to assemble into triple helical structures referred to as tropocollagen molecules (see schematic in figure 2). The elastic collagen matrix is hardened by the binding of the hydroxyapatite crystals through the bone mineralization process that gives bones rigidity (Voet, 1995).

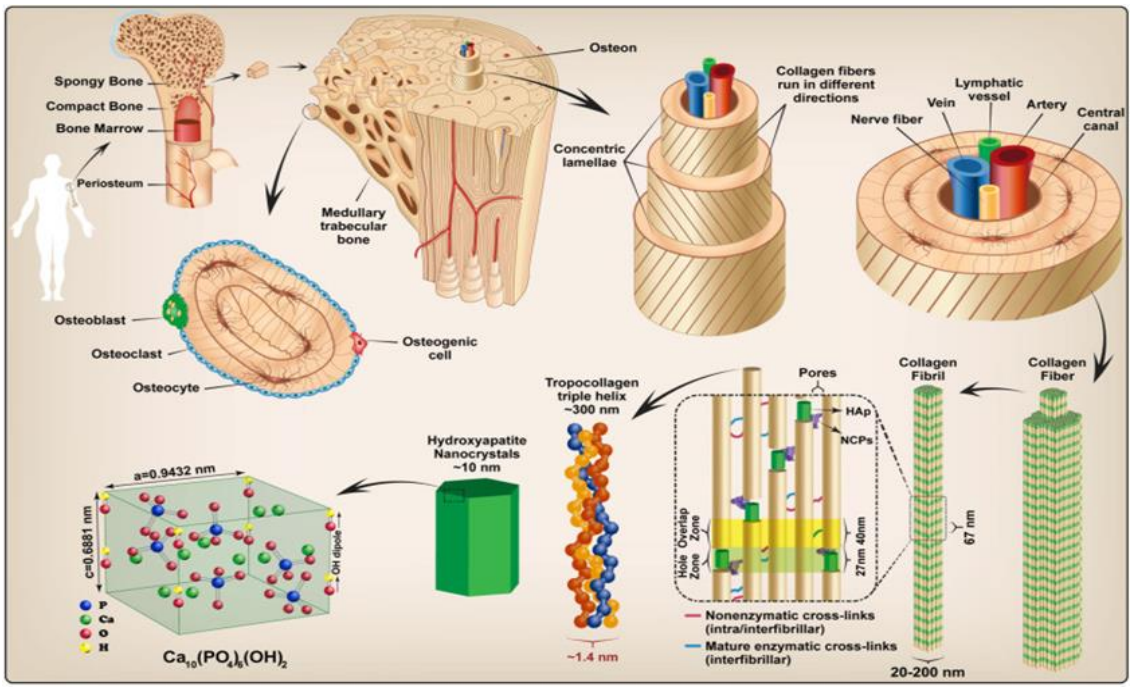

Figure 2: Structure of bone tissue. Bone is divided into a hard compact bone and spongy bone. Bone is formed by overlapping cylindrical units (osteons) which contain blood vessels, lymphatic vessels, nerves and osteocytes along with the calcified matrix. The organic part of the bone is mainly elastic collagen fibres in which protein is assembled into triple helical structures (tropocollagen molecules). The collagen is hardened by binding of inorganic hydroxyapatite crystals. The bone is filled with bone morrow containing multipotent mesenchymal and hematopoietic stem cells (Adapted from https://www.sciencedirect.com/science/article/pii/S0734975017301210).

The bone has two surfaces; the internal (endosteal) and external (periosteal) surfaces, and are each lined with cellular layers called the endosteum and periosteum respectively. The mature bone (Lamellar bone) is characterized by regular and parallel alignment of collagen fibres into concentric sheets (lamellae) and osteocytes embedded within the calcified matrix. Morphologically, lamellar bone is classified into 2 types, cortical bone (compact or dense bone) and trabecular bone (cancellous or spongy bone). Cortical bone forms the hard outer layer of bones and it is formed by overlapping cylindrical

units called osteons or Haversian systems. Osteons contain blood vessels, lymphatic vessels, nerves and osteocytes along with the calcified matrix. Trabecular bone is sponge-like manner bone found principally at the ends of long bones, and in the vertebral bodies and the flat bones. It is composed of a meshwork of trabeculae with intercommunicating spaces for blood vessels and bone marrow. The differences in bone structure are related mainly to bone function. Cortical bone provides mechanical and protective functions while trabecular bone provides metabolic function (Marks and Odgren, 2002). However, differences in their protein contents was also shown (Ninomiya et al., 1990).

The bone is filled with bone marrow which is a loose vascular connective tissue that exists in direct contact with the endosteal surfaces. The connective tissue network of the bone marrow is called stroma. The stroma itself is a heterogeneous mixture of cells including adipocytes, reticulocytes, endothelial cells, and fibroblastic cells which are in direct contact with the hematopoietic elements (Jaiswal et al., 1997). Bone marrow contains multipotent stem cells localised in a determined micro-environment in which synthesis of blood cells take place (Yin and Li, 2006). These stromal cells are capable of differentiating along multiple mesenchymal and hematopoietic lineages.

The mesenchymal stem cells (MSCs) differentiate into various cell types including osteoblasts, chondroblasts, fibroblasts, adipocytes and myoblasts (Aubin, 1998b) while, the hematopoietic stem cells differentiate into erythrocytic, leukocytic and thrombocytic lineages in addition to osteoclasts.

Bone mesenchymal stem cells (BMSCs) differentiate toward an osteogenic lineage under the control of specific growth and transcriptional factors involving a number of developmental stages, beginning with transformation into osteoprogenitor cells through to preosteoblasts and osteoblasts and finally osteocytes (Long, 2001). During the early stages, osteoprogenitors maintain a certain degree of plasticity allowing de- and trans-differentiation to other mesenchymal lineages whereas osteoblasts and osteocytes are regarded as specialised functional cells that represent a terminal stage of cell differentiation (Rottmar et al., 2010).

Osteoblasts are the bone forming cells which after several stages of differentiation become osteocytes trapped in mineralised matrix (Acquavella and Owen, 1990). The differentiation of mesenchymal stem cells to osteoblasts is mainly stimulated by Cbfa1/RUNX2 expression which induces the expression of other genes encoding matrix proteins such as osteocalcin, type I collagen and bone sialoproteins (Karsenty, 1999, James et al., 2006). The main function of osteoblasts is production and secretion of bone matrix proteins such as type I collagen and non-collagenous proteins (Rodan, 1992). Production and secretion of many cytokines and signalling proteins such as bone morphogenetic proteins (BMPs) transforming growth factor beta (TGF-β) and bone matrix proteins were also mediated by osteoblasts (Marks and Popoff, 1988, Fu et al., 2007).

1.5 Osteoblast gene expression profile

Three differentiation stages were described for BMSCs entering the osteoblast lineage; cell proliferation, extracellular matrix (ECM) formation and mineralization. Each of these stages is regulated by specific osteoblast gene expression profiles (Owen et al., 1990).

- COL1 gene is highly expressed by osteoblasts during the proliferation phase (8-12 days for osteoblasts cultured in vitro) (Jaiswal et al., 1997) and becomes down regulated when extracellular matrix mineralisation begins (Dunn et al., 1995). Therefore, the regulatory role for the COL1 gene is predominant during the osteoblast proliferation phase.

- Alkaline phosphatase (ALPL) is an early post proliferative osteoblastic marker gene that is thought to be associated with the mineralisation procedure. However, the expression of ALPL gene is ultimately decreased in highly mineralised mature bone matrix (Shalhoub, 1992; Jaiswal et al., 1997). It represents an early marker of BMSCs osteogenic differentiations in vitro, and bone formation in vivo. ALPL gene encodes alkaline phosphatase (ALP) glycoprotein which is a hydrolase co-enzyme that is responsible for hydrolysing phosphate groups from various organic and inorganic biological molecules. As calcium levels increase during mineralisation, calcium binds ALP and activates

its phosphohydrolytic activity, which can increase local concentrations of inorganic phosphate and destroy pyrophosphate (a local inhibitor of mineral crystal growth). It has been reported that ALP protein levels begin to be detectable between days 12 to 18 in monolayer culture of human primary osteoblasts (Wessinger and Owens, 1990, Jaiswal et al., 1997).

➢ *RUNX-2* gene is an important transcription factor for bone formation (Komori et al., 1997). It is a member of the Runt domain proteins that play a crucial role in early stages of pluripotent mesenchymal cells differentiation to osteoblasts (Yamaguchi et al., 2000). RUNX-2 regulates bone development by promoting the up-regulation of ALPL, osteopontin (OPN), osteocalcin (OCN), bone sialoprotein (BSP) and type I collagen alpha chains (COL1A1) (Teplyuk et al., 2008). In addition, RUNX-2 triggers the expression of major bone matrix protein genes during early osteoblast differentiation but does not play a major role in the maintenance of the expression of collagen I or OCN in mature osteoblasts (Komori, 2009). RUNX-2 was shown to modulate RANKL gene expression by the osteoblasts, hence indirectly affect osteoclast differentiation (Mori et al., 2006). Moreover, RUNX-2 has been shown to negatively control osteoblast proliferation by acting on pathways associated with cell cycle (Yoshida et al., 2004).

➢ *OCN* gene is a post proliferative expressed gene that encodes the matrix protein osteocalcin (Shalhoub et al., 1992, Dunn et al., 1995). The regulatory role for the *OCN* gene is expressed predominantly during mineralised nodule formation in in vitro cultures and during the mineralisation of the bone matrix (Owen et al., 1990). It is considered to be a marker of mature osteoblast differentiation since it is expressed at the later stages of differentiation (Frenkel et al., 1997, Jaiswal et al., 1997).

➢ *OPN* gene encodes osteopontin which is a cell-matrix adhesion protein. OPN and bone sialoprotein (BSP) were described as major sialoproteins in the extracellular matrix of bone (Zhang et al., 1990). OPN is a member of the SIBLING family of proteins which are known to bind to cell integrin receptors

(Denhardt et al., 2001). In addition, OPN protein has the potential to serve as a bridge between cells and hydroxyapatite through its cell binding amino acid RGD sequences (Oldberg et al., 1986). It was revealed that OPN is produced by osteoblastic cells at various stages of differentiation (Zohar et al., 1997).

1.6 Biology of bone healing following implant placement

During and following implantation, blood components come into contact with the implant surface resulting in a cascade of biological processes that take place at the bone-implant interface until the implant surface becomes covered with newly formed bone (Mavrogenis et al., 2009). Bone healing around dental implants is similar to fracture healing with the hallmark cascade of hemostasis, inflammation, regeneration and remodelling. However, the presence of a foreign implant surface may influence these phases (Larsson et al., 2001). Healing around the implant ends in a distinctive continuous layer of mature bone in intimate contact with the implant surface, while fracture healing ends in reproduction of the original bone shape and its associated tissues. Further, the process of bone formation at the bone-implant interface is not preceded by obvious chondrogenic activity (Cooper, 1998), which represents a prominent phase during fracture healing. Figure 3 shows the cellular reaction at the implant- bone interface during the peri-implant healing process.

The biological cascade of peri-implant healing process includes:

1. Protein deposition and adsorption onto the implant surface:

Within few seconds of blood-implant contact, a monolayer of specific blood proteins is adsorbed on the implant surface. The composition of the protein layer is highly determined by the surface properties of the implant and these adsorbed proteins determine the host response to the material and the resultant peri-implant healing (Kuzyk and Schemitsch, 2011). For example, proteins like fibronectin and vitronectin contain peptide sequences that are responsible for mediating cell adhesion for many different kinds of cells (Kieswetter et al., 1996). Fibrinogen, complement and IgG proteins are important for platelet activation, coagulation and inflammatory response (Kuzyk and Schemitsch, 2011). Whereas, fibrin has the potential to form scaffold that promotes bone

mesenchymal stem cells (BMSCs) recruitment into the implant surface arriving as early as the first day and stimulate cell differentiation in the healing process (Mavrogenis et al., 2009).

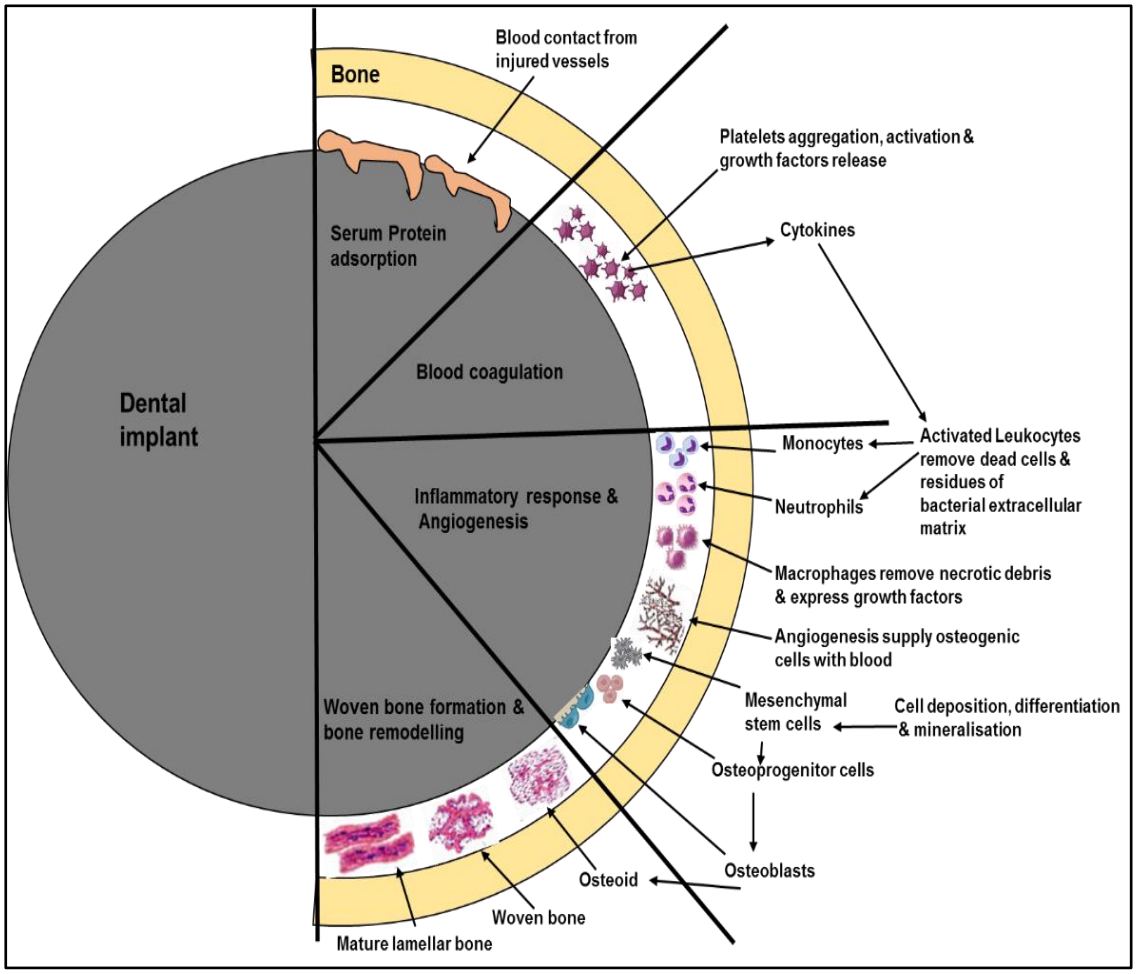

Figure 3: Diagram showing the biological cascade at implant- bone interface during the healing process. Platelets initiate the coagulation cascade and release inflammatory cytokines and growth factors that lead to migration and proliferation of phagocytic cells. Neutrophils peaking at the first three days remove the residues of bacterial extracellular matrix. Macrophages remove the necrotic debris and express more cytokines, inducing further recruitment of osteogenic and endothelial progenitors that initiate the angiogenesis. The formed fibrin matrix acts as a scaffold for attachment and differentiation of the migrating stem cells into osteoblasts. Osteoblasts deposit osteoid, followed by woven bone formation and mineralisation. Then the immature woven bone starts remodelling at the second week and becomes replaced by mature lamellar bone within three months.

2. Coagulation and platelet activation:

Platelets are the first cells to arrive at the implant surface. Subsequent platelet activation is triggered by tissue injury or through interacting with foreign materials like an implant surface or in response to factors such as thromboxane A2 and thrombin which are released by other platelets or cells (Kanagaraja et al., 1996). Platelet activation induces the platelets to aggregate, form a blood clot and release cytokines and growth factors (GFs) (Kuzyk and Schemitsch, 2011). GFs such as platelet-derived growth factor (PDGF), transforming growth factor β (TGF- β) and insulin-like growth factor I (IGF-1) serve as signalling molecules for recruitment and differentiation of mesenchymal stem cells at the implant surface (Gaβling et al., 2009; Zhang et al., 2013).

3. Inflammatory response:

Inflammation is the early tissue response to implant surgery and the presence of the implant (Marco et al., 2005). The inflammatory response is facilitated by a number of leukocytes (neutrophils and monocytes) which migrate into the peri-implant space after platelets followed by phagocyte macrophages. Leukocytes peak at the first three days following surgery to remove the dead cells and residues of bacterial extracellular matrix. They become activated in response to platelets cytokines (e.g., β-thromboglobulin and PDGF) resulting in the release of many inflammatory cytokines which are the first signalling molecules to initiate bone formation (Kuzyk and Schemitsch, 2011). Macrophages remove necrotic debris created by the drilling process of implantation surgery. Moreover, macrophages replaces the platelets as the primary source of growth factors after the third day of the surgery and begin to express some cell surface proteins and growth factors such as fibroblast growth factors (FGF-1,2,4), TGF-α and β, epithelial growth factor (EGF), bone morphogenetic proteins (BMPs) and growth & differentiation factors (GDFs) (Canalis et al., 1989). These osteoinductive factors have been shown to enhance bone formation at the surgical site (Anil et al., 2011). Macrophages also produce numerous cytokines, growth and angiogenic factors that are important in the regulation of fibro-proliferation and angiogenesis (Martin and Leibovich, 2005).

Angiogenesis (formation of new blood vessels) is required to supply the osteogenic cells with blood. It is regulated by some growth factors like PDGF, angiopoietin, FGFs and vascular endothelial growth factor (VEGF) which may also modulate osteoblast function (Carmeliet, 2000).

4. Woven bone formation:
The complex collaboration of the signalling molecules within the peri-implant space exhibits osteoconductive and osteoinductive potential leading to recruitment, migration and differentiation of mesenchymal cells into osteoblastic (osteoprogenitor) cells that participate significantly in the formation of a woven bone (Marco et al., 2005). The osteoblasts start to deposit non-collagenous bone matrix proteins on the implant surface (e.g.osteocalcin, osteopontin and bone sialoprotein) that have nucleation sites for calcium phosphate mineralisation. The mineralisation process is regulated by the alkaline phosphatase enzyme secreted from osteoblasts by increasing localised inorganic phosphate levels, leading to formation of calcified layer on the implant surface (Marco et al., 2005; Mavrogenis et al., 2009). Few days after implantation, osteoblasts begin to deposit collagen matrix directly on the early formed mineralised layer on the implant surface. This process of osteogenesis results in immature woven bone formation (characterised by haphazard organization of collagen fibres) around the implant that eventually remodels into a mature lamellar bone (characterised by regular parallel alignment of collagen) Bone remodelling starts at the second week following the surgery and becomes replaced by mature lamellar bone within three months (Marco et al., 2005). The final remodelling results in mature bone in direct contact with most of the implant surface (i.e. proper implant osseointegration) (Davies, 2003; Marco et al., 2005).

1.7 Influence of implant surface properties on osseointegration

Histological and biomechanical data indicated that bone cells respond differently when interfacing to different implant surfaces (Larsson et al., 2001; Albrektsson and Wennerberg, 2004). Moreover, it was indicated that the biological host response of the bone to an implant is essentially influenced by

the chemical, physical, mechanical and topographical properties of the implant surface (Figure 4), which in turn have great impact on the speed and strength of the osseointegration (Marco et al., 2005; Grassi et al., 2006).

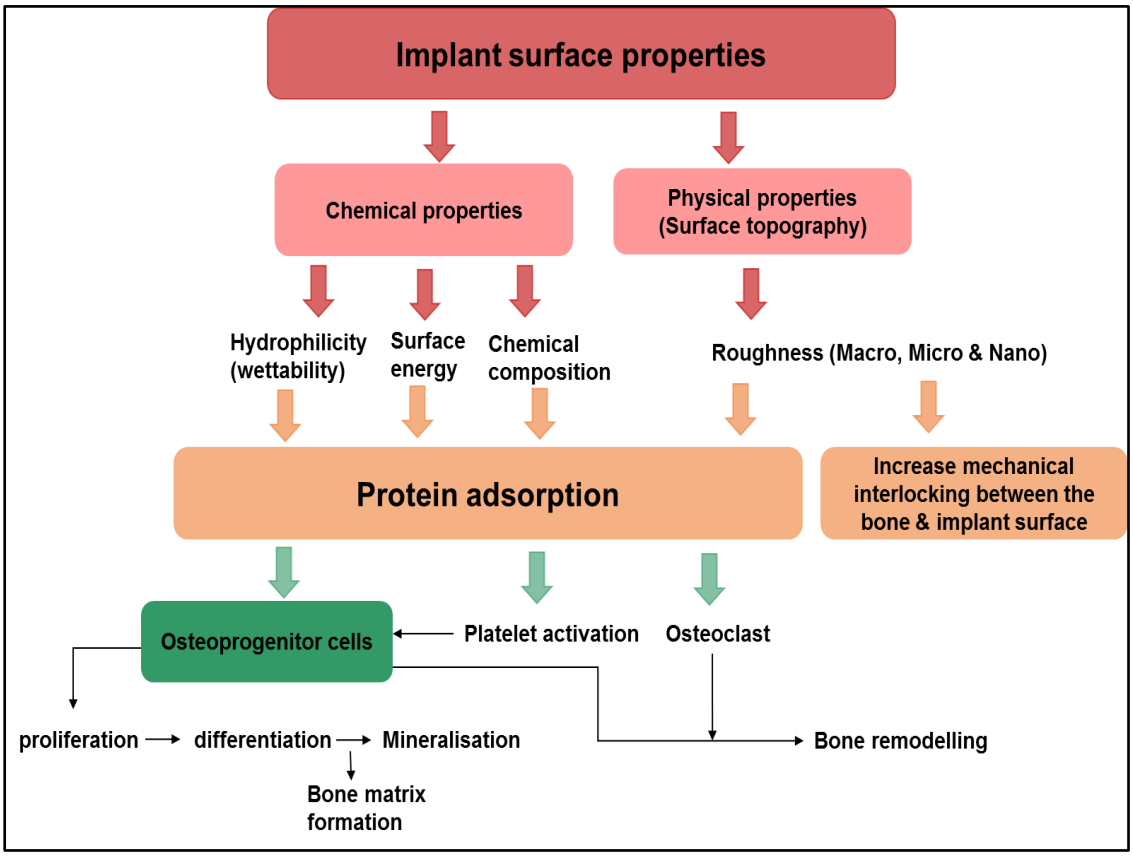

Figure 4: Effect of surface characteristics of the implant on the osteogenic response. Chemical properties including hydrophilicity, surface energy and composition of the implant surface affects ionic interactions, protein adsorption and cell attachment. Surface physical properties such as surface topography and roughness (macroscopic and microscopic features) play an important role in the biomechanical fixation of dental implants by enhancing protein adsorption and the consequent osteoblastic cell migration, adhesion, proliferation and differentiation as well as collagen synthesis leading to better bone deposition adjacent to the implant.

1.7.1 Chemical properties of implant surface:

Albrektsson et al. (1981) pointed to the hydrophilicity (wettability) and surface energy as the most important factors influencing bone-implant contact. Previous in vivo evidence has supported the modification of implant surface chemistry to enhance implant osseointegration (Schliephake et al., 2005). The chemical composition of the implant surface affects ionic interactions, protein adsorption, cell attachment and the hydrophilicity of the surface. Highly hydrophilic surfaces seem more desirable than hydrophobic ones in view of their interactions with biological fluids, tissues and cells (Le Guéhennec et al., 2007). Furthermore, the expression of bone-specific differentiation factors is reported to be higher on hydrophilic surfaces (Le Guéhennec et al., 2007; Anil et al., 2011).

1.7.2 Physical properties of implant surface:

Surface physical properties such as surface topography (macroscopic and microscopic features of the implant surface) and roughness play an important role in the biomechanical fixation of dental implants (Cochran et al., 2002). The osseointegration process can be affected by the surface roughness of the implants because the cells react differently to smooth and rough surfaces. For example, epithelial cells and fibroblasts adhere more strongly to smooth surfaces (Wennerberg and Albrektsson, 2000; Boyan et al., 2001). While rough implant surfaces have a positive influence on osteoblastic cell migration, adhesion, proliferation and differentiation as well as collagen synthesis leading to better bone deposition adjacent to the implant (Wennerberg and Albrektsson, 2000; Boyan et al., 2001; Novaes Jr et al., 2002; Cochran et al., 2002). Depending on the dimension of the measured surface features, implant surface roughness is divided into macro, micro, and nano-roughness. When macro roughness is appropriate, it can enhance the primary implant fixation and long-term mechanical stability by promoting the mechanical interlocking between the macro rough features of the implant surface and the surrounding bone. Macro roughness comprises features in the range of millimetres to tens of microns. This scale of roughness directly relates to implant geometry, with threaded screw and macro porous surface treatments (Wennerberg et al., 1996, Shalabi et al., 2006). Micro roughness is defined as being in the range of 1–10 microns.

This range of roughness increases the interlocking between mineralised bone and implant surface. Micro roughness resulted in greater bone deposition at the implant surface according to some clinical studies (Shalabi et al., 2006, Junker et al., 2009). Nano-sized surfaces provided with nanoscale topographies are widely used in recent years. Nanotechnology involves materials are composed of nano-sized materials with a size range between 1 and 100 nm. Brett et al. (2004) proved that nanoscale roughness plays an important role in the adsorption of proteins, adhesion of osteoblastic cells and thus the rate of osseointegration. Roughness of the implant surface can be induced by different methods including: titanium plasma-spraying (TPS), acid-etching, anodisation and grit-blasting with hard ceramic particles like alumina (Al_2O_3), titanium oxide (TiO_2) and calcium phosphate ($CaPO_4$) (Anil et al., 2011).

1.8 Surface modifications of dental implants

Even though the reported success rate of implant osseointegration is higher than 90% after 5 years and more than 78% after 15 years (Adell et al., 1981), some important conditions remain to be a challenge in dental implant applications such as the long latency period between implant placement and loading with dental prosthesis and the poor bone quality in medically compromised patients including diabetics, osteoporotic, oncology patients and smokers (Elsubeihi and Zarb, 2002). Therefore, surface modification of the dental implant using ceramic coatings has been extensively proposed to improve the clinical survival rates of the implant, to reduce the healing period and to enhance bone anchorage to the implant. It involves improving the surface chemistry, morphology and bio-mechanical properties (Anil et al., 2011). There are 2 types of ceramic coating; bioactive such as calcium phosphates and bioinert such as aluminium oxide and zirconium oxide.

1.8.1 Modification of implant surface by coating with calcium phosphate

Coating implants with calcium phosphate $Ca_3(PO_4)_2$ ceramic materials has been extensively studied since these compounds have relatively similar chemical composition to the mineral matrix of the bone (hydroxyapatite; $Ca_5(PO_4)_3OH$). Calcium phosphate coatings have low thermal and electrical conductivity. They

do not exhibit any unsatisfactory tissue response such as local or systemic toxicity or immune response (Muddugangadhar et al., 2011).
Following implantation, the release of calcium ions (Ca^{2+}) and phosphate ions ($PO4^{3-}$) from the coating into the peri-implant region precipitates a biological apatite layer onto the surface of the implant. The apatite layer stimulates the adsorption of specific blood proteins serving as a matrix for osteogenic cell attachment and growth. This allows direct bone-implant contact without an intervening connective tissue layer leading to a better and faster biomechanical fixation of dental implants compared to uncoated surfaces (Le Guéhennec et al., 2007). The dental implants are usually coated with ceramics by using plasma or flame spray techniques. Various calcium phosphate materials were used as coatings for dental implants with different degradability depending on calcium/phosphorus (Ca/P) ratios, such as bioglasses, tricalcium phosphates (TCP) and tetra- calcium phosphates (Klein et al., 1994). However, the most extensively investigated material is hydroxyapatite (HA) and recently fluorapatite (FA). It has been found that HA (Ca/P ratio of 1.67) and tetra-calcium phosphate (Ca/P ratio of 2) induce an intimate bone- implant contact with lower bone remodelling activity around the implant surface compared to uncoated and tricalcium phosphate coated implants (Klein et al., 1991). The in vitro solubility reports indicated that solubility of tetra- calcium phosphates and tricalcium phosphates is much higher than HA (Klein et al., 1990), while FA has better solubility than HA (Dhert et al., 1991).

1.8.1.1 Hydroxyapatite

HA [$Ca_5(PO_4)_3OH$] is similar in composition and structure to natural bone (Pullen and Gross, 2005), but has low strength and toughness which precluded its clinical use (De Aza et al., 2005). However, using HA as a coating on metallic substrate can combine the good biological properties of the HA layer while retaining the mechanical superiority of the metallic substrate (Yang et al., 2010). In vivo studies of HA coated implants revealed good fixation to the surrounding bone and a greater amount of new bone formation (McPherson et al., 1995). Therefore, HA coated implants were recommended in areas with relative poor bone quality (Junker et al., 2009).

Different coating processes were used for the dental implants with HA such as plasma spraying methods, vacuum deposition techniques, sol-gel coating, electrophoresis and electrolytic deposition (Muddugangadhar et al., 2011). However, plasma spraying is the most commonly used method to produce the commercial HA coatings (Strnad et al., 2000). To coat a dental implant with HA using a plasma spray coating process, the implant surface is first roughened to increase the surface area available for mechanical bonding with HA. Then a plasma is created by an electric arc between an anode and cathode that ionizes HA particles. A carrier gas (argon or nitrogen) blows a stream of HA powder through the very high temperature plasma flame that melts the powder. When the molten powder hits the implant surface, it condenses and forms a glossy and crystalline ceramic coating (Thornton and Bunshah, 1982; Groot et al., 1987). A robotic technique is usually used to build up a thin layer of HA coating of usually 40-50 µm on a roughened titanium or alloy surface (Groot et al., 1987). Major shortcomings of plasma-sprayed HA coatings have been recognised when used for bone regeneration including lack of mechanical strength, cracking and separation from the metallic substrates which results in loss of a firm fixation between the implant and surrounding bone tissue (Sun et al., 2001; Yang et al., 1997). Recently, many studies suggested the incorporation of inorganic materials (strontium, zinc, magnesium, sodium, silver, silicon and yttrium) into HA to promote the bone formation and to enhance bone mineral characteristics such as crystallinity, degradation behaviour and mechanical properties (Sato et al., 2006; Xue et al., 2008; Boanini et al., 2010; Yang et al., 2010; Yang et al., 2012a). HA thermal sprayed coatings have been modified with zirconia (Chou and Chang, 2002) and alumina (Kim et al., 1998) to increase the strength and fracture toughness of the coatings. Moreover, in vivo studies indicated that strontium-substituted hydroxyapatite prepared using electrochemical deposition process showed higher and faster bone to implant contact compared to HA coated implant (Fu et al., 2012; Yang et al., 2012b). It has been found previously that strontium enhances preosteoblast differentiation and inhibits osteoclast differentiation (Canalis et al., 1996). However, the limited stability of plasma sprayed HA has stimulated interest in other bioactive

materials with high resorption resistance like fluorapatite (Fazan and Marquis, 2000).

1.8.1.2 Fluorapatite

Fluorapatite crystals [$Ca_5(PO_4)_3F$] are hexagonal crystals known to have the highest symmetry found among the apatite minerals (Bayliss et al., 1986). The structure of FA crystal is composed of calcium ions (Ca^{2+}) and phosphate ions (PO_4^{3-}) arranged around fluoride ions F^- which extends throughout the crystals in the c-axis direction forming the central column of the crystals (Brown and Constantz, 1994). In the last few decades, FA coating has been studied extensively in order to be used in tissue engineering applications. The excellent biocompatibility of FA is closely related to its chemical and biological similarities with hydroxyapatite based human hard tissues.

Naturally, fluoride ions from the blood accumulate in the bone forming fluoride containing HA. Fluoride is the most electronegative element. Its small ionic diameter and high charge density enable the fluoride to have a great capacity to form strong ionic and hydrogen bonds and to have a high potential for interacting with mineral phases and organic macromolecules (Robinson et al., 2004). Fluoride ions substitute the hydroxyl ions (OH^-) within the apatite lattice creating a tighter lattice structure [$Ca^5(PO_4)_3F$] (Figure 5) with higher stability and lower solubility than HA because this substitution leads to reduction in (a) and (b) lattice parameters of the crystal lattice and a consequent reduction in the crystal energy. This, in turn dramatically decreases the acid solubility of the crystals and generates a more stable crystal structure (Robinson et al., 2017). This could also improve the mechanical strength, decrease the dissolution rate of HA and enhance bone tissue growth (Fathi and Zahrani, 2009). Moreover, fluoride is believed to stimulate bone growth and mineralisation by suppressing osteoclast maturation, inhibiting phagocyte activity and minimizing fibroblast proliferation (Sakae et al., 2000, Cooper et al., 2006). These properties have encouraged the use of FA coatings for dental and orthopaedic implants. In vivo studies have observed a direct bone apposition at the interface of FA coatings with no signs of degradation of the coatings compared to the partial resorption of HA coatings (Dhert et al., 1991; Dhert et al., 1993; Gineste et al., 1999).

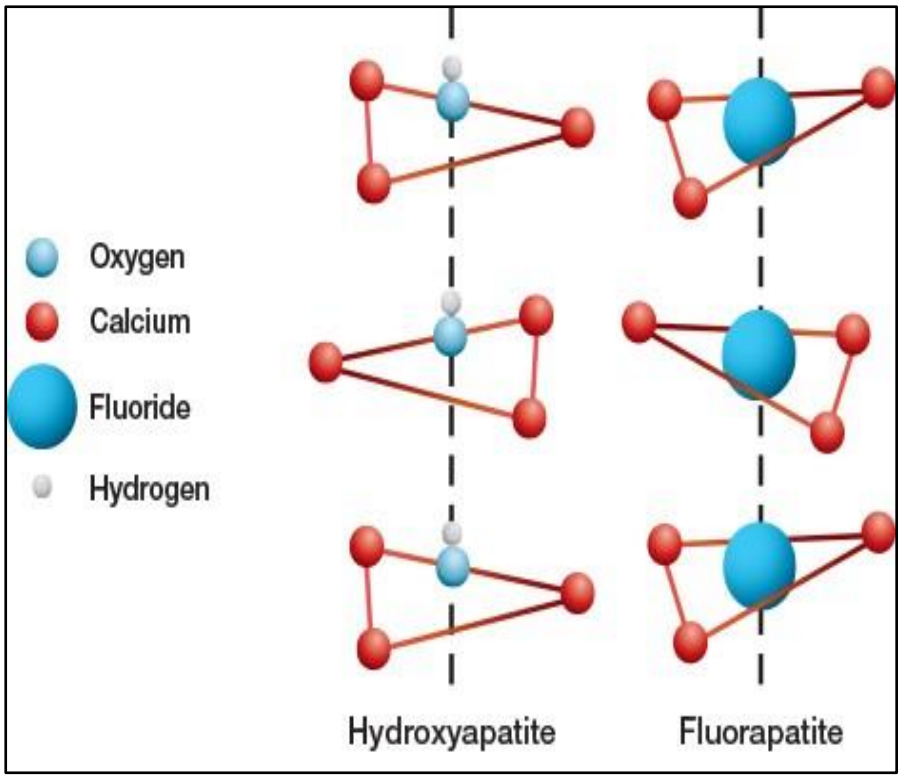

Figure 5: Schematic diagram for hydroxyapatite and fluorapatite. The hydroxyl group of HA is substituted with high charge density fluoride creating tighter lattice structure with higher stability and lower solubility than HA as this substitution leads to reduction in (a) and (b) lattice parameters of the crystal lattice and a consequent reduction in the crystal energy. This, in turn dramatically decreases the acid solubility of the crystals and generates a more stable crystal structure (Adapted from https://www. dentalcare.com/mechanism-of-action-of-fluoride).

FA coatings have been applied to implants by plasma spraying (Ranz et al., 1997). FA is the most stable plasma-sprayed calcium phosphate coating as to a large part, it retains its stability, its fluorine content and its crystallinity during the high temperature process. However, the rapid cooling process does cause a change in the orientation of the FA crystals (Klein et al., 1994). In general, all coating processes are likely to alter the composition of the coating materials, influence their microstructure and crystallinity as well as biological responses to

the materials (Yang et al., 1997, Sun et al., 2001). Therefore, new coating methods have been introduced and studied.

Chen et al. (2006a) demonstrated and compared two novel methods to synthesize FA crystals. One produced short crystals under ambient pressure in which the synthetic crystals prepared at pH 6 -11 and aged at 70°C for 5 days had a length of 20–50 nm and a cross section of about 10 nm. The synthetic nanorods have a typical apatite crystalline structure with a Ca/P ratio between 1.6–1.7, which approaches the theoretical ratio of FA (Ca/P = 1.67). The second method synthesised longer and very well aligned or ordered FA nanorods, by simply controlling pH and using etheylenedeiaminetetraacetic acid (EDTA) as a stabiliser in the precipitation solution under mild hydrothermal conditions (121°C, 2 atm for 6 hours). The FA crystals were of 1–5 μm in length and 30–100 nm in cross section. They are approximately similar to those seen in human enamel but of different shapes and sizes. Chen et al. (2006a) reported that the formation of FA crystals is determined by two processes, one is the initiation of nucleation and the other is the continued growth of the nucleate. The EDTA chelates strongly with Ca^{2+} and this chelating ability depends on the pH of the solution. EDTA can exist in several ionic forms (in up to 7 different acid-base forms) depending on the solution pH. When the pH value of the solution is high (7-12), the more negative anions of EDTA will predominate and provide the strongest EDTA-Ca complexing ability (Liu et al., 2004), thus Ca^{2+} is not released resulting in prevention of FA crystal formation. Whereas, at low pH (pH 4), the chelated Ca^{2+} is not stable under hydrothermal conditions, resulting in explosive release of Ca^{2+} which produces a large quantity and size of nucleates. These nucleates aggregate together and adopt a spherical structure in order to minimise their surface energy. Each spherical structure will have many active growth sites, and with the continuous release of Ca^{2+} will result in the growth of the FA crystals from these sites. The large size of each nucleate on the spherical aggregate induces the formation of many defects during the fast growth, that will produce small branches at the end of the crystal. However, the stability of Ca-EDTA complex is enhanced by increasing the pH to 5 which will result in the formation of smaller spherical structures containing smaller nucleates and only single nanorod forms from each nucleate

with no branching structures. When the pH is increased to 6, a stronger chelating of Ca^{2+} to EDTA is produced, leading to the formation of small nucleates in size and quantity, and because each individual nucleate will develop into individual single nanorods, individual well-separated and long nanorods are synthesized. The FA crystals may grow faster in one of the polar directions. The fastest growth direction will form the leading tip due to diffusion-limited growth, which results in a spear-like crystal formation with one end of the crystal being sharper than the other (Liu et al., 2004).

Chen et al. (2006b) demonstrated another hydrothermal technique to grow a layer of well aligned FA crystals on metal substrates at 121^{o}C and 2 atm for 10 hours using EDTA to stabilise the release of Ca^{2+}. This direct growth method was able to produce fluorapatite dental enamel prism like structures (10–30 μm in cross section) on iron substrates. The crystal structure was very similar in chemical composition to natural tooth enamel, the crystals are of 1–3 μm in cross section and approximately 50 μm in length. Other metal substrates may support the growth and orientation of the FA crystals but do not produce the closely aligned prism-like structures. The morphology of the synthetic FA crystals developed from amorphous deposits to hollow balls and finally to well-defined crystals as the autoclave time increased from 5 min to 10 hours as shown in figure 6. The FA rod- like structures have the tendency to aggregate side by side to form a bundle because of the stronger van der Waals attraction along the long axis of the rods. Then, a long FA nanorod that undergoes rapid growth may act as a leader crystal in the centre of the bundle while some shorter nanorods become closely aligned parallel to the surface of the leader crystal resulting in a shuttle-like structure of a large well-defined hexagonal crystal. With increasing autoclave time, all the Ca^{2+} from the EDTA-Ca complex are diminished and the bundles stop growing longer (Chen et al., 2006b). Chen et al. (2006b) proposed that it might be possible to induce dentin and pulp formation on the synthetic enamel layer in vitro and to regenerate teeth for implantation into humans in the future.

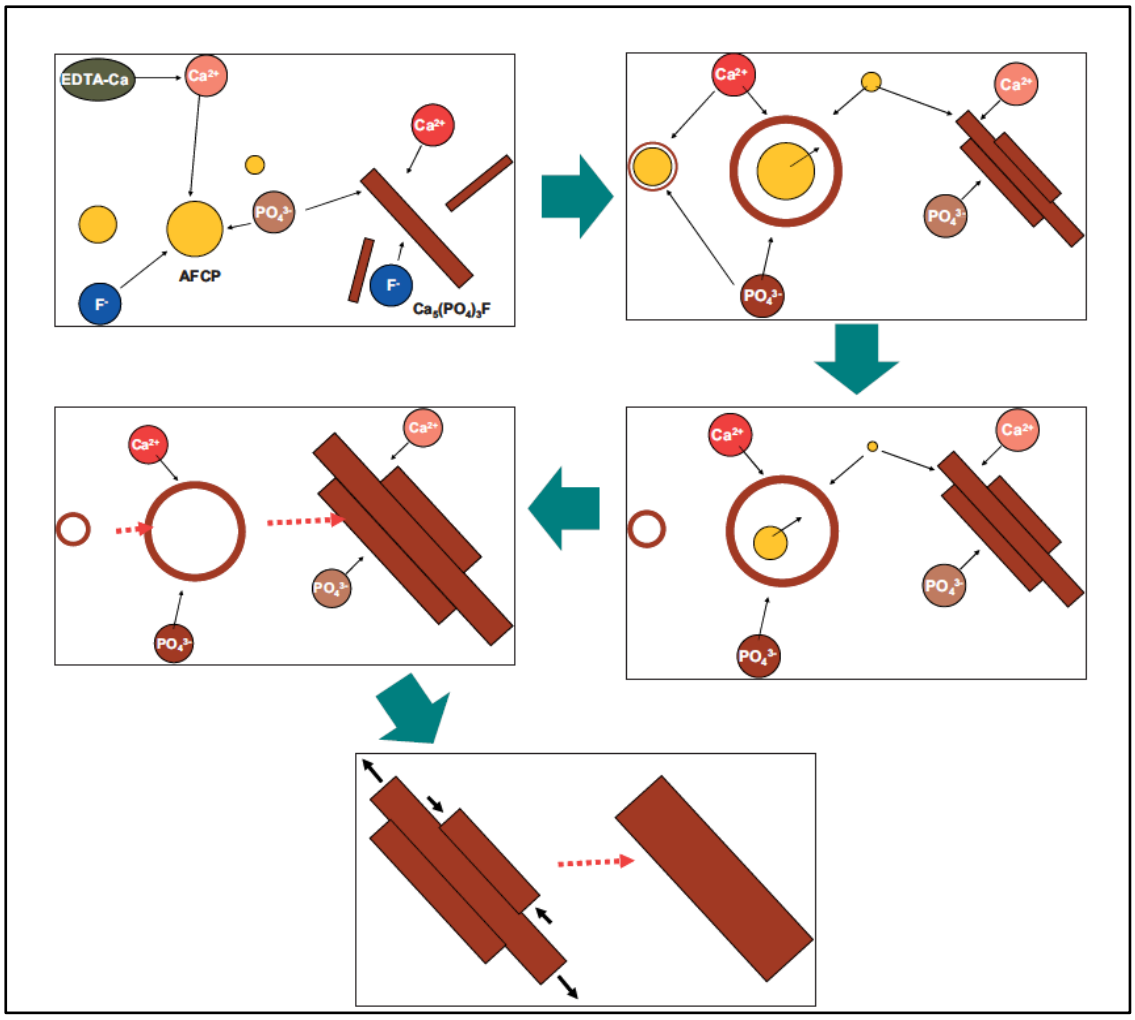

Figure 6: Growth of FA crystals as the autoclave time increased from 5 minutes to 10 hours using a hydrothermal technique. The morphology of the synthetic FA crystals developed from amorphous deposits to hollow balls and to well-defined crystals as the autoclave time increased. At pH 6, Ca^{2+} dissociate slowly from the EDTA-Ca complex and react with phosphate and fluoride ions leading to the formation of small nucleates in size and quantity and because each individual nucleate will develop into individual single nanorods, individual well-separated and long nanorods are synthesized. The FA rod- like structures have the tendency to aggregate side by side to form a bundle of crystals. Then, a long FA nanorod that undergoes rapid growth may act as a leader crystal in the centre of the bundle while some shorter nanorods become closely aligned parallel to the surface of the leader crystal resulting in a shuttle-like structure of a large well-defined hexagonal crystal (Adapted from Chen et al. 2006b).

Czajka-Jakubowska et al. (2009a) have successfully changed the surface morphology of the FA crystals from ordered to disordered when produced individually on the under surfaces and upper surfaces of the substrate respectively. They also attempted to grow FA on different substrates; they found that only etched stainless steel and titanium substrates could produce surfaces completely covered with FA crystals of uniform composition, alignment, size, shape and structure (Czajka-Jakubowska et al., 2009b).
Interestingly, some in vitro studies revealed that the well aligned FA crystals grown by the mild hydrothermal method appeared to promote cell differentiation and mineralization process better than the disordered crystals. This would suggest that ordered FA crystals may enhance osseointegration of dental implants (Liu et al., 2010; Liu et al., 2011; Liu et al, 2012). However, more research is required to develop the understanding of the exact effect of fluoroapatite as a dental implant coating.

1.8.2 Modification of implant surface by coating with platelet-rich plasma

Recent tissue engineering developments have improved the osseointegration of dental implants through stimulating the regeneration of new bone by using growth factors (GFs), plasma proteins and stem cells (Anil et al., 2011). The potential effects of GFs in the repair and regeneration of bone have been well documented. GFs are secreted locally during blood clotting by activated platelets at the site of implantation and stimulate a series of events that leads to the wound-healing response. They promote proliferation, chemotaxis and differentiation of cells which are essential to osteogenesis and angiogenesis (Kanno et al., 2005) (Figure 7). Thus, they have been suggested as bio-coatings for endosseous implants to accelerate and enhance bone growth (Anitua et al., 2008; Anitua et al., 2009b; Albanese et al., 2013).
Coating implants with bone morphogenetic protein-2 (BMP-2) has been suggested as a means of inducing local bone formation (Liu et al., 2007; Wikesjö et al., 2008) and platelet-derived growth factor (PDGF) accelerated soft tissue attachment (Bates et al., 2013). However, the clinical application of commercial GFs is problematic due to their short shelf life and high cost. Additionally, high doses may be required to achieve any therapeutic effect.

Alternatively, an easy and cost-effective way to obtain high concentrations of GFs for tissue healing and regeneration has been achieved by using autologous platelet concentrates (Nikolidakis and Jansen, 2008). Pure platelet concentrates were developed for topical use as an additional application of the classical transfusion platelet units and were first used for maxillofacial surgery by Whitman et al. (Whitman et al., 1997). Platelet concentrates were prepared and used in different forms and platelet-rich plasma (PRP) is one of the forms that were extensively used as a substitution for the commercial GFs.

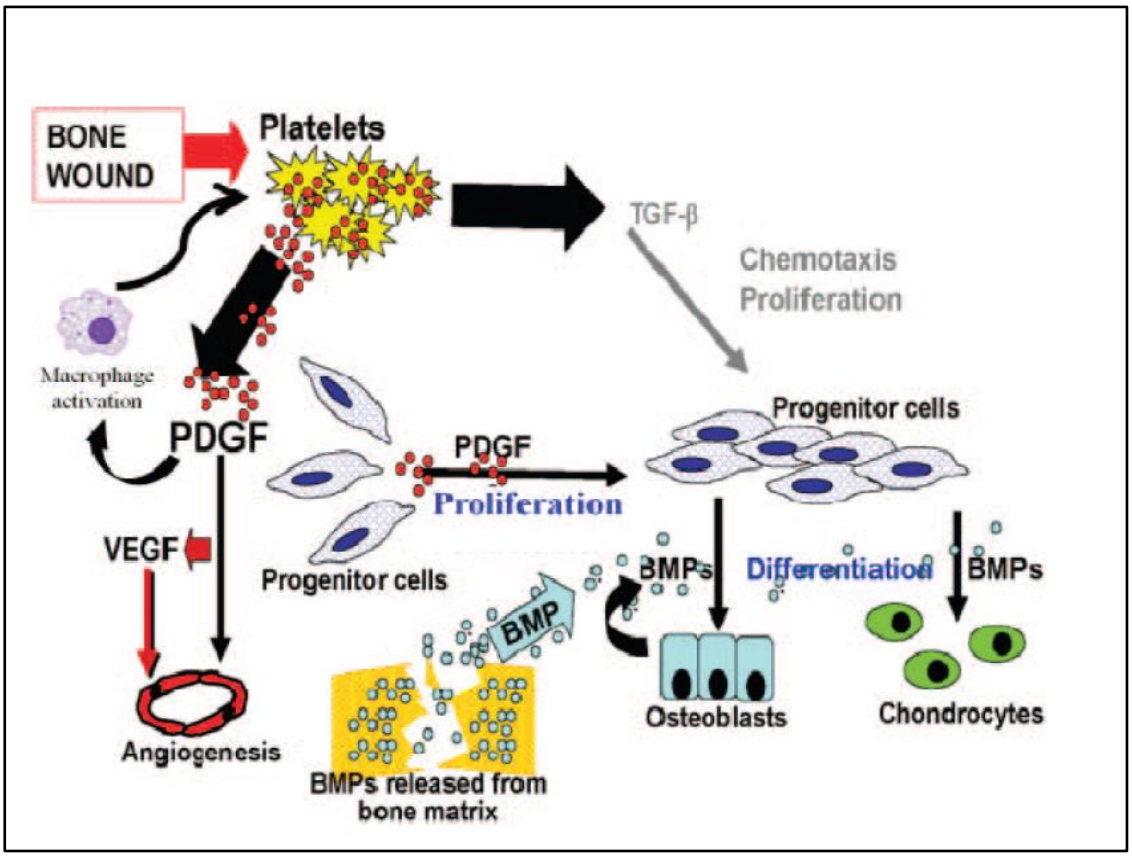

Figure 7: The role of platelets and some GFs in bone healing. After 10 minutes of platelets aggregation induced by tissue injury, platelets begin releasing GFs into the injury site. GFs such as PDGF, TGF- β and IGF-1 serve as signalling molecules for recruitment and differentiation of mesenchymal stem cells into different lineage to initiate different activities including angiogenesis and osteogenesis. Platelets GFs also activate the macrophages that replaces the platelets as the primary source of growth factors after the third day of the healing process (http://www.joionline.org/doi/pdf/10.1563/AAID-JOI-D-11-00173).

Platelet-rich plasma (PRP) is safe because it is an autologous preparation (i.e prepared from the patient's own blood), and thus, poses no risk of infection, disease transmission or immunogenic reaction. It is easily obtainable and not time-consuming to use for the patient and the clinician (Albanese et al., 2013). Such advantages have increased the interest in the application of PRP to promote tissue healing in dental and orthopaedic applications (Anitua, 1999) and as a dental implant coating for improving the osseointegration of dental implants (Anitua et al., 2004; Kanno et al., 2005).

PRP is defined as a high concentration of autologous platelets in a small volume of autologous plasma. A concentration of 1,000,000 platelets/μL in a 5mL volume of plasma or approximately 5 times higher than that of whole blood was proposed to be the working definition of PRP (Marx, 2001). PRP is effective in the early stage of bone healing process, because the life of a platelet is only about 5–7 days. Within 10 minutes of platelets aggregation, platelets begin releasing GFs into the injury environment with full release within an hour (Pietrzak and Eppley, 2005). Although proteins can be released for an hour, the half-life of the GFs and other cell factors last just a few minutes. However, macrophages aggregated by PDGF released by platelets, might play a more important role in the following stage of healing process.

1.8.2.1 Preparation procedures of PRP

To prepare PRP, blood samples should be drawn into a tube containing anticoagulation factors. There are several choices of anticoagulants such as citrate dextrose-A, which is the preferable agent. The citrate binds with calcium and subsequently prevents blood coagulation, whereas the dextrose and other ingredients support platelet metabolism and viability. Citrate phosphate dextrose anticoagulant has fewer supportive ingredients and therefore may be less effective at maintaining platelet viability (Marx, 2001).

Ethylenediaminetetra-acetic acid (EDTA) is also used as an anticoagulant to chelate calcium but is potentially more harmful than citrate to the platelets (Landesberg et al., 2000). While, trisodium citrate solution was used as an anticoagulant that has no negative effects on PRP preparation (Anitua, 1999).

PRP is prepared by centrifugation using several automated systems and manual protocols. However, each method results in a different PRP product with different biological properties and uses (Marx, 2001).

1) Automated protocols of PRP preparation

The first automated method of producing platelet concentrates was called plasmapheresis, in which the patient stays connected to a cell separator and the blood filtering continues until the desired quantity of platelets has been collected (Weibrich et al., 2003).

The ideal cell separator must use a double centrifugation technique. The blood sample is drawn into a tube containing an anticoagulation factor and spun in double centrifuge cycles. The first spin (hard spin) separates the red blood cells at high force (3000 g in general) from the plasma that contains the platelets and white blood cells (buffy coat). Then the buffy elements in the plasma are detected by an optical reader and automatically collected into a separate bag using a soft spin as a platelet concentrate (PRP) (Weibrich et al., 2003; Pietrzak and Eppley, 2005). The platelet collection is interrupted when the optical reader detects elements of RBCs, thus RBCs mixed with leucocytes and some residual platelets are directed towards a third collection bag and re-infused in to the donor blood. Recently, newer systems have been introduced that can be used more easily, both for auto-transfusion during surgery and for topical application e.g. the Electa cell separator (Sorin group, Italy).

Another automated system called PCCS (Platelet Concentrate Collection System) uses centrifuges that consist of two connected chambers or compartments. The citrated blood is transferred into the first chamber and centrifuged briefly to obtain three layers (RBC, buffy coat, platelet-poor plasma or PPP). Then, by using air pressure, the superficial layers (PPP and buffy coat) are transferred to the second chamber and centrifuged again for a longer period. Finally, most of the PPP layer is transferred back into the first chamber using the same air pressure system.

Automatic devices allow around about 5mL to 10mL of PRP to be obtained from 40- 60 mL of whole blood which is sufficient for most minor surgical procedures, including ridge augmentation, bilateral sinus grafts and periodontal regenerative

surgeries (Gibble and Ness, 1990). Therefore, in maxillofacial reconstruction therapies, up to 500mL of blood should be drawn from the patient to obtain larger amount of PRP required for larger surgical defects.

Several commercial systems are also available for preparing platelet concentrate, such as SmartPReP system (Harvest Autologous Hemobiologics, Norwell, MA), the Tisseel system (Baxter Health Corporation, Deerfield, IL) and the Curasan PRP kit (Curasan, Pharma Gmbh AG, Lindigstrab, Germa ny) (Nikolidakis and Jansen, 2008). However, not all the commercially available devices are able to produce adequate platelet concentration and this might explain some of the variation in clinical efficacy of PRP reported by different studies (Weibrich and Kleis, 2002). Some studies have compared these systems and found that the PCC System may produce the greatest platelet concentrations in a short time with great ease of handling (Appel et al., 2002; Marx, 2004).

Although this sophisticated technology is the more accurate method from a technical point of view, it still can result in PRP containing residual RBCs and leucocytes. Moreover, the platelet collection efficiency is rather low and the platelets could be damaged during the process (Leitner et al., 2006). Platelet-poor plasma (PPP) cannot be collected using automated PRP preparation techniques as it is re-infused in to the blood donor. In addition, the main drawback of all these automated techniques is that they are unwieldy and labour-intensive as they often require the help of a haematologist, thus, their use in daily practice remains rare. Therefore, developing alternative manual protocols was necessary to make it possible to use platelet concentrates in daily practice without the need for transfusion laboratory support.

2) Manual protocols of PRP preparation

The first platelet concentrate manual protocol was described by Anitua to prepare plasma rich in growth factors (PRGF) (Anitua, 1999; Anitua et al., 2007). In this protocol, blood is collected and centrifuged to obtain the three typical layers: RBCs, buffy coat and platelet-poor plasma (PPP). The PPP is discarded from each tube by careful pipetting to avoid creating turbulences. The remaining plasma rich in growth factors is collected with a pipette, using only

eyeballing as a measuring tool. The pipetting steps are associated with possible pipetting and handling errors. Therefore, this technique may be more prone to errors leading to a low platelet collection efficiency because platelets and leucocytes are found together in the intermediate layer (Weibrich et al., 2005). Anitua's PRGF method is an inexpensive manual protocol for the preparation of leucocyte-poor PRP or pure PRP. However, the lack of reproducibility of the procedure is problematic.

In another protocol uses also a two-step centrifugation procedure, the blood components are separated into three parts (RBCs, buffy coat and PPP) in the first centrifugation step. The PPP and the buffy coat are carefully collected in another tube, avoiding RBC contamination and are subjected to a second centrifugation step at high speed to separate the platelets from the platelet-poor plasma (PPP). Most of the PPP fraction, identified by simple visual inspection, is discarded and the platelet pellet is re-suspended in a low volume of plasma to obtain the PRP. The PRP obtained with this method is composed of a high quantity of platelets, leucocytes and circulating fibrinogen, but it also may contain residual RBCs.

The manual PRP preparation process is time consuming and yields small volumes of PRP, but PPP fraction can be well preserved. PPP contains fibrinogen and can be used to increase the final volume of PRP (Pietrzak and Eppley, 2005). In general, it is necessary to point out that the success of the manual method depends on the operator and results are not always reliably reproduced. This is especially true considering that various authors use different centrifuges and different g forces to spin the blood samples. Consequently, PRP samples obtained by different labs differ in platelet concentrations which in turn leads to variability in the published results. Furthermore, platelet activation might be triggered inadvertently during PRP preparation and can result in the early release of GFs in the PPP and their subsequent loss (Marx, 2001).

1.8.2.2 Components of PRP

1) Platelets

Platelets are small discoid blood cells (1–3 µm). The average platelet count in human blood is 200,000 platelets/µL (ranging between 150,000 and 350,000

platelets /µL). The in vivo half-life time of platelets is about 7 days (5 to 9 days). Platelets are synthesized in bone marrow by the pinching off of pieces of megakaryocyte cytoplasm that are extruded into the blood circulation. Platelets have a cytoskeleton comprising a peripheral ring of microtubules containing actin and myosin. Platelets contains a number of intracellular molecules such as glycogen, lysosomes, and two types of granules; dense granules which contain ADP, ATP, serotonin and calcium, and α-granules which contain clotting factors, growth factors and other proteins (Zucker-Franklin, 1988). Normally, in the resting state, platelets are non-thrombogenic and require a trigger before they become an active player in the wound healing process. On activation by contact with a foreign surface or by thrombin, they change shape and develop pseudopodia, which promote platelet aggregation and the subsequent release of the GFs from the granules through the open canalicular system (Figure 8).

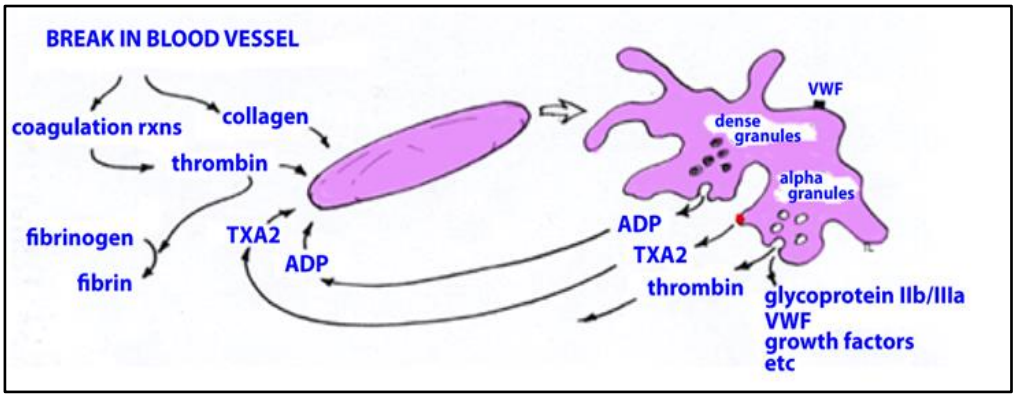

Figure 8: **Schematic overview of a resting and activated platelet. Normally platelets are in a resting state. On activation with an activator, platelets change their shape with the development of pseudopods to promote platelet aggregation and subsequent release of granules content through the open canaliculi system (https://courses.washington.edu/ conj/bloodcells/plateletScheme.png).**

2) Fibrin

Liquid PRP formulations also contain soluble fibrinogen which is the precursor molecule to fibrin monomers. Thrombin cleaves soluble fibrinogen into fibrin monomers that assemble into networks of insoluble fibrin polymers at the site of injury in which platelets, leukocytes, and other cells can proliferate and perform

specific functions (Laurens et al., 2006). The structure and function of fibrin matrices used as scaffolds for tissue regeneration therapies are determined by several conditions, including; clotting, fibrinogen concentration, fibrin density and polymerization rates (Brown et al., 1994; Laurens et al., 2006).
Cellular responses to fibrinogen or fibrin matrices within PRP applications may be greatly individualised because of the differences in fibrinogen which is depending on posttranslational protein modifications and genetic variants (de Maat and Verschuur, 2005). Fibrinogen regulates the activity of monocytes and macrophages and therefore mediates the transition between inflammatory and regenerative stages of the response to injury response (Kells et al., 1995).
Fibrin density is determined by the concentration of native fibrinogen during preparation (Clark, 2001). Fibrin polymerization is determined by the ratio of fibrinogen and thrombin where high thrombin concentrations trigger rapid polymerization, leading to the formation of a dense network that hampers cytokine signalling and cellular migration. In contrast, slow polymerization induced by low thrombin concentrations creates a more flexible scaffold that is more conducive to cellular migration and cytokine signalling (Hinsbergh et al., 2001).

3) Growth factors and cytokines

As outlined in table 1, PRP contains numerous growth factors (GFs), whose properties vary significantly. Many of the GFs and cytokines that are believed to be responsible for the biological effects of PRP are released from the α-granules of the platelets. VEGF, PDGF, and TGF-β1 are the main growth factors derived from platelets. PRP typically contains 3 to 5 fold increase in growth factor concentrations over baseline blood levels (Doessing et al., 2010; Wasterlain et al., 2012).

Table 1: Some important biologically active molecule contained in PRP cited by Sell et al. (2012)

General category	Specific molecules	Physiological role
Adhesive proteins	Fibrinogen, fibronectin, vitronectin, thrombospondin-1, von Willebrand factor, laminin-8	Cell contact interactions, cellular adhesion, chemotaxis, ECM composition, clotting
Clotting factors and associated proteins	Factor V, factor XI, protein S, antithrombin, tissue factor pathway inhibitor	Thrombin activation and its regulation, eventual fibrin clot formation
Fibrinolytic factors and associated proteins	Plasminogen, plasminogen activator inhibitor	Plasmin production and regulation
Proteases and anti-proteases	Tissue inhibitor of metalloproteases 1–4 (TIMP 1–4), MMP-1, -2, -4, -9	Regulation of matrix degradation, regulation of cellular behavior, etc
Growth factors, cytokines and chemokines	TGF-β, PDGF, insulin-like growth factor (IGF)-I and -II, FGF, EGF, VEGF, ECGF, KGF, GM-CSF, hepatocyte GF, TNFα, RANTES,IL-8,IL-1β, BMP-2, -4, -6	Chemotaxis, cell proliferation and differentiation,promotion of ECM production, regulation of inflammation, angiogenesis.
Antimicrobial proteins	Thrombocidins, kinocidins	Bactericidal and fungicidal properties
Membrane glycoproteins	αIIbβ3, αvβ3, CD-40 ligand, P-selectin, tissue factor, PECAM-1, CD63	Platelet aggregation and adhesion, inflammation, platelet–leukocyte interactions
Lipids	Sphingosine-1-phosphate, thromboxaneB2, prostaglandin F2α, leukotriene B4	Inflammation modulation, cell migration and proliferation, etc
Basic proteins and others	Platelet factor 4, β-thromboglobulin, endostatins, albumin, immunoglobulins G and M	Regulation of endothelial cell chemotaxis and angiogenesis, platelet activation, etc

1.8.2.3 Mechanism of GF and cytokine action of PRP on bone healing process

The application of PRP amplifies the surge of chemical mediators to the microenvironment of the injured area. Therefore, many studies have focused on the role of PRP on the molecular mechanisms of bone healing process through three aspects of bone repair; inflammatory cytokines, growth factors, and angiogenic factors.

1. The role of inflammatory cytokines to promote bone healing process

Inflammatory reactions involve a number of biochemical and cellular alterations depending on the initial trauma (Kamoda et al., 2012). Histamine and serotonin are released by dense granules of the platelets. They increase capillary permeability in the healing area, which allows inflammatory cells greater access to the wound site and activates macrophages (McManus and Pinckard, 2000). Adenosine, also released from the dense granules, is a potent endogenous physiological mediator that regulates a wide variety of physiological processes. In addition to its effects on angiogenesis, adenosine is a potent regulator of inflammation, the first stage of the wound-healing process (Montesinos et al., 2002).

2. The Role of growth Factors to promote bone healing process

The action of PRP on the natural healing pathway of bone is related to the increased concentration of growth factors and bioactive proteins released by activated platelets (Pietrzak and Eppley, 2005). The best known growth factors are PDGF, TGF-βeta and IGF-1.

- **Platelet-derived growth factor (PDGF):** it is mainly found and stored in the alpha granules of the platelets (Antoniades, 1981), and thus is directly proportional to the number of platelets in PRP. PDGF can also be found in other cells, such as macrophages (Rappolee et al., 1988), fibroblasts (Antoniades et al., 1991) and in bone matrix (Hauschka et al., 1986). Human PDGF was originally identified as a disulfide-linked dimer of two different polypeptide chains, A and B (Johnsson et al., 1982) and found as three isoforms; two

homodimers (AA and BB), one heterodimer (AB) (Miyazono and Takaku, 1989). The reason for three distinct forms remains unclear, but a differential binding between the three distinct forms and various target cells such as macrophages, fibroblasts, endothelium and marrow stem cells has been suggested (Ross et al., 1986). This view lasted for more than 15 years until combinations of genomic and biochemical efforts identified two additional PDGF genes and proteins, PDGF-C (Li et al., 2000) and PDGF-D (LaRochelle et al., 2001). PDGF isoforms signal through a homo- or heterodimeric receptor of PDGF receptor- α (PDGF-R α) or PDGF receptor- β (PDGF-R β) subunits (Andrae et al., 2008). One heterodimer (PDGF-AB) has been found in human platelets (Ekman et al. 1999). The biological activities of PDGF are mostly involved in the stimulation of mitogenesis, angiogenesis and macrophage activation (Raines et al., 1990), fibroblast chemotaxis and collagen synthesis (Matsuda et al., 1992) and proliferation of bone osteoblast cells (Yang et al., 2000). Cell migration is one of the well-documented effect of PDGF in vitro (Heldin and Westermark 1999). It also promotes the deposition of fibronectin and glycosaminoglycan (Anitua et al., 2005). The effect of PDGF on mesenchymal stem cells (MSCs) has been intensively studied. PDGF signalling has been identified as the key pathways involved in MSCs differentiation into osteogenic lineage where genes of the PDGF pathway are expressed strongly in undifferentiated MSCs (Ng et al., 2008).

- **Transforming growth factor (TGF):** TGF-β1 and β2 are members of a super-family of growth and differentiation factors including the bone morphogenetic protein (BMP) which are involved in connective tissue healing and bone regeneration (Celeste et al., 1990). The most important function of TGF-β1 and -β2 is chemotaxis and mitogenesis of preosteoblasts during bone formation (Beck et al., 1993). TGF-β1 has been reported to promote the biosynthesis of type I collagen and fibronectin, to stimulate the deposition of bone matrix (Bonewald and Mundy, 1990), and to inhibit osteoclast formation and bone resorption (Mohan and Baylink, 1991). Accordingly, TGF-β not only initiates bone regeneration but also supports long term healing and remodelling (Hsiao et al., 2012).

➢ **Insulin-like growth factor (IGF-1):** it is produced by the liver and is primarily found in plasma, and is therefore found at fixed levels in most PRP preparations regardless of the platelet count (Doessing et al., 2010). IGF-1 is known to enhance bone formation when it binds to a specific receptor on the cell membrane of preosteoblasts and stimulates their proliferation and differentiation (Hock et al., 1988). The presence of IGF-1 could also inhibit apoptosis of bone cells (Joseph et al., 1996). It is known to be responsible for the bone formation-bone resorption interaction (Mohan and Baylink, 2002).
The biological effect of IGF-1 could be regulated by IGF binding proteins (IGFBPs) where IGFBPs could be involved in transporting IGF-1 and increasing its half-life (Govoni et al., 2005).

3. The Role of angiogenesis factors to promote bone healing process
Angiogenesis is essential in the bone healing process where osteogenesis needs a sufficient blood supply. It is, therefore, vital to promote angiogenesis rapidly in the bone healing area in the early healing stages and also during the long-term process of ossification. There are two independent pathways stimulating angiogenesis; one depends on vascular endothelial growth factors (VEGF) released from platelet granules, and the other depends on angiogenin. VEGF mainly stimulates the growth of new-born local blood vessels and specific mitogen of endothelial cell, whereas angiogenin mainly affects large vessels and collateral circulation formation (Behr et al., 2011).
The vascularisation potential of PRP was found to be associated with some important factors such as; the concentration of plasma, activation of Ca^{2+}, the release of VEGF and the formation of platelets (Karp et al., 2005).

1.8.2.4 PRP activation

PRP activation initiates 2 main processes within PRP preparations; degranulation of platelets to release α-granules containing growth factors, and fibrinogen cleavage to initiate fibrin matrix formation (Wasterlain et al., 2012). Once the PRP is activated, the extracted PRP fraction is often called the PRP releasate. PRP activation can be achieved using 3 mechanisms; addition of

calcium chloride and thrombin, freeze/thaw cycles, and direct exposure to collagen in vivo.

➢ **Calcium chloride and thrombin activation**

At the time of clinical application, the PRP is combined with a certain amount of a sterile saline solution containing 10% calcium chloride and thrombin which causes the platelets to degranulate and release GFs and cytokines. Calcium chloride is a citrate inhibitor that allows the plasma to coagulate by replenishing the binding site that were previously bound by anticoagulant. Thrombin directly activates platelets through a proteolytic G-coupled protein receptor and also allows polymerization of the fibrinogen into an insoluble fibrin gel. Different protocols for PRP activation exist. However, the standard clinical approach uses a ratio of thrombin to $CaCl_2$ of 142.8 U/mL thrombin to 14.3 mg/mL $CaCl_2.2H_2O$ as suggested by Marx et al. (1998). A mixture of 1,000 UI of thrombin powder suspended in 10mL of sterile saline with 10% calcium chloride was also reported for the initiation of the coagulation process (Sánchez et al., 2003). While, Anitua (1999) suggested that 50 µL of 10% calcium chloride can be utilised to activate 1.2mL of PRP for 15 to 20 min, then a PRP gel can be formed without using thrombin.

One of the disadvantages of using calcium chloride and thrombin as exogenous activators is the increased risk of infections and allergic or other reactions. This is especially true with the use of bovine thrombin, which is immunogenic. Therefore, calcium can be used independently as an alternative way to stimulate platelet activation (Anitua et al., 2012).

➢ **Freeze/thaw cycle activation**

PRP is stable for 5 days at room temperature (Cognasse et al., 2009) and for longer when frozen. However, freeze/thawing cycles are reported to physically damage and lyse the platelets, and hence initiate the de-granulation and release the contents of the α-granules (Johnson et al., 2011). It seems that activation through freeze/thaw cycles initiates platelets degranulation only, whereas addition of thrombin and calcium chloride is effective in activating both platelets and fibrinogen polymerisation. The precise number of freeze/thaw

cycles necessary for complete degranulation is not clear. Many protocols suggest 4 freeze/thaw cycles for in vitro studies. The freeze/thaw cycle activation method is useful for in vitro PRP applications and laboratory experiments because it does not use chemical substances to activate the platelets and therefore does not alter the composition of the sample. However, this method is time consuming and thus is impractical for clinical applications (Wasterlain et al., 2012).

- **In vivo collagen activation**

It was suggested that the liquid form of PRP (non-activated) can be injected directly into the injured tissue to be activated on contact with collagen. Thrombogenic fibrillar collagen types I and III (COL1 and COL3) are regarded as the most potent activators of platelet adhesion and aggregation because of their high content of von Willebrand factor, which is an important substrate that mediates the interaction between collagen and platelets (Farndale et al., 2003) Many clinical applications prefer the use of in vivo collagen activation for activating PRP, as it leads to a slower and more sustained release of growth factors, compared with thrombin. It was proved that collagen activation leads to a more sustained release and 80% greater cumulative release of TGF-β1 over a seven-day period, compared with thrombin activation (Fufa et al., 2008; Harrison et al., 2011). While, cumulative release of VEGF appears unaffected by the activation method used, and PDGF has shown mixed results.
One of the main benefits of using in vivo collagen activation is that it enables the PRP to be injected through a smaller-gauge needle as the clotting as not occurred. Furthermore, its use eliminates the risk of immunologic reactions to exogenous activating substances such as calcium or thrombin (Wasterlain et al., 2012).

1.8.2.5 The Application of PRP in bone tissue engineering

The application of PRP in dentistry have been intensively published to clarify the clinical efficiency of PRP as a source of many growth factors on bone regeneration and healing process (Schliephake, 2002; Sánchez et al., 2003; Tozum and Demiralp, 2003; Freymiller and Aghaloo, 2004; Grageda, 2004;

Nikolidakis and Jansen, 2008; Plachokova et al., 2008; Anitua et al., 2012; Albanese et al., 2013).

1) PRP in dental implant applications

Many human and animal studies using PRP have yielded promising results in dental implant applications. PRP was used topically at the implant site to enhance bone regeneration (Zechner et al., 2002). In 2006, Anitua indicated that coating the dental implant with PRP prior to its insertion into the jaw bone might generate a new active surface which could potentially enhance the osseointegration process. Similarly, Gentile et al. (2010) reported the efficacy of PRP treatment in postoperative patients' satisfaction of 15 cases including maxillofacial surgery, post-extraction bone regeneration and dental implantation. Anitua et al. (2008) and Anand and Mehta (2012) have suggested the use of a PRP coated implant to improve the prognosis of immediate loading protocol with dental prosthesis. However, PRP efficiency in dental implant applications was controversial. Thor et al. (2005) in a conflicting study failed to show a positive effect for PRP gel in association with autogenous bone graft on the survival rates of the dental implants of severely resorbed maxilla. Likewise, Garcia et al. (2010) did not find a significant enhancement in bone formation around sandblasted acid etched dental implants placed in association with PRP gel.

2) PRP and bone grafts in dental surgery

Clinical studies have shown that the bone density and the maturation rate increased significantly after implanting bone grafts in combination with PRP into mandibular bone defects compared to using grafts alone (Marx et al., 1998). The combination of mesenchymal stem cells (MSCs) with PRP and autogenous bone grafts also showed a significantly higher maturation of bone in a canine model (Yamada et al., 2004). Moreover, it was demonstrated previously that PRP combined with autologous cancellous graft could significantly improve the bone regeneration compared to graft applied alone in a critical size defect of load-bearing long bones of minipigs (Hakimi et al., 2010). In another published article, the effect of PRP as an autologous source of growth factors combined

with autograft was evaluated in bone defect model of 23 rabbits. They found that the use of PRP in this study enhanced type III to type I collagen ratio and the chemotaxis of CD34+ bone progenitor cells (Giovanini et al., 2010). The use of PRP with bone graft was also proved to significantly enhance the quality of bone healing in rabbit model (Kanthan et al., 2011).

3) PRP and biomaterials in dental surgery

Studies of tissue engineering have obtained more favourable clinical results in bone repair when PRP was used in association with biomaterials which resulted in better bone inductivity (improved the cells ability to induce bone formation) and conductivity (support the bone growth on the biomaterial).

Some investigators reported that using PRP in combination with hydroxyapatite or tricalcium phosphate scaffolds and bone substitute materials may hold some promise for tissue engineering purposes by enhancing in vivo bone regeneration compared to the use of the scaffold alone (Okuda et al., 2005; Abhijit, 2006; Rai et al., 2007; Chevallier et al., 2010; Bi et al., 2010, Klein et al., 2010; Qi et al., 2015).

Kim et al. (2002) introduced a combination of particulate dentine, plaster of paris (calcium sulphate) and PRP around titanium dental implants in a canine model where they observed a better histological outcome of bone formation when PRP was added to the biomaterials. Bone density and the maturation rate was increased significantly after implanting calcium phosphate scaffolds in combination with PRP in mandibular bone defects compared to using scaffolds alone (Kovács et al., 2003). Yamada et al. (2004) in an animal study observed a well-formed mature bone in osseous defects when injected with PRP gel and MSCs compared to PRP alone or autogenous bone graft. They found a progressive and complete resorption of PRP gel and relatively mature bone. Another animal study showed that the bone regeneration around dental implants was promoted when the implants were placed simultaneously with a combination of MSCs, PRP and fibrin glue (a composite contains fibrinogen and thrombin) in areas with poor bone quality or low bone volume (Ito et al., 2006). The fibrin glue was used as an osteoconductive scaffold for the stem cells and as a carrier for PRP growth factors. Another study introduced calcium sulphate

and PRP combinations as a novel biomaterial that is able to induce bone formation in bone defects. They assumed that the exothermic reaction generated by the mixture of calcium sulphate with PRP activates the platelets contained within the PRP and that this combination behaves as time-controlled releasing matrix for all platelet GFs (Intini et al., 2007). The effect of PRP in the treatment of periodontal intrabony defects was also evaluated by Yamamiya et al. (2008) who observed a more favourable clinical improvement in the periodontal defects when treated with a combination of HA, PRP and human periosteum sheet (contain osteoprogenitor cells and extracellular matrix) compared to HA and PRP combination. They attributed this result to the additional benefit of the osteogenic cells found in the periosteum sheet. However, Sammartino et al. (2009) did not find a higher grade of bone regeneration in vivo when combined PRP with a resorbable collagen membrane compared to PRP alone (Sammartino et al., 2009).

Studies on the effect of PRP on bone healing were not all positive. In previous animal studies, it was revealed that the use of PRP gel did not have any effect on the bone-implant contact of trabecular bone (Nikolidakis et al., 2006) and cortical bone (Nikolidakis et al., 2008) to calcium phosphate coated implants, while non-activated PRP in a liquid form induced an increase in bone apposition to roughened titanium implants. They related this difference to the mechanical trauma caused by the pressure of the PRP gel on the bone walls of the already tightly fitted implant leading consequently to bone resorption and necrosis of interfacial bone. They supported their hypothesis by indicating remnants of PRP gel around the implant surfaces which couldn’t be seen around calcium phosphate coated implants, suggesting that calcium phosphate coating may enhance macrophage activation (Silva et al., 2003) and play a role in the faster degradation of PRP gel. Kasten et al. (2008) investigated in vitro effect of PRP on MSCs seeded on calcium phosphate scaffold and found that PRP improved cell proliferation on the scaffold but reduced the osteogenic differentiation compared to calcium phosphate scaffold alone, relating the reason to inefficient PRP preparation and storage method. Another recent animal study also suggested that treatment of bone defects with tricalcium phosphate (TCP)/PRP

did not show a significant difference compared to PRP alone (Sebben et al., 2012).

Despite some benefits demonstrated to date, mixed results were reported about the potential establishment of platelet therapy as a reliable therapy in managing the bone, and therefore no definitive conclusions could be drawn. In addition, limited information is available regarding the biological effect of PRP alone or in combination with other biomaterials on osseointegration of dental implants which would require the completion of high quality clinical trials with long-term follow up.

1.9 Stem cells used in bone tissue engineering

For tissue engineering purposes, it has been proposed that a complex of interactions involving osteoprogenitor cells, osteoinductive mediators and osteoconductive matrices would be the ideal restoration of both soft and hard tissues (Giannoudis et al., 2007).

Stem cells are one of the most obvious source of cells that are known for their unique ability to self-renew to be used for bone tissue engineering (Caplan, 1991). Pluripotent Stem cells can give rise to different progenitors of all body tissues, whereas multipotent stem cells are cells that have the capacity to develop into multiple specialised cell types present in a specific tissue or organ. Most adult stem cells are multipotent stem cells. They usually remain inactive but in cases of disease and injury, they become activated to regenerate the damaged tissues (Castro-Malaspina et al., 1981, Caplan, 1991, Ying et al., 2002).

Osteoblasts were also used for tissue engineering purposes. Nevertheless, many limitations for using these cells were highlighted including; the osteoblast cells available for harvesting are usually low in number, and their expansion in vitro is limited, expensive and slow (Salgado et al., 2004).

Stem cells are divided into different categories on the basis of origin:

- **Embryonic stem cells (ESCs)**: are pluripotent stem cells, isolated originally from the inner cell mass of mouse early pre-implantation blastocyst that can give rise to almost all lineages (Evans and Kaufman, 1981). ESCs were used

for drug discovery, immunotherapy and regenerative medicine. However, their use in humans has been restricted due to ethical issues.

➢ **Mesenchymal stem cells (MSCs):** are self-renewable multipotent cells (differentiate into more than one cell type) that exist in adult tissues. They have the ability to differentiate in vitro into adipocytes, chondrocytes and osteoblasts (Dominici et al., 2006).They are easily obtainable and can be expanded in vitro. Their exceptional genomic stability and ethical acceptance made MSCs important tools in cell therapy and regenerative medicine (Horwitz et al., 2005). To identify MSCs in mixed population of cells, the cells should possess specific set of cell surface markers called cluster of differentiation (CD) including CD73, CD90, CD105, CD34, CD45 and human leucocyte antigen-DR (HLA-DR) (Dominici et al., 2006).

MSCs isolated from bone marrow have been reported to be an efficient population of MSCs (Pittenger et al., 1999). Cells which exhibit characteristics of MSCs were also isolated from different tissues such as adipose tissue and umbilical cord (Wagner et al., 2005), amniotic fluid (Scherjon et al., 2003), placenta and fetal membrane (Raynaud et al., 2012), salivary gland (Rotter et al., 2008), synovial fluid (Morito et al., 2008) and dental tissues (Huang et al., 2009).

Recently, a distinct population of human postnatal dental pulp stem cells (hDPSCs) have been described and have offered promising prospects for tissue engineered constructs including dentin and bone (Miura et al., 2003; Shi et al., 2005). Normally, dental pulp tissue comprises of condensed connective tissue that contains a mixture of fibroblasts, lymphocytes, macrophages, dendritic cells, nerve cells, pericytes, endothelial cells and undifferentiated mesenchymal cells, embedded in a fibrous vascular stroma (de Oliveira et al., 2003). This mixed population of cells originates mainly from the neural crest and first branchial arch mesoderm and later on from the dental follicle. Dental pulp cells retain a mitotic potential even in the adult tissue (Tecles, 2005), and hence they were expected to act as adult stem cells (Mrozik et al., 2010). hDPSCs were proved to be a generic source of mesenchymal stem cells. They retain the characteristic stem cell features of high proliferative ability after prolonged

culture (Papaccio et al., 2006, Govindasamy et al., 2010). Moreover, hDPSCs were known to express various mesenchymal stem cell markers such as CD29, CD44, CD146, CD90, CD105, STRO-1, CD106, and OCT4 (embryonic stem cell marker) (Gronthos et al., 2002; Lindroos et al., 2008). hDPSCs were shown to undergo self-renewal and multi-lineage differentiation. They are able to differentiate into odontoblasts, adipocytes, chondrocytes, and osteoblasts in vitro (d'Aquino et al., 2008, Koyama et al., 2009). The ability of hDPSCs to differentiate into functional osteoblasts and produce a mineralised matrix have been reported in many in vitro studies (Pisciotta et al., 2012, Riccio et al., 2010). In addition, the ability of hDPSCs to reconstruct bony structures were confirmed in some in vivo studies (d'Aquino et al., 2009, Giuliani et al., 2013, Sheth et al., 2017). hDPSCs were shown to have comparable behaviour to human bone marrow stem cells (El-Gendy, 2010). hDPSCs are easily collected from third molars and premolars that were extracted for clinical reasons and are easily banked (Volponi et al., 2010). Wisdom teeth are the preferred source for hDPSCs as they are the last teeth to develop, thus their cells retain maximum pluripotency and proliferative potential (Couble et al., 2000). The cells are usually isolated from pulp tissues via two main methods; explant outgrowth cultures and enzyme digestion. The method of explant outgrowth simply involves excavating the pulp tissue from the extracted teeth under aseptic conditions and growing it in culture medium (Huang et al., 2006). The enzyme digestion method is achieved by mincing the pulp tissue and immersing it in a digestion cocktail of collagenase type I and dispase, then the digested cell solution is passed through a cell strainer to obtain a suspension of single cells (Gronthos et al., 2000, Huang et al., 2006). The enzyme digestion method results in a higher yield of cells that have faster proliferation compared to the former method. Further, it can give rise to a distinct variety of cells that were not reliably obtained using the outgrowth method (Tsukamoto et al., 1992, Couble et al., 2000).

Chapter 2: Aim of the study

The purpose of the present study was to investigate *in vitro,* the synergistic effect of FA coatings and PRP on cell adhesion, growth, differentiation and mineralization, with the long term and ultimate goal of enhancing bone formation and hence osseointegration of dental implants.

Objectives:

1. To investigate the growth of FA crystals grown by a hydrothermal method on stainless steel discs.
2. To characterise PRP fraction extracted from total human blood.
3. To evaluate the biocompatibility of the FA coatings and PRP.
4. To investigate the effect of the FA coatings on the release of osteogenic growth factors from PRP.
5. To assess the adsorbed proteins of PRP on FA coatings.
6. To investigate the attachment and growth of osteoblast cell line on FA coatings and PRP combinations.
7. To evaluate the synergistic effect of FA coating and PRP on the osteogenic differentiation and mineralisation of human dental pulp stromal cells (hDPSCs).

Chapter 3: Materials and Methods

3.1 Fluorapatite coatings (FA)

3.1.1 Synthesis of the FA coatings on metal substrates

3.1.1.1 Principle

The methodology of FA coating synthesis on metal substrates used herein has been previously described by Chen et al. (2006b) and modified by Czajka-Jakubowska et al. (2009a). In this method, EDTA was used in the precipitation solution to stabilize the release of Ca^{2+} ions under a specific pH and under mild hydrothermal conditions (121°C, 2 atm for 10 hours). The morphology of synthetic FA crystals changes during this time from amorphous deposits to hollow balls and finally ends with well-defined, long nanorods crystals.

3.1.1.2 Materials

The details of the materials and chemicals that were used in FA coating procedure are recorded in table 2, unless otherwise stated.

Table 2: List of materials and chemicals used for FA coating synthesis

Material/ Chemical	Company	Cat no.
Stainless steel (SS grade 316) bar	Metals 4U LTD	NA
Sulphuric acid 98% Analar -Analytical Grade	VWR Chemicals	102765G
Hydrogen peroxide 35% wt. in H_2O	Sigma	349887
Etheylenedeiaminetetraacetic acid calcium disodium salt (EDTA.Ca.Na_2)	Sigma-Life sciences	ED2SC
Sodium phosphate monobasic monohydrate 98.0-102.0% ($NaH_2PO_4.H_2O$)	Sigma-Aldrich	S3522
Sodium fluoride (NaF)	Sigma-Aldrich	30105

3.1.1.3 Method

A bar of SS was purchased and cut into discs of 12 mm diameter and 1mm thickness. Their flat surfaces were ground smoothed using an aluminium oxide 60,000 grit grinding wheel (Mester Tooling, UK). The discs were treated with

piranha solution comprising of equal volumes of sulphuric acid 98% and hydrogen peroxide 35% for 24 hours. The discs were then rinsed generously under tap water, sonicated in distilled water for 1 hour with changing of the water every 15 min and left to dry. Etched SS discs were then hydrothermally coated with FA as shown in figure (9). In brief, 9.36g of EDTA.Ca.Na_2 (0.25 M) and 2.07g of $NaH_2PO_4.H_2O$ (0.15 M) were mixed with 80mL distilled water. The suspension was stirred continuously and the pH was adjusted to 6.0 using NaOH. The suspension was then made up to 90 mL with distilled water. Meanwhile, 0.21g NaF (0.05 M) was dissolved in 10 mL distilled water (pH 7.0) and added to the mixture to produce 100mL of coating (mineralising) solution. FA crystal growth on the SS discs was achieved by immersing the discs, positioned vertically or tilted at 45° as illustrated in figure 1, in the freshly prepared FA coating solution. The coated discs were then autoclaved (Rodwell, UK) at 121°C, at a pressure of approximately 2 atmospheres for 10 hours.

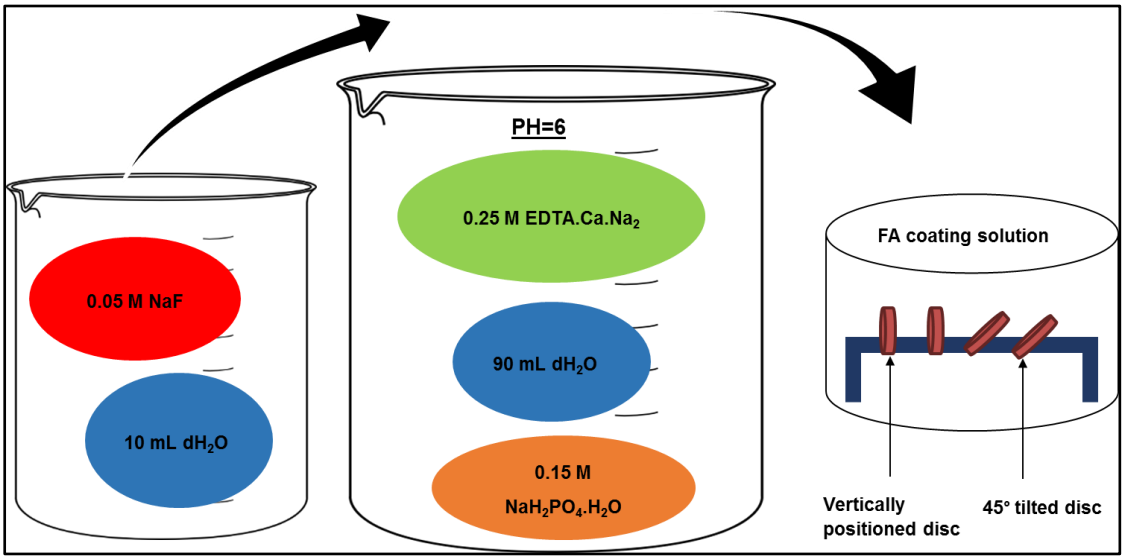

Figure 9: Diagram showing the mild hydrothermal method used to synthesise FA coatings on SS discs (dH_2O, distilled water).

3.1.2 Optimisation of post synthesis treatment of the FA coatings

After the autoclaving cycle of 10 hours was completed, the coated discs were washed with distilled water for about 5-7 times until the washing water became

clear. The discs were then left to dry overnight in a dryer. The effect of the subsequent washing and drying process on the FA coatings was observed. The following groups were set up with using three samples in each group:

Group I: Discs tilted at 45°, dried in vacuum desiccator for 24 hours without washing (no washing but dried i.e. unwashed group).

Group II: Discs tilted at 45°, dried in vacuum desiccator for 24 hours then rinsed several times with distilled water (dried- washed group) and dried again.

Group III: Discs tilted at 45°, rinsed several times with distilled water (pH7.0), then dried in vacuum desiccator for 24 hours (washed- dried group).

Group IV: Discs positioned vertically (unwashed but dried group).

Group V: Discs positioned vertically (dried- washed group).

Group VI: Discs positioned vertically (washed- dried group).

3.1.3 Characterisation of FA-coated substrates

3.1.3.1 Scanning Electron Microscopy (SEM)

3.1.3.1.1 Principle

Scanning electron microscopy (SEM) is used to investigate the microstructure and topography of a surface. Under the SEM, the specimen surface is scanned with a finely focused electron beam emitted from an electron gun fitted with a tungsten filament cathode toward the conductive sample. The electrons are detected by detectors to obtain images for the surface with different signal characteristics. Two types of electrons can be detected; secondary electrons (SE) and back scattered electrons (BSE). SE are low energy electrons. They are generated very closely to the surface within a few nanometers allowing for high resolution images to be produced. The electron beam hits the sample leading to interaction between the sample surface and the electron. As a result of this interaction, the electrons are displaced from within the sample resulting in energy converted into image for the surface of the sample. Backscattered electrons mode (BSE) consists of high energy electrons that are back scattered out of the specimen interaction. It is used to detect the contrast between areas with different atomic numbers and chemical compositions. Since heavy elements (high atomic number) backscatter electrons more strongly than light

elements (low atomic number), they appear brighter in the image (Khursheed, 2007).

3.1.3.1.2 Method

Back scattered SEM (Hitachi S-3400N) was used to characterise the synthesised FA coatings by looking at the microstructure, topography, morphology and orientation of the crystals of upper and under surfaces of FA coated discs. Prepared FA coated specimens were mounted on aluminum stubs at a 5 mm distance and scanned under low vacuum with an accelerating voltage of 20kV and a beam current of 50 µA using different magnifications. SEM images showed disorganised FA coatings on upper disc surfaces and organised FA coatings on the under surfaces.

3.1.3.2 Energy dispersive x-ray spectroscopy (EDS)

3.1.3.2.1 Principle

The elemental composition of a specimen surface can be determined using energy dispersive x-ray spectroscopy (EDS). EDS is based on generating secondary X-rays in a specimen through electron bombardment. Subsequently, the elements of the specimen and their relative percentages are identified using the wavelengths and intensities of the produced X-rays (Gruia, 2017). EDS is regarded as a semi-quantitative analysis which can provide a comparative information about the relative proportions of the elements within a sampling depth of 1-2 microns (Goldstein et al., 2017).

3.1.3.2.2 Method

The EDS apparatus used to analyse the chemical composition of the FA coatings (Bruker 4030 Quantax SDD-EDS system, Germany) was attached to the SEM (operated at 20kV with a beam current of 50 µA). Analysis was carried out for each sample prepared for SEM imaging with 10 mm working distance (n = 3).

3.1.4 Biocompatibility assessment of FA coatings

According to the results of FA coating characterisation conducted previously, it was decided to use group III FA-coated discs (i.e. discs tilted at 45°/ washed then dried) for the subsequent cell culture experiments. The biocompatibility of FA coatings was assessed under the microscope on the basis of cell adherence and colonisation of osteoblast-like cells (human osteosarcoma G292 cell line) on the FA coated surfaces. All cell culture experiments were carried out aseptically in a class II biological safety laminar flow hood. G292 cells were purchased from the European Collection of Cell Cultures (ECCAC) and received as frozen cells. The cells were revived, expanded and seeded on FA coated discs for the biocompatibility test.

3.1.4.1 Materials

All reagents and materials used in cell culturing and biocompatibility testing were listed in table 3, unless otherwise stated.

Table 3: List and details of the materials that were used for cell culturing

Materials/ chemicals	Company	Catalogue no.
Alpha minimum essential medium without L-Glutamine (α-MEM)	Lonza, BioWhittaker	BE12-169F
Fetal bovine serum (FBS)	Sigma - Aldrich	F9665
Penicillin (10,000 units/mL) – Streptomycin (10 mg/mL) (P/S)	Sigma- Aldrich, Life science	P4333
L-glutamine (200 mM) (L-G)	Sigma - Aldrich	G7513
Phosphate buffered saline 1x, pH 7.4 without Ca or Mg (PBS)	Lonza, BioWhittaker	BE17-516F
Trypsin-EDTA (Ethylenediaminetetra-acetic acid) 0.25 % (w/v) solution (T/E)	Sigma- Aldrich, Life science	T4049
Trypan blue 0.4%	Sigma- Aldrich	T8154
Agarose low gelling temperature	Sigma- Aldrich	A9045
Neutral buffered formalin (10%) (NBF)	Cellpath	BAF-0010-01A
Ethanol	Sigma-Aldrich	E7023

3.1.4.2 Recovery of Cryopreserved Cells

3.1.4.2.1 Principle

The cells are commonly cryopreserved (frozen) at −80°C or in liquid nitrogen for long-term storage. Cell freezing allows secure preservation of the cells without contamination, senescence and genetic drift. The cells should be cryopreserved in culture medium supplemented with 10% to 20% (v/v) serum and 10% (v/v) preservative like dimethylsulfoxide (DMSO). The DMSO allows gradual freezing of the cells with a slow cooling rate of 1°C/ minute. This minimises the risk of ice crystal formation and consequent cell damage. To recover the cells with a high survival rate, they need to be thawed as quickly as possible to prevent formation of ice crystals that can cause cell lysis. The cell freezing medium should be diluted for about 10-20 fold in order to reduce the potential cytotoxicity of DMSO on the cells. During cell recovery, DMSO should be completely removed from the cell culture by centrifuging and re-suspending the cells in fresh medium or alternatively changing the medium once the cells are attached (Freshney, 2006).

3.1.4.2.2 Method

Frozen cells were thawed by agitating the cell vial in a water bath (37°C) for about 1 minute and pipetting the content into falcon tube containing 10 mL of α-MEM supplemented with 10% FBS, 1% P/S and 1% L- G. Then the resulting cell suspension was centrifuged at 200 g for 5 minutes. The supernatant was discarded and the cell pellet was re-suspended in 15 mL cell medium and plated in 75cm^2 cell culture flask at 37°C in 5% (v/v) carbon dioxide (CO_2) in air and 98% relative humidity. The cells were cultured for 2-3 days until they became 80-90% confluent and were then passaged (expanded).

3.1.4.3 Cell expansion

3.1.4.3.1 Principle

Cells in monolayer culture are usually subcultured when becomes 80-90% confluent so as to expand the cell population. The first step in subculturing monolayers is to detach cells from the surface of the culture vessel by trypsinisation. Trypsin is a serine protease that digests the proteins that

facilitate cell adhesion to the culture vessel and to other cells. Trypsin is inhibited by serum and calcium (Ca^{2+}) and magnesium (Mg^{2+}) ions. Therefore, EDTA (disodium ethylenediamine tetraacetic acid) is added to trypsin solution as a chelating agent to bind to Ca^{2+} and Mg^{2+} ions found in the culture. The resultant cell suspension is then subdivided and reseeded into new cultures. Secondary cultures are monitored for growth and nourished with fresh medium every 3-5 days. Cells are once again passaged when they become 80-90% confluent (Phelan and May, 2007).

3.1.4.3.2 Method

Cell culture medium was aspirated from the cell culture flasks ($75cm^2$) and the cell surface monolayer was washed twice with PBS (without Ca or Mg). The PBS was then thoroughly aspirated and the cells were detached using Trypsin / EDTA. Five mL of 0.25 % (w/v) Trypsin / EDTA solution was added to the cell culture flask and incubated with the cells for no longer than 2 minutes at 37°C. Following incubation, the culture was checked for cell detachment with an inverted microscope to be sure that the cells are rounded and detached from the surface. On successful detachment, 5 mL of complete cell medium (α-MEM and 10% FBS) was added to each flask to deactivate and stop further action of trypsin that might be harmful to the cells. Flask contents were then transferred into a universal tube and centrifuged at 200 g for five minutes. Following centrifugation, the supernatant was discarded and the cell pellet was resuspended and homogenised in complete culture medium. A viable cell count was performed before being seeded at a specific cell density according to the design of the experiment.

3.1.4.4 Viable cell counting

3.1.4.4.1 Principle

Seeding the cells in culture with a specific cell density is important in performing accurate quantitation experiments for standard culture conditions. Cell number is determined by a hemocytometer. It is a thick glass slide with a counting chamber of a specific volume. The chamber has 9 major squares with a volume of 0.1 mm^3 per square. Each square is 1 mm x 1 mm and the depth is 0.1 mm,

so the final volume of each square is 0.1 mm^3 (0.0001 mL). The cells are stained with Trypan blue dye to distinguish between live and dead cells. Nonviable cells which take up the dye through the damaged cell membrane are not counted. While live cells with intact cell membrane are impermeable to the dye (Phelan and May, 2007).

3.1.4.4.2 Method

To count the cells, a mixture of a 20 µL cell suspension and 20 µL trypan blue was loaded into the hemocytometer chamber. Under a light microscope (x10 objective lens), the cell number was manually counted in 4 corner squares. The total viable cells were counted and the average cell number was calculated. The total number of the cells per mL was calculated by multiplying the average cell count by the dilution factor of trypan blue (2), then by 10,000:
Cell number (cells/mL) = average of cell number of 4 squares x 2 x 10,000

3.1.4.5 Agarose wells preparation

3.1.4.5.1 Principle

Agarose wells (12 mm in diameter) were used to accommodate and restrict cell attachment and growth on FA coated discs

3.1.4.5.2 Method

Agarose solution was prepared by mixing 3% (w/v) agarose of low gelling and melting points (congealing temperature 26-30°C and melting point ≤ 65°C) in PBS. The agarose solution was then autoclaved at 121°C. Subsequently, the agarose solution was left to cool down for 5 minutes before being poured into a 12-well plate containing 12 mm diameter moulds suspended in the wells. Once the agarose had gelled, the moulds were gently removed leaving agarose wells of 12 mm diameter (Figure 10).

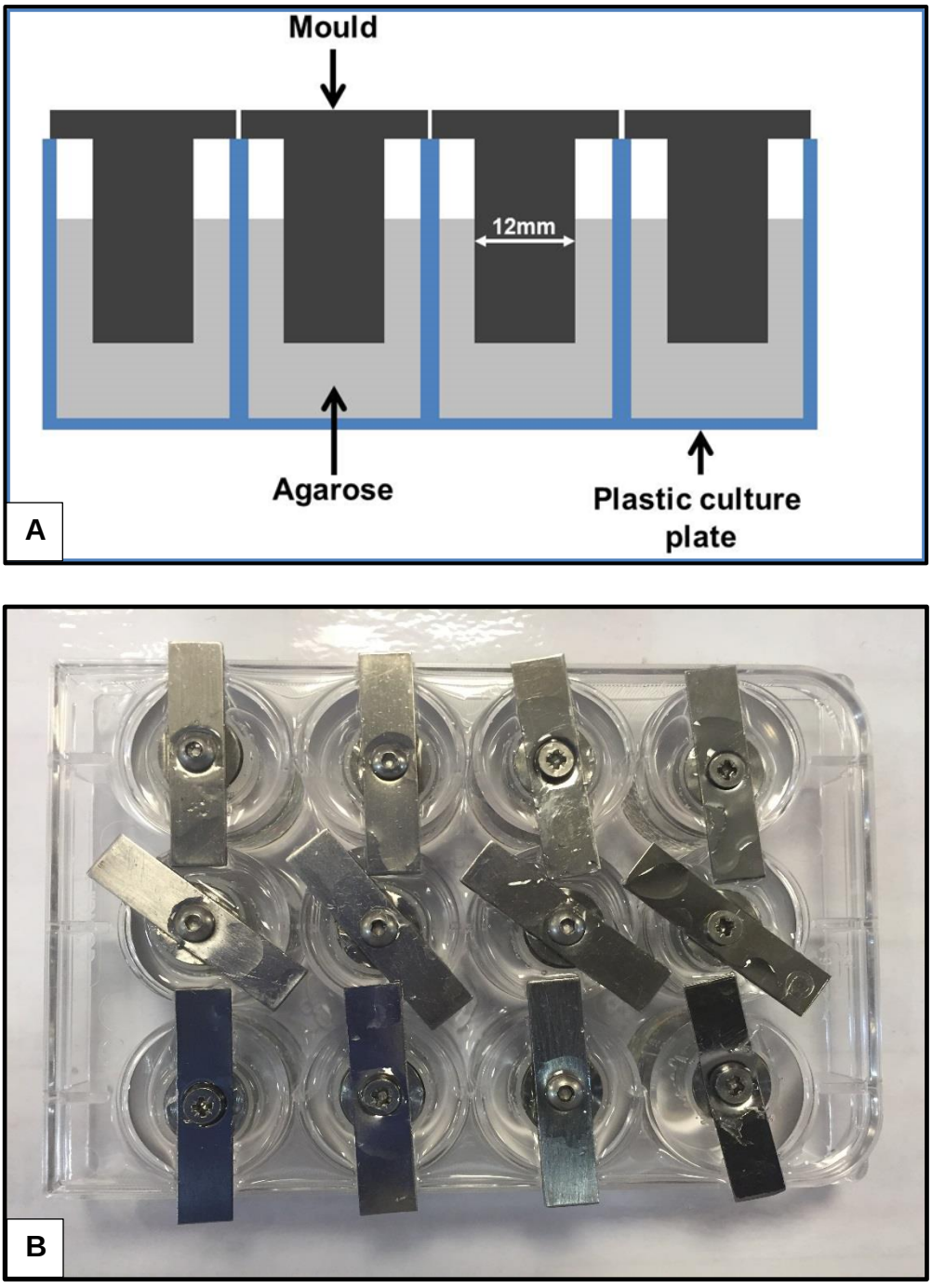

Figure 10: Schematic diagram (A) and photograph (B) for agarose wells preparation. SS moulds of 12mm diameter are suspended inside the wells of 12-well plate with agarose poured around them.

3.1.4.6 Cell seeding procedure on FA coatings

FA coated discs and uncoated etched SS discs were autoclaved at 121°C for at least 30 minutes by using saturated steam under at least 15 psi above

atmospheric pressure. Sterile FA-coated discs (three with ordered and three with disordered FA crystals) and three control uncoated discs were placed in the agarose wells and equilibrated with 10% FBS culture medium for 2 hours. Subsequently, G292 cells were seeded on each disc of the three groups at a density of $1x10^4$ cells/cm^2 in 500 µL media. After 3 - 4 hours, 500 µL 10% FBS media was equally added into each well and cultured for 2 days (Figure 11).

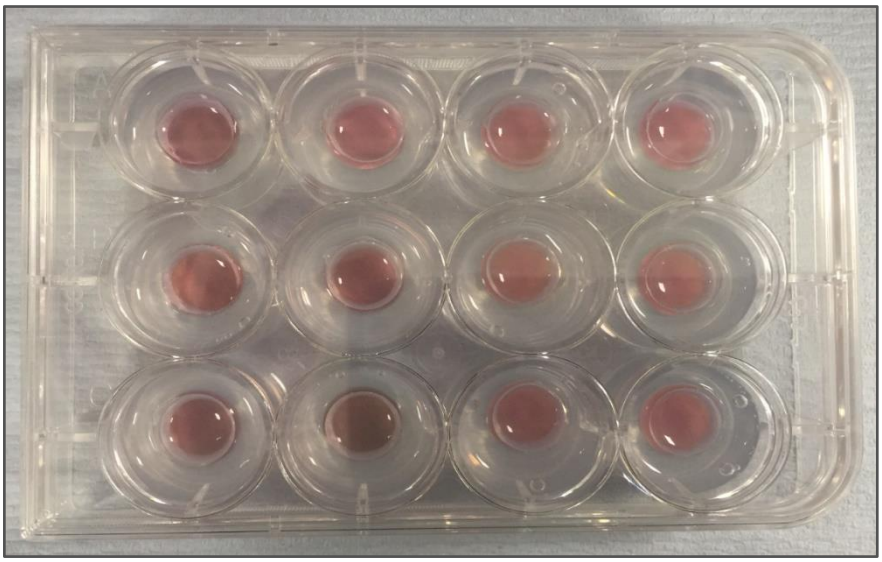

Figure 11: G292 cells seeded on uncoated and FA coated discs placed inside agarose wells.

3.1.4.7 SEM observation for the cells

3.1.4.7.1 Principle

SEM (BSE) could be used to detect contrast between areas with different chemical compositions. The high beam energy of BSE penetrates deeply into the cells, producing an image with Z contrast and allowing the identification of major cellular compartments such as cellular cytoskeleton. If the scanned sample is not conductive as is the case of cells and tissues, a discharge of the electrons will happened when they hit the sample surface resulting in unclear image with low resolution. Therefore, it is preferable to sputter- coat the sample with a thin gold or copper layer to conduct the incident electrons (Khursheed, 2007). FA coated discs were opaque and were not suitable for normal

transmitted light microscopy. Thus, cell morphology and the distribution of G292 grown on FA coated discs were observed under the SEM using BSE.

3.1.4.7.2 Method

After 2 days of cell culturing, the discs were removed from the agarose wells and gently washed with PBS. The cells on the discs were fixed with 10% neutral buffered formalin (NBF) overnight at 4ºC. To minimise tissue shrinkage, a graded series of ethanol was used for tissue dehydration instead of absolute ethanol. Thus, after fixation, the specimens were thoroughly washed with PBS and serially dehydrated in ethanol for 30 minutes in each concentration (30%, 50%, 70%, 90% and 100%). After that, the discs were left to dry in a vacuum desiccator overnight before being sputter-coated with about 5 nm gold film to prevent specimen charging and image artefacts using an argon sputter coating unit (Agar Scientific, Stanstead, UK). The samples were then mounted on aluminium stubs at a 5 mm distance and scanned under low vacuum with an accelerating voltage of 20Kv using BSE.

3.1.4.8 Confocal laser scanning microscopy (CLSM)

3.1.4.8.1 Principle

Alexa Fluor 488 Phalloidin and TO-PRO-3 nucleic acid stain are used to label the cells' cytoskeleton and nucleus respectively. Phalloidin conjugated to bright, photo stable, green fluorescent Alexa Fluor 488 dye is a bicyclic peptide commonly used to selectively label F-actin. TO-PRO-3 is a dye composed of carbocyanine monomers that have very strong binding affinity for dsDNA giving a strong and selective staining of the nucleus in cultured cells. In this study, the cells that were grown on FA coated discs were stained with Alexa Fluor 488 Phalloidin (Life Technologies, A12379) and TO-PRO-3 (Life Technologies, T3605) according to manufacturer's instructions. The cells were then analysed under a laser scanning confocal microscopy (LSCM). LSCM uses Argon laser as a light source at visible wave lengths giving five different excitation lines in the blue/blue-green range. The light beam becomes a parallel beam of expanded diameter when it passes through a pinhole aperture, encounters a dichromatic mirror and reflected onto objective lens. The light beam is reflected

90° when it hits the dichromatic mirror and is focused onto the desired focal plane on the sample when it passes through the objective lens (Paddock, 2000). When the light is absorbed by the fluorophore molecules of Alexa (i.e becomes excited) at a particular wave length (488nm), the fluorophore emits light at longer wave lengths (emission at 580nm). The emitted light is collected by the objectives and sensitive photomultiplier tube (PMTs) detectors. The microscope use TIFF images which are acquired with software for subsequent measurement and analysis. TO-PRO-3 dye exhibits fluorescence with excitation at 590 nm and emission at 700 nm.

3.1.4.8.2 Method

Briefly, the FA-coated samples were rinsed with PBS and fixed in 10% NBF for 15min. After rinsing with PBS for 3 x 5 mins, 0.1% Triton X-100 in PBS was used to permeabilise the lightly fixed cell membrane for 15 min at room temperature. The samples were then rinsed with PBS (3 x 5 mins) before being stained with Alexa Fluor with a dilution of 1/10 in PBS for 2 hours in the dark and at room temperature. The samples were subsequently washed with PBS (3 x 5 mins) and incubated in TO-PRO-3 nucleic acid stain (1/100 in PBS) for 20 mins in the dark and at room temperature. Later, the staining solution was aspirated and replaced with fresh PBS. The cells were then analysed under a Spectral Confocal Leica TCS SPE microscope (Leica, GmbH) in conjunction with x10 and x40 dipping lenses to obtain three-dimensional images for the cells.

3.1.5 Cytotoxicity of FA coatings

3.1.5.1 Direct contact cytotoxicity test

3.1.5.1.1 Principle

The direct contact cytotoxicity test allows both qualitative and quantitative assessment of cytotoxicity after direct exposure to the test sample. Qualitatively, the cells are checked under the microscope for any changes in morphology and growth rate compared to the control. In the quantitative assessment, the cells could be counted manually and checked for release of lactate dehydrogenase enzyme (LDH) in the culture media. Measurement of

LDH release is an important and frequently applied test to measure cell death and inhibition of cell growth. LDH is a stable cytosolic enzyme that is released upon cell lysis, cellular membrane permeabilisation and severe irreversible cell damage. According to the International Standard Organisation's ISO 10993-5:2009E (DIN) standard, a decrease in cell viability by more than 30 % is regarded as a cytotoxic effect. LDH release is measured by recording the conversion of a tetrazolium salt (INT) into a red formazan product. The amount of formazan red colour is proportional to the number of dead cells. In this colorimetric reaction, LDH strips an electron from lactate and this electron is transferred to NAD to yield NADH. The NADH subsequently reduces the INT and causes a color change from yellow to red, as follows:

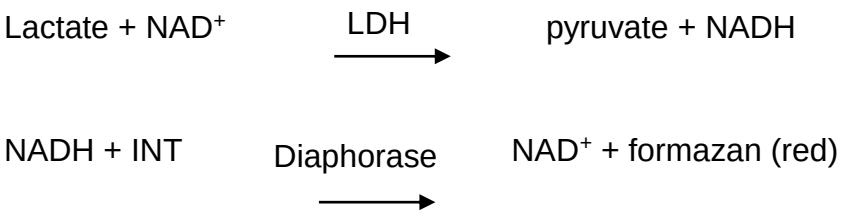

3.1.5.1.2 Method

➢**Test sample and control preparation**

Sterile FA coated and uncoated discs were placed in 6-well plate in triplicate. The discs were attached to the underlying culture plate surface by a biocompatible collagen gel. One drop of collagen gel (15 µL collagen gel and 7.5 µL of sterile 0.1% NaOH to neutralise the gel) was loaded into the centre of each well. The discs were placed immediately over the drops and left to set for 15 min. Subsequently, G292 cells were seeded in the wells at a cell density of ($10^4/cm^2$) and cultured in 10% FBS supplemented A-MEM (3mL/well) for 2 days. Cells cultured on collagen gel drop with no discs in 10% FBS MEM were used as a negative control (nontoxic group). The positive control (100% toxic) was performed by placing a drop of cyanoacrylate contact adhesive into the centre of a one well. Blanks (culture medium background control) were prepared for LDH assay using the same conditions described above but without

cells. The absorbance value determined from the blank is used to normalize absorbance values obtained from the other samples.

➢**Qualitative evaluation of direct contact FA cytotoxicity**

After 2 days of incubation, the growing cells alongside the discs were examined microscopically to record any changes in the cell morphology and cell detachment and membrane integrity. Images were taken by digital camera attached to the inverted microscope (Olympus, CKX41).

➢**Quantitative evaluation of direct FA cytotoxicity**

The media was collected in eppendorf tubes and stored at -80°C to be investigated later for the release of LDH. The cells were detached by trypsin (0.25%) and counted using Trypan blue and hemocytometer as described in section 3.1.4.4.2. To measure LDH release, a 30-minute coupled enzymatic assay (CytoTox 96 colorimetric assay, Promega, Cat. no: G1780) was carried out according to the manufacturer's instructions. Briefly, the collected media was thawed on ice and centrifuged at high speed (10000 g) for 10 min. Then, 50 µL of the supernatant of each experimental sample, control and blanks were transferred into 96-well plate (flat bottom enzymatic assay plate) in triplicate. To each well, 50µL of reconstituted substrate mix was added and incubated at room temperature in the dark. After 30 minutes, the reaction was stopped by adding 50µL of stop solution into each well. The absorbance (optical density) was measured using VARIOSKAN FLASH spectrophotometer (Thermo scientific, UK) at 490nm. To calculate the results, the average of absorbance values of the culture medium background was subtracted from all absorbance values of experimental. The corrected values obtained were used in the following formula to compute percent cytotoxicity for each experimental group:
% cytotoxicity= Absorbance (experimental)/ Absorbance (positive control) x 100%

3.1.5.2 Indirect contact cytotoxicity test

3.1.5.2.1 Principle

Indirect cytotoxicity tests are used to determine cell lysis and growth inhibition caused by a sample extract according to International Standard Organisation (ISO/EN 10993). The result of this indirect test depends on the concentration of the test material, the extraction volume, pH, chemical solubility, diffusion rate of molecules out of the test sample, temperature and time. Culture medium with serum is the preferred extraction vehicle because of its ability to support the cellular growth and to extract the polar substances (ionic compounds) and non-polar substances (organic compounds). However, the use of culture medium without serum should be considered in order to specifically extract the polar substances as serum proteins are known to bind to some extractable ions and therefore mask and prevent the release of these ions (ISO 10993-5, 2009).

3.1.5.2.2 Method

➢**Preparation of liquid extracts of FA crystals**

A schematic diagram showing the steps of the indirect cytotoxicity test is shown in figure 12. FA crystals were prepared using the same mild hydrothermal method mentioned previously (section 3.1.1.3) but without adding SS discs to the mineralising solution. The synthesized crystals were rinsed several times with distilled water and dried in a dryer for 24 hours. The crystals were weighted and autoclaved at 121°C for at least 30 minutes by using saturated steam under at least 15 psi above atmospheric pressure. Subsequently, FA crystals were incubated in serum free α-MEM at a ratio of 200mg/mL at 37°C in 5% (v/v) carbon dioxide (CO_2) in air and 98% relative humidity for 24 hours (Wei et al., 2011; Forghani et al., 2013). The mixture was then centrifuged at high speed (5000 g) and the supernatant was filtered (0.2 µm) to get rid of any FA crystal or debris. In the same time, a 50 mL of serum free unconditioned medium was exposed to the same incubation conditions of the FA extract and used to prepare control and blank groups.

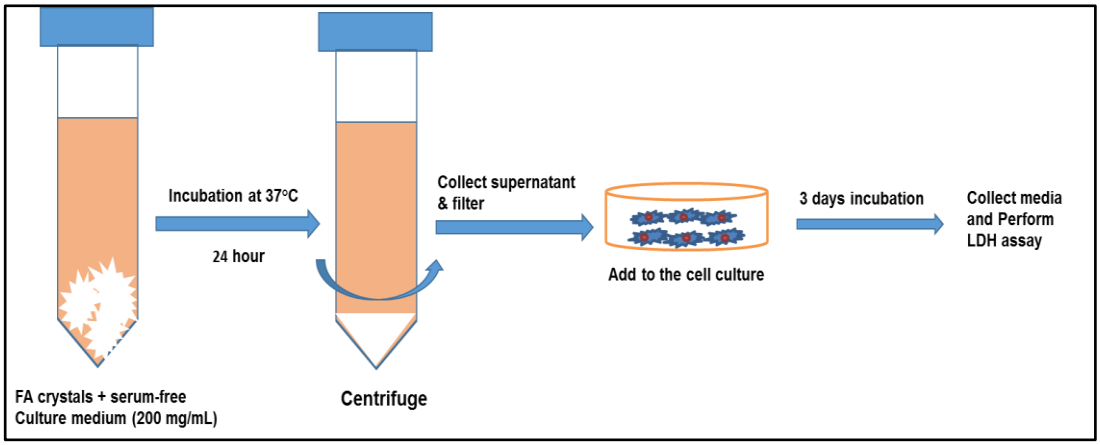

Figure 12: Schematic diagram for indirect cytotoxicity test of FA crystals. Sterile FA crystals were incubated in serum free α-MEM at a ratio of 200mg/mL and incubated at 37°C for 1 day. The mixture was then centrifuged and the supernatant was filtered and added to the cell culture. After 3 days, the cytotoxicity of FA- conditioned medium was analysed quantitatively using LDH assay.

➢**Test sample and control preparation**

G292 cells were plated in a 24-well plate at a density of $10^4/cm^2$, and cultured in 10% FBS culture medium. After 24 hours, the culture medium was removed and replaced by 1 mL FA extract medium supplemented with 10% FBS (test group) or 1 mL unconditioned medium with 10% FBS (negative control). All the groups were prepared in triplicate. Corresponding blanks (10% FBS unconditioned medium) were prepared by omitting the cells.

➢**Quantitative evaluation of FA indirect contact cytotoxicity (FA extract)**

After 1, 4 and 7 days of incubation, the media were collected and assayed for lactate dehydrogenase enzyme (LDH) released from dead cells using the same spectroscopic assay according to the manufacturer's instructions previously described (section 3.1.5.1.2). Triton X-100 was used to provide the positive control by adding Triton (1% in PBS) for about 30 min to cells grown in unconditioned complete medium (assumed to kill 100% of the cells present).

3.2 Platelet-rich plasma (PRP)

3.2.1 Preparation of PRP

3.2.1.1 Principle

The principle of PRP preparation is to generate plasma that contains a higher concentration of platelets than baseline blood. PRP used herein was prepared by a two-step centrifugation process following a protocol described by Xie et al (2012).

3.2.1.2 Method

Venous blood samples were donated by healthy volunteers who were not taking any medication. Consents were obtained from the donors and ethical approval was issued by University of Leeds research ethics committee on 20th May 2015.

The blood was withdrawn from antecubital region of the participants into sterile 4.5 mL vacutainer tubes containing sodium citrate anti-coagulant (0.105M) (Greiner Bio-one, Cat. no: 12306949). The blood was first centrifuged without brake (centrifuge 5810R; Eppendorf, Darmstadt, Germany) at low speed with centrifugal force (RCF) of 200 g for 10 minutes at room temperature resulting in separation of the whole blood into plasma and erythrocytes sediment. To obtain concentrated platelets, the plasma was collected into sterile falcon tubes under the hood (class II laminar flow hood) and centrifuged for 10 minutes at high speed (1000 g). Subsequently, 80% of the supernatant comprising platelet-poor plasma (PPP) was decanted and the platelet pellet was then re-suspended in the remainder of the PPP to form the PRP samples (Figure 13).

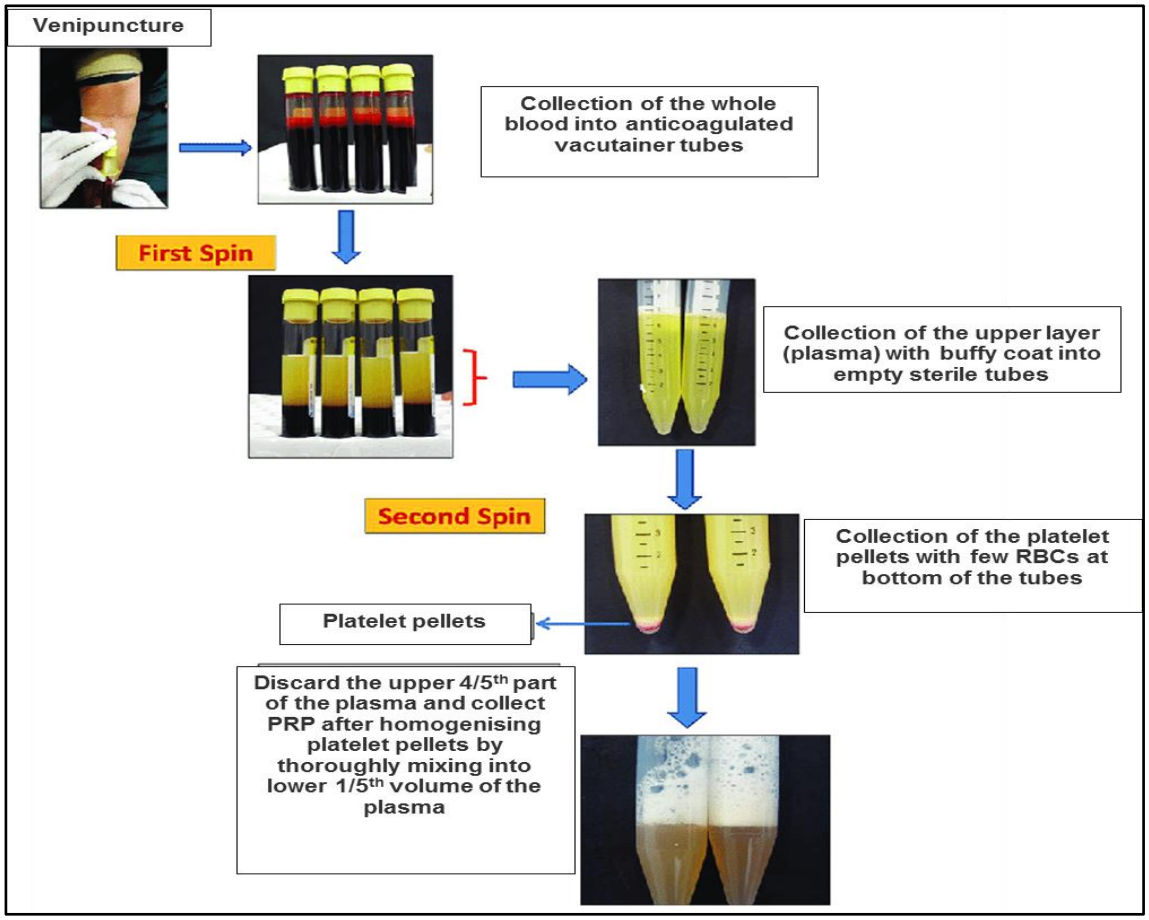

Figure 13: Preparation steps of platelet-rich plasma (PRP) fraction by two-step centrifugation cycle process. In the first cycle, the blood is separated into plasma and erythrocytes sediment and in the second one, the platelets are pelleted down and separated from the plasma. Platelets re-suspended in low amount of plasma is collected as PRP (Adapted from https://www.researchgate.net/publication/273952492_ Principles _and_Methods_of_ Preparation_ of_ Platelet-Rich_Plasma_ A_Review_ and_ Author's_Perspective).

To obtain liquid serum from the PRP samples (PRP releasate), PRP samples were activated in a sterile centrifuge tube under the cell culture hood (class II safety cabinet) using a final concentration of either 23 mM $CaCl_2$ for 1/2 hour or 20 U/mL thrombin from bovine plasma reconstituted in 0.1% (w/v) BSA solution (Sigma- Aldrich, T4648) for 1/2 hour. After PRP activation and formation of fibrin gel, PRP releasate was separated from the cellular debris and fibrin gel by centrifugation at high speed (15000 g) for 10 min and the supernatants were then collected as PRP releasate samples.

Both of PRP and PRP releasate samples were either prepared fresh before the experiment or stored at -80°C for use within a maximum of 2 weeks. PRP samples were usually collected in cryogenic vials and frozen at -80°C using Mr Frosty freezing containers (Nalgene, Sigma, Cat. no: C1562) overnight before being transferred to a normal freezing box. This was to achieve the optimal platelets preservation by providing a rate of cooling very close to -1°C/minute using Mr Frosty.

3.2.2 Determining of platelets concentration in the PRP samples

3.2.2.1 Principle

Platelet concentration in PRP samples is analysed manually using a haemocytometer and phase-contrast microscopy. In order to facilitate the recognition of the small sized platelets, the PRP samples are diluted 1:100 in PBS (standard dilution). The isotonic balance of the diluent (PBS) results in erythrocytes lysis while the platelets and leukocytes remain intact (Brecher and Cronkite, 1950). Recently, automated counting techniques have become more commonly used to count platelets and they are regarded as a more rapid and precise technique compared with manual counting (Harrison and Briggs, 2013). Manual and automated counting techniques were used herein to count PRP platelets.

3.2.2.2 Method

In the manual counting procedure, 20 µl of diluted PRP (1:100 in PBS) was placed onto the counting chamber of the haemocytometer. The platelets were allowed to settle and then were counted under the microscope. The counting chamber has 9 major squares with a volume of 0.1 mm^3 per square. Each square has 20 small squares except the middle one which has 25 square. The platelets in the middle major square were counted under the light microscope using a high magnification (x20 objective lens). The platelets were counted in 9 small squares out of the 25. Then, the average platelets number was calculated. The total number of the platelets was calculated by multiplying the average platelets number by number of the small squares (25) then by the dilution factor of PBS (100), and by 10,000:

Platelets number (platelets/mL) = average of cell number of 4 squares x 25 x 100 x 10,000

To further confirm the counting procedure, platelet counts from same PRP samples were obtained using automated platelets counting machine (XP-300 automated CBC analyser, Sysmex). Upon switching on the device, three automatic rinse cycles were performed followed by a background check. Each sample of about 100 µL was mixed by pipette then was held up to the aspiration probe of the machine. The probe aspirated 50 µL to count the platelets in about 50 second. This machine was used to measure and record concentrations of white blood cells (WBCs) and red blood cells (RBCs) in addition to platelets counts for PRP and corresponding PPP samples.

3.2.3 PRP cytotoxicity

3.2.3.1 Principle

It is assumed that PRP preparations containing maximal concentrations of growth factors are ideal for promoting cell proliferation. Therefore, the aim of this study was to assess the effect of different configurations and concentrations of PRP on cell viability using the LDH assay in two experimental set-ups:

3.2.3.2 Method

➢**First cytotoxicity experiment**

This test compared activated and non-activated PRP when added to the cell culture after 30 minutes of activation. G292 cells were seeded in 24-well plates at a density of $1x10^4/cm^2$ in 10%FBS media for 24 hour adhesion period then the media was replaced with α-MEM supplemented with:

1. Non-activated PRP added to the culture medium to a final concentration of 5%. This media was aseptically prepared and left for 30 minutes at room temperature before being added to the adherent cells.
2. Activated PRP with 23 mM $CaCl_2$ added to the culture medium to a final concentration of 5%. This media was also aseptically prepared for 30 minutes at room temperature before it was added to the adherent cells.

3. FBS added to the culture medium to a final concentration of 5% forming the control group.

➢**Second cytotoxicity experiment**

The principle of the second test was to compare between the effect of two PRP gel forms and PRP releasate used at two concentrations on the viability of seeded G292 cells. PRP was added to the cell culture in 96-well plate using the following schemes:

1. PRP gel under the cells (cells seeded on top of a layer of gelled PRP): A volume of 5 µL or 10 µL PRP was pipetted in the wells of the culture plate forming 5% or 10% of the total culture medium (100 µL) respectively. PRP was activated with 23 mM $CaCl_2$ (final concentration). After 1/2 hour, G292 cell suspension was added ($1x10^4/cm^2$) to each well on top of the already established PRP gel.
2. PRP gel encapsulated the cells: The cells were seeded at a density of $1x10^4/cm^2$ in culture medium in the wells followed by adding PRP and its activator (23 mM $CaCl_2$ as a final concentration) to the culture medium to a final concentration of 5% or 10% (vol/vol) of the total culture medium (100 µL). The PRP was homogenised immediately and thoroughly with the cell suspension to embed the cells within the gel.
3. PRP releasate (soluble components extracted from activated PRP): The cells were seeded in the wells of the culture plate at a density of $1x10^4/cm^2$ in culture medium. PRP releasate was added to the wells to a final concentration of 5% or 10% (vol/vol) of the total culture medium (100 µL).

➢**Quantitative evaluation of PRP cytotoxicity**

In both experimental set-ups described above, all the groups were prepared in triplicate included corresponding blanks without cells. Cells seeded in 10% FBS culture medium was used as the controls. After 3 days of incubation at 37°C and 5% (v/v) carbon dioxide (CO_2) in air and 98% relative humidity, cell viability was investigated via LDH assay. Triton X-100 was used to provide the positive control by adding Triton (1% in PBS) for about 30 min to cells grown in 10%

FBS medium (assumed to kill 100% of the cells present).The samples' media were collected and assayed for LDH release using the same spectroscopic assay previously described (section 3.1.5.1.2).

3.2.4 Effect of PRP on cell proliferation (DNA quantification assay)

3.2.4.1 Principle

PicoGreen reagent is an ultrasensitive fluorescent nucleic acid stain, which can detect double stranded DNA in solution at concentration as low as 25 pg/mL in the presence of single stranded DNA, RNA and free nucleotides. Since nucleic acid content can be directly related to cell number, the PicoGreen assay was used to assess the effect of PRP gel and releasate on cell proliferation.

3.2.4.2 Optimisation of cell digestion used for PicoGreen DNA assay

3.2.4.2.1 Principle

It is standard practice to lyse the cells in 0.1% triton to quantify the DNA content of monolayer culture but not of 3-D culture as in the case of PRP gel which might need different lysing solutions such as papain. Papain is a cysteine protease of the peptidase C1 family. Cysteine peptidases of papain catalyse the hydrolysis of peptide, amide, ester, thiol ester and thiono bonds, thereby digesting most cellular and extracellular proteins and liberating DNA from cells and tissues (Dubey et al., 2007). Papain has proven more efficient and less destructive than other proteases on certain tissues. In order to assess the efficacy of Triton and papain in releasing DNA from cells in the presence of PRP gel, a comparative study was undertaken to determine the most effective digestion method.

3.2.4.2.2 Method

➢**Test and control sample preparation**

G292 cells were cultured ($10^4/cm^2$) for 3 days in 2 x 24-well plates in culture medium supplemented with 10% PRP gel or releasate (100 µL) in triplicate. Each plate contained 3 experimental groups; PRP gel under the cells, PRP gel encapsulated the cells and PRP releasate (see the second cytotoxicity test in section 3.2.3.2). Cells seeded in 10% FBS culture medium was prepared as the

control group. Corresponding sample blanks were also prepared. One plate will be treated with triton and the other papain. After 3 days in culture at 37°C and 5% (v/v) carbon dioxide (CO_2) in air and 98% relative humidity, the 24 well plates were centrifuged at 300 g for 5 min to pellet down the gels and their embedded cells. The culture media was gently discarded and the cells and PRP gels were carefully washed twice with PBS before being digested.

➢**Triton digestion**

The cells of the first culture plate were lysed in 0.1 % triton followed by three freeze/thaw cycles. The cells and PRP gels were scraped off the wells and mixed using a pipette to assist cell break-up. The complete lysis of the cells was confirmed under the light microscope.

➢**Papain digestion**

PRP gels and cells of the second culture plate were digested with papain (Sigma, Cat. no: P4762) using 0.25 mg/mL papain in 5 mM L-cysteine, 100 mM sodium phosphate dodecahydrate and 5mM Ethylenedinitrilo-tetraacetic acid disodium salt dihydrate (pH= 6.5) at 65°C overnight (Kim et al., 1988; Hoemann et al., 2002).

➢**Picogreen DNA assay**

PicoGreen DNA quantification assay (Invitrogen, Life Technologies, Cat. no: P7589) was used to measure the DNA content of the cell digests. The lysates of the two digestion methods were centrifuged at 10000 g for 10 minutes and the supernatants were diluted (1:20) in Tris-EDTA buffer (TE ,10 mM Tris-HCl, 1 mM EDTA, pH 7.4, Sigma-Aldrich, Cat. no: 93283). Lambda DNA standard (100µg/mL in TE) was supplied with the kit and the sample fluorescence was measured against 7 standards made up at 2000, 1000, 500, 250, 125, 62.5, 31.3 ng/mL and standard blanks (TE buffer alone). Aliquots of 100 µL of each standard, diluted test samples and diluted sample blanks were added to 96 well plates in triplicates. An aliquot of 100 µL PicoGreen (1:200 in TE buffer) was then added to each well and the plates were incubated in the dark at room temperature for 5 minutes. Fluorescence was measured using a Thermo

scientific (ELISA) microplate reader (VARIOSKAN FLASH spectrophoto-meter) with an excitation wavelength of 480 nm and an emission (detection) wavelength of 520 nm. The unknown values of DNA concentrations (ng/mL) were then calculated using the standard curve generated. The total amount of DNA (ng) per well was generated from the calculated DNA concentrations multiplied by cell lysis harvest volume from each well. Graphs of the mean ± SD was plotted using GrapPad Prism 7. The results showed a higher amount of DNA content detected in papain lysis compared to triton lysis indicating the suitability of using papain for digestion (results are shown in results section).

3.2.4.3 Effect of PRP on cell proliferation

Cell culture of G292 cells for test samples, control and corresponding sample blanks were prepared. The cells were seeded at a density of $10^4/cm^2$ in 24-well plates in 10% PRP supplemented culture medium using the same four culture conditions described above (PRP gel under the cells, PRP gel encapsulated the cells, PRP releasate and FBS as a control). All the groups were prepared in triplicate and the experiment was repeated twice using PRP samples derived from 2 different blood donors. The DNA content was assessed after 5 hours (day 0), 1 day, 4 and 7 days. At each time point, the 24 well plates were centrifuged at 300 g for 5 min, the culture medium was discarded. The cells and the gels were washed twice with PBS and digested with papain as described above. The DNA content was measured using PicoGreen DNA assay as described in the previous section.

3.3 FA coatings and PRP combinations

3.3.1 Evaluation of growth factor release from PRP/FA combinations

3.3.1.1 Principle

This experiment was aimed at studying the effect of FA coatings on the release of growth factors (GFs) from PRP using sandwich enzyme linked immune-sorbent assays (ELISA). ELISAs were designed to detect and quantify substances such as peptides, proteins, antibodies and hormones in aqueous samples. In the simplest form of the sandwich technique, the antigen must be immobilized to the microplate surface and complexed with an antibody that is

linked to an enzyme capable of catalysing a colour generating reaction (Figure 14). The amount of colour, determined by spectroscopy, is proportional to the concentration of antigen bound to the well, and can be quantified if standard concentrations of the antigen in question are assayed at the same time. A most commonly used enzyme label is horseradish peroxidase (HRP). The ability to wash away non-specifically bound proteins makes the ELISA a powerful tool for measuring specific antigens. ELISA has several formats but the most powerful, specific and sensitive one is the sandwich assay. In the sandwich assay, the targeted antigen is specifically selected out from a sample of mixed antigens via a capture antibody and sandwiched between two primary antibodies (capture antibody and detection antibody). This eliminates the need to purify the antigen from a mixture of other antigens and simplifies the assay (Gan and Patel, 2013).

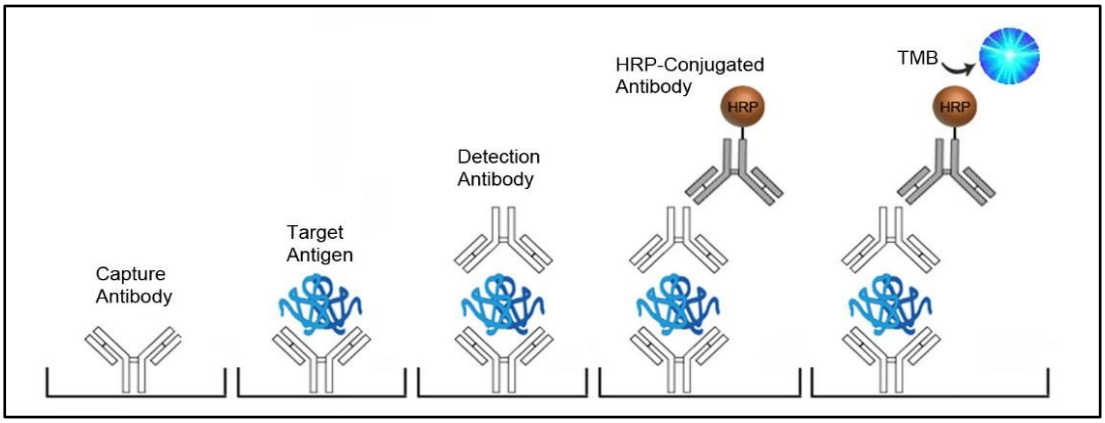

Figure 14: Diagram of Sandwich ELISA. The antigen of interest is immobilized by a capture antibody previously attached to the microplate surface and sandwiched between the capture antibody and a primary detection antibody. The detection of the antigen can then be performed using an enzyme-conjugated secondary antibody.

3.3.1.2 Materials

A list of the materials that were used in sandwich ELISA technique is shown below in table 4, unless otherwise stated.

Table 4: List of the materials and chemicals that were used in ELISA

Materials/ Chemicals	Company	Catalogue no.
Human IGF-1 DuoSet	R&D Systems	DY291
Human PDGF-AB DuoSet	R&D Systems	DY222
ELISA Plate-coating Buffer (PBS, 137 mM NaCl, 2.7 mM KCl, 8.1 mM Na_2HPO_4, 1.5 mM KH_2PO_4, pH 7.2-7.4)	R&D Systems	DY006
Reagent Diluent Concentrate 2 (1% BSA in PBS)	R&D Systems	DY995
Reagent Diluent Concentrate 3 (5% Tween 20 in PBS, pH 7.2-7.4)	R&D Systems	DY004
Quantikine Wash Buffer (0.05% Tween® 20 in PBS, pH 7.2-7.4)	R&D Systems	WA126
Substrate Reagent (1:1 mixture of Color Reagent A (H_2O_2) and Color Reagent B (Tetramethylbenzidine)	R&D Systems	DY999
Stop Solution 2N Sulfuric Acid (H_2SO_4)	R&D Systems	DY994
96 well microplate, polystyrene, sterile	Greiner Bio-One	655161
ELISA Plate Sealers	R&D Systems	DY992

3.3.1.3 Method

➢**Test sample and control preparation**

In this experiment, a loading volume of PRP activating solution comprising thrombin from bovine plasma (20 IU/mL as a final concentration) or calcium chloride $CaCl_2$ (23 mM as a final concentration) and 40 µL of PRP were sequentially pipetted onto uncoated etched SS discs, disorganised FA coated discs (DS FA) and organised FA coated discs (OR FA) placed in 24-well plates at 37°C. Similarly, 40 µl of non-activated PRP was loaded onto uncoated (control) and FA coated discs. The loading volume was determined based on the surface area of the discs. SS and FA coated discs treated with thrombin, $CaCl_2$ or left untreated served as blanks. Figure 15 shows an illustration of sample preparation. Three samples were adopted for each experimental group and the experiment was repeated twice using PRP derived from 2 blood donors.

One hour after the initiation of PRP clotting, 1 ml of PBS was added into each well and incubated at 37°C. After 2 hours, 1 day, 3 and 7 days, the PBS was collected and stored at -80°C for analysis. At each time point, the PBS was completely removed and replaced with fresh PBS. The sandwich ELISA technique was used to determine the temporal (not cumulative) release of IGF1 and PDGF-AB growth factors from PRP gels into the PBS following the manufacturer's instructions of the relevant Duo Set kit.

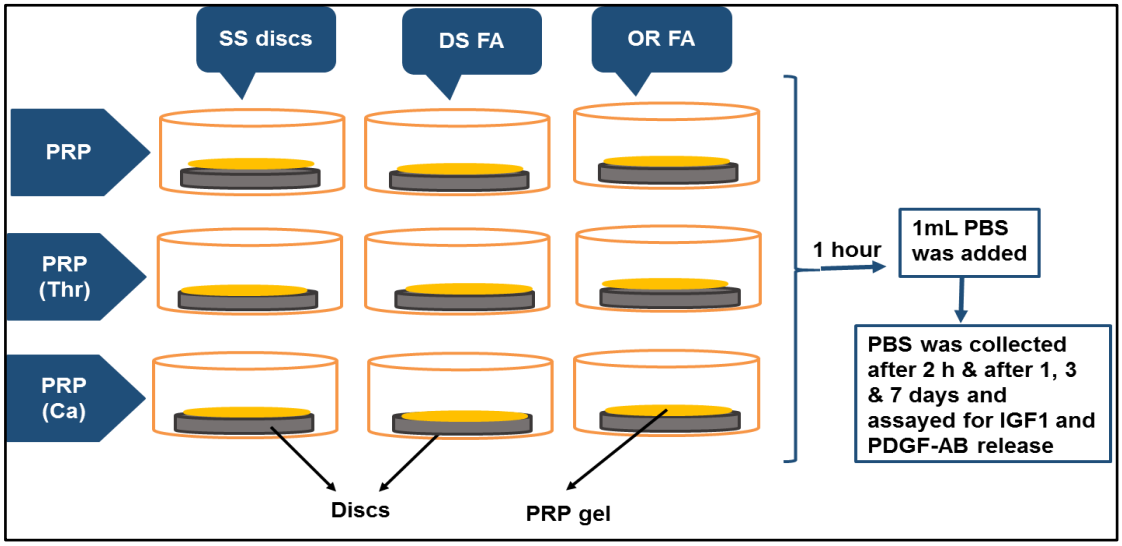

Figure 15: Diagram for samples prepared for ELISA used to measure the release of GFs from PRP gel inducted by FA coatings into PBS (SS, stainless steel; DS, disorganised FA; OR, organised FA; PRP, platelets rich plasma; Thr, thrombin; Ca, calcium).

➢**Assay procedure (Measurement of IGF-1 concentrations)**

IGF-1 concentrations was assessed according to IGF-1 DuoSet protocol. First of all, diluted capture antibody (mouse anti-human IGF-1) at 4 µg/mL in PBS was used to coat 96 well microplate (100µL/well) and the plate was incubated overnight at room temperature. On the following day, the plate was washed with 400µL of diluted washing buffer (1:25 v/v) in deionized water (0.05% Tween 20 in PBS) for a total of three washes. Plates were blocked using 300µL of diluted reagent diluent concentrate 3 (1:5 v/v) in PBS (5% Tween 20 in PBS) and incubated for 1 hour at room temperature. Then, the aspiration/wash step was repeated three times. The samples and the blanks were thawed on ice before

being centrifuged at 10000 g and 4°C for 10 min. Recombinant Human IGF-1 standard (STD) was reconstituted with 0.5 mL of distilled water (110ng/mL) and seven standards using 2-fold serial dilutions in reagent diluent were prepared in a range between 2000 pg/mL and 31.3 pg/mL. Subsequently, 100µL of the sample supernatants, blanks supernatants and standards were loaded in duplicates (n=3 for each blood donor for 2 donors) into the 96 well plate and incubated for 2 hours at room temperature. The plates were washed again as above and 100µL of detection antibody (Biotinylated Goat Anti-Human IGF-1 Detection Antibody) reconstituted with 1.0 mL of reagent diluent were added at a working concentration of 150 ng/mL in reagent diluent for 2 hours at room temperature. After 3 aspirations/ washings, 100µL of working dilution of Streptavidin conjugated to horseradish-peroxidase (HRP) (1:40, v/v) in reagent diluent was added and the plates were incubated for 20 minutes in the dark at room temperature followed by similar washing steps. A 100µL of substrate solution (colour reagent A: H_2O_2 and colour reagent B: Tetramethyl-benzidine, 1:1 v/v) were added per well and the plate was incubated for 20 minutes at room temperature in the dark. Finally, 50µL of stop solution (2 N H_2SO_4) was added to the substrate solution and the absorbance was immediately measured at 450 and 570 nm to eliminate background signal using a VARIOSKAN FLASH plate reader (Thermo scientific, UK). The unknown values of IGF-1 concentrations (pg/mL) were then calculated using the standard curve generated.

➢**Assay procedure (Measurement of PDGF-AB concentrations)**

For PDGF-AB growth factor, the assay was performed following the Duo Set kit instructions. It was the same protocol and assay procedure of IGF1 with the exception that, for PDGF-AB, reagent diluent concentrate 2 was used for blocking of the plate. It was diluted 1:10 (v/v) in deionized water (1% BSA in PBS). The standard used was recombinant human PDGF-AB reconstituted with 0.5 mL of reagent diluent. The prepared standards (STDs) ranged from 1000 pg/mL to 15.6 pg/mL. The sample supernatants were diluted 1:2 in corresponding reagent diluent and the dilution factor (2) was put into consideration during the calculations of the concentrations. The human PDGF-

AB detection antibody was reconstituted with 1.0 mL of reagent diluent and diluted to a working concentration of 50 ng/mL in reagent diluent. Streptavidin-HRP was dilute to a working concentration of 1:200 (v/v) using reagent diluent.

3.3.2 Evaluation growth factor release from PRP gel and PRP releasate

3.3.2.1 Principle

The release of the GFs present in PBS supernatants of PRP gel and releasate loaded onto FA and uncoated discs was compared. Based on the previous findings of this study, it was decided to use organised (OR) FA coating only in this experiment because the organised coatings showed better potential to induce cell proliferation and to stimulate sustained release of GFs from PRP compared to the disorganised coating.

3.3.2.2 Method

➢**Test and control preparation**

Uncoated SS and organised FA coated discs were placed in 24-well plates and loaded with 10 µL thrombin (20 IU/mL as a final concentration) and 40 µL of PRP. Likewise, 40 µl of PRP releasate were loaded onto SS (control) and OR FA coated discs. All the experimental samples were in triplicates. Relative blanks were prepared by omitting PRP. The discs were incubated at 37°C for 30 minutes allowing the formation of PRP gels. Then, 1 ml of PBS was added into each well and incubated at 37°C for 3 days.

➢**Assay procedure**

After 3 days, the PBS was collected and stored at -80°C to quantify, at a later day, the concentrations of IGF1 and PDGF-AB growth factors cumulatively released from the PRP gels or releasate into the PBS were measured using sandwich ELISA according to the manufacturer's instructions of the Duo Set kits and as described in the previous section (3.3.1.3). No dilution was used for the samples of IGF1 assay but a dilution of 1:2 in the corresponding reagent diluent was used for all samples of PDGF-AB assay. The samples, standards and blanks were loaded in triplicate in the 96-well plate. The experiment was repeated twice for 2 blood donors.

3.3.3 Calcium ion release from FA coatings in presence of PRP

3.3.3.1 Principle

In order to observe the dissolution behaviour of FA coatings in presence of PRP gel, the concentration of calcium ions (Ca^{2+}) dissolved from the coatings into the PBS was measured using inductively coupled plasma-optical emission spectroscopy (ICP-OES). The principle of ICP is based on generating plasma by argon gas. The component elements (atoms) of the sample are excited and emission rays (spectrum or photon rays) are emitted and measured. The spectrum obtained is characteristic of the elements present and the intensity of the spectral lines is proportional to the amount of each element present.

3.3.3.2 Method

Disorganised (DS) and organised (OR) FA coated discs, either bare or loaded with 10 µL thrombin (20 IU/mL) and 40 µL PRP, were placed in 12-well plate in triplicate. PRP gellification was allowed for 30 min, then PBS was added into the wells (2mL/well) and incubated at 37°C. Corresponding PBS and PRP blanks were prepared without FA coatings. After 2 hours, 1 day, 3 days, 7 days, 10 days and 14 days, the PBS was collected and stored at 4°C for analysis. At the end of each incubation period, the PBS was completely removed and replaced with fresh buffer. Prior to the test, all collected PBS and blank samples were diluted 1:10 in distilled water and the concentrations of Ca^{2+} ions dissolved from FA and FA/PRP coatings into the PBS were kindly measured by the School of Geography/ University of Leeds using inductively coupled plasma-optical emission spectroscopy (Thermo Scientific iCAP 7000 Series ICP-OES).

3.3.4 Indirect contact cytotoxicity of FA/PRP combinations (LDH assay)

3.3.4.1 Principle

In this study, cytotoxicity of FA in presence of PRP was investigated using the LDH assay. LDH release as explained previously (section 3.1.5.1.1) is measured by recording the conversion of a tetrazolium salt (INT) into a red formazan product and the amount of formazan red colour is proportional to the number of the dead cells.

3.3.4.2 Method

➢**Preparation of liquid extracts of FA crystals**

FA crystals extract was prepared as described previously in section 3.1.5.2.2. At the same time, serum free unconditioned medium exposed to the same incubation conditions of the FA extract was used to prepare the controls and blanks.

➢**Test and control sample preparation**

The filtered FA extract was added to the cell pellet of human osteosarcoma cell line (G292) to be seeded in 24-well plate at a cell density of 1 x 10^4 cells/cm^2. The cell culture was supplemented with either 10% FBS or 10% activated PRP using $CaCl_2$ (23 mM as a final concentration). The cells were also cultured in unconditioned α-MEM medium with 10% activated PRP or 10%FBS (negative control). Triton X-100 (1% in PBS) was used to provide a positive control (100% cell death). Corresponding blanks were prepared by omitting cells. All PRP groups were prepared in triplicate for 2 blood donors. All the groups were incubated at 37°C in 5% (v/v) CO_2 in air and 98% relative humidity for 3 days. Then, the media were collected and assayed for LDH released from dead cells using spectrophotometer as described previously (section 3.1.5.1.2).

3.3.5 PRP protein adsorption on the FA coatings

3.3.5.1 Principle

The effect of the FA surface characteristics on adsorption of PRP proteins is important for cell adhesion and attachment. PRP proteins adsorbed to the FA coatings were extracted and subjected to Sodium Dodecyl Sulfate (SDS)-polyacrylamide gel electrophoresis (SDS-PAGE) analysis. SDS-PAGE is commonly used for the separation of proteins based on their molecular weight and on their differential rates of migration through a polyacrylamide gel under the influence of an applied electrical field. SDS is an anionic detergent that has a negative charge. It denatures the proteins and gives them a uniform net negative charge making them move in a single direction through the porous gel toward the positively charged electrode. The denatured protein molecules are loaded onto the polyacrylamide gel made of acrylamide, bisacrylamide,

TEMED, ammonium persulfate and Tris-HCl buffer. The gel has two phases, a stacking gel and a separating (running) gel. Under an applied electric field, the stacking gel concentrates the denatured linear protein molecules while the separating gel separates the proteins according to their molecular weight (Saraswathy and Ramalingam, 2011).

3.3.5.2 Method

➢Test sample preparation

Uncoated (etched) and FA coated discs (disorganised and organised coatings) were placed in 24- well plate in triplicates and loaded with either PRP gel (10µL thrombin + 40µL PRP), 40 µL PRP releasate or 40 µL FBS and were incubated at 37°C and 5% (v/v) CO_2 and 98% relative humidity overnight. The experiment was done using PRP from 2 blood donors.

➢Protein extraction

To solubilise and extract PRP proteins adsorbed to the surfaces of SS, disorganised FA and organised FA, the discs were first washed gently 3 times on a shaker with Tris buffer (50 mM, pH 7.4) (5 minutes each wash). After the last wash, the discs were placed on a clean filter paper to absorb the extra buffer from the discs. Phosphate buffer (0.1 M, pH 7.4) was prepared containing equal amounts of Na_2HPO_4 $2H_2O$ (0.5M) and $NaHPO_4$ (0.5M) to desorb the proteins from the discs. Phosphate buffer desorbs proteins from apatite by competitive binding to the apatite surface. The surface of each disc was loaded with 40µl of the phosphate buffer at room temperature and in a humid environment. After 30 min, the phosphate buffer was collected slowly and gently from each disc and kept at -20°C until analysis.

➢SDS-PAGE analysis

The desorbed protein samples were denatured (3:1) with 4x Laemmli sample buffer (BIO-RAD, Cat. no: 161-0747) at 100°C for 2 minutes. Equal amounts of the protein extract samples were separated by SDS-polyacrylamide gel electrophoresis using mini-protean TGX stain-free™ precast gels (8-16%) (BIO-RAD, Cat. no: 456-8103). The samples were loaded into the gel wells using a

Hamilton syringe (20µL/well). In addition, 3µL of a suitable molecular weight markers (precision plus protein molecular weight blue marker, 10 -250 kD) was loaded in a lane next to the samples. The molecular mass (kDa) markers were used to assess the relative molecular weight of the target proteins. The marker was diluted 1/20 in 1x Laemmli sample buffer. Gels were run with 1 X TRIS/glycine/SDS running buffer at 200V for 1/2 hour. Afterward, the gels were transferred to polystyrene boats filled with distilled water.

➢**Silver staining of SDS gels**

The protein bands were visualized with silver stain using the Pierce® silver stain kit (ThermoFisher Scientific, Cat. no: 24612) according to the manufacturer's instructions. Briefly, each gel was washed 2 × 5 minutes in ultrapure water and fixed in 30% ethanol: 10% acetic acid solution (2 × 15 minutes). The gel was then washed in 10% ethanol (2 × 5 minutes) and 2 × 5 minutes in ultrapure water. The gel was sensitized for 1 minute with a prepared sensitizer working solution (50µL sensitizer with 25mL water). The gel was washed 2 × 1 minute with water before being stained for 30 minutes in a prepared silver stain working solution (0.5mL Enhancer with 25mL Stain). Later, the gel was washed 2 × 20 seconds with ultrapure water and developed for 2-3 minutes in a prepared developer working solution (0.5mL Enhancer with 25mL developer). When the protein bands became visible, the developing was stopped with 5% acetic acid for 10 minutes. The intensity of the protein bands was determined and recorded using a ChemiDoc imager (BIO-RAD).

3.3.6 Effect of FA/PRP combinations on cell proliferation

3.3.6.1 Principle

This study aimed at investigating the growth pattern of G292 cells on FA/PRP coated disc surfaces using PicoGreen DNA quantification assay. PicoGreen reagent as mentioned before (section 3.2.4.1) is an ultrasensitive fluorescent nucleic acid stain used to detect double stranded DNA in solution at a concentration as low as 25 pg/mL in the presence of single stranded DNA, RNA and free nucleotides.

3.3.6.2 Method

➢Test and control preparation

Agarose wells were prepared in 12-well plates as described previously (section 3.1.4.5). Sterile FA coated discs with disorganised and organised coating surfaces and uncoated etched SS discs (control group) were placed in the agarose wells. The discs were loaded with either PRP gel (12.5 µL thrombin and 50 µL PRP), 50 µL PRP releasate or 50 µL FBS forming 10% of cell culture medium. The samples were incubated for two hours at 37°C in 5% (v/v) CO_2 in air and 98% relative humidity. Subsequently, G292 cells were seeded on the substrates at a density of 1 x10^4 cells/cm^2 in 450 µL of a serum-free medium. Blanks were also cultured under the same conditions of the samples with no cells. The schematic diagram shown in figure 16 summarises the experimental set-up of the test samples.

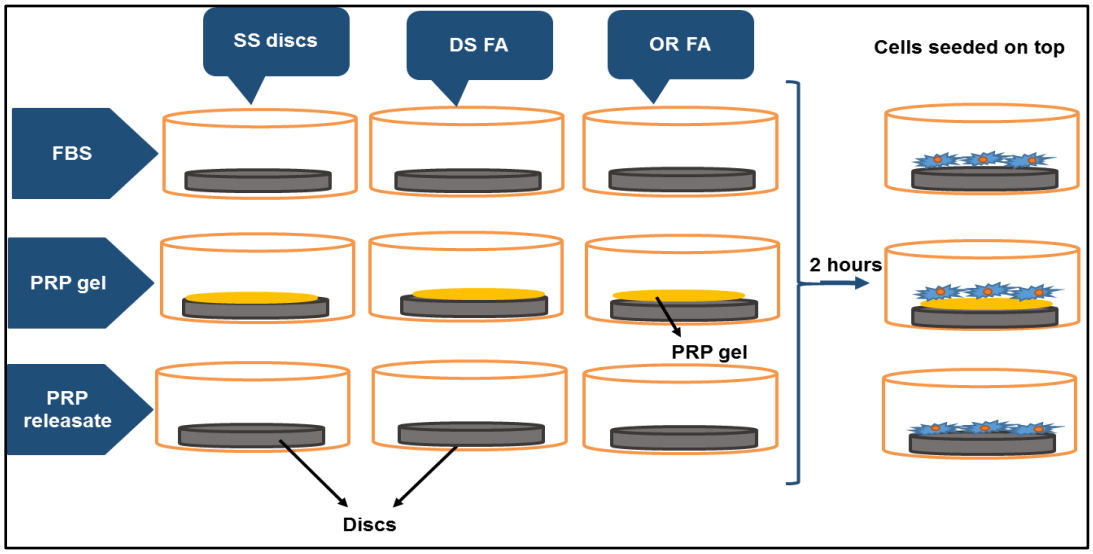

Figure 16: Schematic diagram of sample preparation for DNA content assay of cells cultured on FA/PRP combination. SS, stainless steel; DS, disorganised FA; OR, organised FA; FBS, fetal bovine serum; PRP, platelet-rich plasma.

➢Papain digestion

After 5 hours and 1, 3 and 7 days in culture, the discs were carefully transferred using a clean tweezer from the agarose wells into a dish filled with PBS. The discs were gently washed with PBS one time then transferred onto clean filter

paper to absorb and remove any residual PBS. Subsequently, the discs were placed in 24-well plates containing 500 µL papain buffer (0.25 mg/mL) to digest the attached cells as described in section 3.2.4.2. The cell lysates were homogenised by micropipette and transferred to eppendorf tubes and left on heat block at 65°C overnight.

➢**PicoGreen DNA assay**

Next day, the lysates and blanks were centrifuged at 10000 g for 10 min. The supernatants were diluted in Tris-EDTA buffer (1:20) and loaded into ELISA flat bottom 96-well plates (100 µL/well) in triplicates, DNA standards were also prepared at concentrations between 2000 ng/mL and 31.3 ng/mL and loaded (100 µL/well). Then, diluted PicoGreen (1:200 in TE buffer) reagent was added to each well (100 µL/well) and the plates were incubated in the dark at room temperature for 5 min. Sample fluorescence was measured using microplate reader with an excitation wavelength of 480 nm and an emission (detection) wavelength of 520 nm. DNA concentrations (ng/mL) were then calculated using the DNA standard curve generated and the total amount of DNA (ng) per well was also calculated from the cell lysis volume harvested from each well multiplied by corresponding DNA concentrations.

3.3.7 Microscopic evaluation of cell attachment and growth on FA/PRP

3.3.7.1 Principle

Morphology and distribution of G292 cells on FA/PRP coated discs were observed under SEM and confocal microscopy. Principles of SEM and confocal microscopy were earlier explained in sections 3.1.4.7 and 3.1.4.8 respectively.

3.3.7.2 Method

G292 cells were seeded and cultured on FA/PRP coatings for 2 days under the same conditions described in section 3.3.6. The discs were then removed from the wells and gently washed with PBS. Subsequently, the cells attached to the coated discs were fixed with 10% neutral buffered formalin (NBF) for 24 hours at 4ºC. Then the specimens were thoroughly washed with PBS, serially dehydrated in ethanol (30-100%) and dried in a vacuum desiccator overnight.

The discs were sputter-coated with gold film and examined under the SEM. At the same time, the cells grown on FA coated discs were labelled using Alexa Fluor 488 Phalloidin cytoskeleton stain and TO-PRO-3 nucleic acid stain according to manufacturer's instructions described previously in section 3.1.4.8.2 and were analysed under confocal laser scanning microscopy.

3.3.8 Osteogenic differentiation of hDPSCs

3.3.8.1 Quantitative real time polymerase chain reaction (qRT-PCR)

3.3.8.1.1 Principle

FA/PRP combinations were investigated for their ability to support the differentiation of hDPSCs towards an osteoblastic phenotype using qRT-PCR technique. qRT-PCR assay is the most powerful and sensitive technique used for the expression analysis of single or multiple genes. This technique involves a series of procedures including; detection of RNA expression levels, quantification of mRNA transcription levels, producing multiple copies of the DNA isolates through amplification and finally measuring the amplification of DNA using fluorescent dyes. In RNA extraction, QIAshredder might be used as a homogenizer for simple and rapid homogenization of the cell lysates. QIAshredder consists of a unique biopolymer-shredding system in a microcentrifuge spin-column format placed in a collection tube. It reduces loss of sample material and filters out insoluble debris like agarose, FA crystals and PRP gel. In a real time PCR assay, a positive reaction is detected by accumulation of a fluorescent signal. The cycle threshold (Ct) determined by the PCR is the number of cycles required for the fluorescent signal to cross the threshold (exceeds background level) (Radonić et al., 2004). In the current study, expression levels of 4 genes (ALP, RUNX2, OCN and OPN) in addition to the house keeping gene or control gene (GAPDH) by hDPSCs were determined by qRT-PCR using TaqMan gene expression assays.

3.3.8.1.2 Materials

Table 5 shows the materials that were used for all steps of PCR assay, unless otherwise stated.

Table 5: List of the materials and chemicals that were used in PCR assays

Materials/ Chemicals	Company	Catalogue no.
RNase, DNase free-Culture plate 24-well plates	Clearline	131020C
RNeasy mini kit	Qiagen	74104
QIAshredder	Qiagen	79654
β-mercaptoethanol	PanReac AppliChem	A4338,0100
Ethy alcohol, pure, for molecular biology	Sigma- Aldrich	E7023
Ultrapure DNAse/RNase-free distilled water	Thermo Fisher Scientific	10977035
RNase- Free DNase set	Qiagen	79254
High Capacity RNA to cDNA kit	Applied Biosystems	4387406
TaqMan gene expression master mix	Applied Biosystems	4369016
TaqMan gene expression assay (Glyceraldehyde-3-phosphate dehydrogenase, House-keeping gene) (GAPDH)	Applied Biosystems	4331182 (Hs99999905-m1)
TaqMan gene expression assay (Alkaline phosphatase, Bone marker) (ALPL)	Applied Biosystems	4331182 (Hs01029144-m1)
TaqMan gene expression assay (Runt-related transcription factor-2, Transcription factor, bone marker) (RUNX-2)	Applied Biosystems	4331182 (Hs00231692-m1)
TaqMan gene expression assay (Bone gamma-carboxyglutamic acid-containing protein, Select calcium binding protein, bone marker) (BGLAP)/ Osteocalcin (OCN)	Applied Biosystems	4331182 (Hs00609452-g1)
TaqMan gene expression assay (secreted phosphoprotein 1, SPP1) (OPN)	Applied Biosystems (ABI)	4331182 (Assay ID: Hs00959010-m1)
96-Well Semi-Skirted PCR Plate for Roche Lightcycler, White	Starlab	I1402-9909

3.3.8.1.3 Validation of using GAPDH as a house keeping gene

It is standard practice to use an endogenous control housekeeping gene in qRT-PCR analysis to normalise the expression of target genes. This housekeeping gene should be expressed at a constant level in all samples and to act essentially as a reference by reducing error in cDNA concentrations or reaction volumes (Ragni et al., 2013). In order to validate that the housekeeping gene of choice (in this case GAPDH) shows constant expression irrespective of scaffold used in cell culture, a validation experiment was carried out. GAPDH expression levels were measured for hDPSCs/P5 cultured under osteogenic condition for 3 days on uncoated and organised FA coated discs combined with either PRP gel, PRP releasate or FBS using qRT-PCR (the procedure of cell seeding will be described in detail in the next section). The results of this experiment (results are shown in results section) showed no change in the GAPDH levels and displayed no statistical differences between levels in all experimental groups indicating the suitability of using GAPDH as a housekeeping gene.

3.3.8.1.4 Method

➢**Test and control preparation**

As organised (OR) FA coating showed better induction of cell proliferation and sustained release of GFs from PRP compared to the disorganised coating, the osteogenic differentiation of hDPSCs was studied on organised FA crystals only. The hDPSCs (P1) were kindly donated by Dr Fahad Al-Dabbagh (Division of Oral Biology, University of Leeds). The cells were expanded in α-MEM supplemented with 10% FBS, 1% L-G and 1% P/S. At passage 5, when reached 80% confluence, the cells were used for the differentiation experiments. By continuous monitoring of cell morphology and rate of proliferation with each passage under the light microscope, the cells showed a good and fast rate of proliferation.

Agarose wells were prepared aseptically in 12-well plates as explained previously (section 3.1.4.5.2) using 4% agarose (w/v) in PBS. Uncoated etched SS and organised (OR) FA coated discs were placed inside the agarose wells and were loaded in triplicate with PRP or FBS as follow:

1. SS/ FBS (50 µL)
2. SS/PRP gel (12.5 µl thrombin + 50 µL PRP)
3. SS/ PRP releasate (50 µL)
4. OR FA/ FBS(50 µL)
5. OR FA/PRP gel (12.5 µl thrombin + 50 µL PRP)
6. OR FA/ PRP releasate (50 µL)

All the groups were incubated at 37°C in 5% (v/v) CO_2 in air and 98% relative humidity overnight. Subsequently, hDPSCs (P 5) were seeded on the discs at a cell density of 2 x $10^5/cm^2$ in 450 µL of serum-free α-MEM osteogenic medium containing 1 µL/mL dexamethasone (10nM) and 2µL/mL of L-ascorbic acid (100µM) in addition to 1%P/S and 1%L-G. Four hours later, the media and the discs were carefully transferred from the agarose wells into new 24-well plates containing 450 µL osteogenic medium supplied with 50 µL PRP gel, releasate or FBS according to the relative group. After 3 days, the cells were examined for mRNA expression of 4 osteogenic bone markers using qRT-PCR. The experiment was performed twice testing PRP extracted from 2 donors.

➢**Extraction of mRNA from hDPSCs cultured on FA/PRP under osteogenic conditions**

Cell seeded-discs were collected, dipped once in PBS and placed on a clean filter paper to absorb any residual buffer from the discs. The discs were then transferred into RNase free 24-well plate for mRNA extraction that was performed according to manufacturer's instructions of Qiagen's RNeasy minikit. To perform the experiment, 500 µL of Buffer RLT containing β-mercaptoethanol (10µL/mL) were added to each disc and the cells were disrupted by pipetting. Then, the cell lysates were transferred into QIAshredder tubes and centrifuged for 2 min at 10000 g. The homogenized lysates were then collected in RNase free centrifuge tubes and 500 µL of 70% ethanol were added to each lysate and mixed well by pipetting. Subsequently, the samples were transferred to RNeasy Mini spin columns placed in 2 mL collection tubes and centrifuged for 15 sec at 10000 g. The silica gel membrane spin columns were utilised to bind RNA in the presence of high concentrations of salts. The RNA attached to the column then

went through multiple wash steps. To ensure that the mRNA was pure and clear of any genomic DNA, RNase- Free DNase set was used to digest any genomic DNA contaminate. The flow-through of the RNeasy columns was discarded and 350 µL of buffer RW1 were added to the RNeasy columns and centrifuged for 15 sec at 10000 g. The flow-through was discarded then 80 µL of DNase I incubation mix (10 µL of DNase I stock solution and 70 µL Buffer RDD) was added directly to RNeasy column membrane and left at room temperature for 15 min. Later, 350 µL Buffer RW1 was added to the columns and centrifuged for 15 sec at 10000 g. The flow-through was discarded and 500 µL of Buffer RPE was added to the spin columns and centrifuged for 15 sec at 10000 g. The flow-through was discarded and another 500 µL of Buffer RPE were added to the columns and centrifuged for 2 min at 10000 g. Finally, after discarding the flow-through, the RNeasy columns were placed in new 1.5 mL collection tubes and 30 µl of RNase-free water were added directly to the spin column membranes and centrifuged for 1 min at 10000 g to elute the RNA. The RNA samples were stored at - 80 until required.

➢**Quantification of mRNA**

The extracted mRNA samples were checked for concentration and quality using a NanoDrop spectrophotometer (ND1000). Simply, 2µL of the samples were pipetted onto the lower pedestal of the NanoDrop and the quantities of mRNA were systematically recorded as ng/µL in addition to the ratio of sample absorbance at 260 and 280 nm to assess the mRNA purity. All ratios were found to be between 1.8 and 2, indicating acceptable purity. A dry clean lens cleaning tissue was used to wipe the pedestals of the instrument upon completion of each measurement to prevent sample carryover and residue build up. Before making the sample measurements, a blank of RNase-free water was measured to ensure that the instrument is working properly and the pedestal is clean.

➢**Reverse Transcription (RT) of mRNA**

High capacity RNA to cDNA kit was used to produce single stranded cDNA samples from the mRNA samples. To perform the assay, 20 µL of RT reaction

mix was aliquoted in 0.2 mL RNase-free centrifuge tubes comprising 9 µL of dilute mRNA sample in nuclease-free water (300 ng of mRNA), 1 µL of RT enzyme and 10 µL of RT buffer. The tubes were centrifuged briefly and placed in the PTC-100 Thermal Cycler to perform the RT at 37°C for 1 hour, followed by an enzyme denaturing step at 95 °C for 5 minutes. Tubes of cDNA samples were then stored at - 20°C until used for the next step within maximum 2 weeks. It was assumed that the reverse transcription reaction was 100 % efficient, so cDNA synthesised was the same amount as the RNA used.

➢**Performing qRT-PCR**

The reactions were carried out in 96- well PCR plates in duplicate using 20µL reaction volume contained 10 µL gene expression master mix, 1 µL of Taqman assay probe (gene of interest) and 9 µL diluted cDNA template (1 µL cDNA and 8 µL water). The plates were sealed securely and centrifuged briefly for 10 sec using spinner, then placed in the Roche LC480 light cycler machine to start the amplification procedure. Amplification curves were obtained using a LightCycler 480 real time QPCR system. All samples underwent a 10 minute 95°C pre-incubation step, followed by 45 cycles of 10 seconds at 95 °C, 30 seconds at 60 °C and 1 second at 72 °C. Samples were cooled to 40 °C at the end of the 45 cycles for 30 seconds. The cycle threshold (Ct) values were generated for each gene of interest and for the house keeping gene or the control gene (GAPDH) in all the samples by LightCycler 480 software.

➢**Calculation of gene expression levels**

First of all, ΔCt was calculated by normalising Ct value of each gene of interest to that of GAPDH determined for the same sample. Then, the relative change in gene expression was calculated using the $2^{-\Delta ct}$. Finally, in order to determine the effect of FA/PRP scaffolds on gene expression compared to the control, the $2^{-\Delta ct}$ value for each sample was normalised to the mean of the control sample (uncoated SS/FBS). The log10 of $2^{-\Delta ct}$ (fold change) ± SD and were plotted for the sample groups.

3.3.8.2 Alkaline phosphatase (ALP) activity quantitative assay

3.3.8.2.1 Principle

Cultures of hDPSCs seeded on FA/PRP coatings were terminated at 2 weeks for further investigation of the cells osteogenic differentiation by analysing alkaline Phosphatase (ALP) quantity. ALP is a cell membrane-bound glycoprotein. It is the most widely recognized biochemical marker for osteogenic activity and hard tissue cell differentiation (Sharma et al., 2014). ALP is involved in skeletal mineralisation by acting both to increase the local concentration of inorganic phosphate (a mineralisation promoter) and to decrease the concentration of extracellular pyrophosphate (an inhibitor of mineral formation) (Golub and Boesze-Battaglia, 2007).

ALP activity was measured by the ability of ALP enzyme released from osteogenic differentiated cells to convert the colourless substrate paranitrophenylphosphate (pNPP) into yellow paranitrophenyl (pNP).

3.3.8.2.2 Method

➢**Test and control preparation**

hDPSCs/P5 were cultured at a cell density of 2 x 10^5 cells/cm^2 on FA/PRP, FA/FBS, SS/PRP and SS/FBS for 2 weeks under osteogenic conditions as described above (section 3.3.8.1.4). Blanks were also prepared for background readings using the same culture conditions but without cells. The experiment was repeated twice using PRP samples of 2 blood donors (the same donors of qRT-PCR assay). The media was changed every 3 days by transferring the discs into new 24-well plate by sterile tweezers. The new wells contained 1mL osteogenic α-MEM supplied with either 10% PRP gel, PRP releasate or FBS.

➢**Evaluation of ALP activity**

At day 14, the cell culture was terminated. The discs were washed once in PBS and dried on clean filter paper. To lyse the attached cells, the discs were added to new 24-well plates containing 500 µL/well of 2 % triton X100 with three freeze/thaw cycles. To assist cells break up, the cell lysates were homogenised thoroughly by pipetting up and down several times after each thawing. Cell lysates were then transferred to clean Eppendorf tubes and centrifuged at high

speed (10000 g) for 10 min. The lysates' supernatants were used to quantify alkaline phosphatase activity using the 4-nitrophenyl colorimetric phosphate liquid assay. Briefly, standards for the ALP activity assay were prepared at concentrations of 5 µM to 300 µM by a serial dilution of 4-nitrophenyl (10 mM solution, Sigma-Aldrich, Cat. no: N7660) in an assay buffer solution [60 µL of 2 % aq. solution of Tergitol type NP-40 (Sigma-Aldrich, Cat. no: NP40S) in 10 mL of 1.5 M alkaline buffer solution (Sigma-Aldrich, Cat. no: A9226) and 20 mL dH_2O]. In triplicate, a 100 µL of each standard was added to wells of an ELISA 96-well plate. A 10 µL of each cell lysate solution and blank was loaded into the plate along with 90 µL of p-nitrophenyl phosphate liquid substrate system (pNPP, Sigma-Aldrich, Cat. no: N7653) and incubated at 37°C for 30 minutes in the dark. The reaction was stopped by addition of 100 µL of 1 M NaOH to all of the standards, samples and blanks. The absorbance was then read at 405 nm using a spectrophotometer. ALP concentrations were calculated using the generated standard curve. DNA concentrations of the lysates were also measured using PicoGreen assay (explained in section 3.2.4.2.2). ALP data were normalised to total DNA concentrations obtained from the same cell lysates.

3.3.8.3 Alkaline phosphatase staining

hDPSCs were seeded on the discs (12×10^4 cells/cm^2) as described above (section 3.3.8.1.4) and cultured for 2 weeks using PRP sample of donor 1 of the previous differentiation assays. The discs were then washed once in PBS and fixed in 98 % ethanol for 15 min in 24-well plate. The ethanol was then fully aspirated and the discs were washed once in distilled water. ALP stain solution was prepared by adding 4.2 mg Fast violet B salt (Sigma-Aldrich, Cat. no: F1631) and 0.4 mL Naphthol AS-MX (0.25% (w/v), buffered at pH 8.6, Sigma-Aldrich, Cat. no: 855) to 9.6 mL dH_2O. The cells were then stained by adding 500 µL of the ALP stain solution to each well and the plates were incubated at 37°C for 60 minutes in the dark. Subsequently, the stain solution was aspirated and the discs were washed one time with dH_2O and analysed under stereo-microscope. A purple coloured stain indicates ALP protein.

hDPSCs/P5 were also tested for ALP deposition on monolayer, therefore, the cells were cultured in 24-well plates under basal and osteogenic conditions in triplicates, at cell density of 1 x 10^5 cells/cm^2. After 2 weeks, the cells were stained for ALP using the same instructions mentioned above and observed under a Leica DMI6000 B inverted microscope.

3.3.8.4 Alizarin red staining for calcium accumulation

3.3.8.4.1 Principle

Alizarin red stain (ARS) was used to evaluate calcium deposits in cell culture inducted by FA/PRP combinations.

3.3.8.4.2 Method

hDPSCs/P5 were seeded on SS/PRP and organised FA/PRP coated discs (2 x 10^5 cells/cm^2) and cultured for 2 weeks using PRP of donor 1 (Section 3.3.8.1.4). Subsequently, the cell seeded-discs were gently washed 3 times with PBS, fixed in 10 % NBF for 15 minutes at room temperature and then washed three times with dH_2O. The samples were then incubated with Alizarin Red solution (40 mM, Caltag Medsystems Ltd, Cat. no: SC-8678) for 20 - 30 min at room temperature with gentle shaking, followed by 5 washes of dH_2O. Cells were then observed under a stereo-microscope. A red coloured stain indicates calcium deposition.

3.4 Statistical analysis

All experiments were carried out in triplicate and repeated twice using PRP of two different blood donors. hDPSCs used in the differentiation experiments were from one donor. The quantitative data of LDH assay, DNA content assay, ELISA and qRT- PCR results were expressed as mean ± standard deviation (SD). Due to small sample size, statistical analysis cannot be reliable. The data were presented and discussed according to data description, notable trends and features.

Chapter 4: Results and discussion (Flourapatite coating)

4.1 Introduction

The use of dental implants for correction of tooth and tissue loss has increased exponentially around the world. Dental implant surfaces are often modified by coating with hydroxyapatite and fluorapatite (FA) to improve the osseointegration process and promote faster bone healing. Fluorapatite [$Ca_{10}(PO_4)_6F_2$,] exhibits a hexagonal unit cell, composed of Ca^{2+} and PO_4^{-3} arranged around a central column of F^- which extends along the c-axis of the crystal (Brown and Constantz, 1994). The release of Ca^{2+} and PO_4^{-3} ions from the coating could control bone cell proliferation, differentiation, modulation of expression of osteogenic genes and synthesis of osteogenic growth factors (Stvrtecky et al., 2003). Fluoride is the most electronegative element and its small ionic diameter and high charge density enable the fluoride to have a great capacity to form strong ionic and hydrogen bonds and to have a high potential for interacting with mineral phases and organic macromolecules (Robinson et al., 2004). It is believed that, fluoride replaces and occupies a column hydroxyl place in the hydroxyapatite crystals leading to reduction in (a) and (b) lattice parameters of the crystal lattice and a consequent reduction in the crystal energy. This, in turn dramatically decreases the acid solubility of the crystals and generates a more stable crystal structure (Robinson et al., 2017). This could also improve the mechanical strength, decrease the dissolution rate of HA and enhance bone tissue growth (Fathi and Zahrani, 2009). Some in vivo studies have proved the increased stability and the lower degradation of FA over hydroxyapatite as an implant coating (Dhert et al., 1991; Dhert et al., 1993; Overgaard et al., 1997; Bhadang and Gross, 2004). Therefore, FA coatings have been selected for investigation in this study to explore their potential to enhance implant osseointegration.

The excellent properties and biocompatibility of FA nanostructures have resulted in many studies focusing on their synthesis. The development of nanotechnology has created many ways to grow 1D nanostructures (Xia et al., 2003) such as the hydrothermal method that was widely used as an effective way to create long nanorods, nanowires and whiskers (Cao et al., 2004). Chen

et al. (2006b) demonstrate a hydrothermal technique to grow a film of compacted well-aligned FA crystals on metal plates at 121°C and 2 atm for 10 hours. The FA crystals were very similar in their chemical composition to natural tooth enamel. Czajka-Jakubowska et al., (2009a) adopted the hydrothermal method of Chen et al. (2006b) but successfully changed the surface morphology of the FA crystals from organised to disorganised depending whether they were deposited on the under surfaces or upper surfaces of the substrate respectively. The same group also attempted to grow FA on different substrates and found that only etched stainless steel and titanium substrates could produce surfaces entirely covered with FA crystals of uniform composition, alignment, size, shape and structure (Czajka-Jakubowska et al., 2009b).

The purpose of the present study was to investigate the topography of the FA coatings including crystal alignment, composition and the effects of post-synthesis treatments such as washing the hydrothermal reaction mixture off the samples. The biological activity of the coatings was also examined to develop a better understanding of their biocompatibility.

4.2 Results

4.2.1 Characterisation of the FA coatings

FA coatings were prepared on SS substrates using a mild hydrothermal method as described in the methods chapter (section 3.1.1.3). The discs were either tilted at 45° or positioned vertically during the coating process.

4.2.1.1 Macroscopic examination

The upper and under surfaces of the discs, tilted at 45° appeared to be completely covered with FA crystals. However, the coating on the upper surfaces looked whiter, denser and thicker than that of under surfaces. Conversely, the discs that were positioned vertically showed a similar thin layer of coating covering both surfaces of each sample. Figure (17) shows etched uncoated SS disc, SS disc with thick coating on the upper surface and SS disc with thin coated under surface.

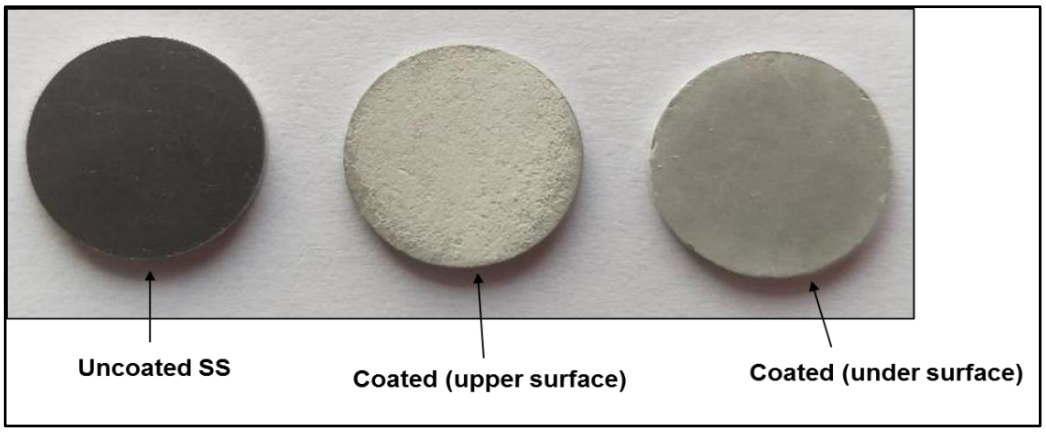

Figure 17: A photograph of etched SS discs that were either left uncoated or had FA coatings deposited on their upper or under surfaces while held at 45° during coating. Note that the coating deposited on the upper surface was visually thicker.

4.2.1.2 Microscopic analysis of FA crystal growth (SEM)

SEM was used to look at the surface topography of the FA coated discs and to make a more detailed comparison between the coatings. After coating, all discs immediately underwent 3 different treatments: dried, dried - washed- dried or washed- dried as described in section 3.1.2. All the SEM images are presented at standard magnifications of x100 and x1000.

➢**Discs tilted at 45°**

In the case of the discs tilted at 45°, upper surfaces of the unwashed discs (group I) that were simply dried following coating showed FA crystals embedded in a magma-like mass of residual material (Figures 18A, 18B). This material was less evident on the under surfaces of the discs (Figures 18C, 18D). The washed discs (groups II and III) were free of magma-like or any residual material and the FA crystals were clearly visible (Figures 19 and 20 respectively). Moreover, no difference was found between groups II (dried-washed-dried coatings) and group III (washed-dried coatings) in terms of crystals morphology and orientation.

In comparing the growth of the FA crystals on upper and under sides of the discs, a different growth pattern of the FA crystals were seen under the SEM.

The upper surfaces displayed randomly arranged hexagonal crystals grown in a disordered manner (disorganised FA coating) with complete coverage of the upper surfaces (Figures 18A, 18B, 19A, 19B, 20A and 20B). In contrast, the under surfaces were completely covered with well aligned and organised hexagonal crystals (organised FA coating). The crystals were compact and deposited parallel to each other in an ordered manner and perpendicular to the substrate surface (Figures 18C, 18D, 19C, 19D, 20C and 20D). Occasionally, some of the organised crystals were aggregated into bundles (Figure 18D). Although it is difficult to measure the dimensions of the crystals accurately due to perspective effects, SEM showed that the crystals were 10-30µm in length and about 1-3 µm in cross section (Figure 21).

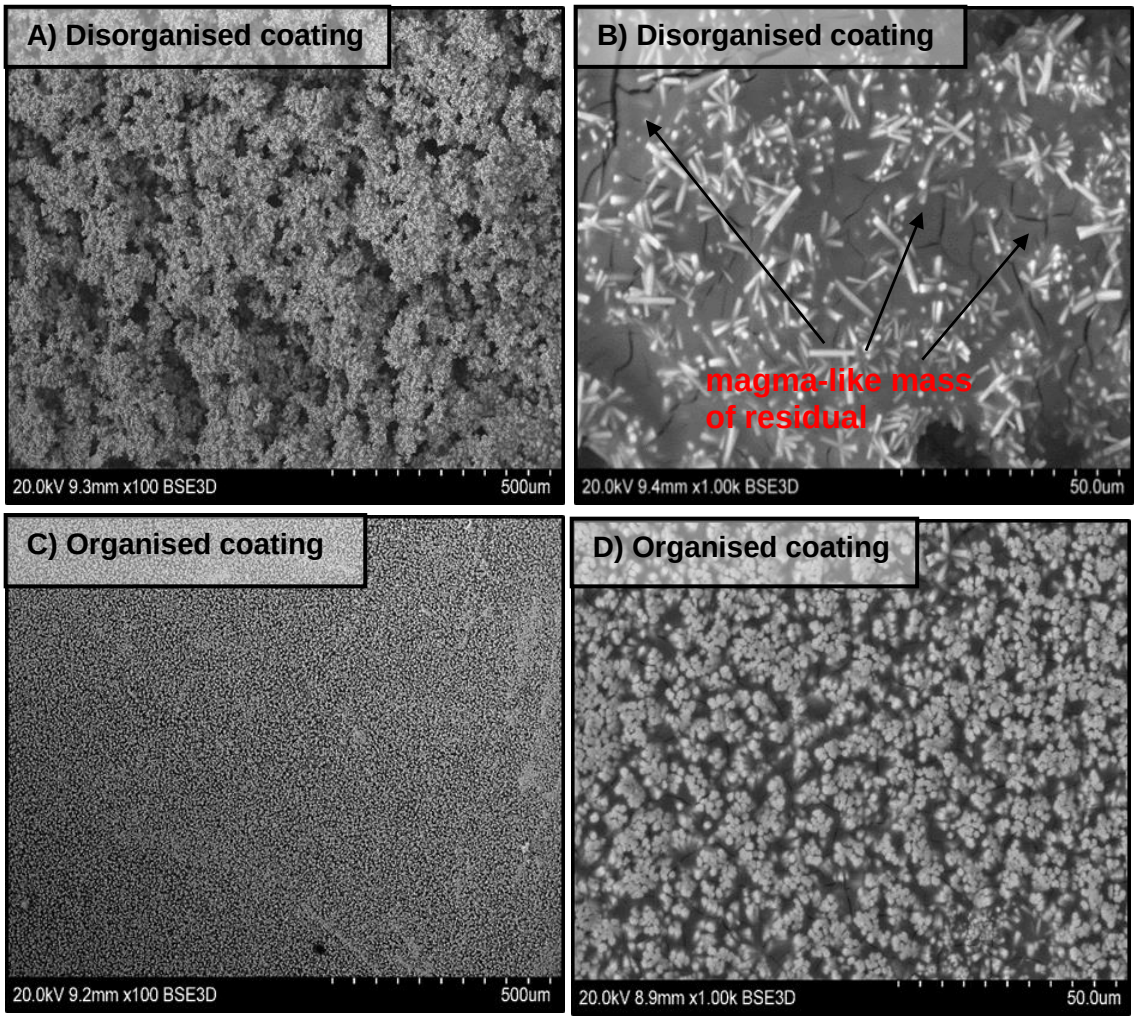

Figure 18: SEM images of group I (unwashed FA coatings of discs tilted at 45°). The crystals of upper surfaces (A, B) were embedded in a magma like mass of material which was seen to a less extent on under surfaces (C, D).

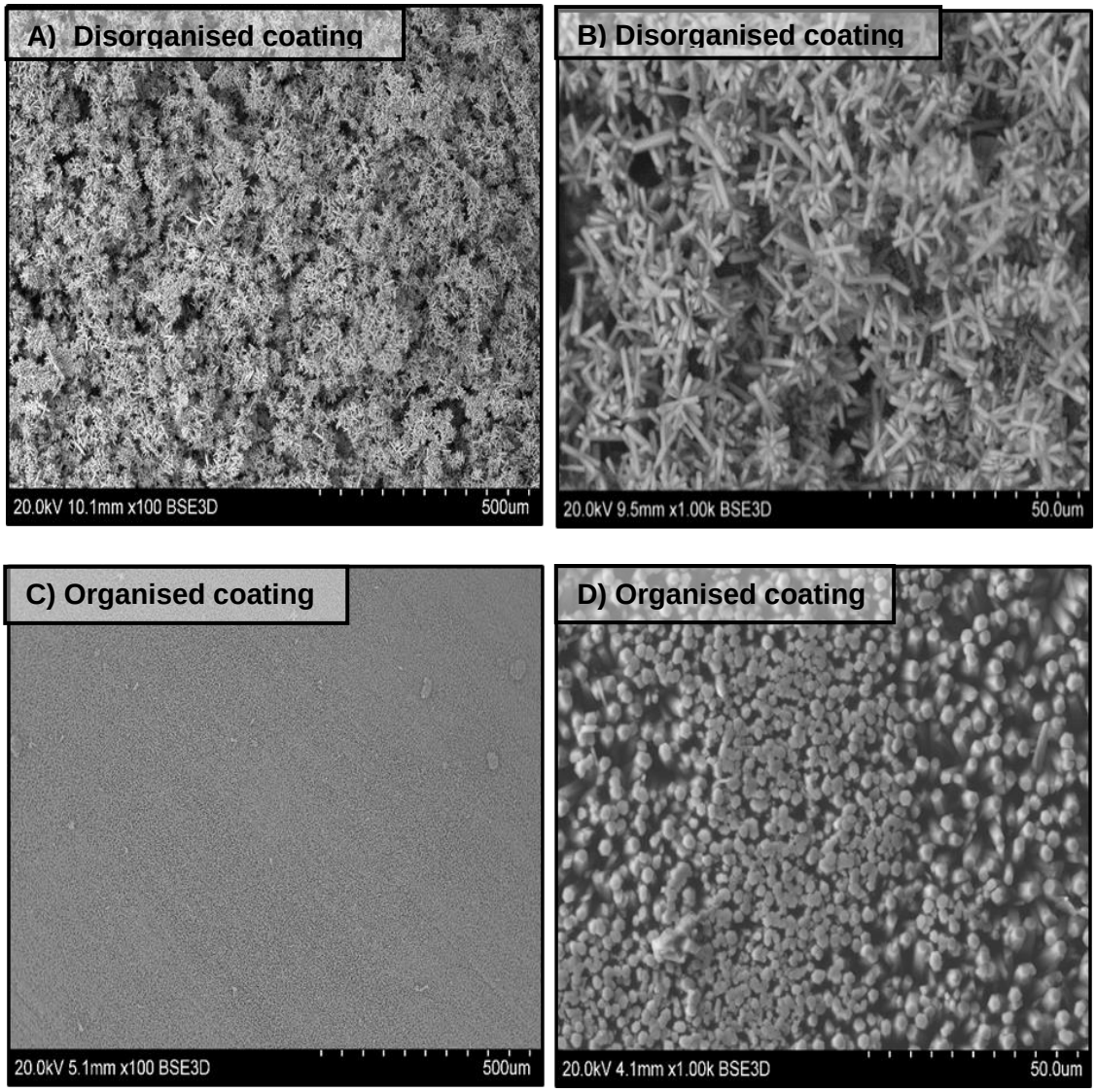

Figure 19: SEM images of group II (Dried-Washed-Dried FA coatings of discs tilted at 45°). The upper surfaces displayed randomly arranged hexagonal crystals or disorganised coatings (A, B). The under surfaces showed well aligned hexagonal crystals or organised coatings (C, D).

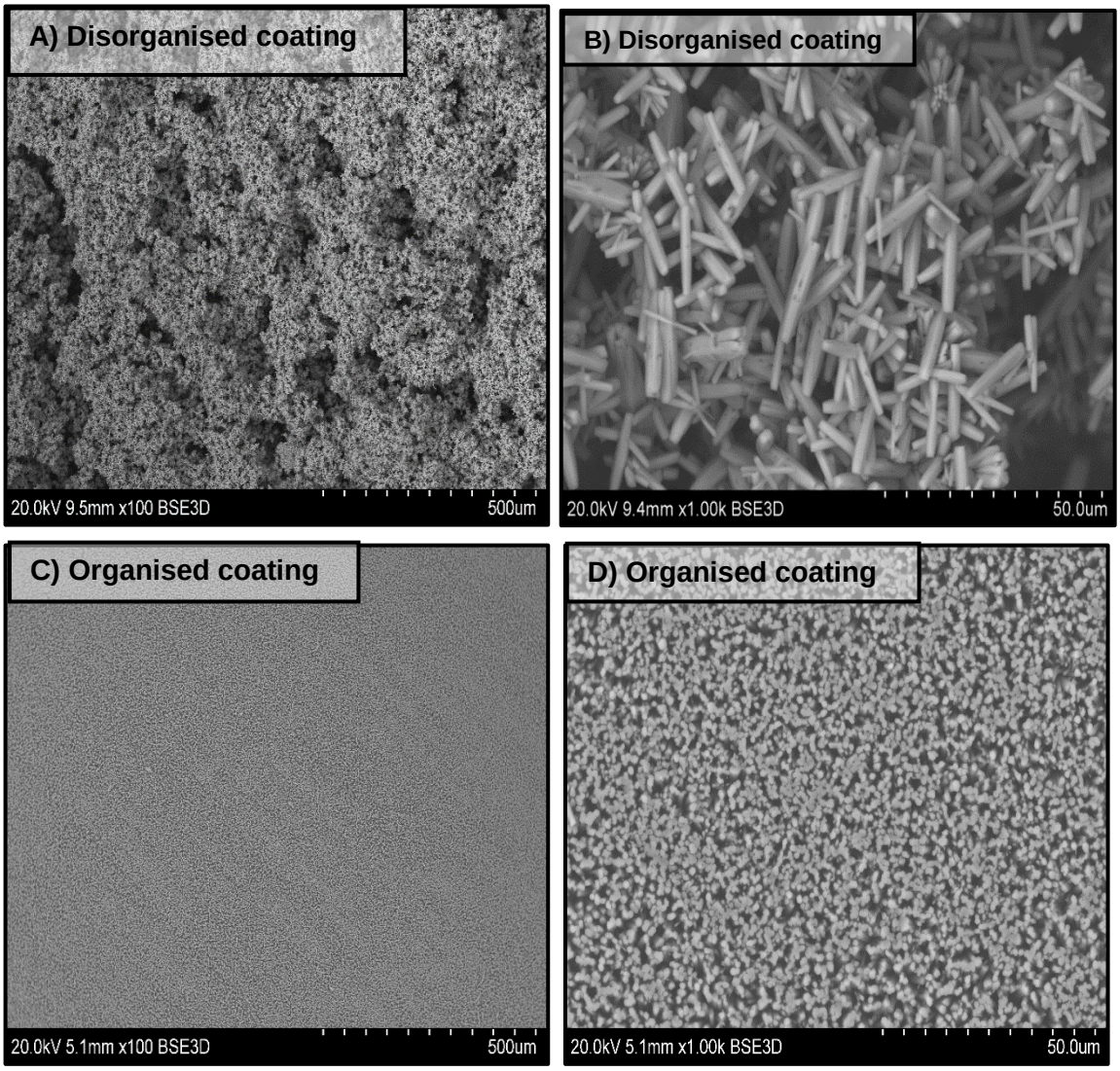

Figure 20: SEM images of group III (Washed-Dried FA coatings of discs tilted at 45°). They displayed the same topography of group II where the upper surfaces exhibited a disorganised FA coating (A, B) and the under surfaces showed an organised coating (C, D).

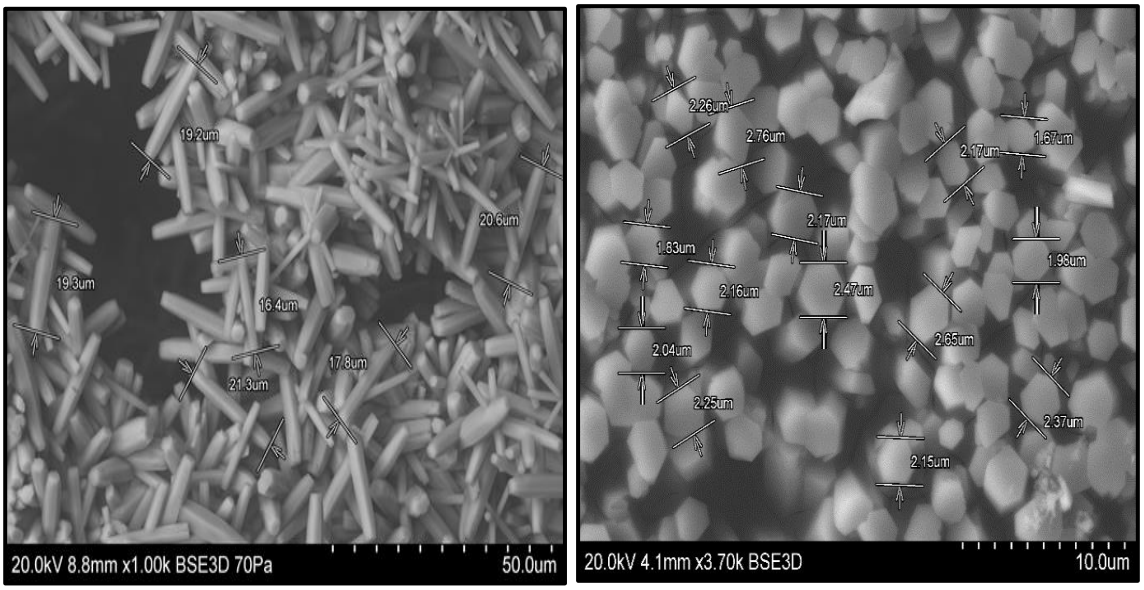

Figure 21: **Micrograph showing the dimensions of the synthesised FA crystals which was about 10-30 µm in length and 1-3 µm in cross-section.**

➢**Vertically positioned discs**

In the case of the vertically positioned discs, unwashed FA coated samples (group IV) also exhibited a magma-like residual material that covered the crystals and accumulated between them (Figure 22). Images of the washed groups (group V and VI) showed clearly visible FA crystals with no residual material (Figures 23 and 24 respectively). SEM analysis for these three groups exhibited complete coverage of both disc surfaces with ordered films of well aligned hexagonal crystals. The crystals were compacted and deposited parallel to each other and perpendicular to the substrate surface. However, many patches of disordered crystals were grown randomly over these organised crystal surfaces (Figures 22C, 23A, 24C), because of that, only the 45° tilted discs were taken forward for the later cell culture experiments.

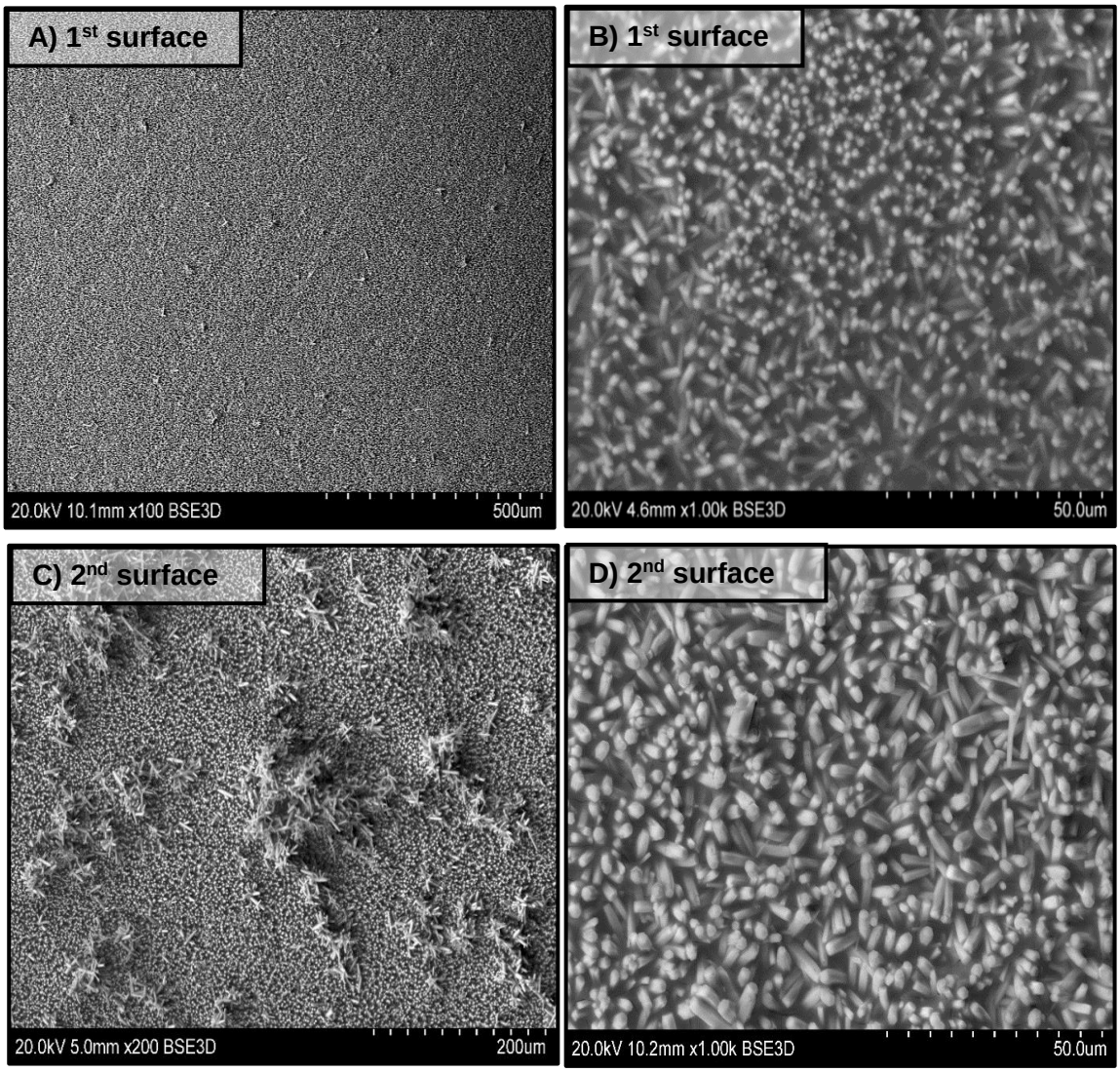

Figure 22: SEM images of group IV (unwashed FA coatings of vertically positioned discs). Residual material covered the crystals on both surfaces of vertically orientated discs; 1st surface (A, B) and 2nd surface (C, D) of each disc.

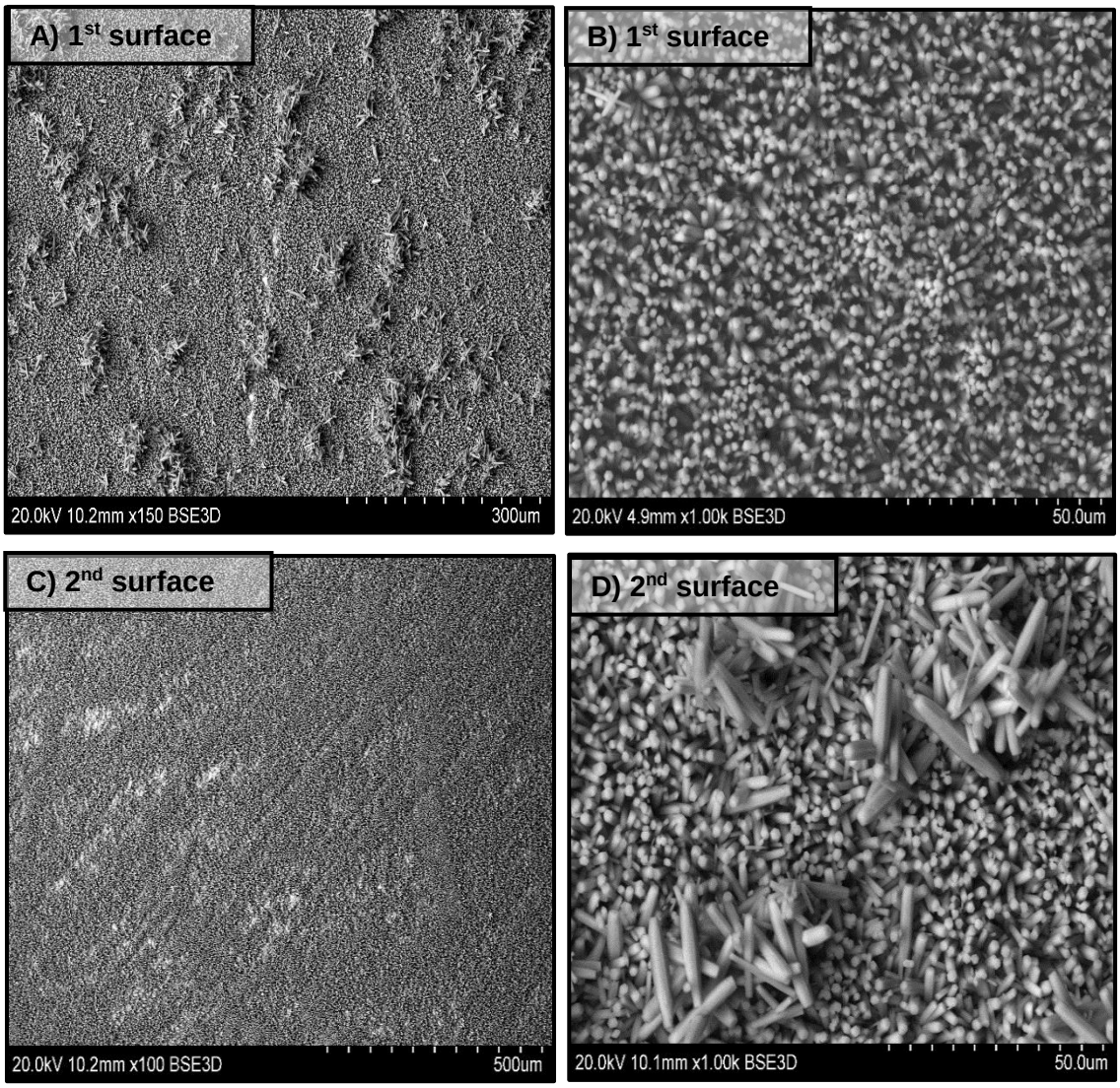

Figure 23: SEM images of group V (Dried-Washed-Dried FA coatings of vertically positioned discs). FA crystals were clearly visible completely covering both surfaces of vertically orientated discs; (A, B) 1st surface and (C, D) 2nd surface with ordered films of well aligned hexagonal crystals or organised coatings.

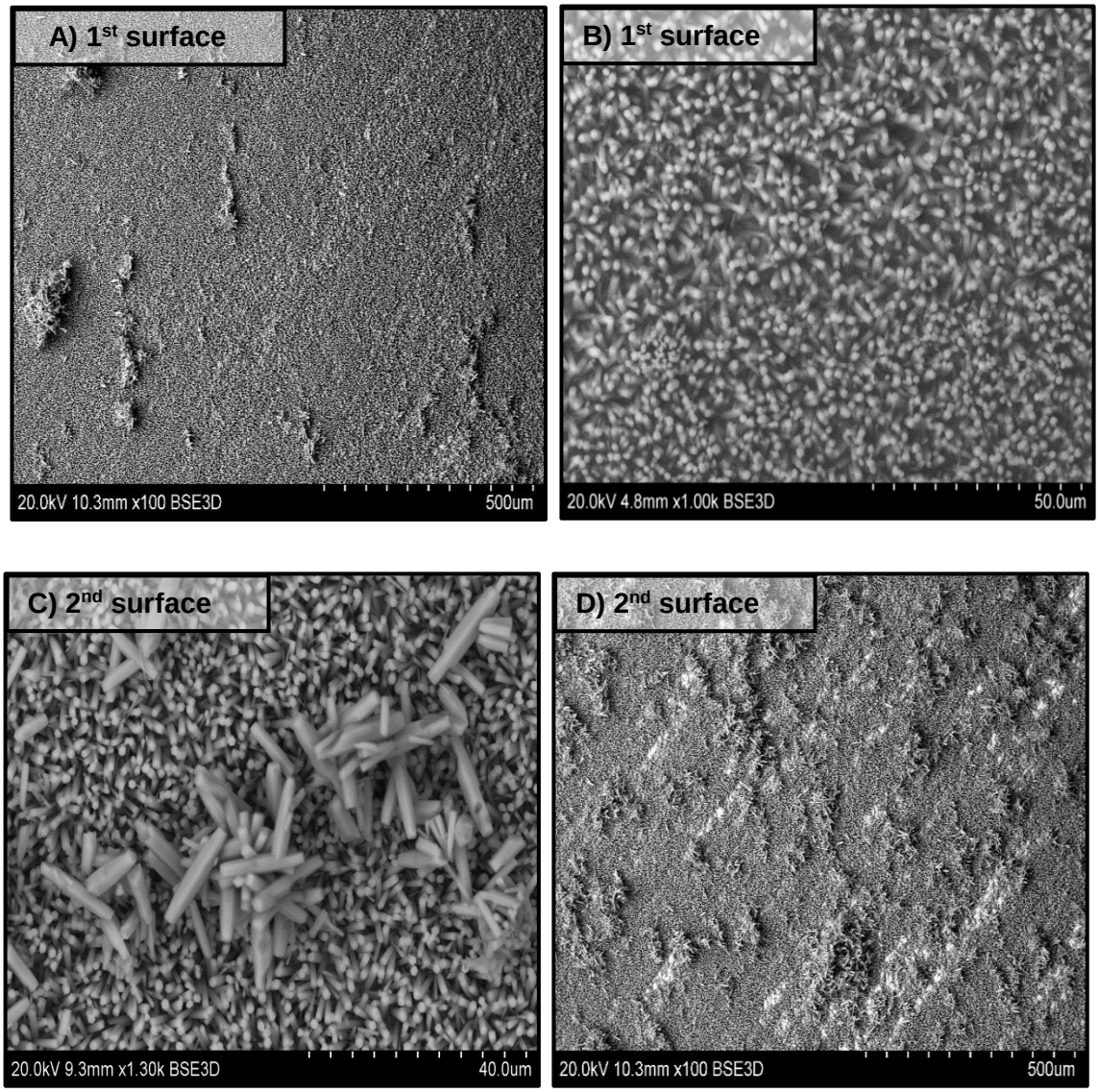

Figure 24: SEM images of group VI (Washed-Dried FA coatings of vertically positioned discs). The FA crystals were not covered with residual material. Both surfaces of vertically orientated discs (A, B) 1st surface and (C, D) 2nd surface were completely covered with organised coatings.

4.2.1.3 Elemental analysis of the FA coatings (EDS)

EDS was conducted for further characterisation of the synthesised coatings by identifying the chemical composition of the FA coatings and measuring the abundance of elements in the sample. Mean values for the atomic percentage of FA coatings elements for both of the 45° tilted discs and vertically positioned discs are illustrated in figures 25 and 27 respectively showing results for unwashed, dried-washed-dried and washed-dried groups. In general, EDS spectra of all groups showed that the elemental composition of the synthesised FA coatings was as expected; comprised of the main elements of FA (calcium, phosphorus and fluorine) in addition to carbon, oxygen, sodium elements.
In both of the 45° tilted discs (Figure 25) and vertically positioned discs (Figure 27), the atomic percentage of all elements in the unwashed upper and under coated surfaces exhibited differences to the corresponding washed surfaces. It was clear that washing the discs considerably reduced the proportion of carbon and sodium detected on the surfaces. Whereas oxygen (the most abundant element), fluorine, phosphorus and calcium were present in proportionally greater amounts after washing the coatings. The elemental composition of the washed coatings was not affected by the order of the washing steps as no difference in the elements level of the coatings was seen between groups II (dried-washed-dried) and group III (washed-dried) of 45° tilted discs (Figure 25) and between group V (dried-washed-dried) and VI (washed-dried) of vertically positioned discs (Figure 27). Further, no difference was noticed between the composition of the disorganised coatings (upper surfaces) and organised coatings (under surfaces) of the 45° tilted discs (Figure 26) or between the compositions of the coatings on either side of the discs of the vertically positioned discs (Figure 28).

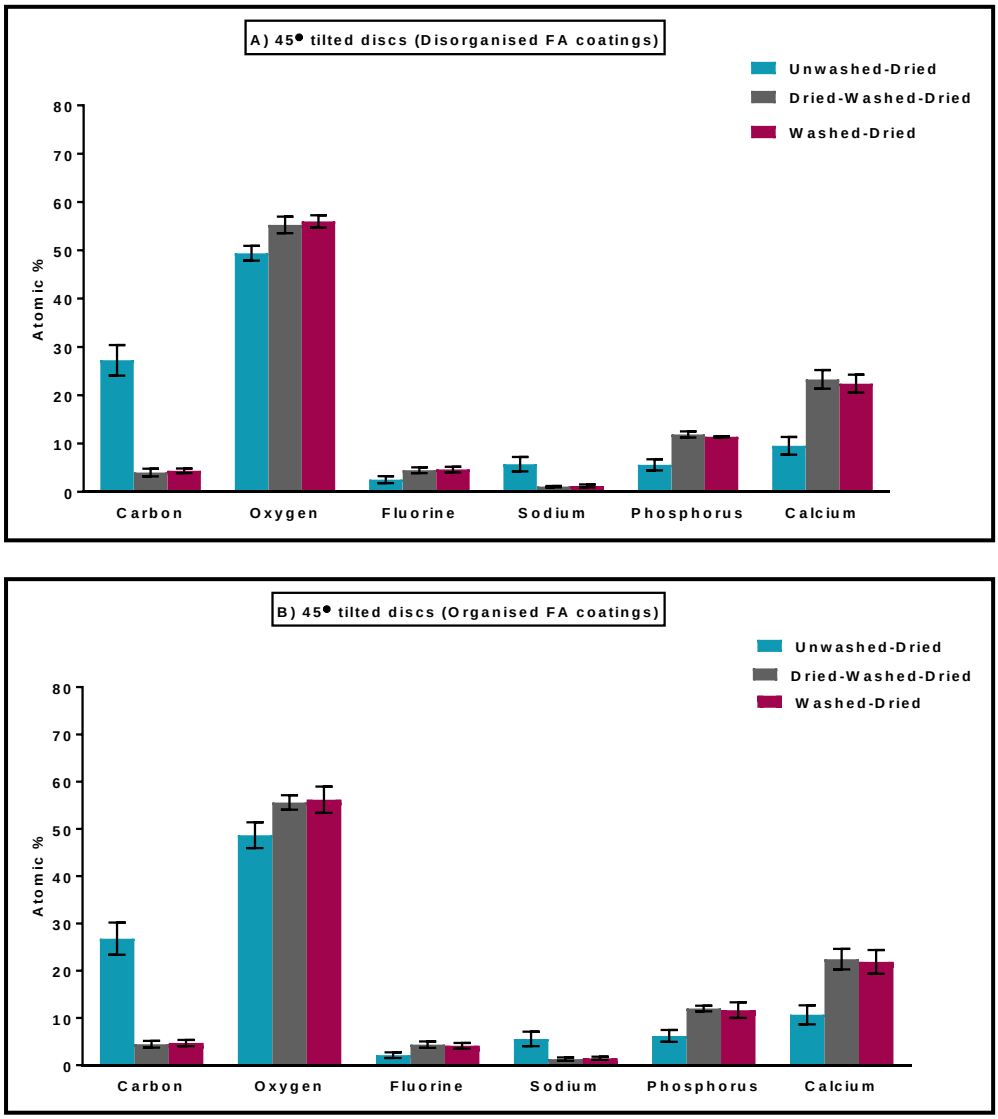

Figure 25: Mean values ±SD for the atomic percentage of the FA coating elements for the discs tilted at 45° (n=3) including disorganised coatings (A) and organised coatings (B). Ca, P and F comprised a larger proportion of the elements present after washing the coatings. No difference was found between either of the washing treatments used.

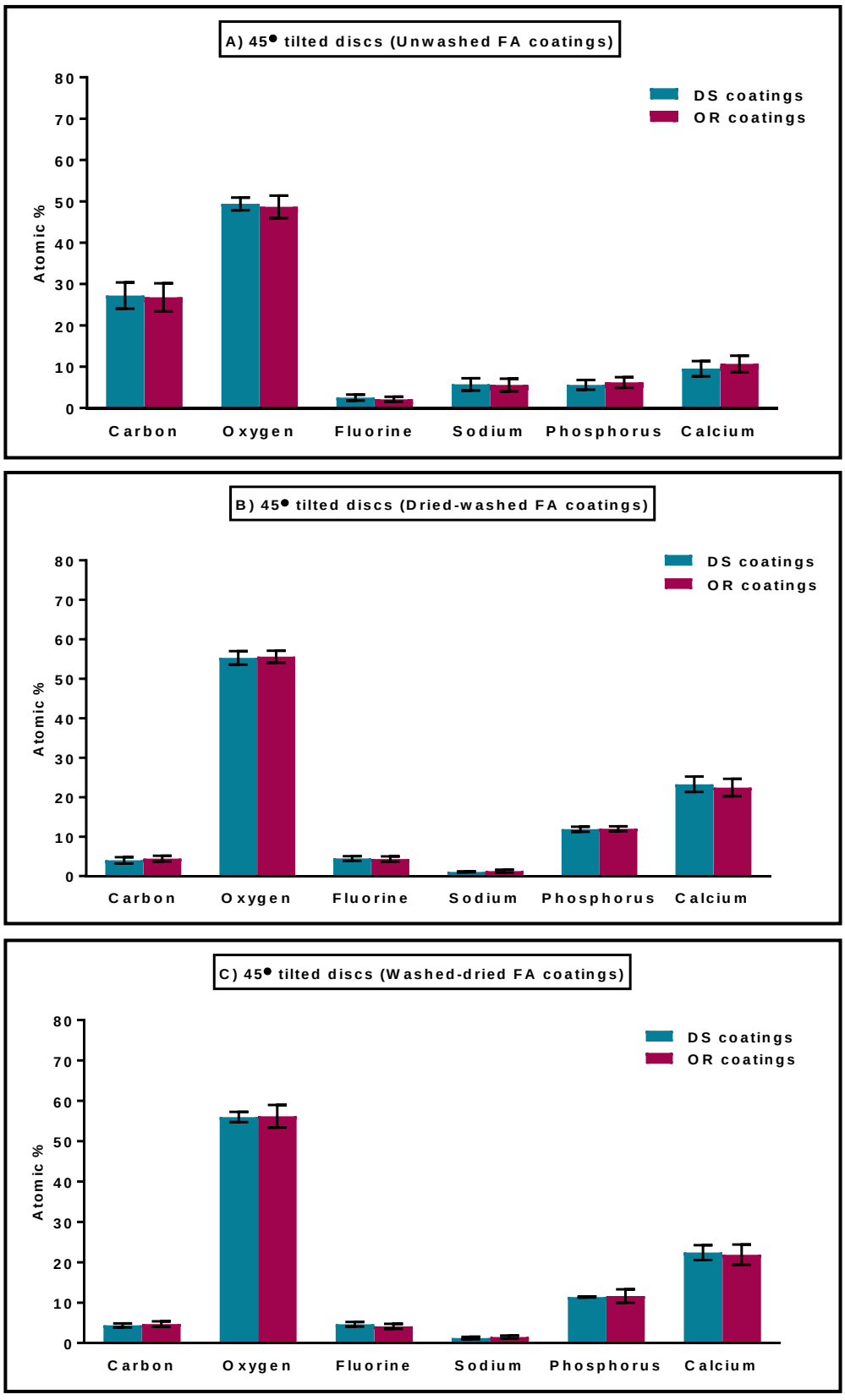

Figure 26: Mean values ±SD for the atomic percentage of the FA coating elements for the discs tilted at 45° (n=3). No difference was found between disorganised (DS) and organised (OR) coatings in any of the coating groups.

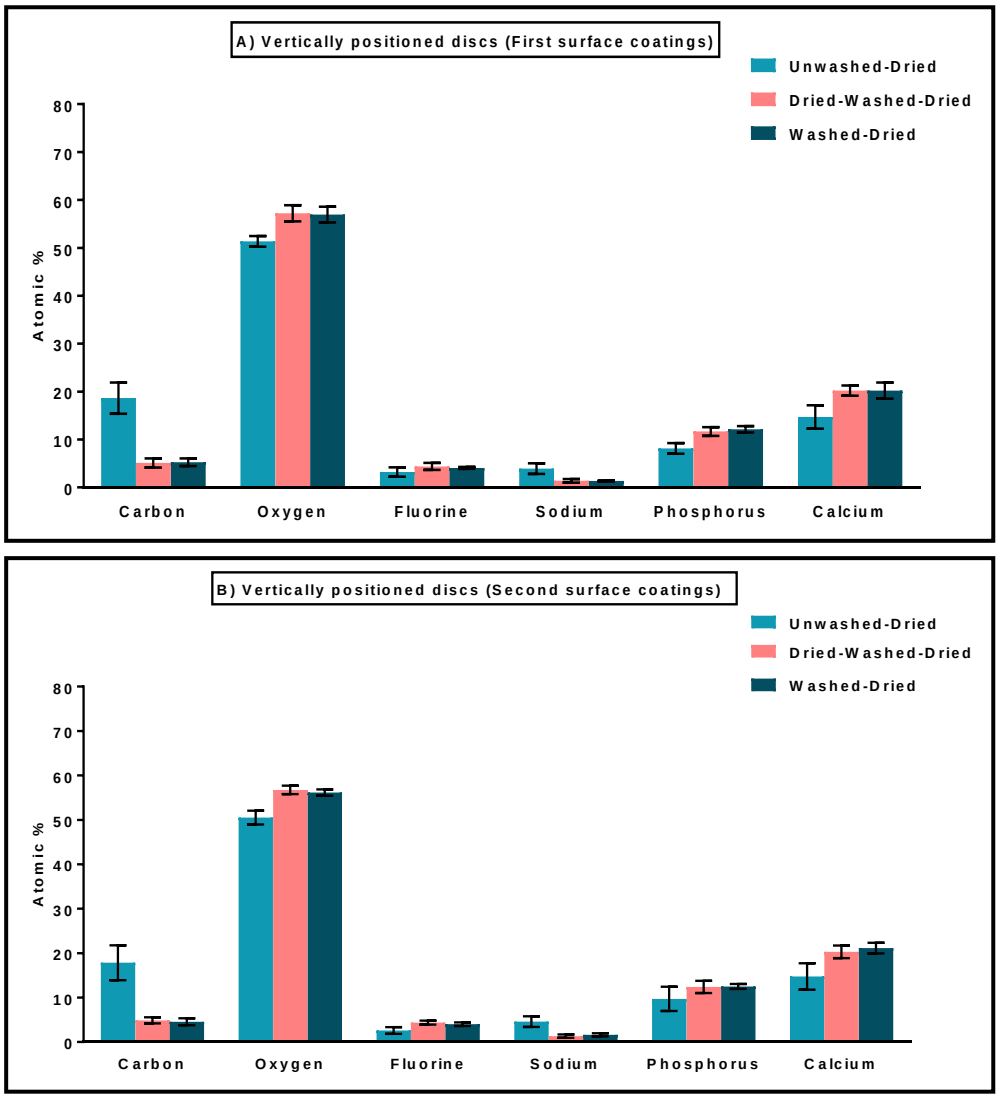

Figure 27: Mean values ±SD for the atomic percentage of the FA coating elements for the vertically positioned discs (n=3). Ca, P and F comprised a larger proportion of the elements present after washing of the coatings of both disc surfaces (A, B). No difference was found in the elements atomic % between both types of the washed coatings.

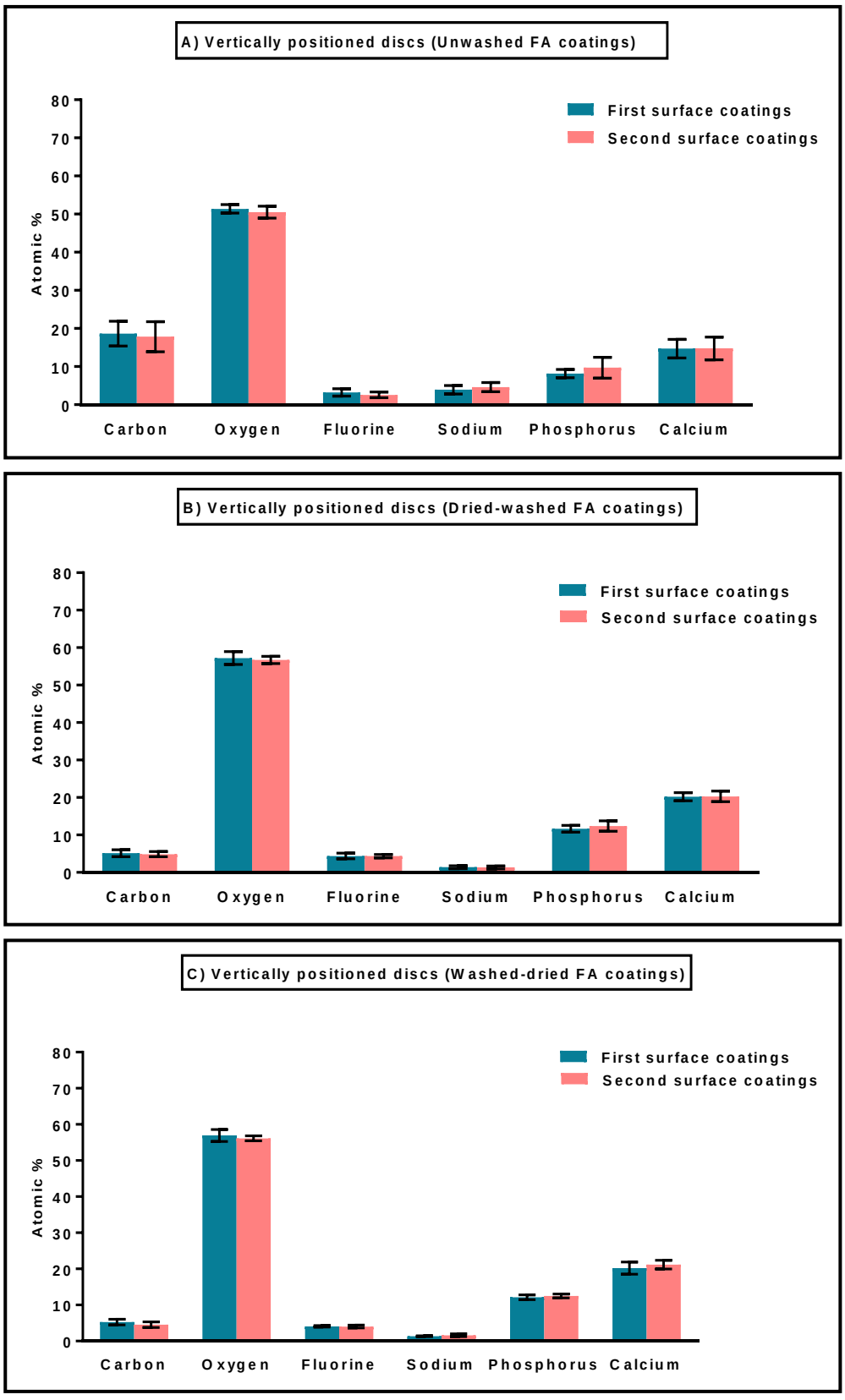

Figure 28: Mean values ±SD for the atomic percentage of the FA coating elements for the vertically positioned discs (n=3). No difference was found between first and second coating surfaces in all coating groups.

The chemical analysis of the coatings also confirmed that the ratio of Ca/P and Ca/F were close to the theoretical values of $Ca_5(PO_4)_3F$ (Ca/P= 1.67 and Ca/F= 5) as shown in table 6 for the 45˚ tilted discs and the vertically positioned discs.

Table 6: Mean atomic ratios ± SD of calcium to phosphorus elements (A) and calcium to fluorine elements (B) in FA coatings of the 45° tilted discs and calcium to phosphorus elements (C) and calcium to fluorine elements (D) in FA coatings of the vertically positioned discs (n=3). The ratios of all the groups were close to the theoretical values (Ca/P=1.67, Ca/F=5). DS, disorganised FA; OR, organised FA; Ca, calcium; P, phosphate; F, fluorine.

A) Means ± STDEV of Ca/P % ratios of the 45° tilted discs					
Unwashed coatings		Dried- washed coatings		Washed- dried coatings	
DS	OR	DS	OR	DS	OR
1.71 ± 0.12	1.75 ± 0.35	1.96 ± 0.19	1.87 ± 0.19	1.97 ± 0.17	1.92 ± 0.43
B) Means ± STDEV of Ca/F % ratios of the 45° tilted discs					
Unwashed coatings		Dried- washed coatings		Washed- dried coatings	
DS	OR	DS	OR	DS	OR
3.97± 0.94	5.28 ± 1.48	5.31 ± 0.89	5.34 ± 1.38	4.93 ± 0.89	5.44 ± 1.11
C) Means ± STDEV of Ca/P % ratios of vertically positioned discs					
Unwashed coatings		Dried- washed coatings		Washed- dried coatings	
1st surface	2nd surface	1st surface	2nd surface	1st surface	2nd surface
1.67 ± 0.08	1.55 ± 0.24	1.73 ± 0.09	1.67 ± 0.30	1.67 ± 0.08	1.69 ± 0.13
D) Means ± STDEV of Ca/F % ratios of vertically positioned discs					
Unwashed coatings		Dried- washed coatings		Washed- dried coatings	
1st surface	2nd surface	1st surface	2nd surface	1st surface	2nd surface
4.96 ± 0.22	6.21 ± 2.58	4.70 ± 0.72	4.69 ± 0.53	4.96 ± 0.22	5.32 ± 0.63

In summary, washing the newly synthesised FA coating either before or after drying proved crucial to get rid of residual magma-like deposits. Therefore, it was decided to use group III discs (45˚ tilted, washed then dried) in the subsequent cell culture work and to study both of the disorganised and the organised coatings.

4.2.2 Biocompatibility assessment of FA coatings

4.2.2.1 SEM analysis for cell attachment to SS and FA coatings

G292 osteoblast-like cells were seeded on SS uncoated and coated discs as described previously (Methods chapter, section 3.1.4), and after 2 days, cell attachment was investigated under the SEM. G292 cells grown on uncoated etched SS were well attached, spindle-like in shape and displayed a characteristic fibroblast-like morphology in monolayer cell culture, indicative of cell spreading. Interestingly, the cells were confluent in the centre of the disc surface and were migrating from the centre toward the edges of the disc surface showing good signs of cell growth (Figure 29).

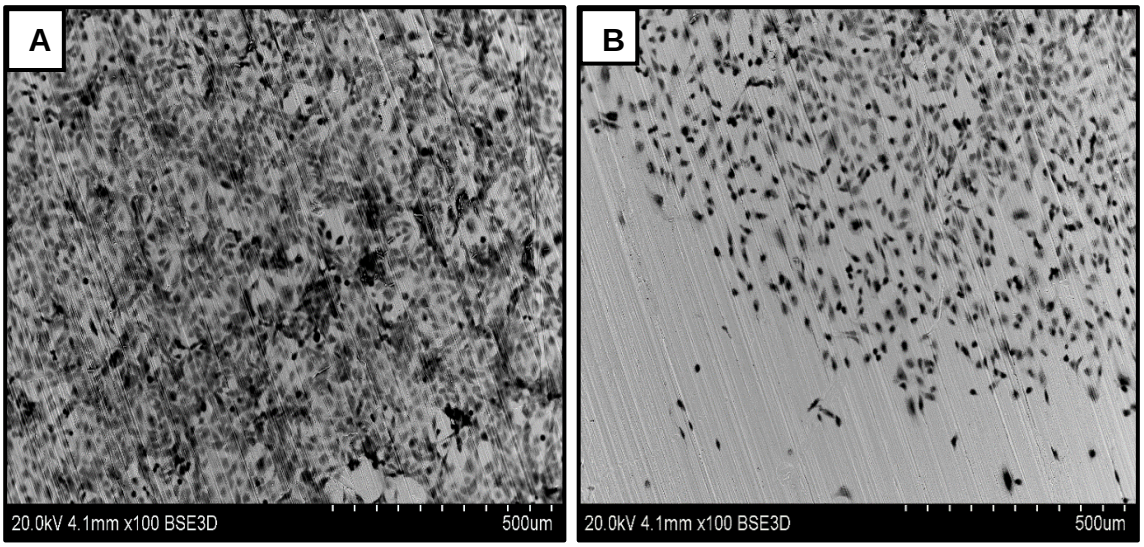

Figure 29: SEM micrograph for G292 confluent cells grown on etched SS surface for 2 days. The cells were spindle-like and well attached on the surface of the discs. The cells were confluent in the centre of the disc surface (A) and migrating from the centre to the edges of the disc surface (B).

The cells that were grown on disorganised and organised FA coatings adopted different configurations. On the disorganised coatings, the cells were seen to adhere very well to the underlying FA crystals by the cytoplasmic extensions. The cells formed small and big clusters that colonised patches of the coating material (Figures 30A, 30B). In the case of the organised coatings, a viable cell layer appeared to have covered the coatings, suggesting cell growth. The cells

were spread evenly on the coating surface either as single spindle cells or small clusters of cells compared to that of the disorganised coating (Figures 30C, 30D).

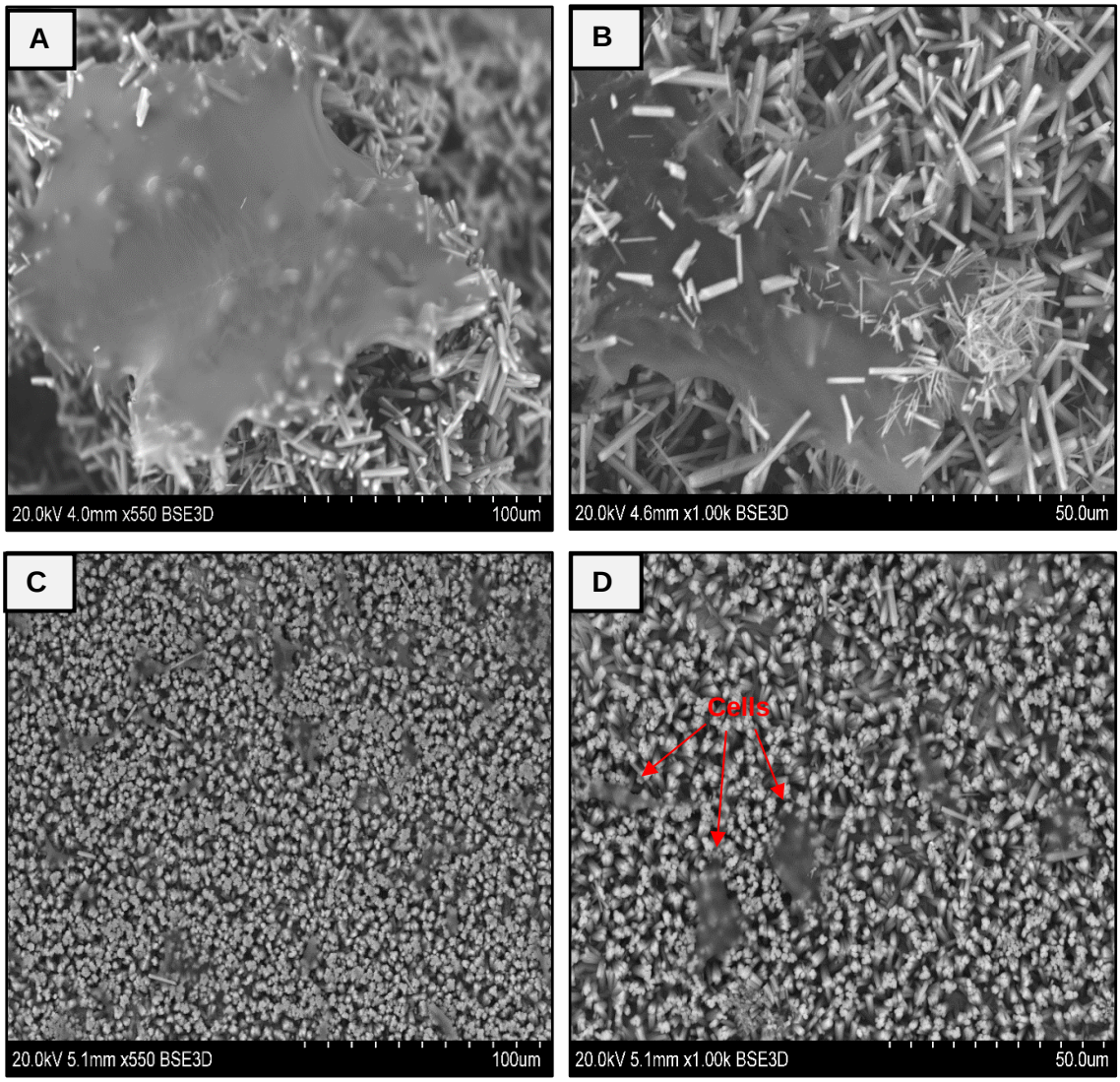

Figure 30: SEM micrograph for G292 cells grown for 2 days on disorganised and organised FA coatings. They show clusters of adhering cells colonising patches of the disorganised coating crystals (A,B) while the organised coatings showed more spindle-shaped cells that were well spread on the organised FA coatings (C,D) as labelled with arrows in picture D.

4.2.2.2 Confocal laser scanning microscopy (CLSM)

Cell attachment and growth were also investigated using Alexafluor 488 phalloidin cytoskeleton stain and TO-PRO-3 nucleic acid stain under the confocal microscope. The morphology of the cells that were spread over both disorganised and organised coating surfaces is shown in figure 31. The cells of the disorganised coatings looked relatively spindle-like in shape with a degree of polygonal appearance (Figure 31A). Most of the cells tended to adhere to each other forming isolated clusters of cells attached to the crystals. However, cells cultured with organised coatings appeared more spindle-like in shape with more pronounced and long cytoplasmic extensions adhering to the underlying crystals (Figure 31B).

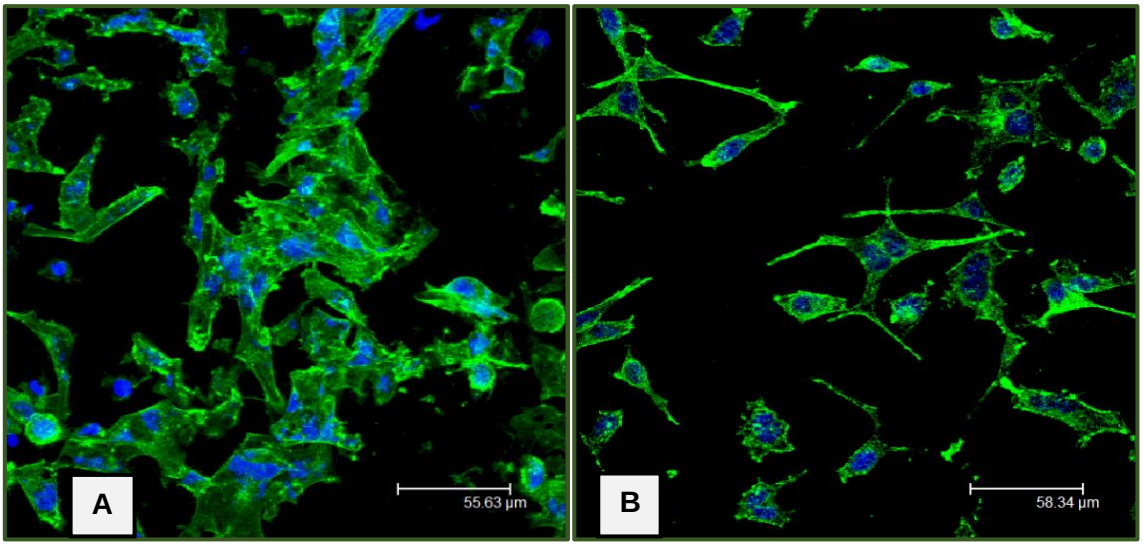

Figure 31: Confocal images showing green stained cytoskeleton and blue stained nuclei of cells attached to disorganised and organised FA coatings. The cells were well attached to disorganised FA coated surfaces (A), where they tended to attach to each other forming clusters. The organised FA surfaces (B) showed well spread and more spindle-like cells with more pronounced cytoplasmic extensions adhering to the underlying crystals.

4.2.2.3 Cytotoxicity of FA coatings

4.2.2.3.1 Direct contact cytotoxicity test

- **Cell morphology**

The cells grown on the plastic wells surfaces alongside the discs were examined under the light microscope and imaged using a digital camera as shown in figure 32. The images of cells cultured on the negative control, uncoated SS and FA coated discs showed a high number of confluent spindle cells adopting the morphology of live and growing cells with no signs of lysis or cell death (detached cells). Whereas the positive control (comprising cells treated with the toxic agent cyanoacrylate) exhibited only dead, round shape and floating, unattached cells.

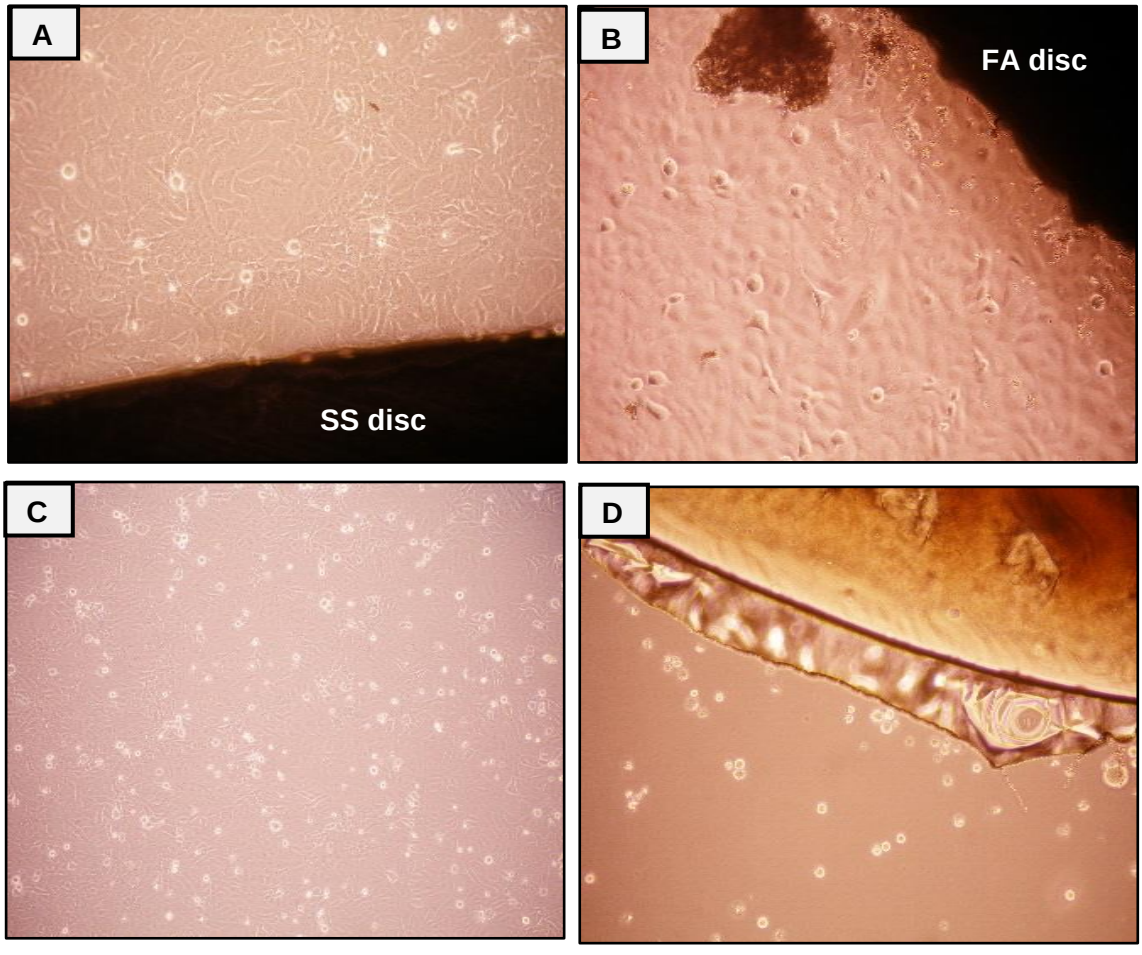

Figure 32: Images taken by a digital camera for osteoblast cells. The cells were cultured for 2 days with uncoated SS discs (A) and FA coated discs (B) revealing a good biocompatibility of the discs compared to the negative control (C) and the positive control (D). All the images were taken at x20.

➢ **Cell counting**

The direct contact cytotoxicity of FA coatings on osteoblast cells (G292) was determined quantitatively by counting the number of the cells cultured with uncoated and FA coated discs after 2 days using a haemocytometer. The media was collected and the cells were harvested by trypsin and counted manually (in duplicate for each group). Mean values of the number of cells of three samples per group are presented in figure 33. The data revealed a higher number of cells in all the tested groups, ranged between 90 $x10^4$ cells/mL and 120 $x10^4$ cells/mL compared to the positive control (100% toxic) (19 ±1.2 $x10^4$/mL). The uncoated SS discs showed a high number of cells (119± 24.8 $x10^4$/mL) comparable to that of the negative control (nontoxic group) (106±6.4 $x10^4$/mL). However, there appears to be less number of cells on FA coated discs (90±12.3 $x10^4$/mL) compared to the the negative control. The number of cells cultured with etched SS surfaces were slightly higher than that of the FA surfaces.

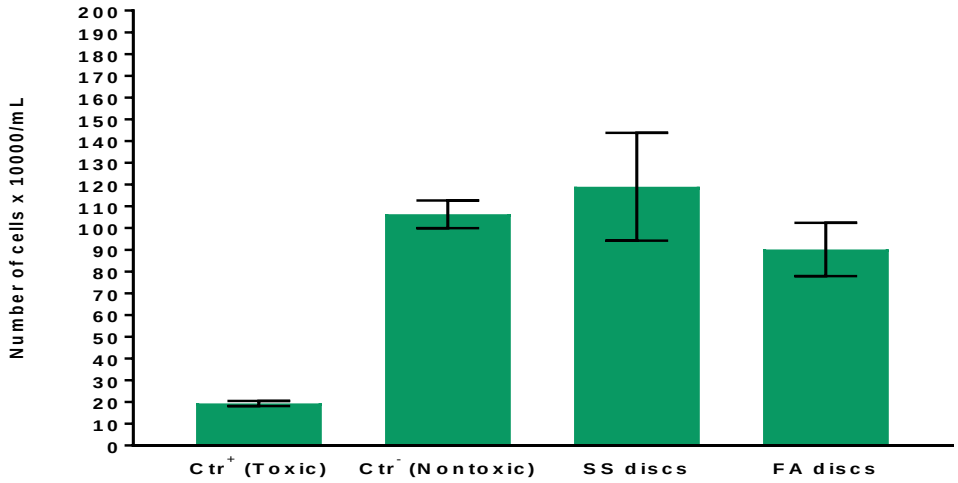

Figure 33: Number of osteoblast cells ±SD cultured directly for 2 days with FA coated and uncoated SS discs and counted manually using a haemocytometer (n=3). The positive control (Ctr^+) or the toxic group showed extremely low number of cells compared to the other groups. There appears to be fewer number of cells on FA coated discs compared to the negative control (nontoxic group) (Ctr^-).

➢ **LDH assay**

The media collected was subjected to LDH assays. Lactate dehydrogenase (LDH) is an easily measured glycolytic enzyme and is commonly used to measure cell lysis. The degree of cytotoxicity (LDH release) for each experimental group was determined as the ratio of released LDH amount and total LDH amount released from the positive control (toxic group) expressed as a percentage (Figure 34). In relation to the positive control (100% cell death), none of the experimental groups were cytotoxic, all of them showed % cytotoxicity less than 30%. The negative control showed the lowest release of LDH (1.4% ±8.2) compared to the positive control. However, LDH release measured in both of uncoated SS (13.3%±24.6) and FA coated (8.1%±19.2) groups were not different to that measured in the negative control group.

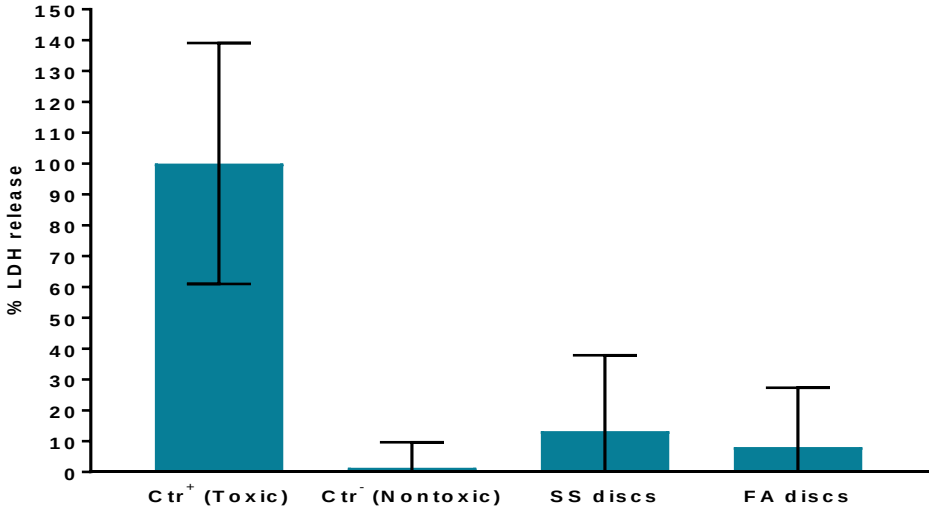

Figure 34: Cytotoxicity (% LDH release) ±SD of uncoated and FA coated SS discs in relation to the positive control (100% toxic) (n=3). Both showed no cytotoxicity compared to the positive control (Ctr^+). LDH release measured in both experimental groups was not different to that measured in the negative control (Ctr^-).

4.2.2.3.2 Indirect contact cytotoxicity test

The toxic potential of any material leaching out of the FA coating was tested by growing G292 cells in preconditoned medium (10% FBS that had been previously exposed to FA as described in section 3.1.5.2) for 1, 4 and 7 days. Cells cultured in unconditioned medium acted as negative control. At each time point, the media were collected and assayed for LDH release. The percentage of LDH release for each experimental group relative to the positive control (cells grown in media containing the cytotoxic chemical Triton 1% in PBS) was determined and plotted as illustrated in figure 35. FA-treated and non-treated groups were not toxic compared to the positive control at all time points. The FA treated groups exhibited less than 30% cell death compared to the control after one day (9.6% ± 1.7) and four days (16% ± 4) of cell culture. However, after 7 days, a slight increase of cell cytotoxicity above 30% was seen in the FA-treated group (30.9% ±11). It is noteworthy that the FA treated cells showed a similar level of LDH release to the untreated cells at any time point indicating that there was no evidence of any potential cytotoxic material leaching out of the FA coatings.

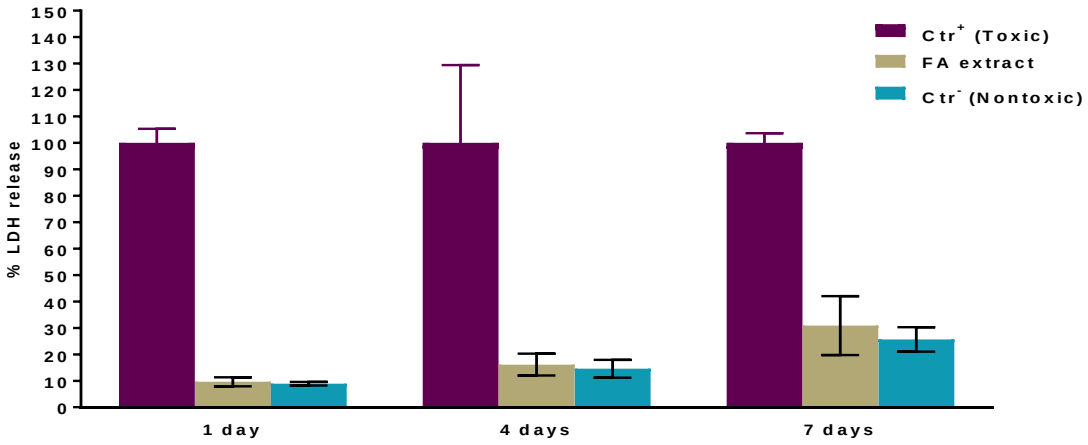

Figure 35: Percentage of LDH release ±SD of FA extract and negative control (Ctr^-) cultures in relation to the positive control (100% toxic) (Ctr^+) after 1, 4 and 7 days of cell culturing (n=3). FA showed no cytotoxicity and showed no difference to the untreated cell culture in LDH release compared to the positive control.

4.3 Discussion:

In this study, FA coatings were synthesised on grade 316 stainless steel (SS) discs using a hydrothermal synthesis as described by Chen et al (2006b) and Czajka-Jakubowska et al. (2009a). The synthesis procedure was carried out by controlling the pH of the reaction solution and by using EDTA to stabilise the calcium ions in the precipitation solution allowing their slow release under the mild hydrothermal conditions (121°C, 2 atm for 10 hours).

Stainless steel (medical grade 316) discs were used in the present study as coating substrates instead of titanium for various reasons. Firstly, Czajka-Jakubowska et al. (2009b) compared FA coatings grown on titanium and SS surfaces, and found that the FA crystal composition, alignment, size, shape and structure were identical for both surfaces. SS metal bars are cheaper and available in more varied sizes when purchased and relatively easy to cut and polish compared to titanium. Finally and most importantly, the present study focuses on investigating the FA coating as an osteoconductive biomaterial or scaffold interfacing between the implant surface and the surrounding bone rather than the underlying substrate surface itself.

Before being coated with FA crystals, the SS discs were etched with a mixture of sulphuric acid and hydrogen peroxide (piranha solution) as recommended by Czajka-Jakubowska et al., 2009a. This solution is an extremely powerful oxidising agent as well as strongly acidic and treatment of the metal substrates is believed to etch the surface material to provide surface roughness, reduce surface energy and decrease the possibility of contamination as any organic contaminates are oxidised (Braceras et al., 2009).

The current study investigated how the orientation of the discs during the coating process would affect the subsequent growth of the FA crystals. The SS discs were coated while tilted at 45° or positioned vertically. The tilted discs showed microscopically two different growth patterns for the FA crystals; disorganised on upper surfaces and organised on under surfaces. This finding was consistent with the research performed by Chen et al. (2006b), Czajka-Jakubowska et al. (2009a and b) who reported that as the crystals grow on the under surface, the densely packed growth mode along the c-axis forced them to align parallel to each other leading to the deposition of highly orientated FA

films with a similar growth rate. Moreover, crystals growing on the under surfaces were self-assembled or packed together in cohorts. This was most likely due to the strong attraction among adjacent crystals which causes the spontaneous aggregation of these rods into bundles reportedly similar to those seen in human enamel (Chen et al., 2006b; Czajka-Jakubowska et al., 2009b). The comparison of these bundles to human enamel prisms should be regarded with caution. The width of a single FA crystal is approaching the width of a real enamel prism which is composed of thousands of crystals and the aspect ratio (length/width) of a real enamel prism may be as much as 400:1 (assuming prisms transverse the full enamel thickness). Whereas the FA crystals here have a ratio of about 5:1 or less.

In contrast to the under surfaces, FA crystals on the upper surfaces were randomly arranged which may be related to precipitation of several crystal layers over the already established crystal film resulting in the disorganised orientation of the crystals, according to Czajka-Jakubowska et al. (2009a). However, the role of gravity cannot be ignored as any mineral particles nucleating in free solution may have a high propensity to settle on the upper surface in a random orientation, and as they elongate, give rise to the random crystal orientation. In contrast, the underside are more likely to be populated by crystals that nucleated on the steel surface (which acts as a nucleating template), rather than settling there randomly under the influence of gravity. Subsequent elongation of these crystals gives rise to a more organised crystal coating. However, the chemical composition of both types of coatings (disorganised and organised) was the same as they were grown from the same mineralising solution under the same conditions. This similarity in the chemical composition of the coatings is in agreement with Czajka-Jakubowska et al. (2009a).

Analysis of the crystal size distribution showed that FA crystals' average diameter ranged between 1-3 μm and length 10-30 μm, similar to the dimensions reported by Chen et al (2006b). However, disorganised and organised FA coatings might have different thickness. Alhilou et al. (2016) revealed that the organised coatings are thinner than disorganised coatings

(7.28 ± 0.46 μm compared to 49.07 ± 6.58 μm), depending on SEM, 3D optical profilometer and diffraction peaks associated with the underlying SS substrate. The chemical compositions and morphological features of the FA coatings produced in this study were similar to that produced by Chen et al. (2006b) who further investigated and identified the phase composition and crystallinity of the synthetic crystals using X-ray diffraction (XRD). They found that all the diffraction peaks can be readily indexed to a pure hexagonal phase with lattice constants a = 9.331 Å and c = 6.840 Å that are characteristic of FA. The same synthesis method of FA was adopted in previous studies (Alhilou et al., 2016; Al-Taie, 2017) in which the apatitic structure and the high crystallinity of FA coatings were confirmed. It is believed that fluoride may aid the stability of the coatings which could be clinically advantageous (Okazaki et al., 1981). Alhilou et al. (2016) also indicated that the diffraction pattern of the organised coatings showed the same peak positions as that of the disorganised coatings, but with different peak heights, confirming the similarity of the material but with preferential orientation of the crystals.

In the current study, vertically positioned FA coated discs were also prepared and investigated. In contrast to the tilted discs, vertical discs generally exhibited an organised crystal alignment on both surfaces. This supports the contention described above that the upper surface of a tilted disc is subject to crystals growing from nucleating centres that settled on the surface randomly. These crystals then grew in addition to nuclei forming directly on the surface to generate the disorganised layer observed. With vertical discs both sides would be subject to nuclei forming directly on the surface as opposed to nucleating centres settling on the surfaces randomly. However, small patches of disorganised crystals were observed on each surface of the coated discs preventing its usage as a typical organised coating.

The impact of washing and drying on the elemental composition, attachment and orientation of FA crystals was investigated and compared between three groups; the first group was only subjected to a drying step following the hydrothermal coating process with no washing, a second group was dried following the hydrothermal coating process then washed then dried again while a third group was washed following the hydrothermal coating process then

dried. Washing is a chemistry term used for removing any excess reactants after a chemical reaction is completed (Nordquist, 2011). In this study, the upper surfaces of unwashed 45° tilted discs showed disorganised crystals embedded in magma of a residual material. The magma was probably the result of the precipitation of excess mineral ions and residues of EDTA hydrolysis. This hypothesis was supported by EDS results which showed a higher percentage of carbon on the upper surfaces of unwashed discs compared to washed upper surfaces, resulting more likely from the precipitation of a mixed salt comprised of EDTA (a carbon rich organic compound) and other reactants as the surfaces dried in air. The magma was also seen on unwashed under surfaces but to a lesser extent. Washing the discs before or after drying eliminated the magma presumably because the salts comprising the magma are relatively soluble. The coatings on washed discs were predominantly composed of calcium, phosphate and fluorine, presumably due to removal of the more soluble salts containing residual EDTA and other salts.

Fluoride is cytotoxic, and as reported by Nordquist (2011), excess fluoride from FA coatings might interfere with the clotting of blood in an implantation site. Therefore, washing of the coatings to remove readily soluble fluoride salts present as contaminats is an essential consideration for future work especially when thinking about how FA coatings might be translated into the clinical setting. Leaching of fluoride may be deleterious biologically and in terms of public acceptance given the passions that surround the debate on fluoridated water. From the results of this study, it can be concluded that the drying process pre or post washing had no effect on crystal alignment, attachment or elemental composition. Therefore, for all the subsequent cell experiments, following hydrothermal synthesis, the coated discs were washed, dried and sterilised autoclaving at 121°C for 1 hour.

PBS has been used previously for washing FA coated discs under sterilized conditions (Liu et al. 2010, 2011 and 2012). How washing with PBS compared to using distilled water at pH 7 (as used in this study) affects the chemistry of the coating and henceforth cell attachment and growth is unclear. However, since discs should be placed in culture medium prior to cell seeding, the nature of the washing solution may be of little consequence. Intuitively, washing with

distilled water is preferable since it would be expected to be more effective than PBS in washing away soluble salts. This is due to the common ion effect where the ions in PBS; phosphate, sodium, potassium and chloride, will inhibit the solubilisation of contaminating salts containing phosphate and sodium from the hydrothermal reaction.

Ca/P and Ca/F ratios in the current study were close to the theoretical values of FA. The ratios were similar in both of the disorganised and organised FA coatings. Unwashed and washed groups had the same ratios as well.

In this study, biocompatibility of uncoated and FA coated SS discs was studied using SEM and confocal microscopy. A high number of evenly spread cells were seen on the etched uncoated SS discs adopting a fibroblastic configuration typical of that observed in traditional 2D monolayer culture. However, the cells grown on disorganised and organised FA coatings exhibited different configurations. On the disorganised FA surfaces, the cells formed isolated clusters. They created a 3D cellular network between the crystals through establishing filopodia and intercellular connections. Filopodia are one-dimensional structures filled with cores of long, bundled actin filaments (Alberts, 2002). The cells of the organised FA surfaces were more spindle-like in shape compared to the cells of the disorganised coatings. They attached to the underlying crystals and exhibited prominent cytoplasmic extensions indicative of cell adhesion, migration and proliferation. The cells seemed to maintain physical contact with each other and migrate using long, thin and dynamic filopodia confirming the potential support of the coatings to the cellular growth. This was in accordance with studies of Liu et al. (2010, 2011 and 2012) and Czajka-Jakubowska et al. (2011) who investigated the cell response to FA coatings. They revealed that both organised and disorganised FA coatings appeared to induce cell adherence, growth, differentiation and mineralization, but to a greater extent for the organised coatings. It is believed that adsorbed proteins may act as mediators for cell adhesion if they have the correct geometry (Roach et al., 2005). The different topographical and physical properties of the two coating surfaces (e.g. van der Waals forces and hydrophobic) have probably led to difference in proteins adsorbed to both surfaces and the subsequent difference in cell behaviour and morphology (Liu et al., 2010). Furthermore, the

capabilities of the cells in sensing the substrate geometry, rigidity and microstructure was reported previously (Vogel and Sheetz, 2006). They stated that the cells transfer these geometrical and physical signals into cellular biochemical signals that regulate various cellular events. Liu et al. (2010) observed enhanced mineralized tissue formation integrated within organised FA coatings where over 80% of the organised FA coating was integrated with the mineralized tissue layer covering the substrate surface after 5 weeks, in comparison to 40% integration in the case of the disorganised FA coating.

The preliminary observation of this study identified a relatively high number of G292 cells under the microscope grown on the disorganised surfaces compared to the organised surfaces after 2 days in culture. This was probably due to the higher roughness and increased surface area of the disorganised surfaces as indicated by Alhilou (2016) compared to uncoated SS and organised FA surfaces. Osteoblastic adhesion and proliferation and collagen synthesis were reported to increase on the rough surfaces (Wennerberg and Albrektsson, 1999; Boyan et al., 2001). However, it is important to appreciate that the current data are only derived qualitatively from a limited number of samples. Thus, further quantitative studies are needed to generate data and conduct a meaningful statistical analysis in order to compare cell attachment, proliferation and differentiation over both types of FA topographies.

Finally, in the current study, both of the direct contact and indirect contact (FA extract) cytotoxicity tests showed clearly that FA was not cytotoxic compared to the positive and negative controls. In addition, FA and uncoated SS showed no difference in LDH release. Under phase-contrast microscopy, a high number of spindle and confluent cells were seen to grown beside the FA coated discs. However, the number of cells cultured with etched SS surfaces were slightly higher than that of the FA surfaces after 2 days of cell culture. This finding was in agreement with earlier studies which investigated the growth of MG-63 osteoblast-like cells and adipose -derived stem cells on SS and FA discs for 3 days (Liu et al. 2010 and 2012). However, the potential release of Ca^{2+} from FA samples may inhibit trypsin enzyme activity used for detachment of the cells prior to cell counting. In addition, the 3D structure of the FA coating could prevent the complete exposure of the cells to trypsin and even when released

cells could be mechanically trapped in the forest of crystals that could compromise the collection of the cells compared to the flat surfaces of SS discs (negative control) and lead to artefactual low cell counts for the FA surfaces. This result was in contrast to a previous study, in which no significant difference was found between the number of dermal-derived human microvascular endothelial cells grown on SS and organised FA surfaces for 1, 7 and 14 day when trypsinised and counted manually (Wang et al., 2013).

In summary, the present work showed that disorganised and organised FA coatings were synthesised successfully on etched SS discs. They have different topography but were very similar in chemical composition. This study indicated that both FA coatings were biocompatible and not cytotoxic.

Chapter 5: Results and Discussion (Platelet-Rich Plasma)

5.1 Introduction

PRP is a concentrated derivative of blood plasma that has a platelet concentration 3-8 times above that of blood. It is potentially a rich source of growth factors (GFs) as these bioactive molecules, sequestered in platelets, can be released after platelet activatation (Marx, 2004). PRP was introduced in 1998 by Marx et al. as a successful, novel approach to tissue engineering in oral surgery. When applied locally in a bone healing site, GFs released from PRP can potentially enhance the recruitment, proliferation and differentiation of stem cells and subsequently promote the initial bone healing response (Garg, 2000; Mehta and Watson, 2008). When the initial, direct influence of PRP fades away with time, the physiological mechanisms of bone repair continue to proceed at a faster rate (Jakse et al., 2003). Currently, there is limited scientific evidence in the dental literature in favour of the clinical use of PRP for bone regeneration. PRP is used clinically in an inactivated liquid form that can be easily injected in the defect area or as a coating on the implant surface so that the platelets can be activated later by contact with the surrounding collagen tissue (Roberts et al., 2004). PRP was also used in the surgical sites in a hydrogel formulation by activating the PRP with an exogenous activator such as batroxobin, chitosan, calcium chloride, thrombin or a combination of the last two activators (Betoni-Junior et al., 2013). The high concentration of platelets and the native amount of fibrinogen have encouraged the use of PRP gel as osteoinductive, osteoconductive scaffold for bone defect bridging (Kawase et al., 2003; Malhotra et al., 2014; Jalowiec et al., 2015). Another form of PRP that was used successfully to enhance cell viability in vitro and to induce the tissue healing process in vivo is PRP lysate or releasate (the active soluble releasate isolated following platelet activation of PRP). It is derived from the PRP gel by centrifuging the gel at high speed and extracting a liquid form of plasma rich in GFs (Aiba-Kojima et al., 2007; Schallmoser et al., 2007; Fallouh et al., 2010). The clinical efficiency of PRP remains controversial as evidenced by contradictory in vivo studies (Thor et al., 2005; Anitua, 2006; Gentile et al., 2010, Garcia et al., 2010). In vitro, studies have also obtained conflicting results

when investigated the effect of PRP on cell function (Liu et al. 2002; Lucarelli et al. 2003; Gruber et al. 2004; Kilian et al. 2004; Soffer et al. 2004; Kanno et al. 2005; Koellensperger et al., 2006; Kocaoemer et al., 2007). It is still uncertain which concentrations of PRP are optimal in promoting cell viability. Also, little has been reported comparing the influence of PRP gel to PRP releasate on cell proliferation. Therefore, the aim of this study was to determine and to analyse in vitro, the effect of PRP gel and PRP-releasate on osteoblast-like cell viability and proliferation.

5.2 Results

5.2.1 Characterisation of the prepared PRP (platelet concentration)

PRP samples were extracted from three blood donors according to the protocol mentioned previously in section 3.2.1. The platelet (Plt) count analysis was performed manually on PRP samples for each study participant using a haemocytometer and by using automated cell counting machine. For each donor, the counting was repeated twice, and the data were represented as a mean ± standard deviation as shown in table 7.

Table 7: Platelet concentration (mean ± SD $x10^3$/ µL) counted manually and automatically in PRP samples from 3 blood donors. PRP concentration resulted in around an 8 fold and 5 fold increase in platelet concentration over reference values for whole blood for manual and automatic counting respectively.

Platelet concentration ($x10^3$ /µL)		
	Manual counting	**Automated counting**
Donor 1	1355 ± 78	469 ± 139
Donor 2	1564 ± 5	1177 ± 239
Donor 3	1992 ± 260	1572 ± 212
Mean ± SD	1637 ± 324	1073 ± 559

Platelet counts performed manually yielded a mean platelet value of 1637 x 10^3 ± 324 $x10^3$ Plt/µL (ranged from 1355 $x10^3$ ± 78 $x10^3$ Plt/µL to 1992 $x10^3$ ± 260 $x10^3$ Plt/µL). Whereas the automated cell counter yielded a lower mean platelet value of 1073 $x10^3$ ± 559 $x10^3$ Plt /µL (ranged from 469 $x10^3$ ± 139 $x10^3$ Plt/µL to

1572 x10^3 ± 212 x10^3 Plt/µL). It was well known that the average platelet count in healthy human adults is about 200 x10^3/µL. Therefore, manual counting indicated that the platelets had been concentrated by a factor of about 8 compared to whole blood while the results obtained using automatic counting indicated that the platelets had been concentrated by a factor of about 5. The 3 donors showed different levels of platelet numbers in the same way when using manual or automated counting.

In addition to the platelets, concentrations of white blood cells (WBCs) and red blood cells (RBCs) in PRP and corresponding PPP samples were also been measured using automated cell counting. The results presented for each donor as mean ± SD in table 8, showed that the PRP samples contained a very low number of WBCs and RBCs. Whereas PPP samples had very low number of platelets (4.2 x 10^3 ± 5 Plt/ µL) and had no WBCs and RBCs.

Table 8: Platelets concentration (mean ± SD x10^3/ µL), white blood cells (WBCs) (mean ± SD x10^3/ µL) and red blood cells (RBCs) (mean ± SD x10^6/ µL) counted automatically in PRP and PPP samples of 3 donors.

	Plt x10^3		**WBC x10^3**		**RBC x10^6**	
	PRP	**PPP**	**PRP**	**PPP**	**PRP**	**PPP**
Donor 1	469.0 ± 139	10.0 ±1	0.3 ±0	0.0 ±0	0.0 ±0	0.0 ±0
Donor 2	1177.0 ± 239	2.0 ±3	0.7 ±0	0.0 ±0	0.1 ±0	0.0 ±0
Donor 3	1572.0 ± 212	0.5 ±1	0.5 ±1	0.0 ±0	0.1 ±0	0.0 ±0

5.2.2 Cytotoxicity of PRP (LDH assay)

Two experimental set-ups were used to assess the cytotoxicity of PRP on G292 osteoblast-like cells after 3 days of cell culture. In the first experiment, the cytotoxicity effect of non-activated and activated forms of PRP was assessed on monolayer culture of G292 cells. In the second experiment, cytotoxicity was assessed when G292 cells were seeded on, or encapsulated in PRP gel (cells-PRP construct) (Methods chapter, section 3.2.3). The cytotoxicity was evaluated by assaying the media for LDH. This is a convenient method to evaluate the cell damage, since LDH is released from lysed cells. All the tested

groups were analysed for LDH release and normalised to the positive control (100% cell death). According to ISO 10993-5:2009E (DIN), a decrease in cell viability by more than 30 % is regarded as evidence of cytotoxicity.

5.2.2.1 Cytotoxicity of non-activated and activated PRP

G292 cells were cultured under standard culture condition for 24 hours then treated with medium supplemented with 5% of either non-activated PRP or PRP activated with $CaCl_2$. Both culture media (non-activated and activated PRP media) were allowed to stand for 30 min at room temperature before being added to the cells and incubated for 3 days. It was revealed that the absorbance values of the negative control, non-activated PRP and activated PRP were much lower than the positive control (Figure 36). As non-activated PRP and activated PRP induced less than 30% LDH release, they are therefore considered not cytotoxic. Interestingly, activated PRP showed lower LDH release (8%) relative to the positive control than non-activated PRP (15%). This result means that activated PRP induced less damage on cell membrane and maintained the cell viability compared to non-activated PRP. Compared to the negative control, non-activated PRP displayed a higher amount of LDH release while activated PRP showed a similar amount of LDH to that of the negative control (8.6%).

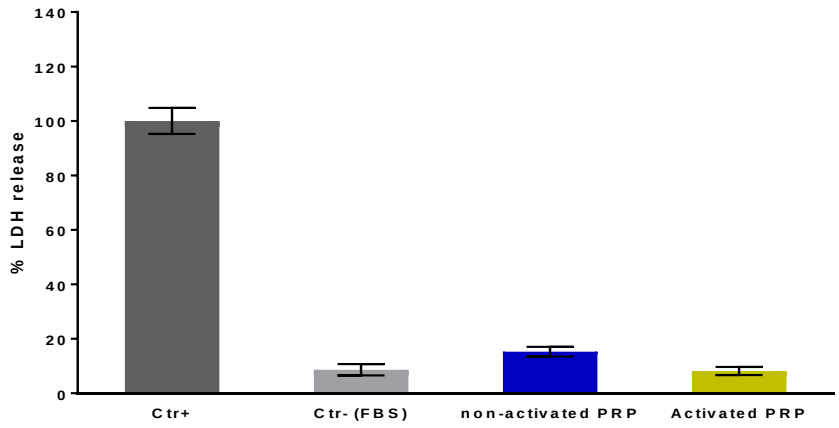

Figure 36: Cytotoxicity (% LDH release ± SD) of 5% PRP added to 24 attached G292 cells as non-activated or activated form in the culture medium. All the groups showed no cytotoxicity. However, activated PRP showed greater influence on cell viability compared to non-activated PRP.

5.2.2.2 Cytotoxicity of cell-PRP constructs

Three approaches were used to incorporate cells to PRP (PRP added to a final concentration of 5% or 10% (vol/vol) of the culture medium). In the first approach, cells were seeded on pre-established PRP gels and overlaid with serum- free media (PRP gel under cells). In the second approach, the cells were mixed with serum-free media containing PRP prior to coagulation with $CaCl_2$ (i.e. cells were grown encapsulated in PRP gel). In third approach, cells were cultured with serum- free media containing PRP releasate. The control comprised cells grown in media supplemented with 10% FBS alone.

As shown in figure 37, all the experimental conditions induced less than 30% of the total LDH release seen in the positive control, and therefore these conditions were considered non-cytotoxic. However, 10% PRP promoted cell viability when compared with 5% PRP in all 3 groups. Furthermore, the groups containing 10% PRP induced LDH release (4- 5%) at comparable levels to that of the negative control (4%). While 5% PRP groups induced an increase in LDH release (12-15%) compared to the negative control.

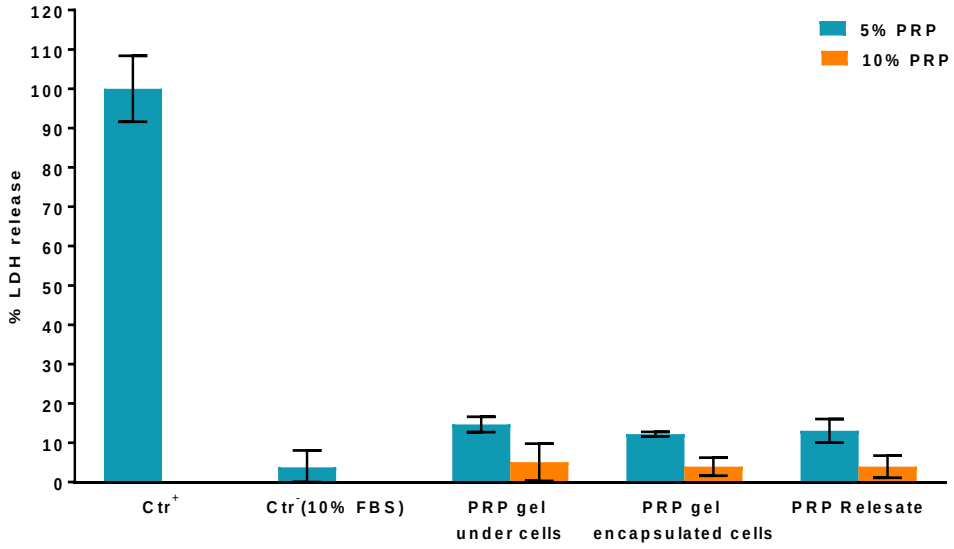

Figure 37: Cytotoxicity (% LDH release ± SD) of two PRP concentrations (5% and 10%) used in 3 different cell culture scenarios. None of the groups showed cytotoxicity but 10%PRP enhanced the cell viability compared to 5%PRP. All 10%PRP groups and the negative control showed the same impact on cell viability.

5.2.3 Effect of PRP on G292 osteoblast-like cell attachment and proliferation

The attachment and proliferation of G292 cells cultured with 10% PRP under the conditions described above in section 5.2.2.2 was investigated by measuring DNA content. This required efficient digestion of the construct and cells in order to release the cellular DNA. The digestion was optimised using two procedures (see section 5.2.3.1).

5.2.3.1 Optimisation of cell and PRP gel digestion procedure

This optimisation experiment was done to determine the most effective digestion method. This was done by comparing the DNA yield obtained to the theoretical amount of DNA present in the seeded cells (assuming 0.0066ng DNA/cell). The doubling time of the cells was obtained in this study following a simple protocol (Korzyńska and Zychowicz, 2008) (data not shown) and it was 27 hours. In this experiment, the cells were seeded in 24-well plates (2 cm^2 surface area) at a density of $10^4/cm^2$ (2 x 10^4 cell/well) for 3 days. Thus, the expected DNA content after 3 days should be around 8 fold (2^3 fold) the initial number of cells (~1000 ng)

Theoretical DNA content = 8 x 2 x 10^4 x 0.0066 = 1056 ng

Optimisation for DNA quantification of G292 cells cultured for 3 days in 10% PRP and 10% FBS supplemented media was carried out using 2 common methods for cell digestion; 0.1% Triton and papain (described in Methods chapter, section 3.2.4.2). DNA content (ng) was obtained and mean data (mean ±SD) were plotted (Figure 38). DNA content of the control (FBS) extracted by Triton was 290ng ± 81, whereas papain extraction of FBS had DNA content of 700ng ± 31 which was closer to the expected values (~ 1000ng) than Triton values. In PRP samples, the result showed a higher amount of DNA extracted by papain ranged from 412 ng ± 18 to 748 ng ± 81 compared to Triton (149 ng±5 - 220ng± 11). Based on the finding of this experiment that papain was more efficient than Triton in digesting the cells, it was decided to use papain for the subsequent DNA PicoGreen experiments.

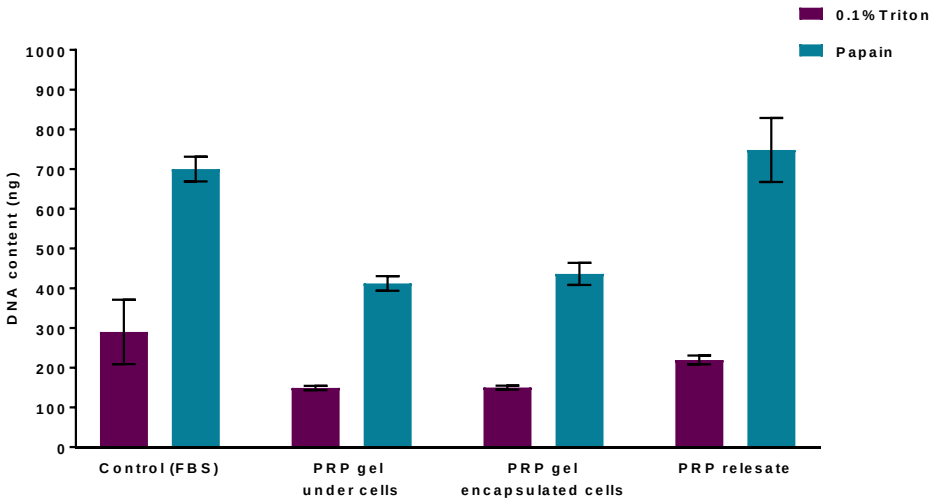

Figure 38: A comparative study for cell digestion using 0.1% Triton and papain. G292 cells were seeded either: on control medium, on pre-established PRP gel, encapsulated in PRP gel or on medium containing PRP releasate for 3 days. DNA content (mean ±SD) for each group was determined using the picogreen assay. The results showed a higher amount of DNA closer to the expected values was extracted by papain compared to Triton in all groups.

5.2.3.2 Effect of PRP on G292 cell attachment and proliferation

G292 cells were cultured under the 3 conditions described above (cells seeded on PRP gel, cells grown encapsulated in PRP gel and cells cultured in PRP releasate supplemented medium) and compared with cells cultured in media supplemented with 10% FBS which acted as control. Cell attachment and proliferation were monitored and assessed by measuring the amount DNA content (ng) after 5 hours of cell seeding (day 0) and after 1, 4 and 7 days. The experiment was repeated twice separately using 2 PRP samples extracted from 2 blood donors. Complete individual data sets for donor 1 and donor 2 are presented in appendix 1. Cell-population density tended to increase in all four groups over the 7 days in cultures associated with both donors. However, PRP releasate greatly enhanced the cell proliferation over time as compared with the others. DNA content of all the groups was normalised to the control (10% FBS) and mean data (mean ±SD) of the 2 PRP donors plotted for each time point (Figure 43 and 44).

After five hours of seeding the cells on the different constructs described above (Figure 39), the number of cells grown in PRP gel groups and in media containing PRP releasate (ranged between 90% and 123%) were not different to that grown in FBS control (100%). In contrast, after one day of cell culture (Figure 39), the cell releasate group exhibited a DNA content of about 96% similar to that of the control (FBS), while both PRP gel groups showed low DNA content (30%- 38%) compared to FBS and to PRP releasate.
Interestingly, PRP releasate increased the proliferation rate of the cells compared to the control to 144% by day 4 and 139% by day 7 as shown in figure 40. PRP releasate induced cell proliferation at higher levels compared to PRP gel groups at both time points. PRP gel under cells group showed lower DNA content compared to the control by 29% at day 7.

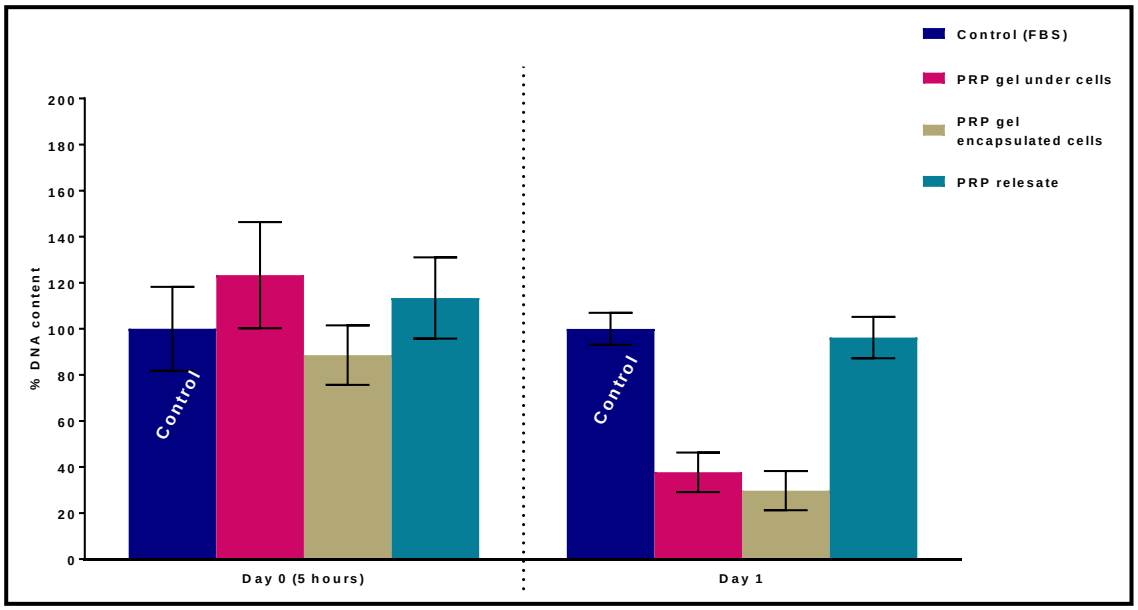

Figure 39: Cell attachment of G292 cells seeded on PRP gel, incorporated with PRP gel and in PRP releasate supplemented medium for 5 hours and 1 day. DNA content of the groups was normalised to the control (10% FBS) and mean data ±SD of 2 PRP donors plotted for each time point. All PRP groups promoted cell attachment for 5 hours at a comparable level to the control. However, PRP gel groups showed lower DNA content compared to the control and to PRP releasate.

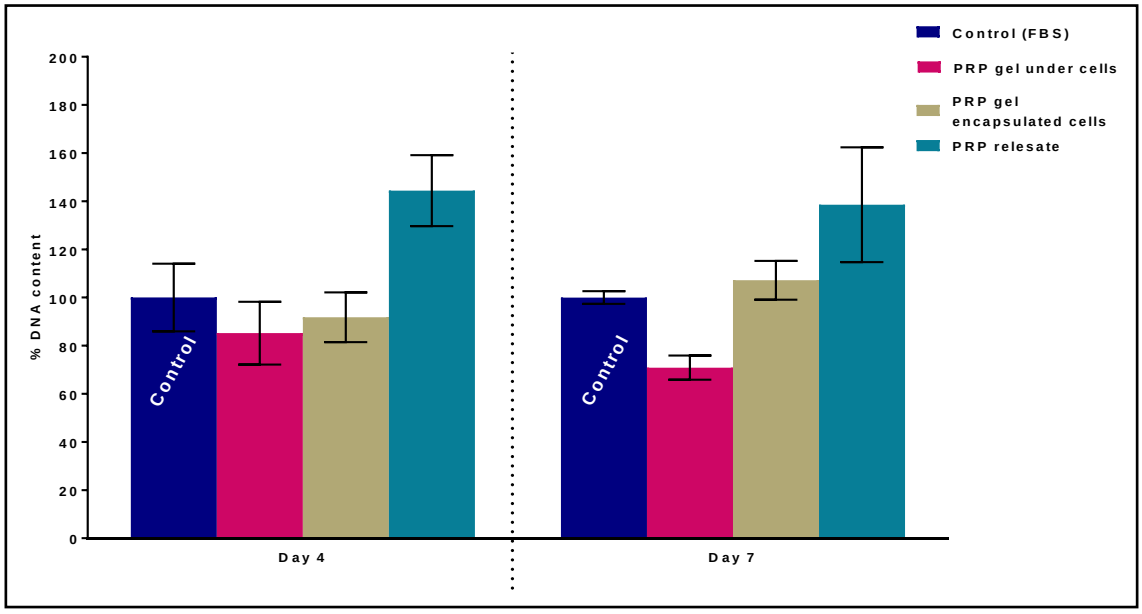

Figure 40: Proliferation of G292 cells seeded on PRP gel, incorporated with PRP gel and in PRP releasate supplemented medium after 3 and 7 days. DNA content of the groups was normalised to the control (10% FBS) and mean data ±SD of 2 PRP donors plotted for each time point. PRP releasate induced the highest rates of cell proliferation over time as compared with the control and the other PRP groups.

5.3 Discussion:

In the current study, blood samples were collected from healthy young donors aged 25-35 years of both genders. No influence of gender or age on platelet count and growth factor concentrations was detected by Weibrich et al. (2002). PRP was prepared manually from whole blood using a two-step centrifugation procedure. In the first step, the blood was subjected to a soft spin (200 g for 10 minutes) and in the second step, the blood plasma obtained was subjected to hard spin (1000 g for 10 minutes). Several automated systems and manual protocols for PRP preparation are available. However, each method generates a different PRP product with different biological properties and uses. It is reported that up to 50% of the variation in GFs concentrations present in PRP can be affected by the degree of contamination with WBCs (Zimmerman et al.,

2001). Ehrenfest et al. (2009) stated that elimination of WBCs is more difficult using manual PRP preparation protocols compared to automated systems. However, the PRP samples produced manually in this study were WBCs-free samples as evidenced by the results shown in section 5.2.1.

PRP is consistently defined by the absolute quantity of platelets. Thus, in the present study, the total number of platelets (per microliter) was determined for aliquots of PRP samples from 3 blood donors. The platelet counting was performed manually using a haemocytometer and automatically using a cell counting machine. There has been some debate over which method counts more accurately. Previous comparative studies reported acceptable agreement between machine counting and the counting using phase contrast microscopy (manual counting) (Rowan et al., 1972; Woodell-May et al., 2005). In contrast to the above studies, Hänseler et al. (1996) reported that automated counting is more precise than the manual counting. In the current study, the quantification of platelets showed lower number of platelets when quantified in the automatic cell counter compared to the manual counting. It may be happened due to platelets clump formation resulting in a miscounting. In order to prevent platelets clumping, the PRP samples have to be adequately mixed for 5 min before automatic counting (Woodell-May et al., 2005).

The average platelet count of the 3 donors performed manually was 1637 $x10^3$ ± 324 $x10^3$ Plt/µL and automatically was 1073 $x10^3$ ± 559 $x10^3$ Plt /µL. Thus, the platelet count obtained in this study was about 5- 8 times greater than the physiological average count in healthy human adult plasma (200 $x10^3$ Plt/µL). The concentration of 1000 $x10^3$ Plt /µL was suggested previously to be the working definition of what constitutes reliable therapeutic PRP levels (Marx, 2001). Lower or higher concentrations might not enhance wound healing (Marx, 2004). In early in vitro studies, platelet concentrations 2- 4 times above the baseline blood levels were suggested to promote the proliferation and differentiation of primary osteoblasts and fibroblasts (Graziani et al., 2006; Anitua et al., 2009a). Interestingly, it was proved earlier that excessively high concentrations of platelets (>2000 x 10^3 Plt/µL) in PRP might have deleterious effects on healing process (Foster et al., 2009; Yamaguchi et al., 2012). Jalowiec et al. (2015) confirmed this when they demonstrated the potential of

PRP gel containing 1000 x 10^3 Plt/µL to promote MSCs' proliferation compared to PRP gels of 2000 x 10^3 and 10000 x 10^3 Plt/µL. In the light of the above studies, the PRP concentration obtained herein was regarded to be within the recommended range required to enhance a cellular response.

The efficacy of PRP is based on the release of multiple GFs when platelets are activated. Hence, the biocompatibility of PRP samples was examined in the current study by examining the viability of pre-attached G292 cells incubated with activated and non-activated PRP supplemented culture medium. The high dose of GFs contained in the activated PRP medium reduced cell death compared to non-activated PRP. By activating the PRP with an exogenous activator such calcium chloride, two key processes may be initiated; activation of platelets to release GFs from their α-granules and the cleavage of fibrinogen into insoluble fibrin (Wasterlain et al., 2012). It was previously demonstrated that the minimal PRP concentration required to obtain the gel formation is as low as 0.5% in the culture medium and gelation occurred as rapidly as 30 minutes post activation (Kawase et al., 2003). Platelets begin actively secreting GFs and clotting within 10 minutes after activation, with more than 95% of the pre-synthesised growth factors secreted within 1 hour. Then, the platelets synthesise and secrete further GFs for the remainder of their life span (5-9 days) (Marx, 2004). The proportional relationship between high GFs concentrations and cell proliferation was evaluated in many studies (Eppley et al., 2004; Cho et al., 2011). The result of this study could be correlated with the findings of Kakudo et al. (2008), who detected a higher proliferative effect of activated PRP and higher levels of PDGF and TGF growth factors compared to the non-activated PRP group. PDGF and TGF are believed to trigger the preosteoblasts to undergo mitosis and differentiation into mature osteoblasts which eventually leads to bone remodeling and mineralization (Marx et al., 1998; Carlson, 2000). In contrast, Han et al. (2009) reported that non-activated PRP has greater positive impact on proliferation of osteosarcoma and stromal cells in vitro and on the osteoinductivity of demineralised bone matrix in vivo compared to thrombin- activated PRP.

In the literature, many studies have investigated the effect of PRP on cell proliferation in vitro but few have investigated the potential cytotoxicity of PRP

gel and its effect on cell viability. The cytotoxicity of two PRP concentrations (5% and 10%) under three PRP configurations was investigated. There were: (i) cells grown on PRP gel and overlaid with serum free media, (ii) cells encapsulated in PRP gel and overlaid with serum free media and (iii) growing cells in serum free media supplemented with PRP relesate. PRP at concentrations of 5% or 10% showed no cytotoxic effects. Previous studies confirmed the positive effect of 5% PRP supplemented medium on proliferation of osteoblast cells (Okuda et al., 2003) and viability of periodontal fibroblast cells in which PRP was activated woth calcium chloride (Tavassoli-Hojjati et al., 2016). In the present study, the viability of the cells was enhanced in 10% PRP samples compared with the 5% PRP. This finding was similar to the report of Kanno el al. (2005) who found that 10% PRP enhanced osteoblast-like cell viability, proliferation and diffrentiation compared to 5% PRP and related this effect to the greater amount of GFs released from the more concentrated preparation. Fallouh et al. (2010) also found in vitro a greater cell viability of anterior cruciate ligament cells in 10% PRP releasate compared to 5% PRP releasate supplemented media. Different GFs concentrations might result in different effects on cell viability. A linear increase of some GFs with increased platelet numbers has been observed and reported earlier (Zimmermann et al., 2001; Eppley et al., 2004; Cho et al., 2011). However, no correlation was detected by Weibrich et al. (2002) between GFs contents and PRP concentration which might be attributed to the fact that they induced the release of the growth factors from PRP by freeze/thaw cycles without any exterior activator. In vitro, certain studies found that 10% PRP releasate caused a marked increase in cell proliferation of mesenchymal stem cells compared to lower or higher concentrations (Gruber et al., 2004; Mishra et al., 2009; Cho et al., 2011). Li et al. (2013) reported that 20% PRP releasate caused a significant increase in human muscle derived progenitor cells proliferation compared to 10% PRP releasate. In contrast, Choi et al. (2005) showed that the viability and proliferation of alveolar bone cells were suppressed by high PRP concentrations compared to low concentrations (1% and 5% in media). Kakudo et al. (2008) as well could not find any significant differences between the effects for 10% and 20% PRP releasate samples on human adipose derived stem cells and human

dermal fibroblast cells compared to lower doses (1% and 5%). Hsu et al. (2009) attributed the reason of the cellular anti-proliferative effect of high concentrations PRP to the presence of negative regulators in PRP (e.g. thrombospondin). While, Liu et al. (2002) related this negative effect to the pH changes associated with high PRP concentrations that adversely affect cell proliferation. In addition, these contrasting data may be related to the possibility that different cell types respond differently to PRP (i.e. the specific cell context may determine cellular response to PRP) and the different methodologies used in these studies (Graziani et al., 2006).

In addition to cytotoxicity, the present study examined G292 cell proliferation when cultured with PRP obtained from 2 blood donors over 7 days compared to the standard culture condition (FBS). The cells were grown in 10%PRP supplemented medium under 3 configurations: (i) cells grown on PRP gel and overlaid with serum free media, (ii) cells growing encapsulated in PRP gel and overlaid with serum free media and (iii) growing cells in serum free media supplemented with PRP releasate. As platelets have no nucleus they cannot replicate and have a finite lifespan of 5 to 9 days (Marx et al., 1998) which raised two questions: (i) during this lifespan of 5 to 9 days, can the platelets provide the cells with sufficient growth supplements to ensure their growth? (ii) which of the 3 PRP configurations described above can provide the best cell microenvironment to ensure their growth? The results showed an increasing trend of the cell-population density over the period of 7 days culture in the three above PRP configuration (Appendix 1). As for the second question, which of the three PRP/cell configurations offered the best micro environment for cell growth, all PRP groups showed the same capabilities to promote cell attachment after 5 hours of cell seeding. However, the trend has been changed after 24 hours and persisted over the 7 days during the cell growth where PRP releasate enhanced the cell proliferation compared to PRP gel groups. A possible explanation for this trend is the weak attachment of PRP gels to the surface of the culture plates leading to sample loss while recovering the gels for DNA quantification. This also might be the cause of the inconsistent results of PRP gel encapsulated cells group which showed reduced cell numbers after one day but high proliferative effect comparable to that of the FBS control after 3 and 7 days

of cell culture. Results of cells grown on PRP gel were also inconsistent where the gel seems to show a comparable results to that of the control after 5 hours and 3 days but didnot promot cell attachment and proliferation after 1 and 7 days compared to the control. Therefore, a conclusive explanation cannot be made as the data of PRP gel groups were not fully reliable and cannot be used to compare between both PRP gel configurations and PRP releasate.

Previous studies have reported a successful culture of cells incorporated into PRP gels, suggesting that the gel environment enhances viability and proliferation of encapsulated cells (Ho et al., 2006; Kawasumi et al., 2008; Xie et al., 2012; Jalowiec et al., 2015). However, the composition of PRP gels used in different studies has a wide variability, mainly because of differences in PRP preparation and activation methods, which in turn leads to remarkable differences in platelet concentration, leukocyte content and GFs release (Mazzucco et al., 2009). In addition, the stiffness of hydrogels may influence the behaviour and differentiation potential of incorporated cells (Brandl et al., 2007; Duarte Campos et al., 2014). The viscoelastic properties of PRP gels were investigated by Jalowiec et al. (2015) through oscillatory rheology and found that the highest storage modulus was achieved by PRP gels with 1000 x 10^3 and 2000 x 10^3 platelets/µL making them slightly stiffer than those with 10,000 x 10^3 platelets/µL. This means that the material tends to maintain its shape rather than creeping and spreading like a viscous fluid. This property, added to the presence of more than 95% culture medium, allows nutrition and waste transport, making the hydrogels as effective cell carriers.

Cell proliferation tests carried out in the present study, indicate that proliferation rates with PRP releasate was consistently high from 1 to 7 days compared to the two other PRP gel configuration’s and to the FBS control at 3 and 7 days. The proliferation- promoting effect is likely due to the high concentration of natural growth factors that PRP releasate contain. The biological actions of GFs in cell proliferation and bone regeneration have been documented in many studies (Sporn and Roberts, 1993; Greenhalgh, 1996; Eppley et al., 2004; Cho et al., 2011). It has been reported in previous studies that PRP releasate significantly increased mesenchymal stem cells (MSC) expansion and proliferation compared to FBS in vitro and has been suggested as a promising

FBS or FCS substitute (Doucet et al., 2005; Kocaoemer et al., 2007; Chevallier et al., 2010). Cho et al. (2011) indicated that the addition of 10% PRP releasate to the culture medium of MSCs induced marked cell proliferation compared to 10% FBS. They also demonstrated the proportional relationship between TGF-β1, PDGF and FGF-b concentrations and cell proliferation. Another in vitro studies confirmed that PRP releasate significantly increased cell proliferation compared to FBS supplemented media in culture of anterior cruciate ligament cells (Fallouh et al., 2010) and human muscle derived progenitor cells (Li el at., 2013).

Many human and animal studies have yielded promising results when PRP has been applied topically at the implant site to enhance bone regeneration (Zechner et al., 2002), or as an implant coating to improve the osseointegration process (Anitua, 2006; Anitua et al., 2008; Anand et al., 2012). Moreover, some investigators have obtained more favourable clinical results in bone repair after implantation when PRP has been used in association with other biomaterials like HA or tricalcium phosphate (TCP) (Okuda et al., 2005; Abhijit, 2006; Yamamiya et al., 2008; Bi et al., 2010). There is very little published information relating to the potential of using PRP synergistically with other biomaterials to promote osteoblastic differentiation. Therefore, in chapter 6, the effect of PRP as an autologous source of GFs on osteogenesis will be compared when used separately or in combination with FA coatings.

In summary, the results showed that the PRP prepared during this study contained platelets at a concentration within the accepted range considered to provide therapeutic value. None of PRP concentrations and configurations used herein were cytotoxic. However, 10% PRP had the greatest effect on cell viability and proliferation. No meaningful data were derived from cell proliferation experiment because of PRP gel detachment from the culture plate prior to the digestion. Thus, it was decided in the future work to test the cell response to both of PRP gel and PRP releasate combined with FA coatings.

Chapter 6: Results and discussion (FA/PRP combinations)

6.1 Introduction

Replacement of lost natural teeth with dental implants is regarded as a major advance in dentistry. The use of calcium phosphate implant coatings such as FA has been shown to enhance the bone response during the initial healing period after implant insertion (Vercaigne et al., 2000; Hayakawa et al., 2000). In the present study, disorganised and organised FA coatings were synthesised on SS metal surfaces using a hydrothermal technique (Chapter 4). Neither FA surface was cytotoxic and both supported initial cellular growth. The new generation of bone scaffolds and implant coatings should not only provide the mechanical architecture to support cell attachment but should also promote cell growth by acting as delivery vehicles for desirable factors such as growth factors (Babensee et al., 2000). PRP was shown to promote the bone healing around the dental implants under the influence of IGF, TGF and PDGF growth factors which are present in PRP in high concentrations (Marx et al., 1998; Vehof et al., 2001; Vehof et al., 2002). With this in mind, to enhance the osseointegration of dental implants, PRP was selected for this study and prepared from whole blood using a manual protocol (Chapter 5). The prepared PRP had platelet concentrations of 5 - 8 times higher than that of the normal blood. A tremendous proliferative effect was detected for PRP releasate on G292 cells in monolayer culture. However, PRP gel showed a comparable influence on cell viability and proliferation to that of the standard cell culture conditions (10% FBS). According to the literature, combined application of PRP with calcium phosphate could facilitate the osteoinductive properties of PRP GFs and might be a promising strategy for stimulating osteogenesis (Vehof et al. 2001). However, the additional use of PRP did not show any significant effect on the early bone response to calcium phosphate coated implants (Nikolidakis et al., 2006; Nikolidakis et al., 2008). Therefore, more research has to be carried out to elucidate this issue. In the present study, the aim was to investigate in vitro, the synergistic effect of FA coatings and PRP on osteoblast-like cell (G292) viability, attachment and proliferation. Furthermore, the release of IGF-1 and PDGF-AB growth factors from PRP/FA coatings was investigated

and the proteins adsorbed from PRP on to surfaces of FA coatings were also analysed. Human postnatal dental pulp stem cells (hDPSCs) were used to investigate whether combinations of FA/PRP can induce cell differentiation and mineralisation, as a result, can provide a scaffold for bone regeneration around the dental implant surface. hDPSCs are easily collected from healthy third molars and are easily banked (Volponi et al., 2010). The ability of hDPSCs to differentiate into functional osteoblasts and produce mineralised matrix have been reported in many in vitro studies (Riccio et al., 2010; Pisciotta et al., 2012).

6.2 Results

6.2.1 Temporal release of growth factors from PRP when used in combination with disorganised and organised FA coatings

PRP was applied to SS surfaces coated with either disorganised FA, organised FA or plain uncoated SS surfaces (control). The loaded PRP samples are either activated with thrombin or calcium chloride or left non-activated. This concomitant activation allowed the release of growth factors and PRP gelification on the surfaces. Non-activated PRP applied to uncoated SS served as the control. The samples were overlaid with PBS and after 2 hours, the PBS was collected and fresh PBS was added and after 1 day collected and again fresh PBS was added and the process was repeated after 3 and 7 days. Collected PBS samples were assayed for IGF-1 and PDGF-AB growth factors using ELISAs. The whole experiment was conducted twice using PRP derived from two separate blood donors. The results for IGF-1 and PDGF-AB are described below as mean ± SD.

Determination of IGF-1 released from PRP when used in combination with disorganised and organised FA coatings

The overall release of IGF-1 from PRP derived from donor 1 and donor 2 into PBS is illustrated in Figure 41. The data revealed that PRP derived from donor 1 released greater amounts of IGF-1 than PRP derived from donor 2. The maximum mean concentrations of IGF-1 occurred within 1 day after PRP gelification reaching around 620 pg/mL in blood donor 1 and 266 pg/mL in donor 2. The lowest concentrations for both growth factors were measured at day 7 post PRP gelification reaching about 25 pg/mL in both blood donors. There was also variation in the kinetics of IGF-1 diffusion out of the PRP gels. For example, in the case of the FA coated samples, PRP from donor 1 tended to release the bulk of the IGF-1 present between 2 hours and 1 day while PRP from donor 2 released the bulk of the IGF-1 present within the first 2 hours. However, a comparative lower sustained release at the later times was detected for all PRP samples in both donors.

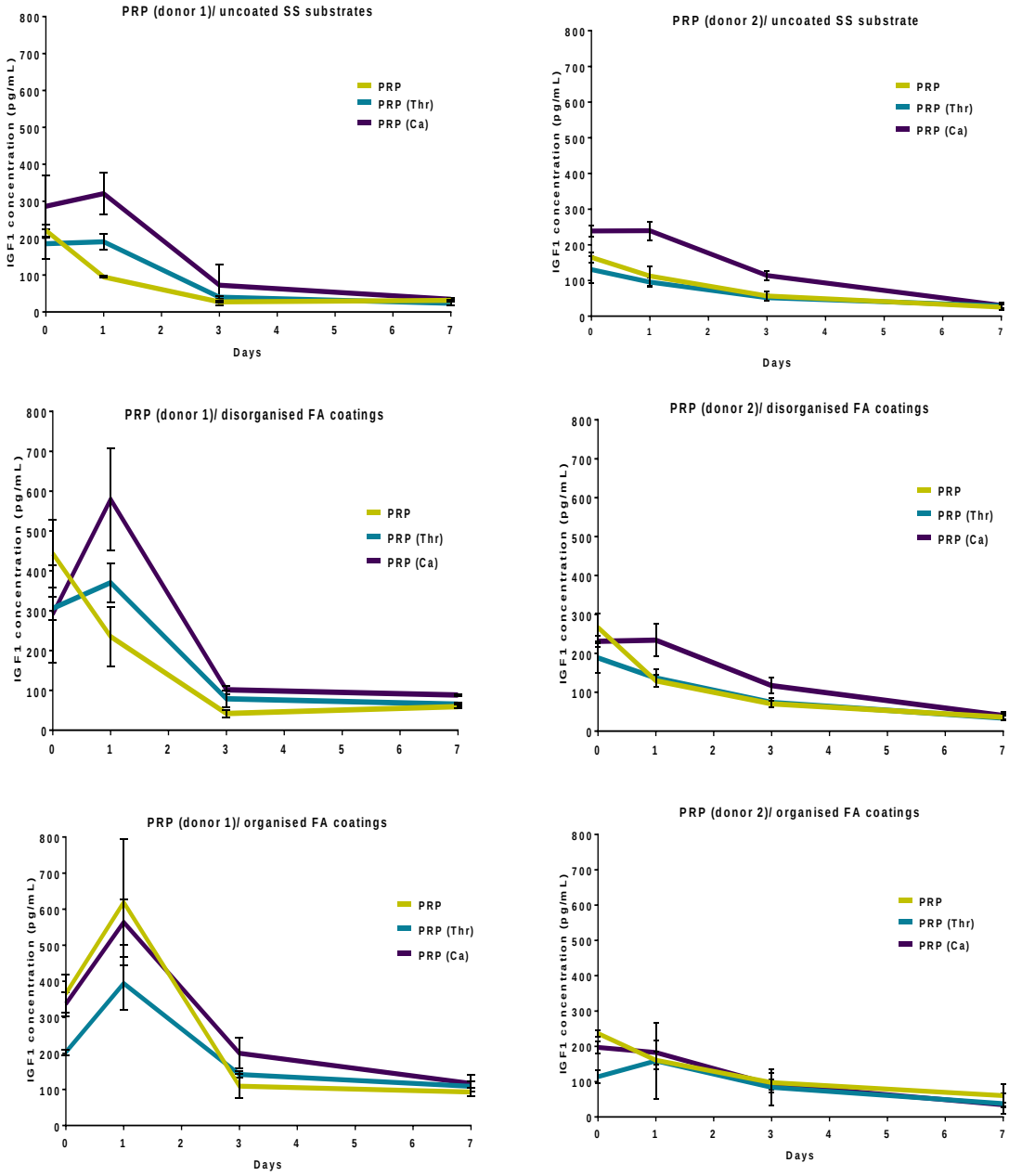

Figure 41: Concentrations of IGF1 (mean ±SD pg/mL) in PBS supernatants released from PRP gel of 2 blood donors combined with FA coatings. PRP samples were activated with either thrombin (Thr) or CaCl2 (Ca) or left non activated (control). Donor 1 showed higher levels of IGF1 compared to donor 2. There was variation in the kinetics of IGF-1 diffusion out of the PRP gels. FA coated samples showed that PRP from donor 1 tended to release the bulk of the IGF-1 between 2 hours and 1 day while PRP from donor 2 released the bulk of the IGF-1 within the first 2 hours with a comparative lower sustained release at the later times. DS, Disorganised FA; OR, organised FA; SS, stainless steel; PRP, platelet-rich plasma.

For further discussion here and to determine the effect of FA coatings and type of PRP activator on IGF-1 release, the quantitative data of IGF-1 release at each time point were expressed below as mean ± SD.

➢**Time point 1: IGF-1 released between PRP gelification and 2 hours post gelification**

As seen in figure 42A, after 2 hours of PRP gelification from donor 1, treatment of PRP with calcium chloride (Ca) appears to induce a higher IGF-1 release compared to non-activated PRP when combined with SS substrate. Interestingly, disorganised FA coatings enhanced the release of IGF-1 from non-activated PRP (443.5 ± 85 pg/mL) compared to thrombin- activated PRP (305.9±28 pg/mL). Similarly, IGF-1 was detected in higher amounts in non-activated PRP samples combined with organised FA (365.8 ± 53 pg/mL) compared to thrombin-activated PRP (203±8 pg/mL).

The same release pattern was detected in the case of donor 2 (Figure 42B). Calcium induced higher release of IGF-1 (239±16 pg/mL) compared to the control (non-activated PRP) (164.9±15 pg/mL) and to thrombin (130.6±38 pg/mL) from PRP samples combined with uncoated SS. The disorganised coatings triggered a greater release of IGF-1 from non-activated PRP compared to thrombin- activated PRP and to calcium- activated PRP by about 30% and 15% respectively. Similarly, organised FA coatings triggered a greater release of IGF-1 from non-activated PRP compared to thrombin- activated PRP and calcium-activated PRP by around 50% and 15% respectively. The release appears to be greater in non-activated PRP samples combined with disorganised FA coatings (266.4 ±35.6 pg/mL) compared to non-activated PRP samples combined with organised FA (236.6± 10 pg/mL). In both PRP donors, it seems that both FA coatings stimulated the release of IGF-1 from non-activated PRP in high amounts compared to uncoated SS.

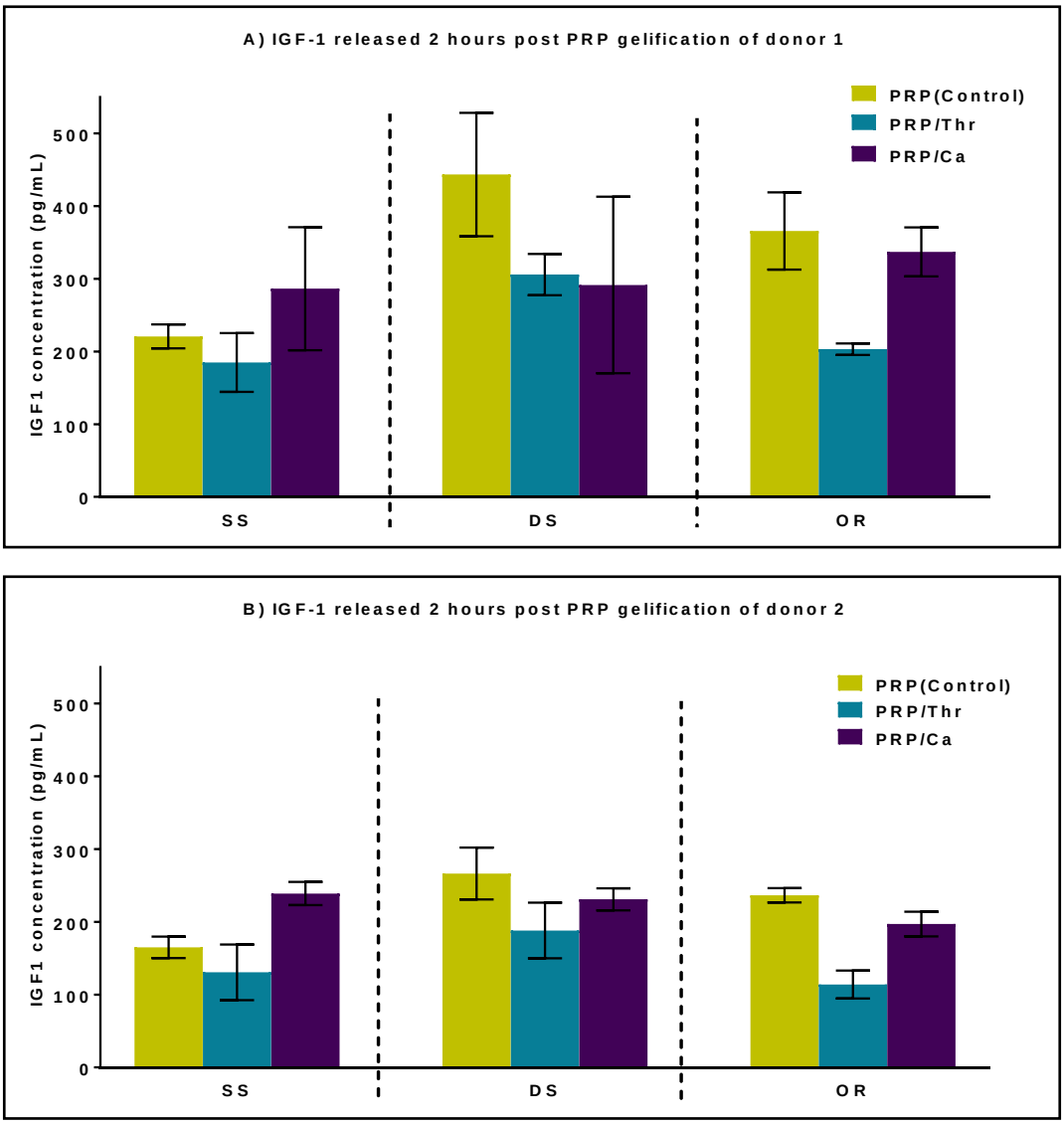

Figure 42: IGF-1 (mean ±SD) released between PRP gelification and 2 hours post gelification. PRP samples of 2 blood donors were loaded on uncoated stainless steel (SS), disorganised FA (DS) and organised FA (OR) coated discs. The loaded PRP samples were either left non-activated (PRP) or activated using thrombin (Thr) or calcium chloride (Ca) and the discs were overlaid with PBS. IGF-1 concentrations diffusing into the PBS were measured using ELISA and plotted. In SS samples, calcium induced the highest release of IGF-1. While both coatings showed higher release of IGF-1 from non-activated PRP compared to thrombin and calcium-activated PRP with a higher release shown in disorganised FA compared to organised FA coating. Both FA coatings stimulated the release of IGF-1 from non-activated PRP in high amounts compared to uncoated SS.

➢**Time point 2: IGF-1 released between 2 hours post gelification and 1 day post gelification**

In the period between 2 hours and 1 day post PRP gelification, both thrombin and calcium induced a greater release of IGF-1 from PRP of donor 1 over that of the control (non-activated PRP) in uncoated SS and disorganised FA substrate groups by around 50%- 200% (Figure 43A). However, in SS groups, the PRP activated with calcium showed a higher IGF-1 content (320.6 ± 57 pg/mL) compared to PRP activated with thrombin (190.3±20 pg/mL). Similarly, in the disorganised coatings, high levels of IGF-1 were detected in calcium-activated PRP (579.3±128 pg/mL) compared to thrombin - activated PRP (370.4±49 pg/mL). Organised FA coatings stimulated a higher amount of IGF-1 release from non-activated PRP (619± 174 pg/mL) and from calcium-activated PRP (563.6±62 pg/mL) compared to thrombin-activated PRP (394±74 pg/mL). The non- activated PRP combined with organised FA showed the highest IGF-1 release (619±175 pg/mL) compared to that of disorganised and SS sample groups.

PRP samples of donor 2 (Figure 43B) showed that calcium was the most potent activator for PRP as it induced the highest release of IGF-1 compared to non-activated PRP and thrombin in uncoated SS and disorganised FA substrate samples by about 100%. In organised FA samples, calcium-activated PRP samples seem to have IGF-1 release (182.6±35 pg/mL) at about similar levels to that of non-activated (160.7±26 pg/mL) and thrombin-activated PRP samples (158.9±108 pg/mL).

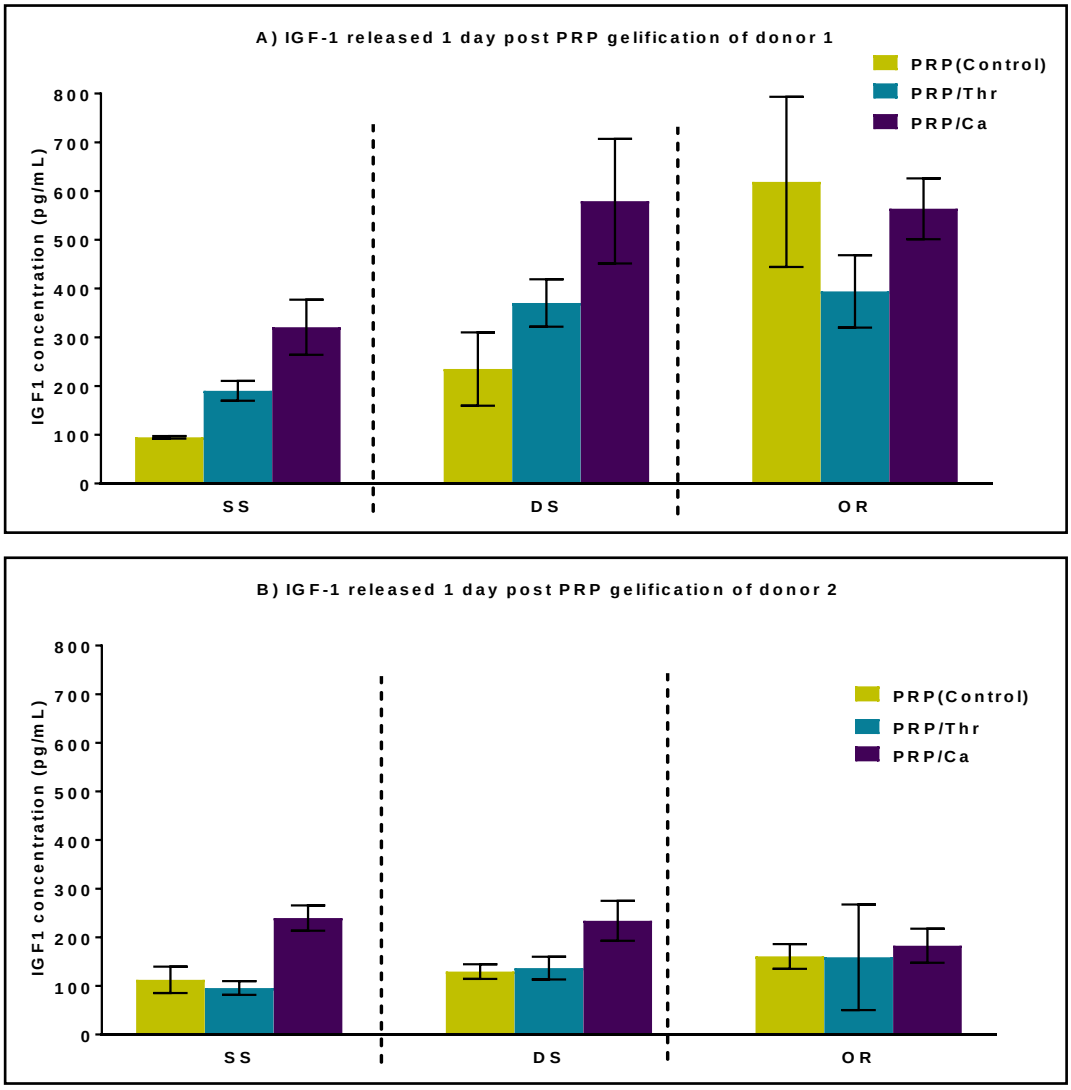

Figure 43: IGF-1 (mean ±SD) released between 2 hours post gelification and 1 day post gelification. Samples from figure 42 were overlaid with fresh PBS and concentration of IGF-1 diffusing into the PBS was measured by ELISA one day later. The mean data for two blood donors were plotted. Calcium induced a greater release of IGF-1 over that of the control (non-activated PRP) in SS and disorganised FA substrate groups in both donors. While in organised FA groups, the non-activated PRP showed amounts of IGF-1 comparable to that of calcium-activated PRP. DS, Disorganised FA; OR, organised FA; SS, stainless steel; PRP, platelet-rich plasma; Thr, thrombin; Ca, calcium.

Time point 3: IGF-1 released between 1 day post gelification and 3 days post gelification

In the period between 1 day post gelification and 3 days post gelifiction of PRP derived from donor 1 (Figure 44A), all FA coatings showed enhanced release of IGF-1 compared to uncoated SS corresponding groups. Calcium was the most potent activator to release IGF-1 from PRP combined with uncoated SS and FA coated substrates compared to non-activated PRP and thrombin. Nevertheless, organised FA increased the release of IGF-1 from calcium-activated PRP (200±42 pg/mL) compared to uncoated SS (72.6±56 pg/mL) and disorganised FA (101.5±10 pg/mL).

In the case of donor 2 (Figure 44B), both non-activated PRP and thrombin-activated PRP exhibited comparable concentrations in all substrate groups. In uncoated SS and disorganised FA samples, 100% and 67% respectively more IGF-1 was released from calcium-activated PRP compared to the non-activated PRP. In contrast, in organised FA samples, non-activated PRP yielded a comparable amount of IGF-1 (97.6±29 pg/mL) to that of calcium-activated PRP (92±15 pg/mL).

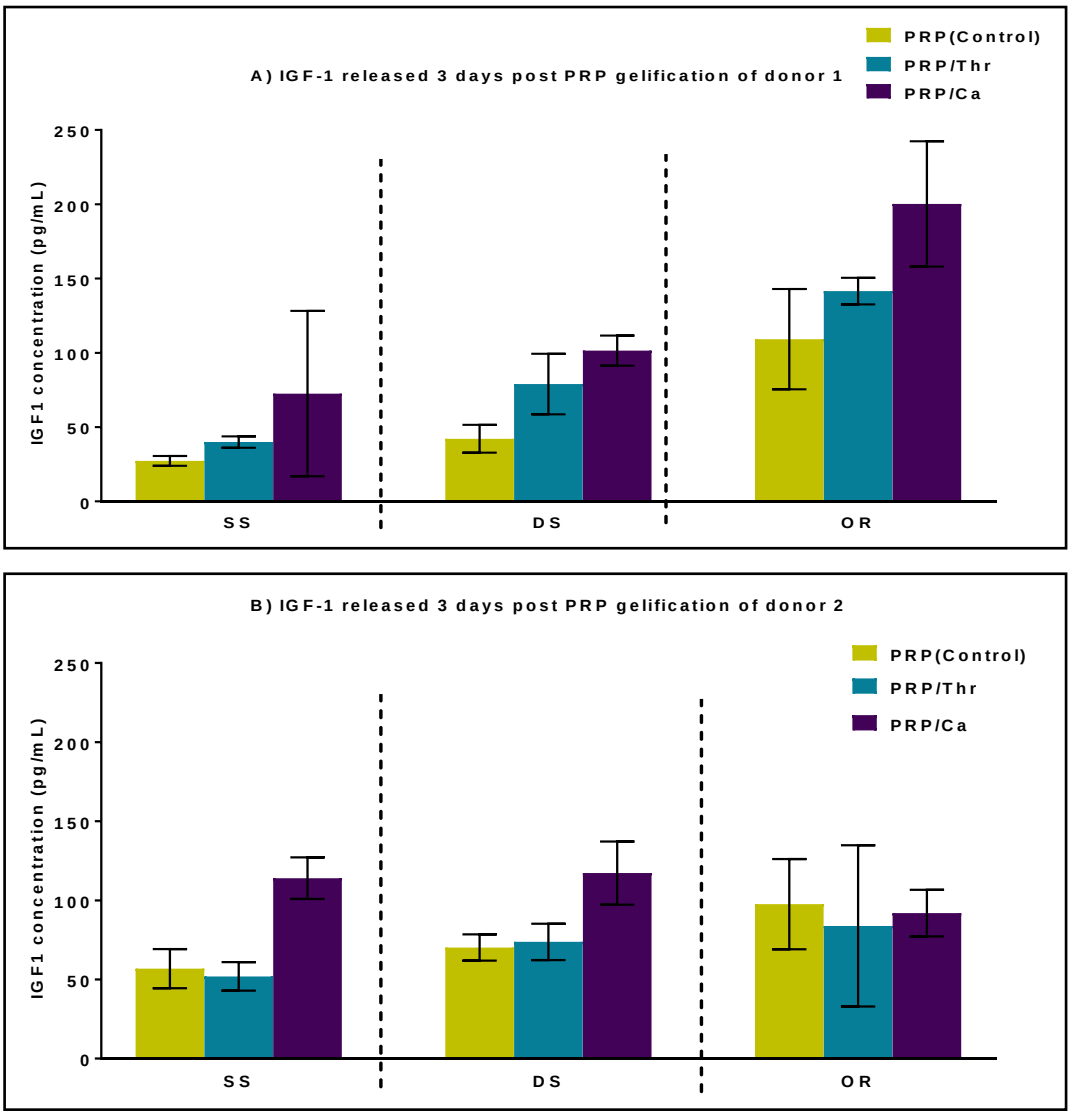

Figure 44: IGF-1 (mean ±SD) released between 1 day post gelification and 3 days post gelification. Samples from figure 43 were overlaid with fresh PBS and the concentration of IGF-1 diffusing into the PBS was measured by ELISA at 3 days post gelification. The mean data for the two donors were plotted. All FA coatings showed enhanced release of IGF-1 compared to uncoated SS. Calcium was the most potent activator to release IGF-1 from PRP in uncoated and FA coated samples with one exception that organised FA coatings stimulated the release of IGF-1 from non-activated PRP of donor 2 in a comparable amount to that of calcium-activated PRP. DS, Disorganised FA; OR, organised FA; SS, stainless steel; PRP, platelet-rich plasma; Thr, thrombin; Ca, calcium.

Time point 4: IGF-1 released between 3 days post gelification and 7 days post gelification

At the last time point (Figure 45A), both of the FA coatings continued to induce a greater release of IGF-1 from non-activated and activated PRP of donor 1 compared to uncoated SS. Calcium raised the release of IGF-1 above that of the control by about 49% disorganised FA. However, organised FA displayed a greater amount of IGF-1 in calcium-activated PRP samples (116.8± 24 pg/mL) compared to uncoated SS (34.6±4 pg/mL) and disorganised FA (88.3± 3 pg/mL) substrates.

PRP data of donor 2 (Figure 45B) showed that both non-activated PRP and activated PRP samples displayed similar amounts of IGF-1 in all substrate groups.

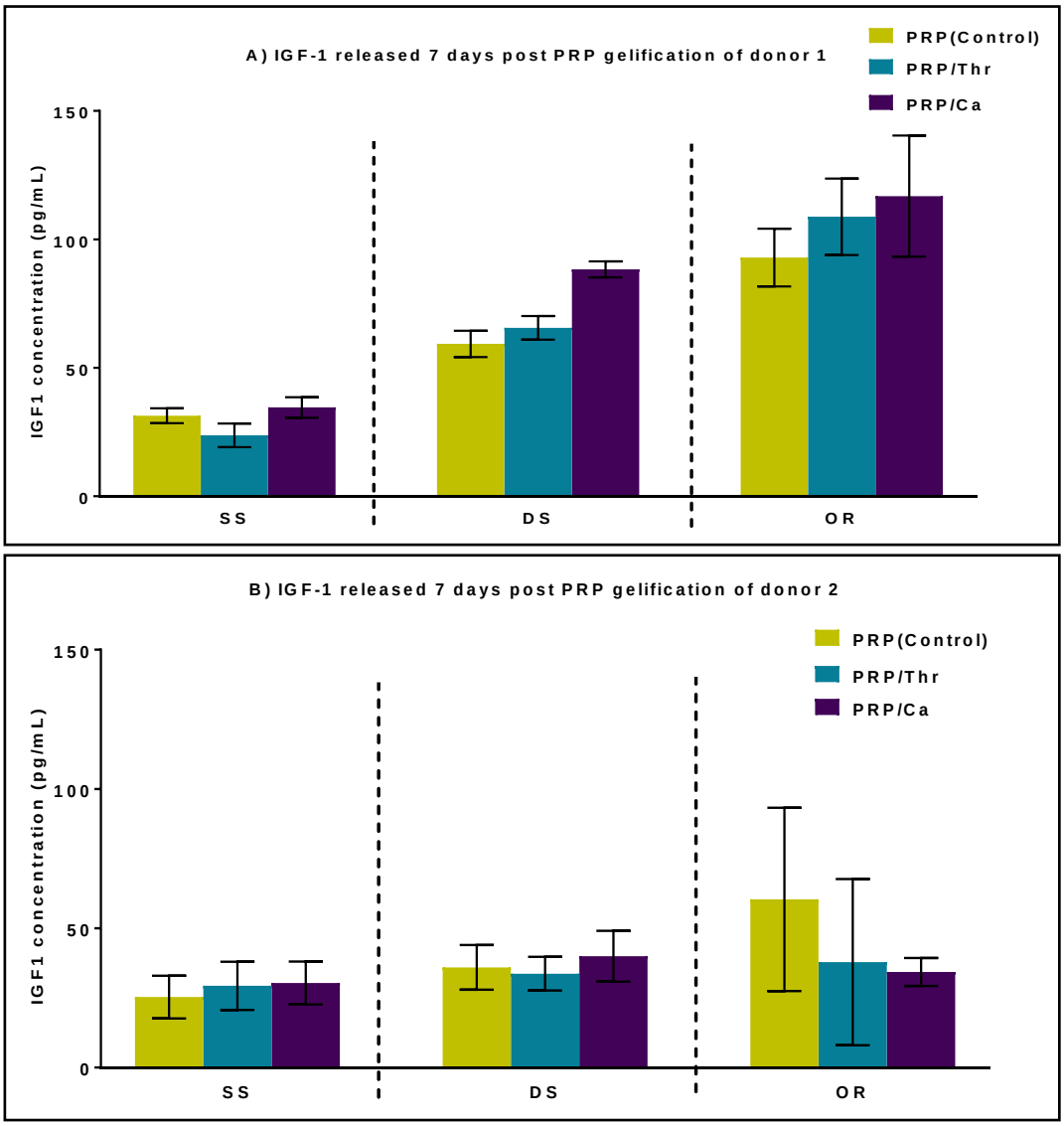

Figure 45: IGF-1 (mean ±SD) released between 3 days post gelification and 7 days post gelification. Samples from figure 44 were overlaid with fresh PBS and IGF-1 concentrations diffusing into the PBS was measured by ELISA at 7 days post gelification. The mean data for the two donors were plotted. All FA coatings showed enhanced release of IGF-1 from PRP of donor 1 compared to uncoated SS. Calcium induced the highest release of IGF-1 from PRP combined with organised FA. PRP samples of donor 2 showed similar amounts of IGF-1 in all substrate groups. DS, Disorganised FA; OR, organised FA; SS, stainless steel; PRP, platelet-rich plasma; Thr, thrombin; Ca, calcium.

Determination of PDGF-AB released from PRP when used in combination with disorganised and organised FA coatings

The temporal release of PDGF-AB from SS/PRP and FA/PRP combinations into PBS was measured over a period of 7 days using ELISAs. PRP samples used were derived from two separate blood donors (the same donors of IGF-1 samples). Complete individual data (mean ±SD) for donor 1 and donor 2 are presented in figure 46. Both donors exhibited higher levels of PDGF-AB compared to IGF-1. In addition, PRP from donor 1 showed higher levels of PDGF-AB release than PRP from donor 2. Most of the release of PDGF-AB appeared mostly within the first 24 hours after PRP gelification with the maximum release seen after 2 hours of PRP gelification in thrombin-activated PRP (~1980 pg/mL and 1730 pg/mL in donor 1 and 2 respectively). It was obvious that the major induction of PDGF-AB was achieved consistently following thrombin activation. A lower sustained release was seen at the later time points. The lowest concentrations for both growth factors were measured at day 7 post PRP gelification reaching about 25 pg/mL for IGF-1 and 50 pg/mL for PDGF-AB in both blood donors.

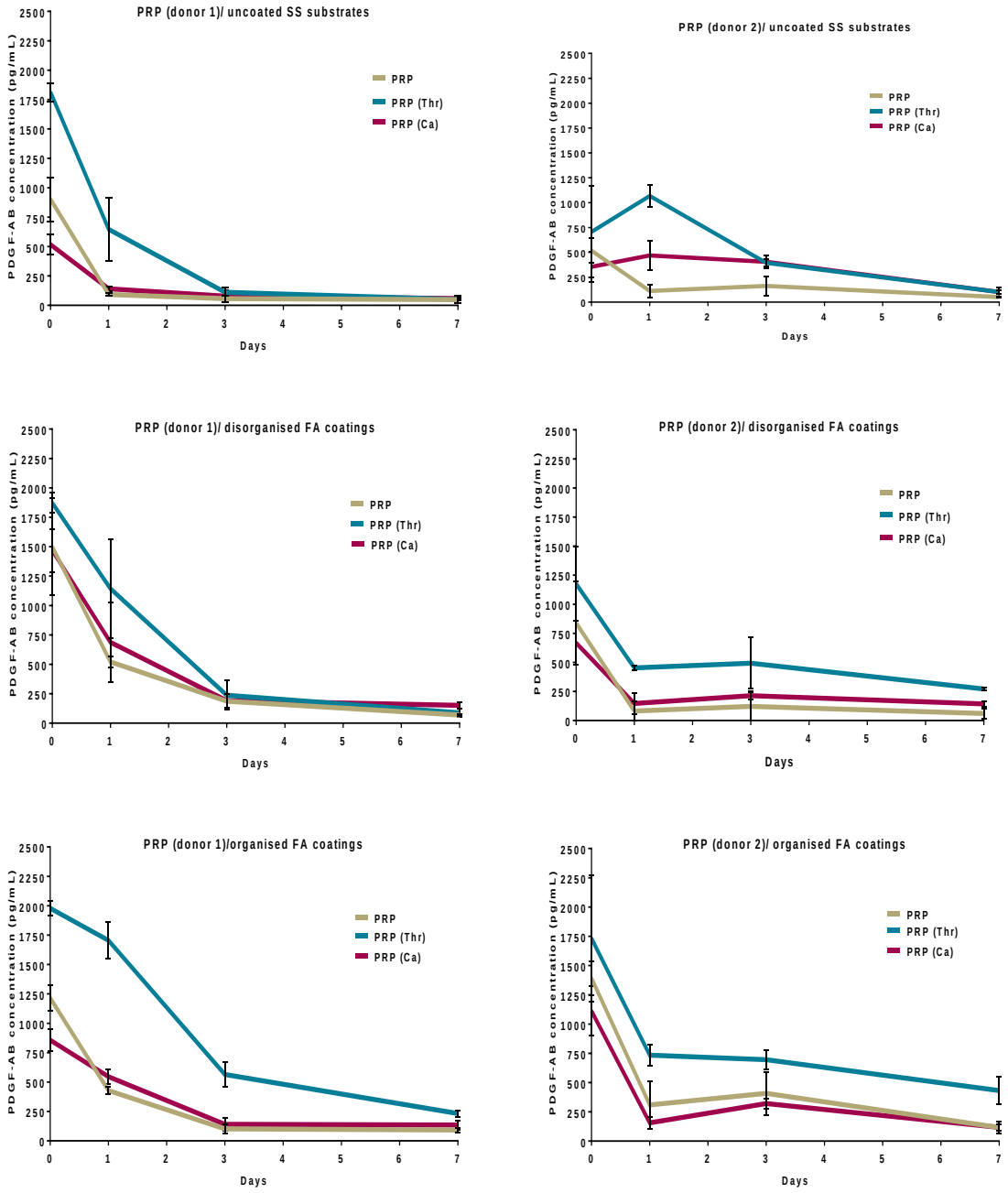

Figure 46: Concentrations of PDGF-AB (mean ±SD pg/mL) in PBS supernatants released from PRP of 2 blood donors combined with FA coatings. PRP samples were activated with thrombin (Thr), $CaCl_2$ (Ca) or left non-activated (control). PRP from donor 1 exhibited higher levels of PDGF-AB than PRP from donor 2. High concentrations of PDGF-AB were detected after 2 hours with a lower sustained release at the later time points. The major induction of PDGF-AB release from PRP was achieved consistently following thrombin activation. DS, Disorganised FA; OR, organised FA; SS, stainless steel; PRP, platelet-rich plasma; Thr, thrombin; Ca, calcium.

For further discussion and comparison here, PDGF-AB concentration of the experimental groups were plotted for each time point and the means of this data are presented below (mean ±SD) and analysed.

- **Time point 1: PDGF-AB released between PRP gelification and 2 hours post gelification**

Two hours after PRP gelification, low concentrations of released PDGF-AB were detected when calcium was used to activate PRP derived from donor 1 (516.6±84 pg/mL) combined with uncoated SS samples compared to the control (non-activated PRP) (901.9±187 pg/mL) as shown in figure 47A. Similarly, calcium did not enhance PDGF-AB release from PRP (857.3±94 pg/mL) compared to the control (1214.7±107 pg/mL) when combined with organised FA coatings. While thrombin activation induced the highest release of PDGF-AB from PRP compared to the control and to calcium reaching 1813±79 pg/mL, 1871.7±87 pg/mL and 1979±59 pg/mL when used in combination with uncoated SS, disorganised FA coatings and organised FA coatings respectively.
Results of donor 2 (Figure 47B) showed that organised FA released a higher amounts of PDGF-AB from non-activated PRP and activated PRP compared to the uncoated and to disorganised FA coated substrates. Moreover, organised FA induced the highest release from thrombin-activated PRP (1732±539 pg/mL) compared to uncoated SS (706.6±461 pg/mL) and to disorganised FA (1175±320 pg/mL).

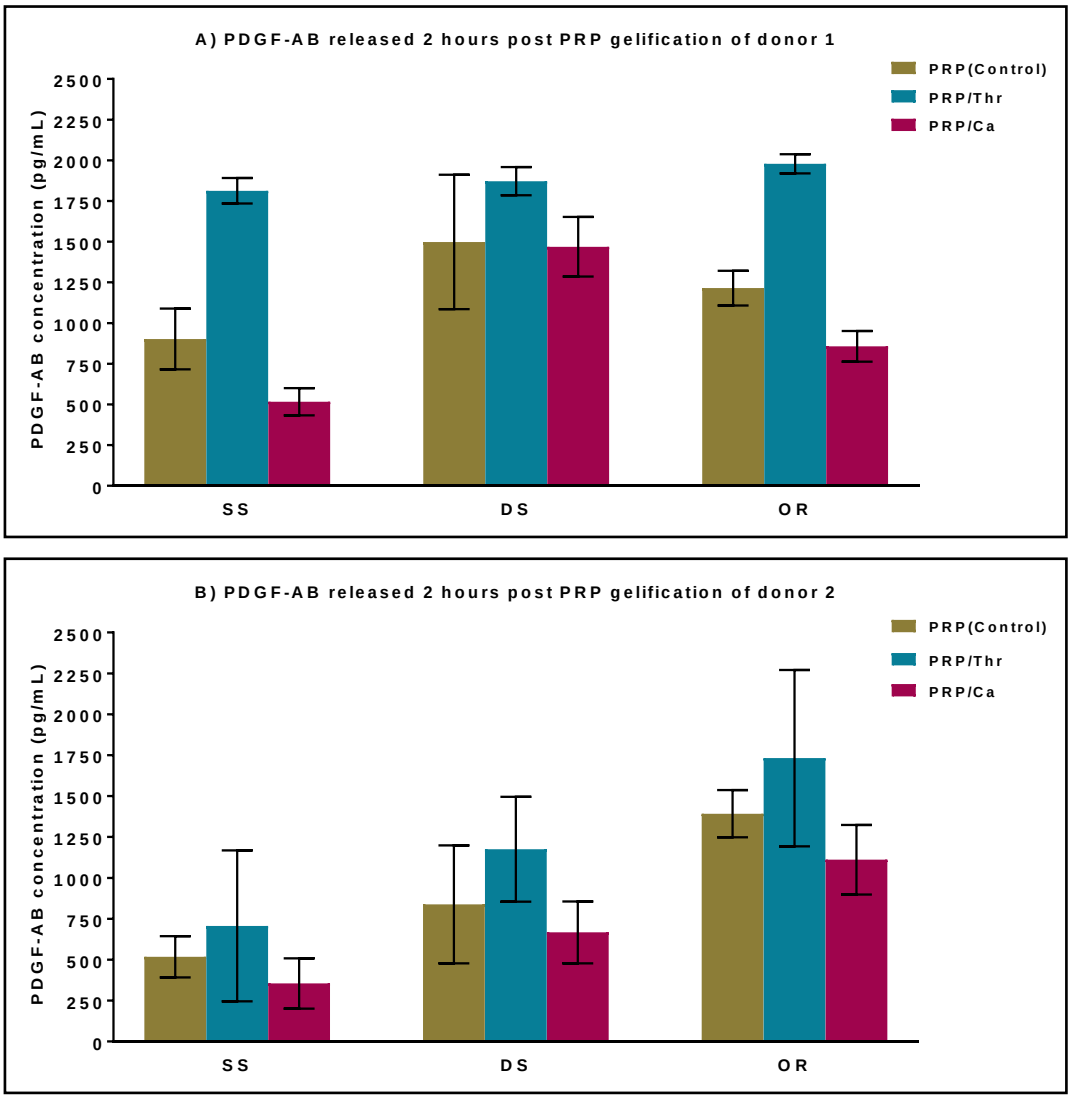

Figure 47: PDGF-AB (mean ±SD) released between PRP gelification and 2 hours post gelification. PRP samples were loaded on uncoated SS, disorganised FA (DS) and organised FA (OR) coatings. The loaded PRP samples were either left non-activated (PRP) or activated using thrombin (Thr) or calcium chloride (Ca) and the discs were overlaid with PBS. PDGF-AB concentrations diffusing into the PBS were measured using ELISA and mean data for the two donors were plotted. Both FA coatings stimulated the release of PDGF-AB in high amounts compared to the uncoated SS. However, thrombin activation induced the highest release of PDGF-AB from PRP loaded on organised FA coated discs.

➢ **Time point 2: PDGF-AB released between 2 hours post gelification and 1 day post gelification**

Increased amounts of PDGF-AB were measured from PRP samples of donor 1 combined with FA coatings after one day of PRP gelification compared to uncoated SS (Figure 48A). It seems that the non-activated PRP used in combination with SS released most of its PDGF-AB within the first 2 hours. Calcium showed a slight increase in PDGF-AB release in all substrates groups compared to the corresponding controls (non-activated PRP). While, thrombin enhanced PDGF-AB release in great amounts above that of the control by about 600%, 120% and 300% when PRP used in combination with SS, disorganised FA and organised FA respectively. However, the highest release was triggered by organised FA from thrombin-activated PRP (1705 ±153 pg/mL) compared to SS (646.6 ±271 pg/mL) and disorganised FA (1143.6±423 pg/mL). Similarly, thrombin demonstrated higher release compared to non-activated PRP of donor 2 in all substrate groups (Figure 48B). In contrast to donor 1, the highest amount of PDGF-AB was seen in thrombin-activated PRP of uncoated SS group (1068.4±113 pg/mL) compared to disorganised FA (453.5±20 pg/mL) and organised FA (734.3±93 pg/mL).

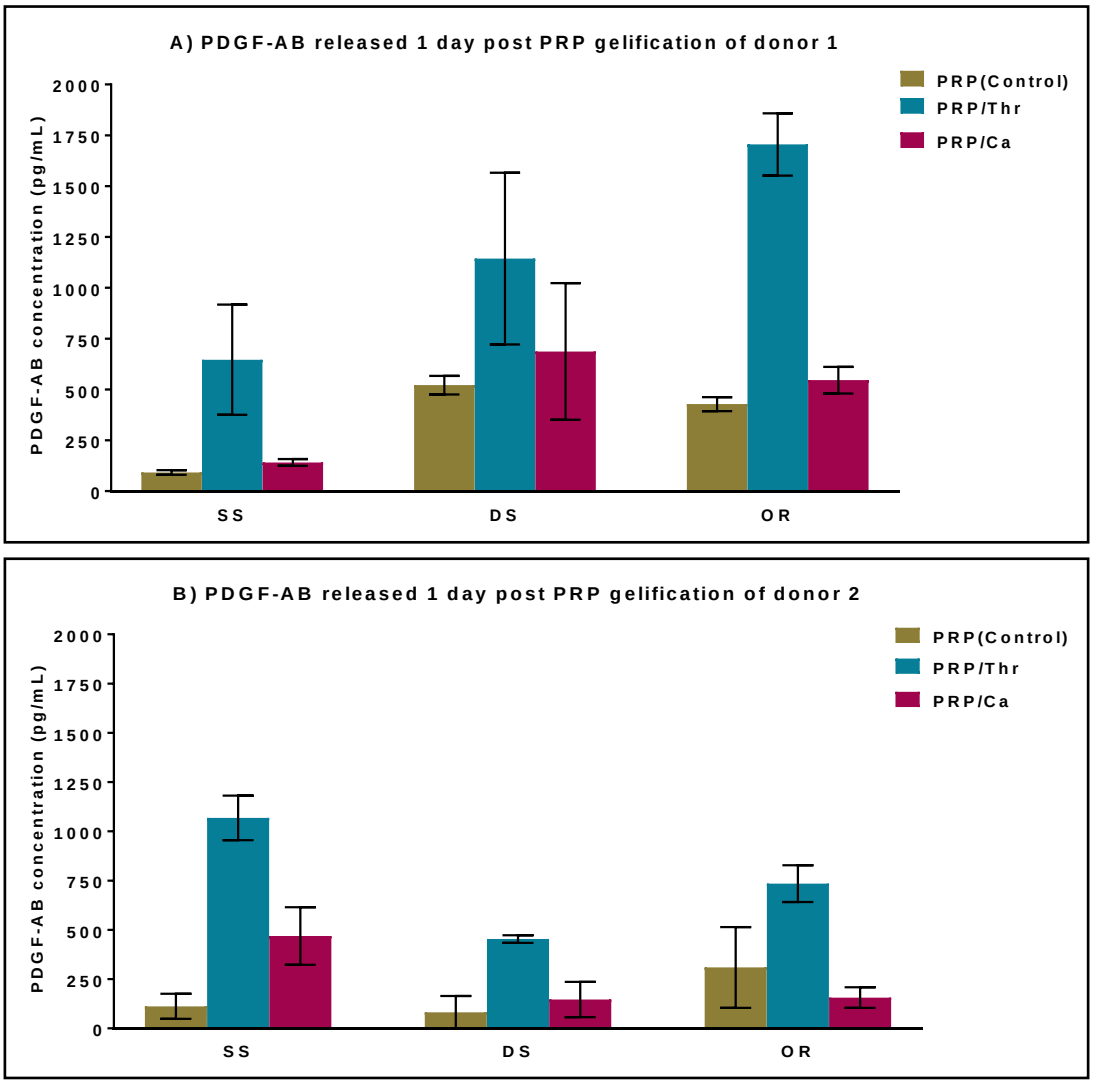

Figure 48: PDGF-AB (mean ±SD) released between 2 hours post gelification and 1 day post gelification. Samples from figure 47 were overlaid with fresh PBS and concentration of PDGF-AB diffusing into the PBS was measured by ELISA and mean data for two blood donors were plotted. Thrombin enhanced PDGF-AB release above that of calcium and non-activated PRP in all the substrate groups. DS, Disorganised FA; OR, organised FA; SS, stainless steel; PRP, platelet-rich plasma; Thr, thrombin; Ca, calcium.

Time point 3: PDGF-AB released between 1 day post gelification and 3 days post gelification

At day 3, results of PRP samples of donor 1 showed that all FA experimental groups continued to show a high amount of PDGF-AB compared to the uncoated SS groups (Figure 49A). Thrombin burst PDGF-AB release from PRP combined with organised FA compared to non-activated PRP and calcium – activated PRP. There was greater amount of PDGF-AB in thrombin-activated PRP samples of the organised FA coatings (565.4±104 pg/mL) than disorganised FA coatings (237.5±124 pg/mL) and SS uncoated discs (111±40 pg/mL)

Data of donor 2 (Figure 49B) showed the same trend where thrombin stimulated a higher release of PDGF-AB from PRP compared to the control (non-activated PRP) and to calcium in FA substrate groups. Nevertheless, the highest release of PDGF-AB in thrombin-activated PRP samples was induced by organised FA coatings (695.2±85 pg/mL) compared to disorganised FA coatings (493.3±221 pg/mL) and SS uncoated discs (395.3±35 pg/mL).

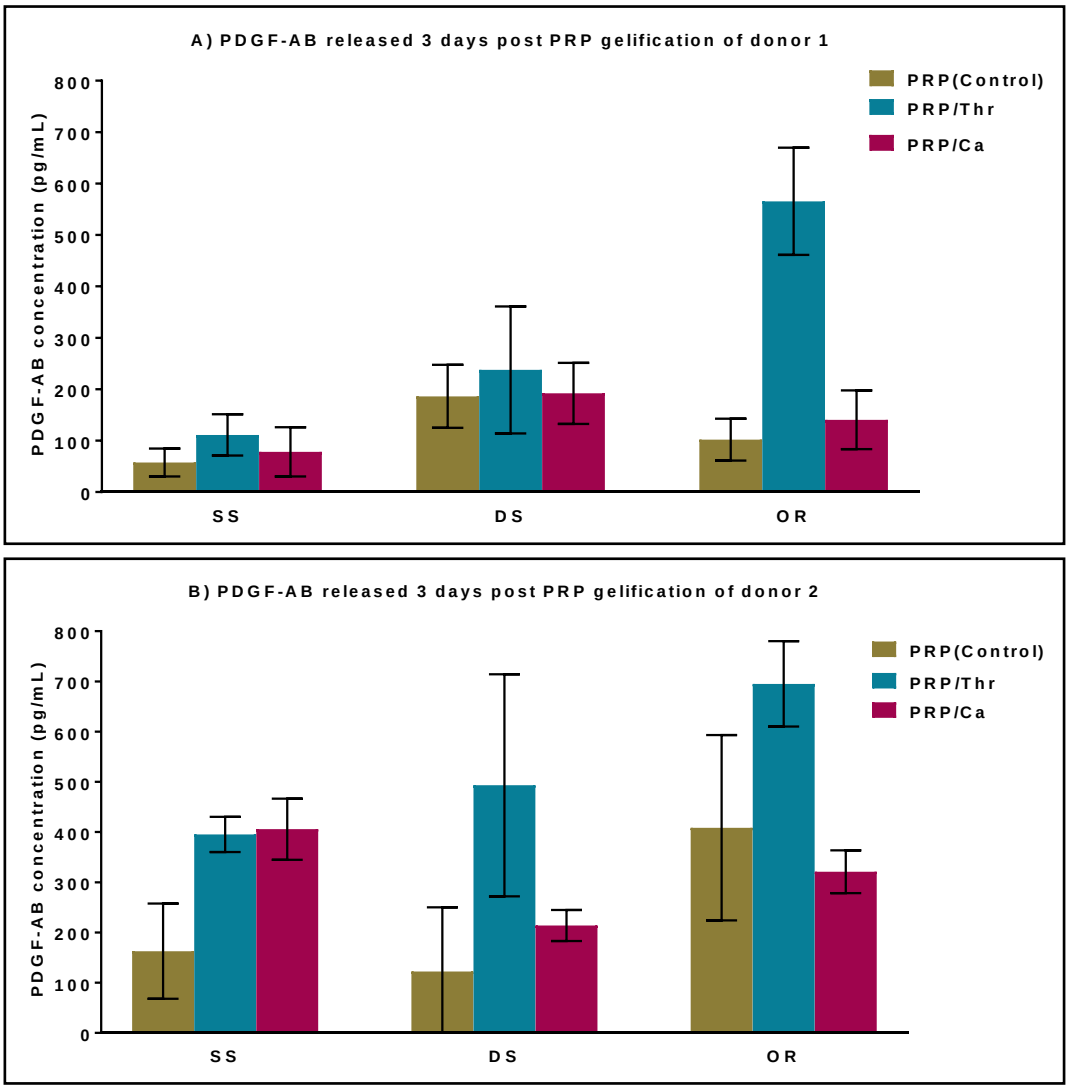

Figure 49: PDGF-AB (mean ±SD) released between 1 day post gelification and 3 days post gelification. Samples from figure 48 were overlaid with fresh PBS and the concentration of PDGF-AB diffusing into the PBS was measured by ELISA 2 days later at 3 days post gelification. The mean data for two blood donors were plotted. Thrombin burst the release of PDGF-AB compared to non-activated PRP and calcium –activated PRP with a greater amount triggered by the organised FA coatings than disorganised FA coatings and SS uncoated discs. DS, Disorganised FA; OR, organised FA; SS, stainless steel; PRP, platelet-rich plasma; Thr, thrombin; Ca, calcium.

Time point 4: PDGF-AB released between 3 days post gelification and 7 days post gelification

Data obtained at day 7 showed that thrombin and calcium induced the release of PDGF-AB from PRP of donor 1 at a comparable levels to that of the control (non-activated PRP) when combined with uncoated SS (Figure 50A).rr This was not the case in FA coating groups where the highest release was induced by calcium in disorganised FA and by thrombin in organised FA groups. However, the thrombin-activated PRP of organised FA showed a greater release of PDGF-AB (232.9±26 pg/mL) than the calcium-activated PRP of disorganised FA (151±28 pg/mL).

In PRP samples data of donor 2, thrombin and calcium activation triggered a greater release of PDGF-AB compared to non-activated PRP in all substrate groups (Figure 50B). PDGF-AB released from thrombin-activated PRP used in combination with organised FA coatings (431.7±117 pg/mL) was higher than with disorganised FA coatings (271.6±14 pg/mL) and SS uncoated discs (102.3±16 pg/mL).

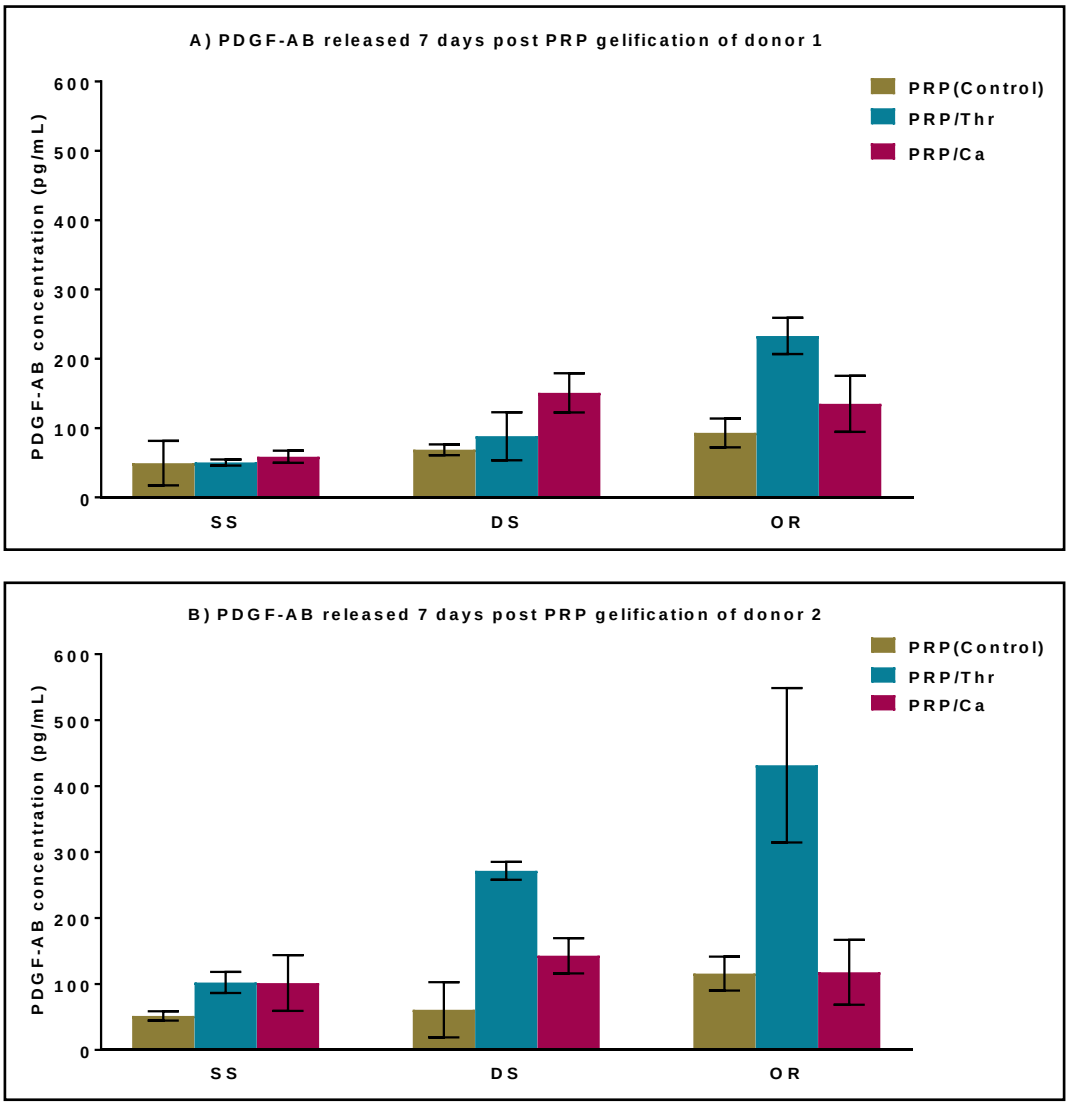

Figure 50: PDGF-AB (mean ±SD) released between 3 days post gelification and 7 days post gelification. Samples from figure 49 were overlaid with fresh PBS and the concentration of PDGF-AB diffusing into the PBS was measured by ELISA at 7 days post gelification. The mean data for two blood donors were plotted. Thrombin activation triggered the greatest release of PDGF-AB compared to calcium- activated and non-activated PRP groups from organised FA coatings. DS, Disorganised FA; OR, organised FA; SS, stainless steel; PRP, platelet-rich plasma; Thr, thrombin; Ca, calcium.

6.2.2 Growth factor released from PRP gel and PRP releasate when combined with uncoated SS and organised FA coatings

In the previous section, growth factor release from PRP gel used in combination with uncoated SS, disorganised FA and organised FA was determined at different time points. In this section, growth factor release from PRP gel was compared to growth factor release from PRP releasate (obtained by extracting the soluble components from thrombin-activated PRP) when both were combined with uncoated SS and organised FA coated surfaces after being incubated 3 days in PBS. The accumulative amounts of IGF-1 and PDGF-AB released into PBS supernatants were measured using ELISA. The experiment was repeated twice using 2 blood donors and the results are presented below.

➢**IGF-1 released from PRP gels and PRP releasate when combined with organised FA coatings and uncoated SS**

The results based on PRP obtained from donor 1 (Figure 51) showed that the mean IGF-1 level released from PRP gel when combined with uncoated SS (117 ± 17 pg/mL) was lower than that of PRP releasate combined with uncoated SS (409 ± 48 pg/mL). Similarly, the mean IGF-1 level released from PRP gel when combined with organised FA coatings (125 pg/mL ± 42) was lower than that of PRP releasate when combined with organised FA coatings (447 pg/mL ±53). Apparently, the underlying substrate, whether uncoated SS or organised FA had no effect on IGF-1 released from either PRP gel or PRP releasate.
A broadly similar pattern of IGF-1 release was observed when PRP gel and PRP releasate derived from donor 2 (Figure 51) were used in combination with uncoated SS or organised FA surfaces though the absolute amounts of IGF-1 released were higher than for donor 1.

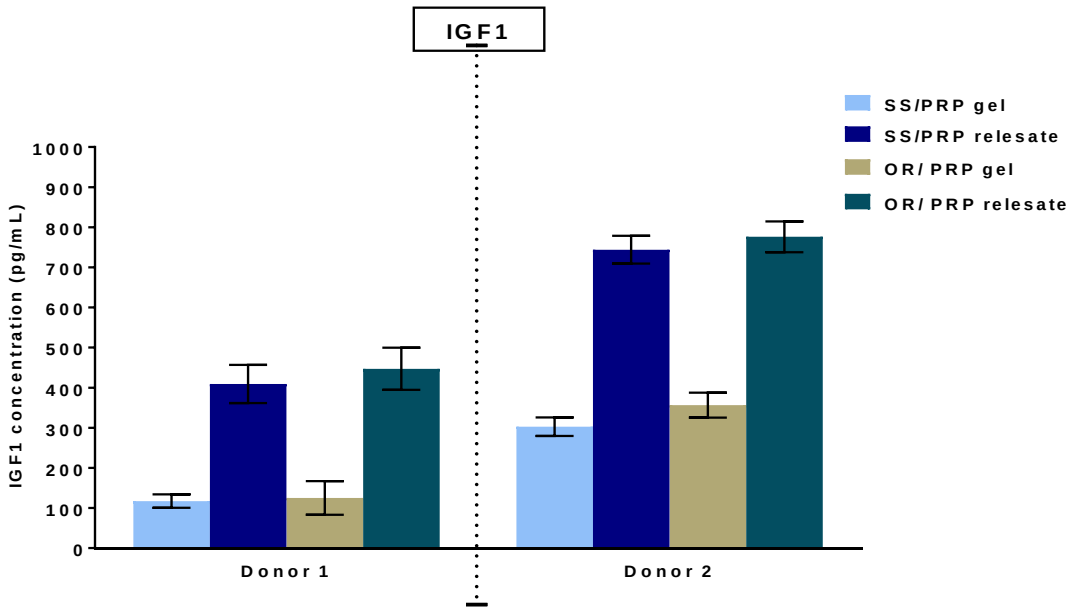

Figure 51: Concentrations of IGF-1 (mean ±SD pg/mL) released into PBS from PRP gel and PRP releasates derived from 2 blood donors and combined with either uncoated SS or organised FA coatings. PRP releasate in both donors exhibited greater release of IGF-1 compared to PRP gel. The underlying substrate (SS or FA) did not affect the release in in either the PRP gel and releasate groups. OR, organised FA; SS, stainless steel; PRP, platelet-rich plasma.

➢**PDGF-AB released from PRP gel and PRP releasate when combined with organised FA coatings and uncoated SS**

The PDGF-AB release profile from PRP extracted from 2 blood donors is illustrated in Figure 52.

For donor 1, PRP gel samples showed a higher level of PDGF-AB release when combined with uncoated SS (1219.6 ±238 pg/mL) compared to PRP releasate loaded on uncoated SS (692.7 ±140 pg/mL). In the same way, PRP gel combined with organised FA coated discs exhibited a higher concentrations of PDGF-AB (1227.5 ±199 pg/mL) compared to PRP releasate loaded on organised FA coated discs (628 ±125 pg/mL). Additionally, no difference was seen in PDGF-AB release between SS and organised FA coatings for both of PRP gel groups and PRP releasate groups.

Sample derived from donor 2 (Figure 52) seemed to have the same release profile as samples derived from donor 1. PRP gel amplified the release of PDGF-AB in the SS group (886 ±130 pg/mL) and organised FA group (834.5 ±178 pg/mL) compared to the PRP releasate corresponding groups of SS (294 ± 67 pg/mL) and organised FA (245 ±63 pg/mL). Similar to donor 1, PDGF-AB concentrations in donor 2 didnot differ between SS and FA coatings for both of PRP gel groups and PRP releasate groups.

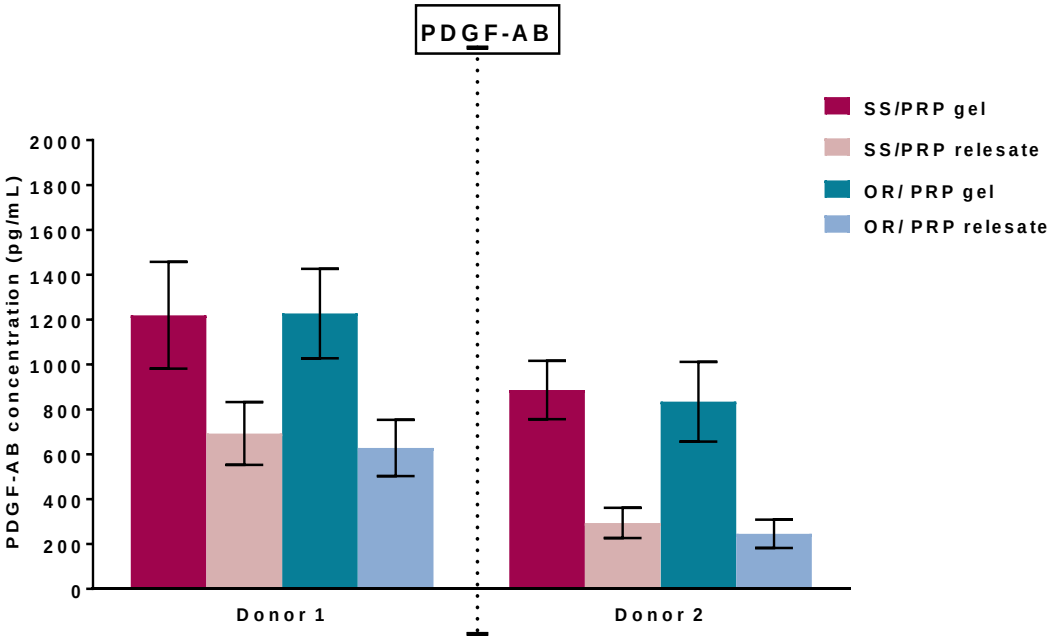

Figure 52: Concentrations of PDGF-AB (mean ±SD pg/mL) in PBS supernatants released from PRP gel and releasate combined with uncoated SS or organised (OR) FA coatings. PRP gel released higher concentrations of PDGF-AB compared to PRP releasate. The underlying substrate (SS or FA) did not affect the release in either the gel or releasate groups. The results were consistent in both donors. OR, organised FA; SS, stainless steel; PRP, platelet-rich plasma.

6.2.3 Release of Ca^{2+} from disorganised FA and organised FA coatings when combined with PRP gel

The release of Ca^{2+} from disorganised and organised FA coatings in presence of PRP gel was investigated by measuring the concentrations of Ca^{2+} ions diffusing into PBS at different time points for up to 14 days using inductively coupled plasma optical emission spectrometry (Figure 53). The PRP samples,

applied to the FA coatings were treated with 20 IU/mL thrombin to activate the platelets and trigger PRP gelification. At 2 hour time point, the concentrations of Ca^{2+} released from disorganised FA (0.07 ±0.01 mg/L) and organised FA (0.07 ±0.009 mg/L) coatings were similar when FA used alone without PRP gel and this was consistently seen at all time points. However, at the 2 hour time point and in the presence of PRP gel, the release of Ca^{2+} ions was increased for organised FA (0.95 ±0.03 mg/L) and disorganised FA coatings (0.68 ± 0.16 mg/L) with the value for the organised FA coating being greater than that of the disorganised coating.

At the one day time point (Figure 53), the absolute amounts released are clearly reduced compared to the 2 hour time point. However, the general pattern of Ca^{2+} release is similar to the data obtained for the 2 hour point described above where Ca^{2+} released from disorganised FA combined with PRP gel (0.118 ±0.01 mg/L) being higher than Ca^{2+} released from disorganised FA alone (0.078 ±0.02 mg/L) and Ca^{2+} released from organised FA combined with PRP gel (0.313 ±0.06 mg/L) being greater than the amount released by organised FA alone (0.055 ±0.001 mg/L). The organised FA combined with PRP gel induced a higher Ca^{2+} (0.313 ±0.06 mg/L) than the disorganised FA combined with PRP gel (0.118 ±0.01 mg/L).

At day 3, the calcium release dropped. As can be seen from figure 53, the difference between disorganised FA and organised FA samples was small. Over the remaining 14 days of the test, the amounts of Ca^{2+} released remained low for all groups with slight difference between them.

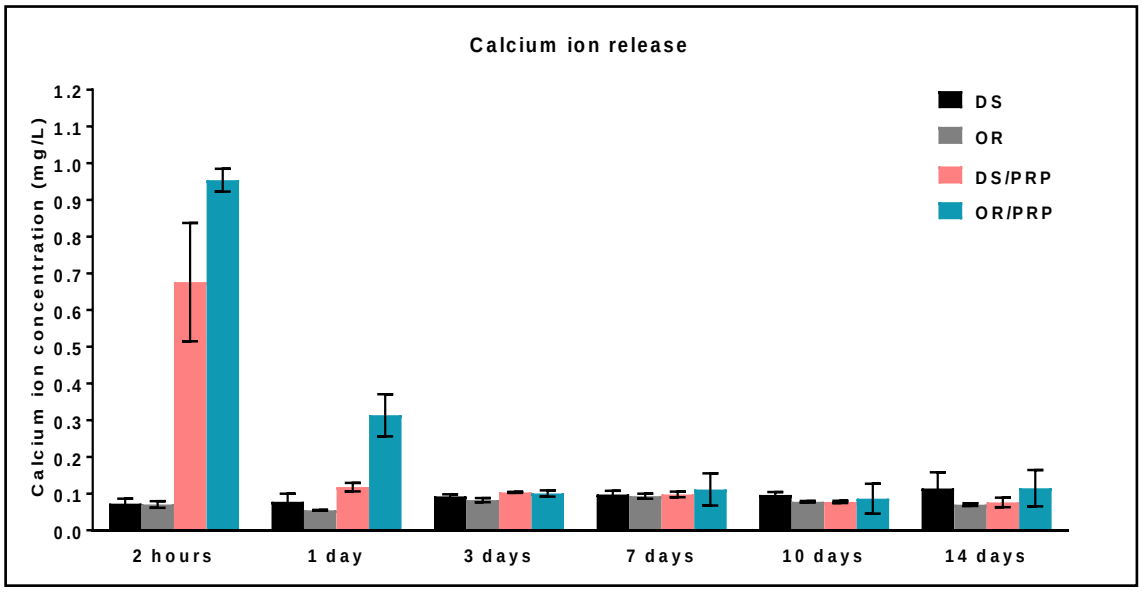

Figure 53: Concentrations of Ca^{2+} (mean ±SD) released from FA and FA/PRP combinations in PBS samples. No difference was seen between the concentrations of Ca^{2+} released from disorganised FA and organised FA coatings when used alone without PRP gel at all time points. Samples with PRP gel released more calcium than samples lacking PRP for over 3 days. OR/PRP gel had increased calcium concentrations compared to DS/PRP gel within the first 24 hours. DS, Disorganised FA; OR, organised FA; SS, stainless steel; PRP, platelet-rich plasma.

6.2.4 Cytotoxicity of FA/PRP combinations

Previously in Chapter 4, it was shown that media preconditioned with FA was non-cytotoxic against G292 cells when grown in culture supplemented with 10% FBS. In Chapter 5, it was shown that media supplemented with activated 10% PRP was also non-cytotoxic against G292 cells. The aim of this section was to discover the effect of FA preconditioned media combined with PRP on cell viability. In this test, G292 cells were grown in media supplemented with 10% PRP (activated with $CaCl_2$) and compared to cells grown in FA preconditioned media supplemented with 10% activated PRP. As controls, the cells were grown in media supplemented with 10% FBS providing idealised conditions for cell viability (i.e. the negative control for cell death) and the cells were grown in FA preconditioned media supplemented with 10% FBS. Cell viability was determined by measuring LDH released into the media by the dead cells. The experiment was repeated twice using PRP samples extracted from 2 blood

donors. Cell death was expressed by normalising the amount of LDH released to a positive control (the cells were killed by adding the detergent Triton- X100) and mean data of the 2 blood donors were presented in figure 54.
Relative to the positive control (representing 100% cell death), none of the treatment options were cytotoxic. LDH measurements were similar in the 10% FBS negative control (9.2%±0.6) and 10% FBS combined with FA preconditioned media (9.5%±0.4) which means FA has no cytotoxic effect (confirming the data presented in Chapter 4). Similarly, cells grown in media supplemented with 10% PRP are perfectly viable in that LDH release is not greatly different to the negative control (10% FBS) (10.7%±3.6 versus 9.2%±0.6 respectively). Interestingly, using FA preconditioned media supplemented with 10% PRP (6.3%±1) appeared to reduce the release of LDH compared to using media containing 10% PRP alone (10.7%±3.6). Likewise, FA preconditioned media supplemented with 10% PRP showed less LDH amount compared to FA-conditioned medium supplemented with 10%FBS (9.5%±0.4).

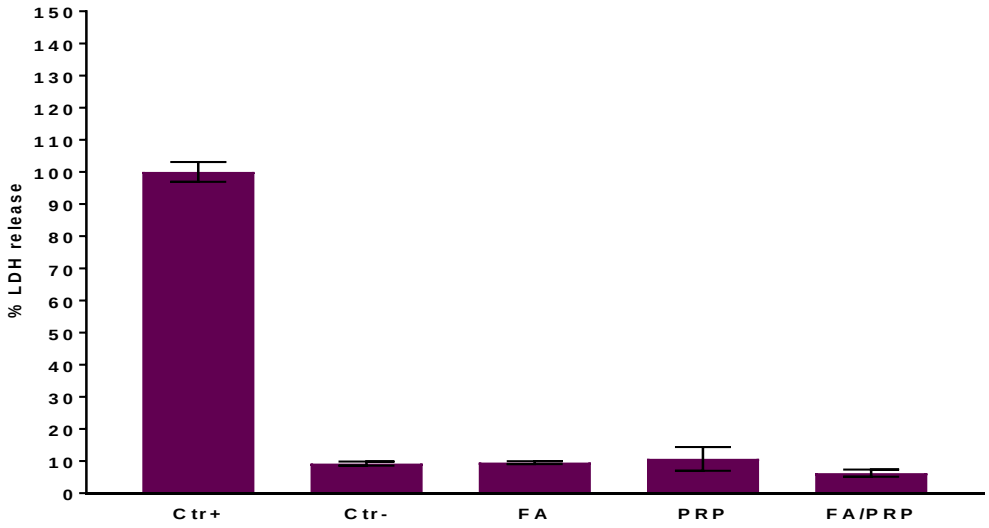

Figure 54: Cytotoxicity (%LDH release mean ±SD) of FA&/or PRP combination on G292 cells after cell culturing for 3 days using PRP samples extracted from 2 blood donors. All the tested groups were normalised to the positive control (100% cell death). The mean data of the 2 donors showed that all the tested groups showed no cytotoxicity. The negative control and FA preconditioned media and PRP groups showed similar amounts of LDH. However, combination of FA and PRP showed low LDH release compared to that of FA or PRP alone.

6.2.5 Protein adsorption of PRP on FA coatings

Adsorption of PRP and FBS proteins on substrates comprised of disorganised FA coatings, organised FA coatings and uncoated SS was investigated using gel electrophoresis (8-16% SDS-PAGE gel). PRP was activated with thrombin to generate PRP gel and PRP-releasate. PRP and FBS samples were loaded on the substrates for an overnight period and competitively desorbed using phosphate buffer. Equal portions of each extract were subjected to SDS-PAGE analysis and the total protein was visualised using silver staining. The experiment was performed using PRP obtained from 2 blood donors and was repeated in triplicate for each donor. Representative data is shown in figure 55. Molecular weight calibrators are shown in the lane labelled Mwt and these indicate that proteins ranging from less than 15kDa to over 250KDa were evident in samples desorbed from the substrates.

For donor 1, PRP gel proteins desorbed from disorganised and organised FA substrates are shown in lanes 1 and 2 respectively. Interestingly, PRP gel proteins appeared to be differentially adsorbed to the disorganised and organised coatings as indicated by the asterisks between the lanes. In contrast, no detectable PRP gel proteins was recovered from the uncoated SS (lane 3). Proteins comprising the PRP releasate from donor 1 appeared to adsorb to the disorganised and organised FA substrates as shown in lanes 4 and 5 respectively with more protein being recovered from the organised FA. Again there was a very clear differential adsorption between the two coatings as indicated by the asterisks between the lanes. No detectable protein was recovered from the uncoated SS (lane 6). The protein comprising the FBS control were also differentially adsorbed to the disorganised and organised FA substrates as indicated by the asterisks in lanes 7 and 8 respectively. With more protein being recovered from the organised FA substrate. As with PRP gel and PRP releasate, no detectable FBS protein was recovered from the uncoated SS (lane 9).

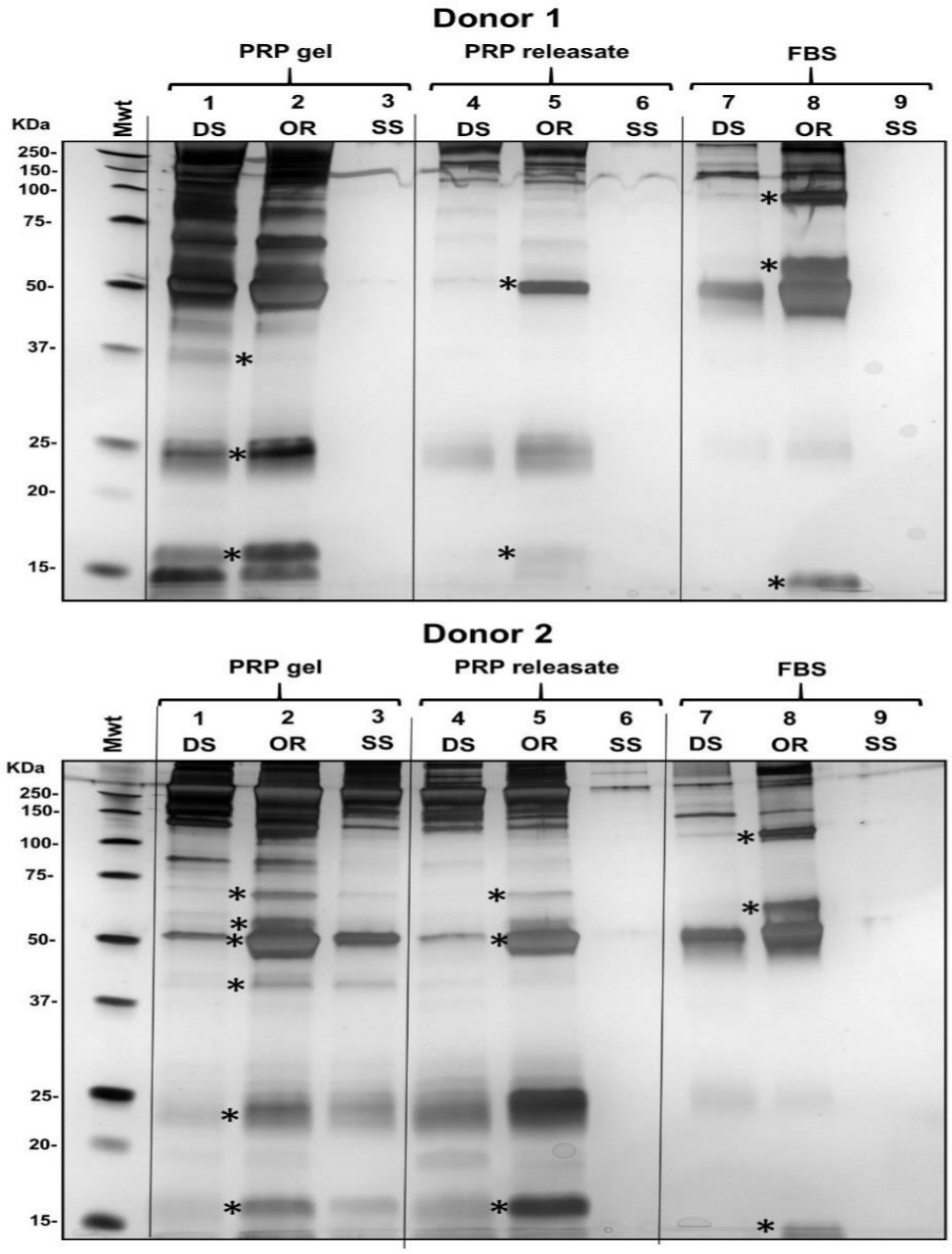

Figure 55: SDS-PAGE of PRP and FBS proteins that were adsorbed overnight on disorganised FA, organised FA and uncoated SS. Disorganised and organised FA appeared to adsorb proteins from PRP and FBS in a differential manner (indicated by the asterisks). Protein recovery was generally greater from organised FA compared to disorganised FA. Variability in the protein banding pattern between donors 1 and 2 demonstrates donor variability. Mwt, molecular weight calibrators; DS, Disorganised FA; OR, organised FA; SS, stainless steel; PRP, platelet-rich plasma; FBS, fetal bovine serum.

In the case of donor 2 (Figure 55), a range of proteins were again present ranging from less than 15kDa to over 250KDa. However, there are inter donor differences between donor 1 and 2. For example, lane 1 (PRP gel adsorbed to disorganised FA) when compared between donors 1 and 2. Asterisks indicate where there is a differential recovery of proteins from disorganised and organised FA coatings in each group. Special attention is drawn to lane 3 of donor 2 which shows that significant proteins were recovered from uncoated SS which is in complete contrast to donor 1 and further indicates the effect of donor variability on PRP composition and behaviour. PRP gel, PRP releasate proteins of donor 2 and FBS control proteins were also recovered in greater amounts from organised FA substrates compared to disorganised FA substrates.

6.2.6 Microscopic analysis of cell morphology and attachment on FA coatings in combination with PRP gel or PRP releasate

The attachment, morphology and distribution of G292 cells cultured for 2 days on discs coated with disorganised FA or organised FA in combination with PRP gel or PRP releasate were examined using SEM and fluorescence confocal laser microscopy.

- **Microscopic analysis of cell growth on FA/PRP gel combinations**

The SEM and fluorescence confocal images of G292 cells growing on both organised and disorganised FA crystal surfaces when combined with PRP gel are shown in figure 56. The analysis of disorganised FA images revealed clumps of small rounded structures that most likely represent platelets embedded within and surrounding the cells and PRP gel. The cells were clustered in groups spreading over the crystals (Figure 56a and 56b).
In the case of organised FA, PRP gel appeared to form a large sheet that spread over the coating surface (Figure 56c and 56d), and was associated with a large number of cells laying down and adhering within PRP gel as seen clearly in confocal microscopy analysis (figure 56d).

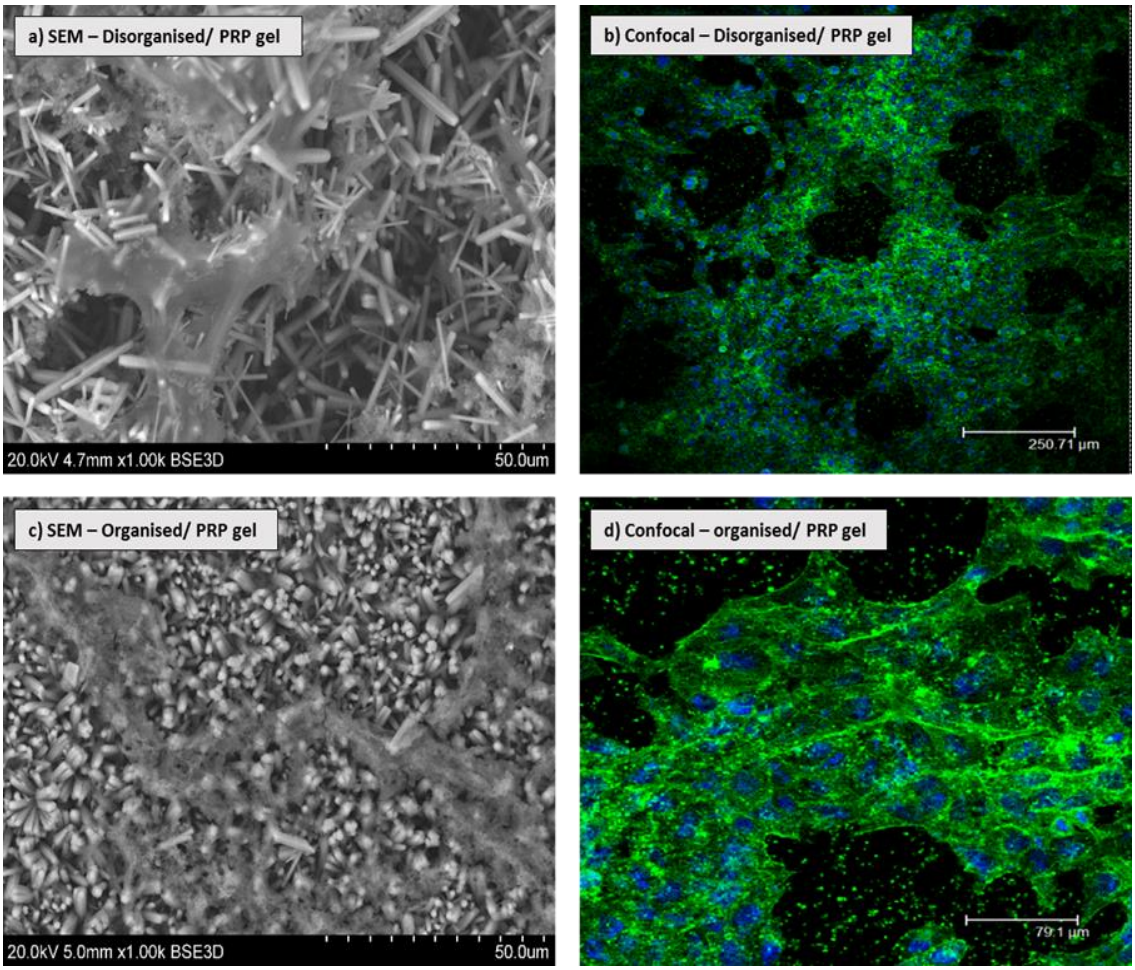

Figure 56: SEM and confocal images of G292 cells attached and grown on FA/PRP gel combinations for 2 days. Cells grown on disorganised coatings were clustered in groups and were surrounded by small round structures which are most likely platelets. PRP gel of organised FA was seen as a big sheet incorporated with many cells.

➢ **Microscopic analysis of cell growth on FA/PRP releasate combinations**

The SEM and fluorescence confocal images of G292 cells growing on both disorganised and organised FA surfaces combined with PRP releasate are shown in figure 57. Cells colonising disorganised FA in combination with PRP releasate adopted a cellular morphology and distribution similar to that observed in disorganised FA coatings in combination with FBS (see figure 31, chapter 4). As shown in figure 57a and 57b, the cells tend to grow as groups of cells and they appeared polygonal with cell processes stretching between the

crystals indicating cell spreading and growth. In organised FA coatings (Figure 57c and 57d), PRP releasate promoted the cellular attachment and growth but the cellular organisation and structure was not similar to that observed in organised FA combined with FBS in that the cells were polygonal but did not have a stellate-like shape and had less prominent cytoplasmic extensions compared to cells grown with FBS.

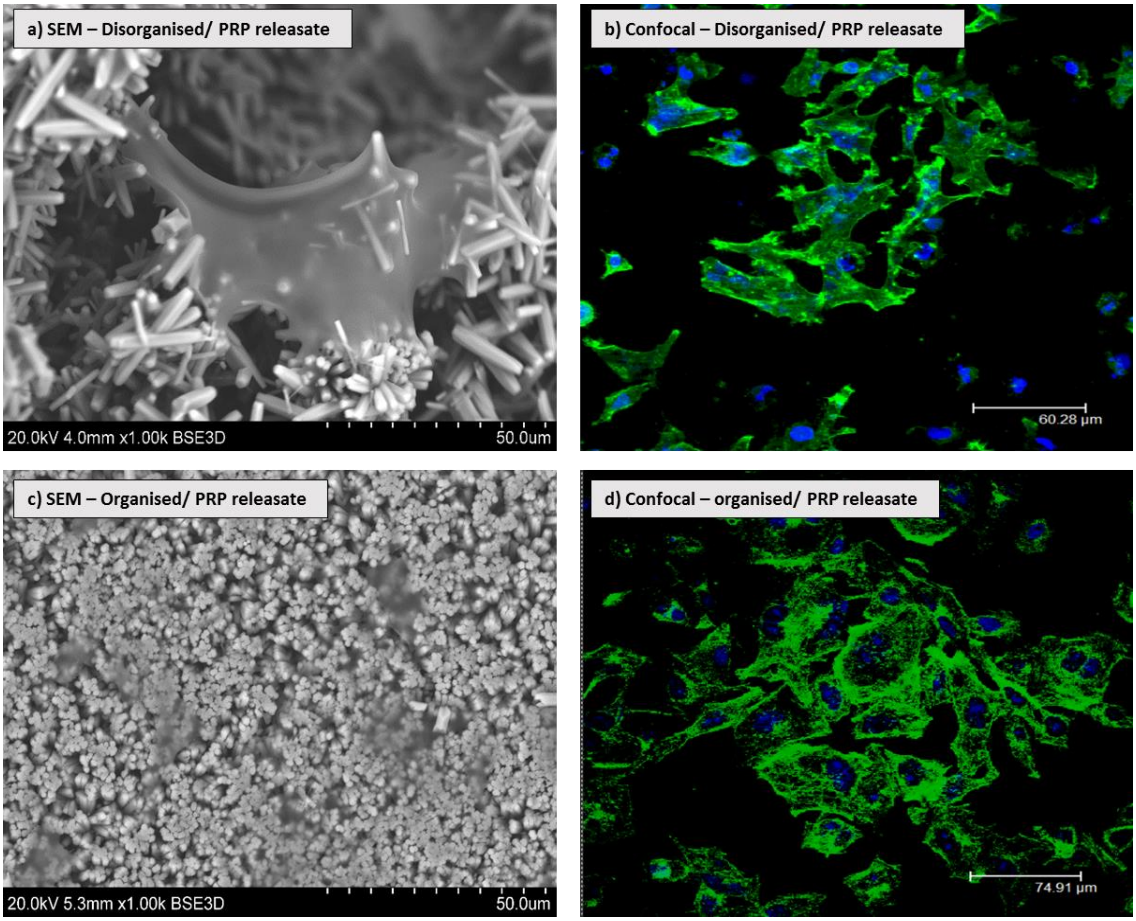

Figure 57: SEM and confocal images of G292 cells attached and grown on FA/PRP releasate combinations for 2 days. The cells grew as groups of cells on disorganised FA with cell processes stretching between the crystals. On organised FA, the cells were polygonal and were spreading with less prominent cytoplasmic extensions compared to cells grown with FBS.

6.2.7 Quantitative analysis of cell attachment and proliferation on FA coatings combined with PRP gel, PRP releasate or FBS

G292 osteoblast-like cells were grown on uncoated stainless steel, disorganised FA coated discs and organised FA coated discs combined with either FBS (control), PRP gel or PRP releasate (obtained by extracting the soluble components from thrombin-activated PRP). In order to examine cell attachment, the DNA content of the grown cells was measured after 5 hours and one day of cell culture and in order to examine cell proliferation, DNA content was detected after 3 and 7 days. The experiment was repeated twice using PRP samples extracted from 2 blood donors. The complete individual data sets for donor 1 and donor 2 are presented in appendix 3 and 4 respectively. The data in each experimental group was normalised to the mean value obtained from the control (uncoated SS combined with FBS) and the mean of the two donors data was plotted for each time point.

- **Quantitative analysis of cell attachment**

The assessment of cell attachment after 5 hours (figure 58) showed that under standard culture condition (cell culture using FBS), no difference was observed between FA coatings and uncoated discs (SS). PRP releasate seemed to have the same effect on cell attachment as FBS in all groups tested. However, compared to FBS, PRP gel increased the cell attachment and the DNA content (as a proxy for cell number) was increased by about 174%, 157% and 149% in SS, disorganised FA and organised FA respectively.

After one day of cell culture (Figure 58), there was no difference between FA coatings and uncoated SS when combined with FBS. However, increase in DNA content was observed when PRP gel was added to the uncoated SS, disorganised FA and organised FA coatings compared to the FBS by about 50%, 40% and 90% respectively. PRP gel promoted cellular attachment on organised FA (191%±56) compared to disorganised FA (140%±40) and compared to uncoated SS (145%±44).

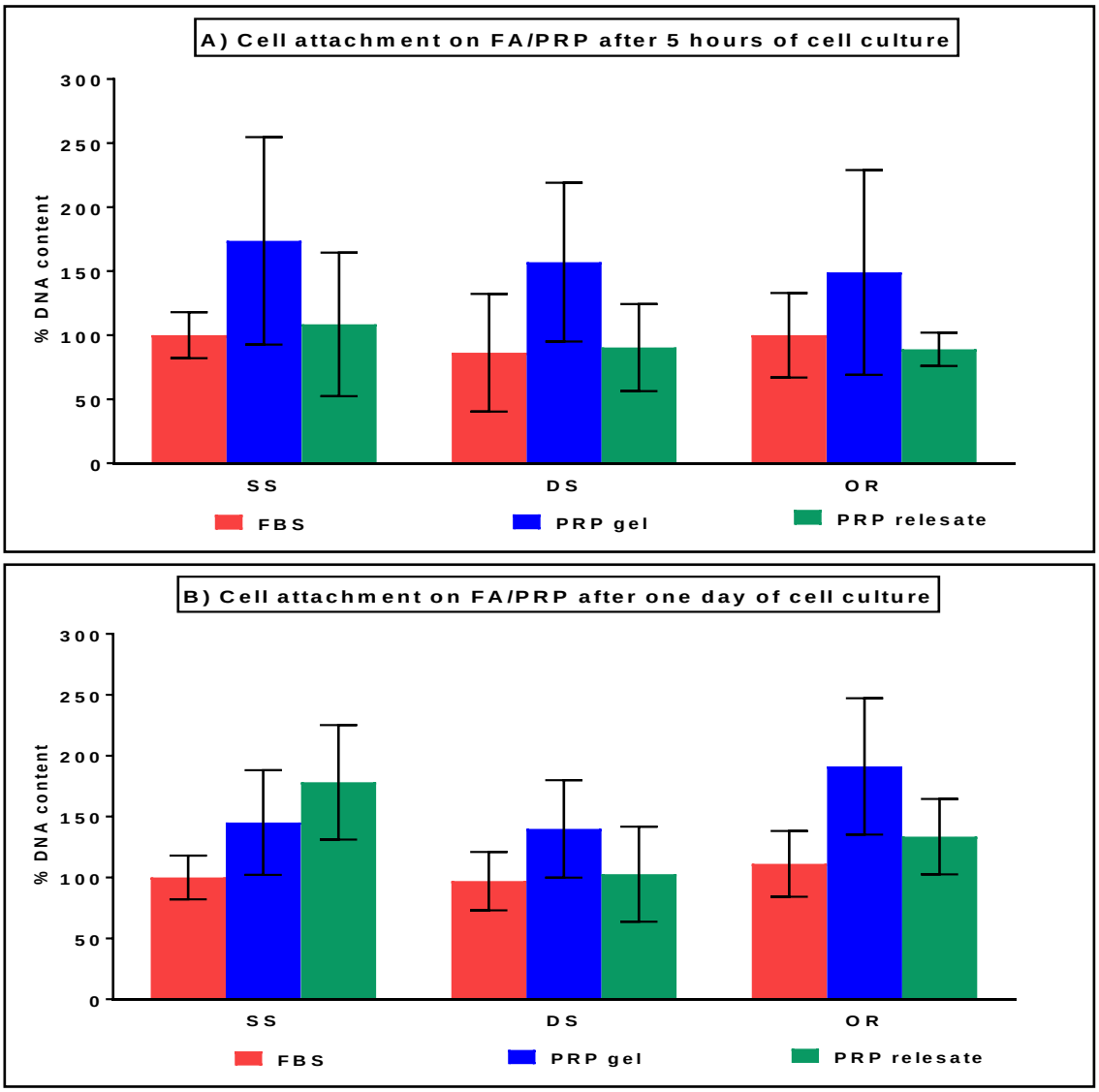

Figure 58: Cell attachment of G292 osteoblast-like cells on FA/PRP (PRP from 2 blood donors) after 5 hours and one day of cell culture, assessed by DNA quantification. All the experimental groups of each donor were normalised to the relative control group (SS/FBS) and mean data of the 2 PRP donors were plotted for each time point. Under standard culture conditions (FBS), FA coatings did not show a different effect on initial cell attachment when compared to uncoated discs. However, addition of PRP gel to FA coatings seemed to enhance cell attachment within the first 24 hours as compared to the control. DS, Disorganised FA; OR, organised FA; SS, stainless steel; PRP, platelet-rich plasma; FBS, fetal bovine serum.

➢ **Quantitative analysis of cell proliferation**

DNA content was determined after 3 days as a measure of cell number and proliferative rate. A similar trend was observed at day 3 (Figure 59) where PRP gel increased the cellular proliferation on both FA coatings above that of the control (uncoated SS/FBS) by 50% and 90% in disorganised and organised FA coatings respectively. A higher amount of DNA was detected in organised FA compared to disorganised FA when the coatings combined with PRP gel .
At day 7 (Figure 59), neither FA coatings enhanced cell proliferation when combined with FBS compared to the control. However, organised FA coatings combined with PRP gel showed increase in DNA content compared to the control (uncoated SS/FBS) by about 30%. Moreover, the increase of cell proliferation induced by organised FA combined with PRP gel was higher than SS and disorganised FA combined with PRP gel.

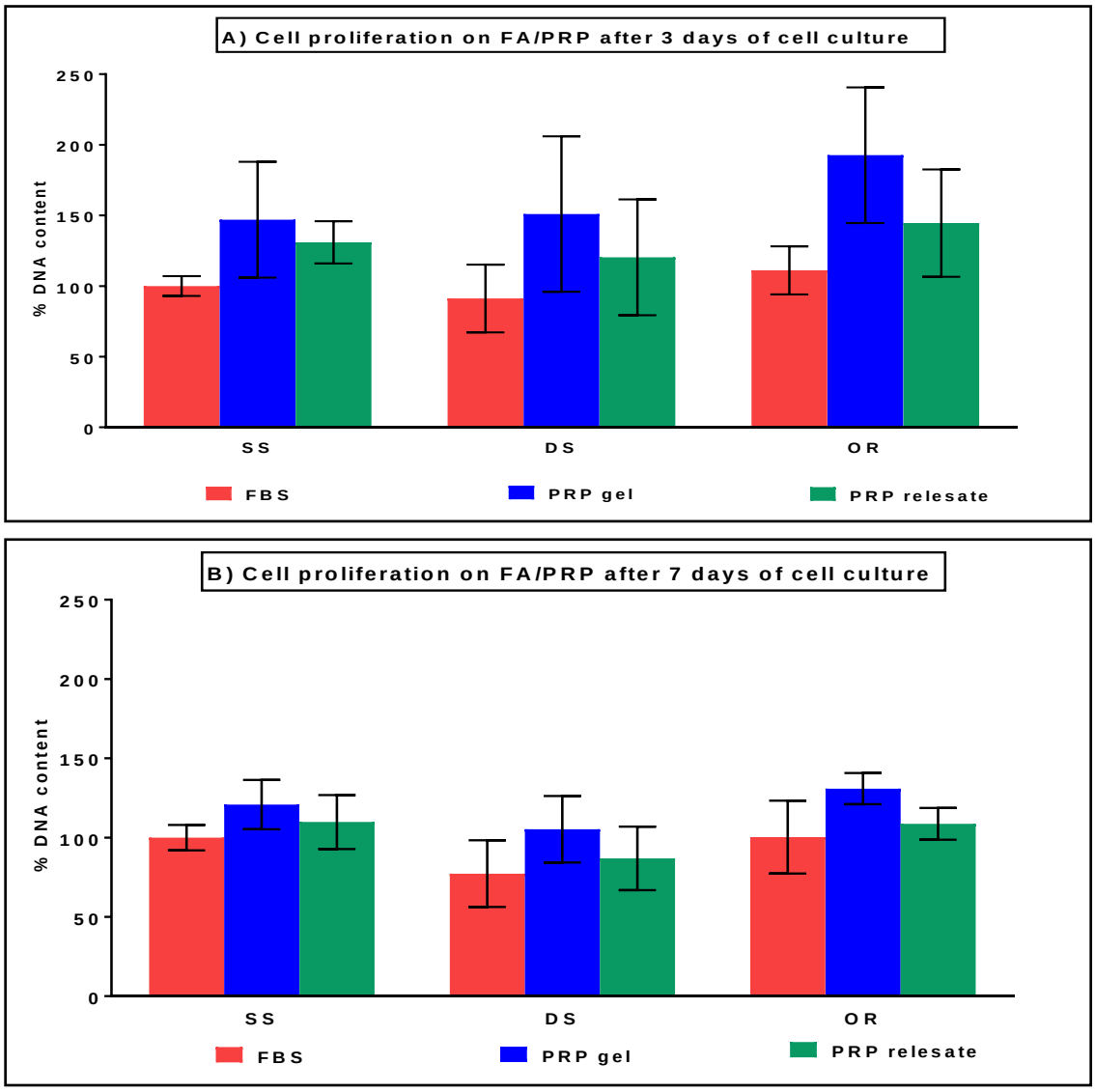

Figure 59: Cell proliferation of G292 osteoblast-like cells on FA/PRP combinations after 3 days and 7 days of cell culture, assessed by DNA quantification. All the experimental groups of PRP obtained from two donors were normalised to the relative control group (SS/FBS) and mean data of the 2 PRP donors were plotted for each time point and statistically analysed. Under standard culture conditions (FBS), FA coatings did not show a significant effect on cell proliferation when compared to uncoated discs. However, addition of PRP gel and releasate to FA coatings seemed to enhance cell proliferation in a consistent manner over the 7 days as compared to the control. DS, Disorganised FA; OR, organised FA; SS, stainless steel; PRP, platelet-rich plasma; FBS, fetal bovine serum.

6.2.8 Osteogenic differentiation of human dental pulp stem cells (hDPSCs) cultured on FA/PRP combinations

6.2.8.1 Determination of expression of osteogenic marker genes by hDPSCs cultured on FA/PRP combinations using qRt-PCR

6.2.8.1.1 Validation of using GAPDH as a housekeeping gene

Changes in gene expression are measured relative to the expression of a specific gene whose expression is thought to be constant during the course of the experiment. GAPDH is an example of a so called “housekeeping gene” which codes for a glycolytic enzyme and is expressed at a constant rate in many cell types as its function is essential to energy metabolism in the cell. In addition, the expression level of a suitable house-keeping gene should not vary significantly between different samples. The suitability of GAPDH to act as a reference housekeeping gene under the experimental condition used here was tested. hDPSCs were cultured for 3 days under osteogenic conditions on uncoated and organised FA coated discs combined with either PRP gel, PRP releasate or FBS. Expression of GAPDH by hDPSCs was investigated using qRT-PCR. Examples of the resulting amplification curves are shown in figure 60. The results showed a constant expression of GAPDH irrespective of the cell culture conditions used with no differences between expression levels across samples. This indicated that GAPDH was suitable to use as a reference gene against which expression of other genes could be compared.

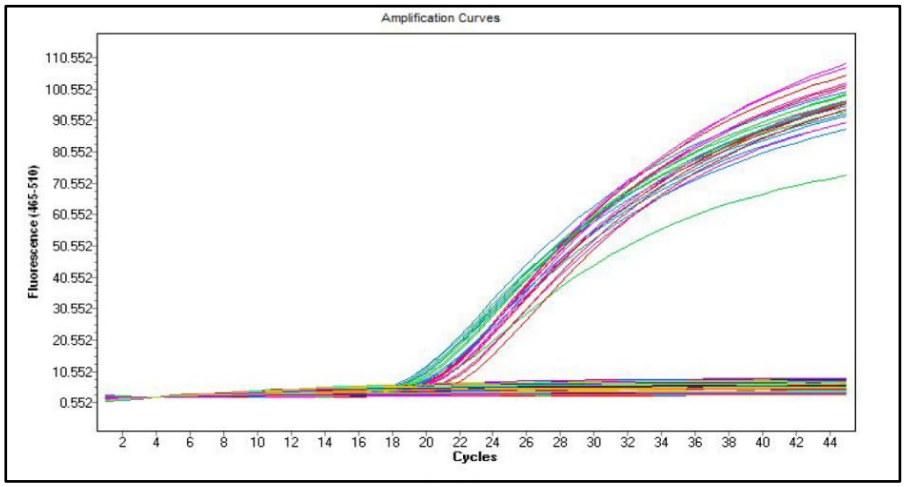

Figure 60: Amplification curves of the qRt-PCR assay using the house-keeping gene (GAPDH) showing a constant expression irrespective of changes of treatment. The straight lines represent the empty wells of the PCR 96-well plate.

6.2.8.1.2 Effect of FA/PRP combinations on levels of osteogenic gene expression in hDPSCs under osteogenic culture conditions

hDPSCs were grown on uncoated stainless steel and organised FA coated discs loaded with either FBS (control), PRP gel or PRP releasate (soluble components extracted from thrombin-activated PRP) in osteogenic media containing dexamethasone and L-ascorbic acid. After 3 days, the level of expression of osteogenic marker genes (ALP, RUNX-2, OCN and OPN) by hDPSCs was determined using qRT-PCR. The effects of PRP extracted from 2 donors on gene expression was investigated. The relative change in gene expression was calculated using the delta Ct (ΔCt) method. By using this method, ΔCt was first calculated by normalising the Ct value of each gene of interest to that of the house keeping gene (GAPDH, see the previous section) determined for the same sample. Then, the relative change in gene expression was calculated using $2^{-\Delta ct}$. Finally, the ratio of gene expression in FA/PRP cultures compared to the control (uncoated SS/FBS) was calculated by normalising $2^{-\Delta ct}$ value for each sample to the mean value of $2^{-\Delta ct}$ of the control sample. The results of the mean of ratio of expression (fold change) ±SD were plotted.

➢**Effect of FA/PRP combinations on expression of ALPL in hDPSCs**

PRP gel and PRP releasate derived from blood donor 1 (Figure 61), caused an up regulation in ALPL expression when used in combination with uncoated SS by about 4.6 fold relative to the control (uncoated SS loaded with FBS). PRP gel showed a slight upregulation in ALPL expression of about 1.7 fold above that of the control when combined with organised FA. In contrast, organised FA failed to cause any significant change in ALP expression compared to the control when used in combination with FBS or PRP releasate. However, both of PRP gel and PRP releasate showed an increase in ALPL expression compared to FBS when combined with organised FA.

In the case of the second donor, all SS and organised FA samples had no effects on ALPL expression compared to the control (Figure 61). However, PRP gel and releasate from both donors showed higher ratios of expression when added to uncoated SS compared to when added to organised FA.

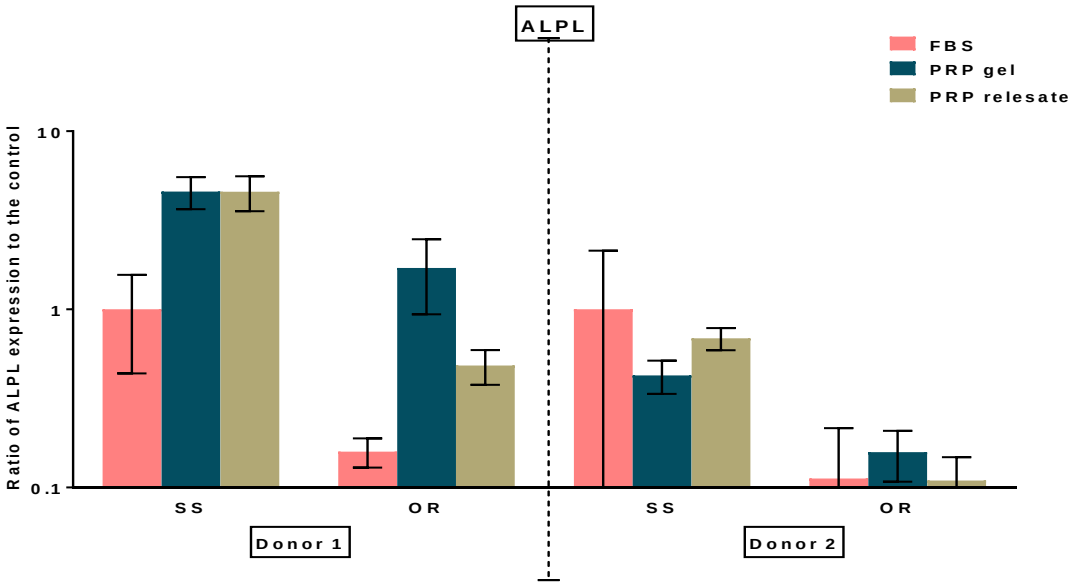

Figure 61: Ratio of ALPL gene expression to SS/FBS control (mean ±SD) in hDPSCs cultured on uncoated and organised FA coated discs combined with FBS, PRP gel or PRP releasate. Compared to the control, PRP extracted from 2 blood donors did not increase the level of ALPL gene expression when combined with organised FA except PRP gel derived from donor 1. PRP of donor 1 showed a high ALPL expression when combined with SS compared to the control. PRP gel and releasate of both donors showed high expression when combined with SS compared to when combined with organised FA. OR, organised FA; SS, stainless steel; PRP, platelet-rich plasma; FBS, fetal bovine serum; ALPL, alkaline phosphatase gene.

➢**Effect of FA/PRP combinations on expression of RUNX-2 in hDPSCs**

After 3 days in osteogenic culture, PRP gel and PRP releasate from donor 1 showed upregulation in RUNX-2 expression when combined with uncoated SS (3 fold difference) and organised FA (2 fold difference) compared to the control (uncoated SS loaded with FBS) (Figure 62). Whereas organised FA displayed a lower level of RUNX-2 expression when loaded with FBS by about two times compared to the control.

In donor 2, RUNX-2 expression was not changed when comparing the levels of all the samples to that of the control (Figure 62). Similar to donor 1, PRP releasate and FBS showed high RUNX-2 expression when combined with SS

compared to organised FA. Nevertheless, and in contrast to donor 1, hDPSCs showed an increase in RUNX-2 expression in organised FA when loaded with FBS compared to when loaded with PRP.

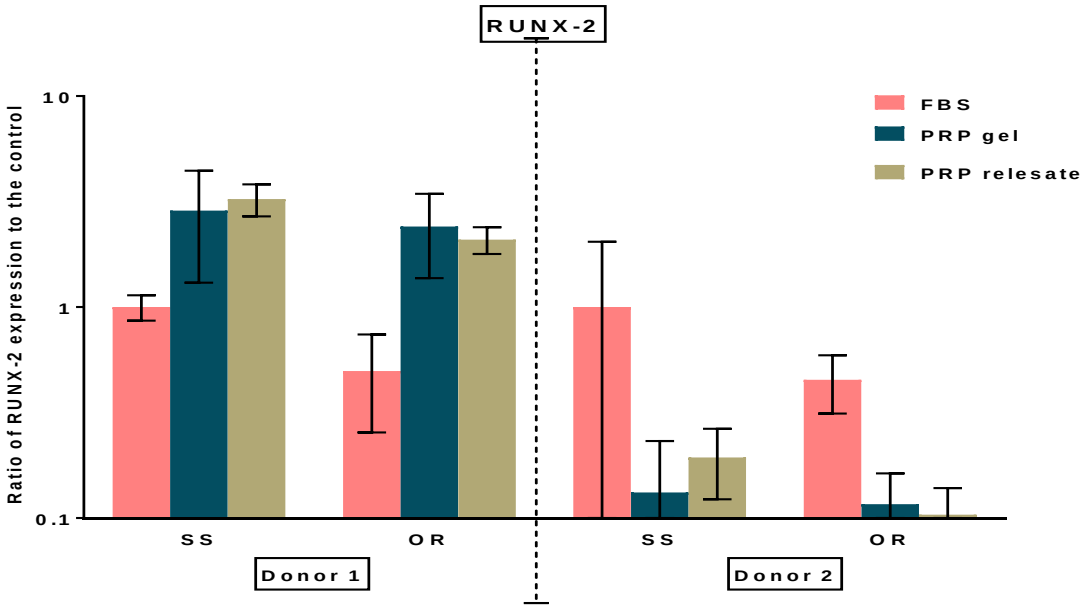

Figure 62: Ratio of RUNX-2 gene expression to the control (SS/FBS) (mean ±SD) in hDPSCs cultured on uncoated and organised FA coated discs combined with FBS, PRP gel or PRP releasate. Compared to the control, PRP gel and releasate of donor 1 showed a high RUNX-2 expression when combined with SS and FA compared to the control. While in donor 2, low RUNX-2 expression was showed by all the samples compared to the control. PRP gel and releasate of both donors showed high expression when combined with SS compared to organised FA. OR, organised FA; SS, stainless steel; PRP, platelet-rich plasma; FBS, fetal bovine serum.

Effect of FA/PRP combinations on expression of OCN in hDPSCs

The levels of OCN expression of FA coated sample groups were not different to those of the control (Figure 63).

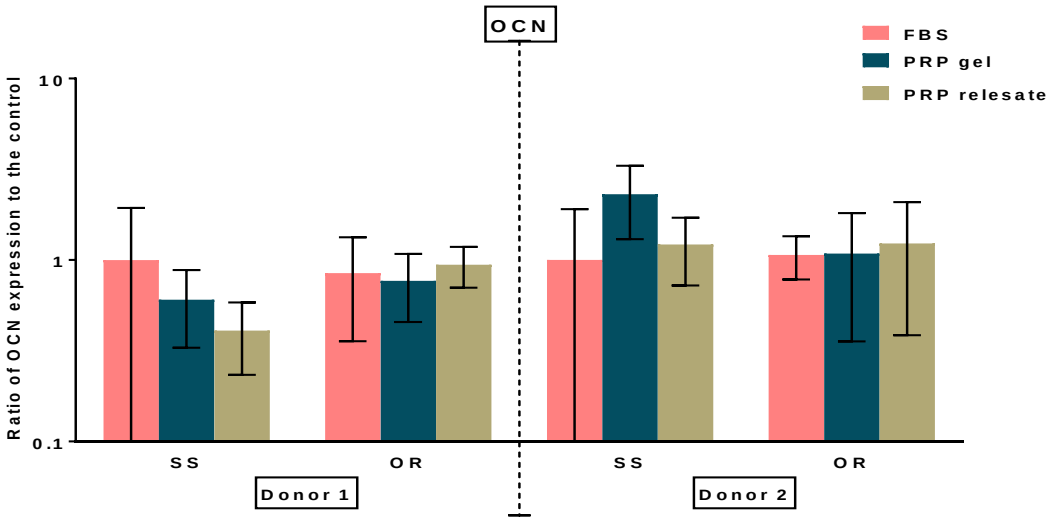

Figure 63: Effects of FA and PRP on levels of OCN gene expression (mean ±SD) in hDPSCs cultured on uncoated and organised FA coated discs combined with FBS, PRP gel or PRP releasate. The levels of OCN expression of organised FA sample groups were almost similar to those of the control in both blood donors' cases. OR, organised FA; SS, stainless steel; PRP, platelet-rich plasma; FBS, fetal bovine serum; OCN, osteocalcin.

➢**Effect of FA/PRP combinations on expression of OPN in hDPSCs**

Compared to uncoated SS loaded with FBS control, OPN expression in hDPSCs was down regulated in PRP releasate of donor 1 when combined with uncoated SS. When SS was coated with organised FA, the level of OPN gene expression was upregulated under standard culture condition (FBS) by about 4 times compared to the control, and was upregulated when organised FA was combined with PRP gel and PRP releasate by about 19 and 17 times respectively compared to the uncoated control (Figure 64).

In the case of the donor 2 (Figure 64), OPN expression was comparable in PRP groups when combined with uncoated SS to that of the control. When PRP gel and releasate were combined with organised FA, they increased the expression levels of OPN compared to the control by 12 and 3 times respectively. The upregulation of OPN expression was higher in PRP gel when added to organised FA compared to PRP releasate. Organised FA showed also up-

regulation in OPN expression under standard culture condition (FBS) compared to the control by about 3.5 times.

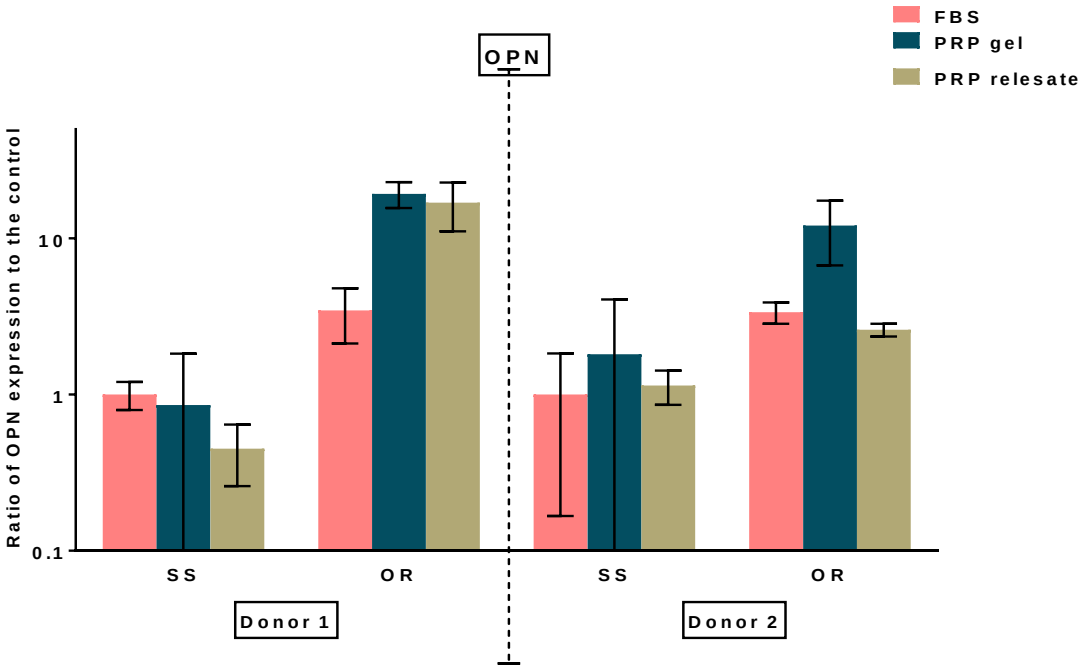

Figure 64: Effects of FA and PRP on levels of OPN gene expression (mean ±SD) in hDPSCs cultured on uncoated and organised FA coated discs combined with FBS, PRP gel or PRP releasate. The levels of OPN gene expression were up regulated in organised FA when combined with FBS or PRP of 2 blood donors compared to the uncoated controls. OR, organised FA; SS, stainless steel; PRP, platelet-rich plasma; FBS, fetal bovine serum; OPN, osteopontin.

6.2.8.2 ALP activity in hDPSCs cultured on FA/PRP combinations

6.2.8.2.1 Quantitative analysis of ALP activity

hDPSCs were grown on uncoated stainless steel and organised FA coated discs loaded with either FBS (control), PRP gel or PRP releasate (soluble components extracted from thrombin-activated PRP) in osteogenic media containing dexamethasone and L-ascorbic acid. After 2 weeks, ALP activity (an early osteoblast differentiation marker) of hDPSCs was determined. The levels of ALP activity was determined in two experiments using PRP samples extracted from blood of 2 donors. The data were first normalised to DNA content and then to the control (uncoated SS/FBS). The mean values ±standard

deviation obtained using PRP from the 2 blood donors were plotted. The results presented in figure 65 showed that organised FA coatings reduced ALP activity under standard culture conditions (FBS), to around 10% relative to the control. The addition of PRP gel and PRP releasate to FA coatings did not restore ALP activity seen in uncoated SS/FBS samples (20% and 17% respectively).

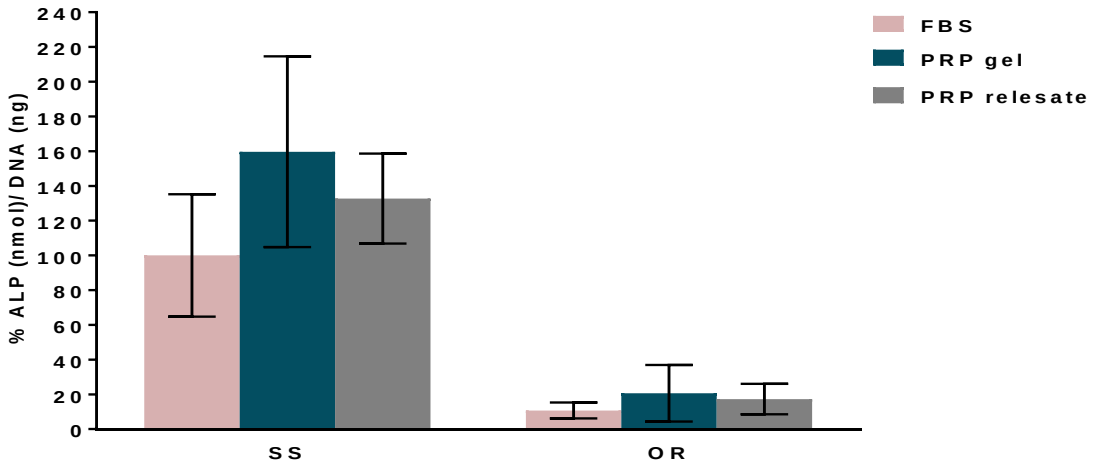

Figure 65: ALP activity normalised to DNA concentrations (mean ±SD) of hDPSCs cultured on uncoated and organised FA coated discs combined with FBS, PRP gel or PRP releasate under osteogenic culture conditions after at 2 weeks of cell culture. ALP/DNA ratios were normalised to the control (uncoated SS/FBS) forming 100% and mean data of 2 blood donors was plotted. The highest level of ALP activity was detected in PRP groups when loaded on SS. In contrast, organised FA had a very low ALP activity compared to the control. OR, organised FA; SS, stainless steel; PRP, platelet-rich plasma; FBS, fetal bovine serum; ALP, alkaline phosphatase.

6.2.8.2.2 Qualitative analysis of ALP deposition in hDPSCs culture

hDPSCs were cultured for 2 weeks on monolayers under basal and osteogenic conditions in order to confirm the capability of hDPSCs for the osteogenic differentiation. The cells showed a transparent cell layer with sporadically distributed ALP positive areas. However, more intense ALP staining was seen visually in hDPSCs cultured under osteogenic conditions compared to cells cultured under basal conditions (Figure 66).

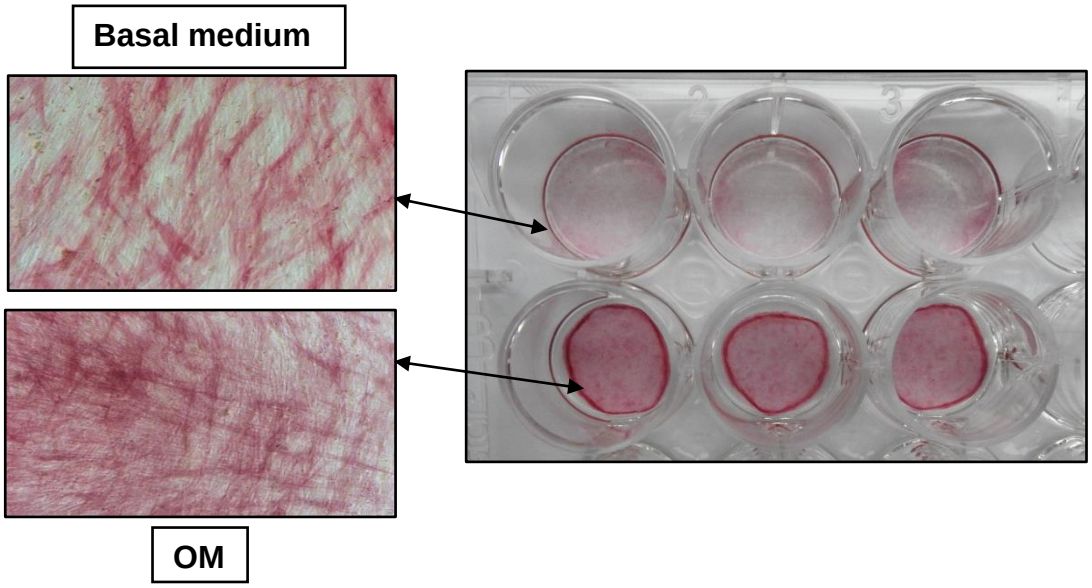

Figure 66: ALP staining for hDPSCs cultured in monolayer under basal and osteogenic conditions (OM). The cells showed positive ALP staining, but the stain was more intense for cells cultured under osteogenic conditions compared to basal conditions.

Osteogenic differentiation of hDPSCs cultured for 2 weeks on SS and organised FA discs combined with FBS, PRP gel or PRP releasate under osteogenic conditions was determined by staining for ALP activity. All the samples showed evidence of positive staining for ALP (dark purple coloration) as shown in figure 67. However, hDPSCs seeded with PRP gel and releasate showed a more intense widespread staining compared to cells seeded with FBS. Interestingly, ALP stain was more evident in SS uncoated discs compared to the corresponding organised FA coated discs. Control SS and organised FA discs (without cells) were also tested for ALP stain. As seen in figure 68, the controls were totally negative for the ALP stain when whether combined with FBS, PRP gel or PRP releasate.

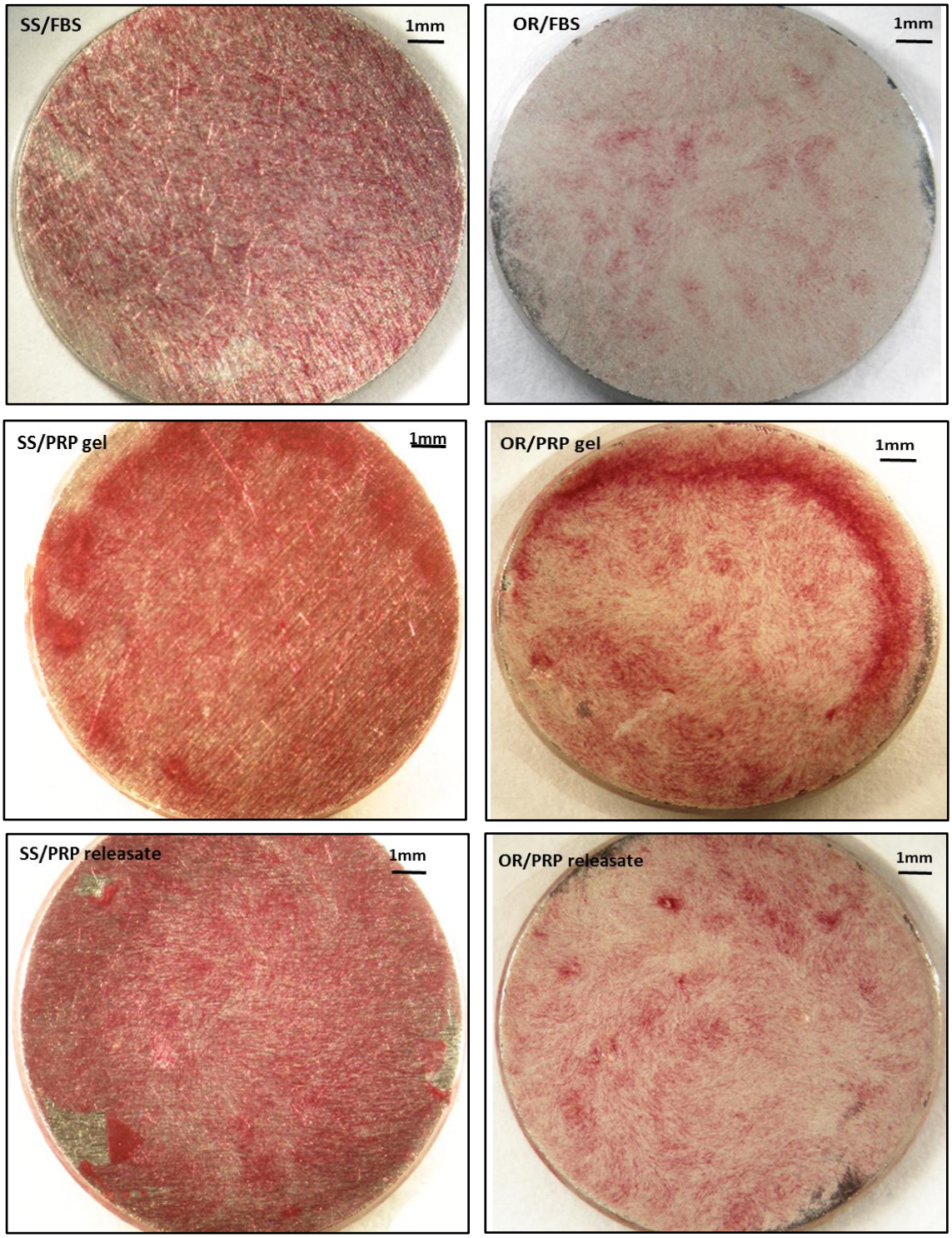

Figure 67: ALP staining (dark purple) of hDPSCs cultured on FA&/or PRP for 2 weeks under osteogenic conditions. All the samples showed positive ALP stain. However, hDPSCs cultured with PRP had a more intense widespread staining compared to cells seeded with FBS. ALP stain was more evident in SS uncoated discs compared to the corresponding OR FA coated discs. OR, organised FA; SS, stainless steel; PRP, platelet-rich plasma; FBS, fetal bovine serum; ALP, alkaline phosphatase.

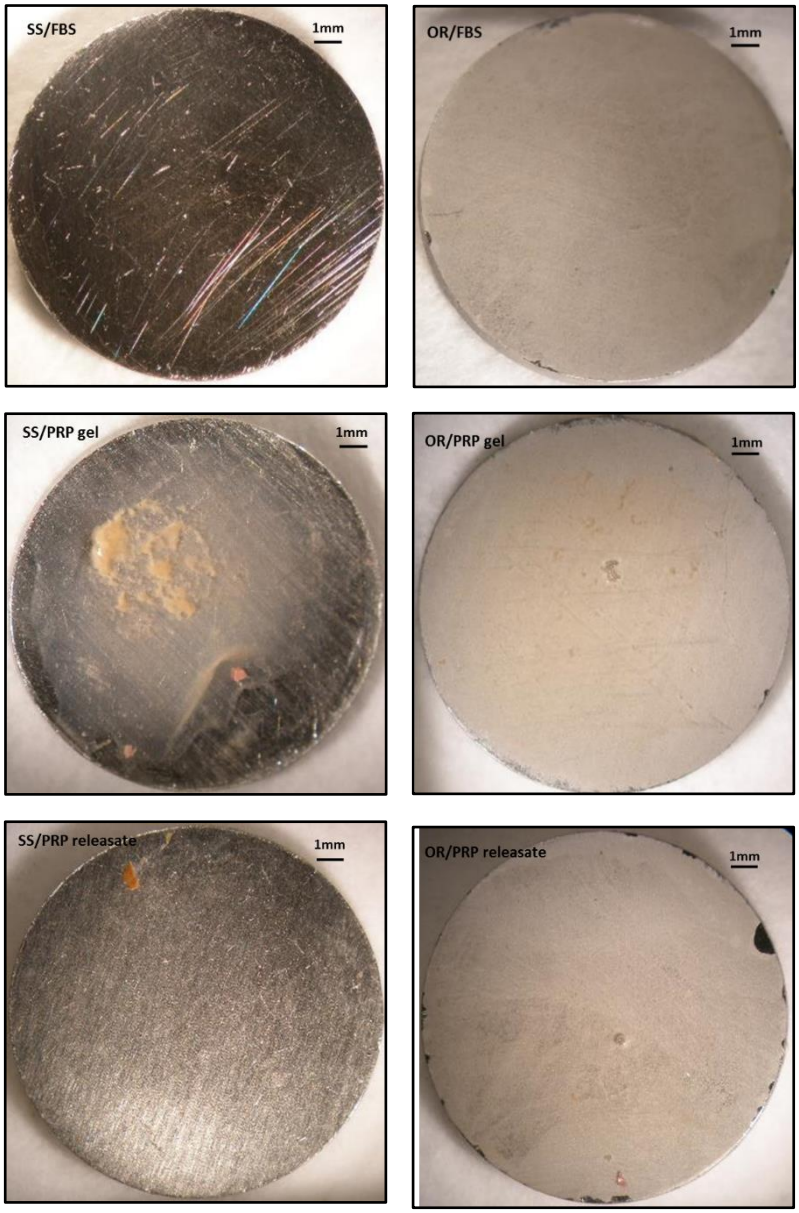

Figure 68: ALP staining of control SS and FA discs cultured under the same conditions of the experimental samples but without cells. They were all negative for the ALP stain. OR, organised FA; SS, stainless steel; PRP, platelet-rich plasma; FBS, fetal bovine serum; ALP, alkaline phosphatase.

6.2.8.3 Effect of FA/PRP combinations on mineralisation induced by hDPSCs

Alizarin red stain (ARS) was used to evaluate calcium rich deposits (mineralisation) in hDPSCs grown in the presence of osteogenic media on FA/PRP combinations for 2 weeks. The results presented in figure 69 showed that all the SS and FA samples displayed positive red staining with Alizarin red. FA coatings themselves contain calcium, even though, it was still possible to distinguish Alizarin red positive calcium deposits within the attached cell layers. The cell layer of FA discs seemed to be more thickened compared to uncoated SS discs. Some calcifying deposits or clumps of mineralisation can be seen on FA coated discs, which was indicative of mineral nodule formation.

Control SS and FA discs (without cells) were also tested with ARS. The results presented in figure 70 showed that the controls were totally negative for the ARS stain when combined with FBS and PRP releasate. However, PRP gel of both substrates had a red coloured stain but with different appearance from that of PRP gel-cell stain where the later was almost dissolved on the SS discs while in the control, the PRP gel was not dissolved. On organised FA discs, the PRP gel of the control took the stain but did not show calcium deposits that were seen on cell-seeded FA coated discs.

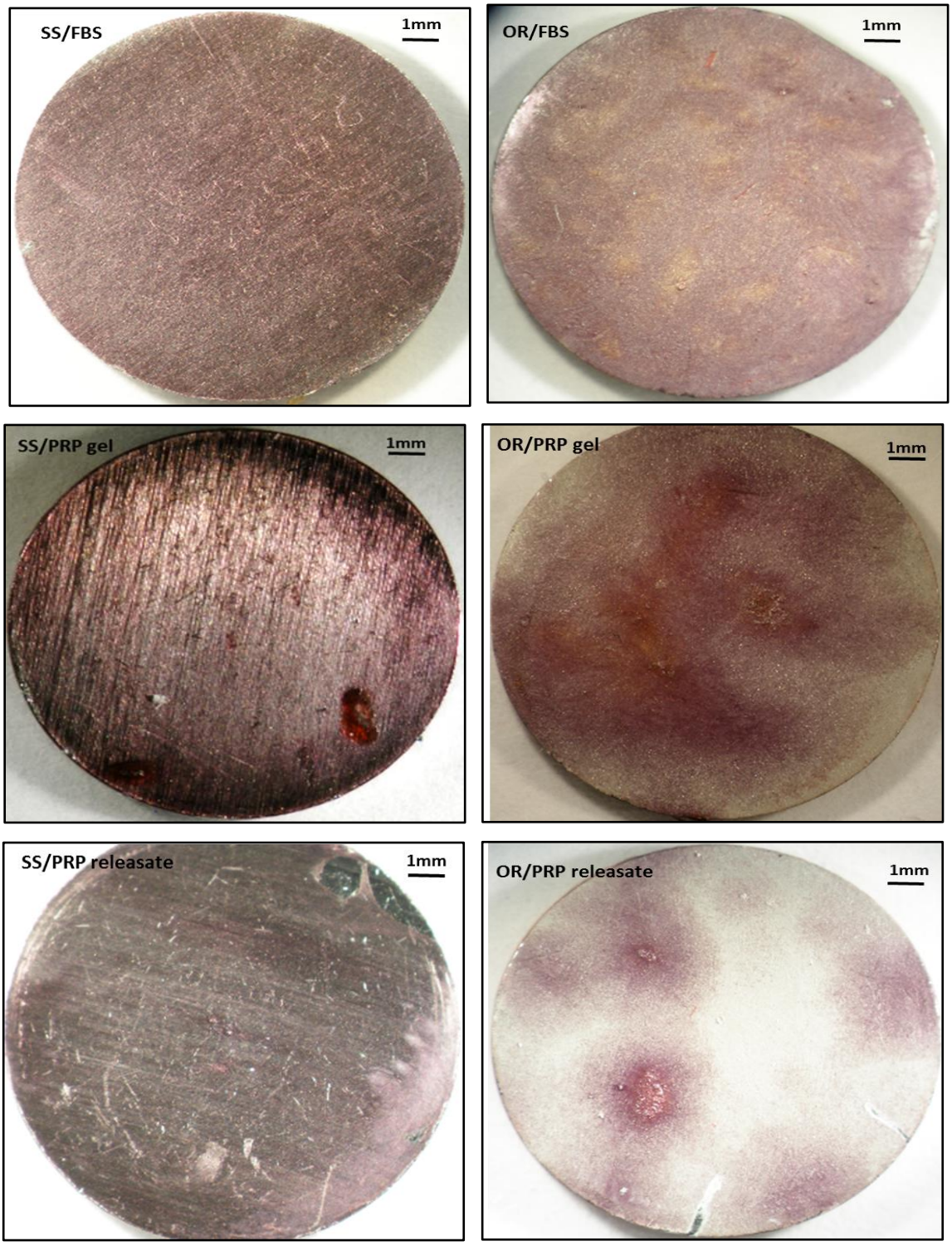

Figure 69: ARS staining (red) of hDPSCs cultured on FA/PRP for 2 weeks under osteogenic conditions. All the SS and FA samples showed positive red staining with Alizarin red. The cell layer of FA discs seemed to be more thickened compared to uncoated SS discs. OR, organised FA; SS, stainless steel; PRP, platelet-rich plasma; FBS, fetal bovine serum; ARS, alizarin red stain.

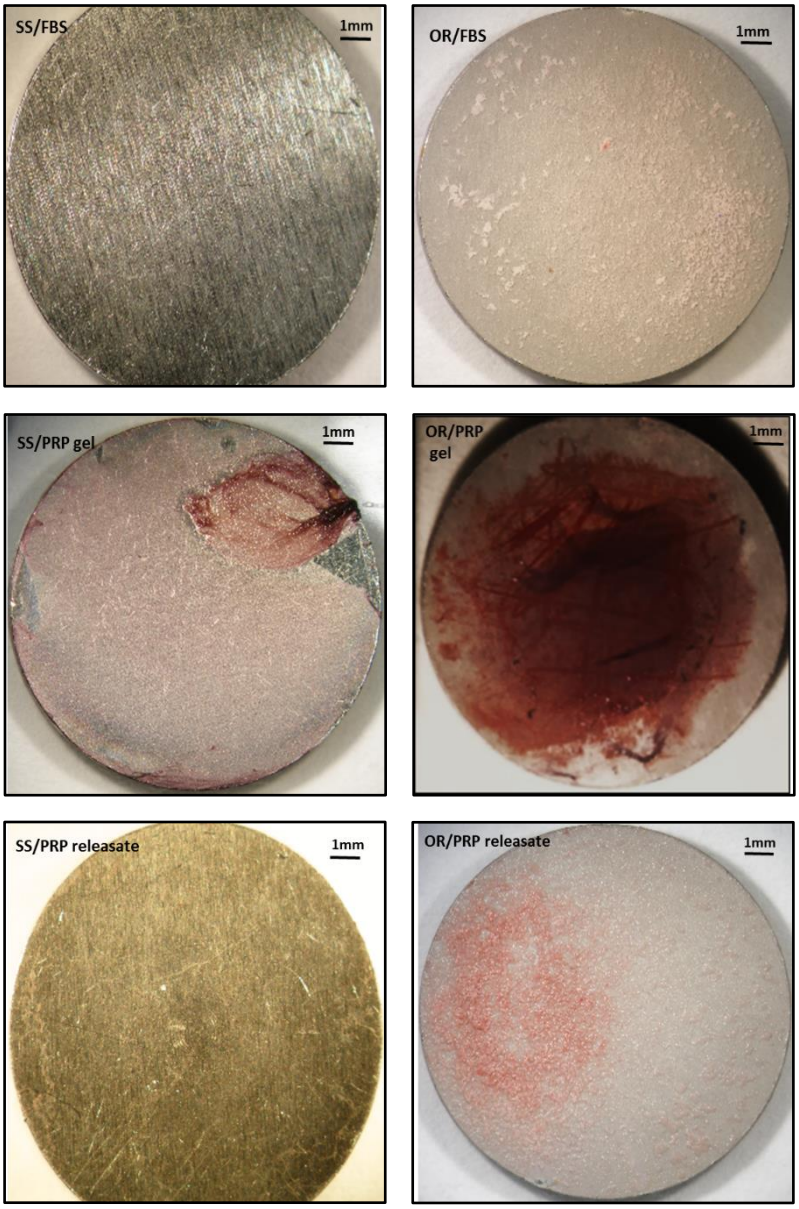

Figure 70: ARS staining (red) of control SS and FA discs cultured under the same conditions of the cells but without cells. They were negative for the ARS stain when combined with FBS and PRP releasate while PRP gel had the stain but with different appearance from that of the cell-seeded discs. OR, organised FA; SS, stainless steel; PRP, platelet-rich plasma; FBS, fetal bovine serum; ARS, alizarin red stain.

6.3 Discussion

FA coatings were synthesised successfully on stainless steel (SS) discs via a hydrothermal method described earlier (Chapter 4, FA results). Deposited FA crystals were arranged in a disordered manner on upper disc surfaces (disorganised FA coatings) and were ordered on the under surfaces (organised FA coatings). Both FA coatings were biocompatible and not cytotoxic. PRP containing high concentration of platelets (5-8 times higher than total blood) was prepared using a simple protocol (chapter 5, PRP results). PRP had a better effect on cell viability when added to culture medium at 10 % (v/v) compared to 5% (v/v). Furthermore, PRP when used in cell culture as either PRP gel or PRP releasate (obtained by extracting the soluble components from activated PRP) enhanced significantly G292 osteoblast-like cell attachment and proliferation compared to the standard culture conditions (FBS).

6.3.1 Temporal release of growth factors from PRP into PBS when used in combination with disorganised and organised FA coatings

It is known that platelets upon activation release a large variety of growth factors (GFs) after they adhere, aggregate and form fibrin mesh (Albanese et al., 2013). IGF-1 and PDGF-AB growth factors are potent mitogens and chemotactic agents for marrow cells and are believed to trigger osteoblast differentiation (Zhang et al., 2013). The ability of FA coatings to influence the temporal release of IGF-1 and PDGF-AB from activated and non-activated PRP into PBS was examined in this study in order to model the release of growth factors (GFs) from FA/PRP implant coatings as they might be used in vivo. Calcium chloride ($CaCl_2$) and thrombin were used to activate PRP. They are commonly used activators to stimulate the release of GFs from platelets. Extracellular ionised calcium serves as a cofactor for the activation of almost every protein factor of the coagulation cascade resulting in indirect platelet activation and the triggering of the prothrombinase catalysed reaction that generates thrombin. Thrombin triggers the conversion of fibrinogen contained in PRP to an insoluble network of fibrin. Activation by $CaCl_2$ is therefore slower than that achieved by the direct addition of externally provided thrombin (Textor and Tablin, 2012).

Several observations were made during this study:

1) After 2 hours of PRP gelification derived from 2 blood donors, a high release of IGF-1 growth factor was observed in the non-activated PRP loaded on FA coatings. Interestingly, the elution of IGF-1 from non-activated PRP increased in FA samples compared to uncoated SS loaded with non-activated PRP (Section 6.2.1). The loosely bound Ca^{2+} ions released from the Stern layer associated with FA coatings might induce this release.

2) At day 1 after PRP gelification, the IGF-1 results indicated that there is a burst-like release of IGF-1 from PRP gel of donor 1 loaded on FA coatings. This might be a consequence of release of IGF-1 bound loosely to FA/PRP surfaces, diffusion of incorporated growth factors out of the combinations and degradation of the PRP gel (Matsumoto et al., 2004).

3) From day 1 to day 7, $CaCl_2$ was the potent stimulator for IGF-1 release from PRP loaded on uncoated SS and FA coated discs. However, organised FA triggered IGF-1 release from the non-activated PRP at a comparable rate to that of calcium-activated PRP at all time points. This confirms that the organised coatings can trigger a sustained release of IGF-1 gradually over time. Moreover, according to the proteomic analysis of the current study, organised FA surfaces induced the adsorption of a larger amount of proteins from PRP gel compared to uncoated SS and to disorganised FA. The adsorbed proteins might facilitate IGF-1 entrapment within the fibrin network and facilitate their adsorption onto the underlying FA coatings for a sustained release later as hypothesised by Anitua et al., (2012) in their review about PRP usage in regenerative medicine.

4) On the contrary to IGF-1 release which was triggered by calcium, thrombin showed a general trend when induced the highest release of PDGF-AB in both blood donors and at all time points. This was in agreement with previous studies (Lacoste et al., 2003, Fufa et al., 2008, Harrison et al., 2011). The use of thrombin resulted in immediate release of amount of PDGF-AB within one day compared to non-activated PRP and calcium-activated PRP loaded on uncoated and FA coated SS discs (see section 6.2.1). However, organised FA coatings increased the release of PDGF-AB and showed a sustained release over time compared to uncoated substrates and disorganised FA when combined with thrombin.

5) Another interesting point in the present study, that IGF-1 was released at considerably lower levels than PDGF-AB. The maximum mean concentrations of IGF-1 occurred within 1 day after PRP gelification reaching around 620 pg/mL in blood donor 1 and 266 pg/mL in donor 2, but the highest concentrations of PDGF-AB were recorded within 2 hours of PRP gelification (~1980 pg/mL and 1730 pg/mL in donor 1 and 2 respectively). The lowest concentrations for both growth factors were measured at day 7 post PRP gelification reaching about 25 pg/mL for IGF-1 and 50 pg/mL for PDGF-AB in both blood donors. The observation that IGF-1 and PDGF-AB are released at different levels was also reported by Rai et al. (2005) who investigated the release of IGF1 and PDGF from thrombin-activated PRP loaded onto polycaprolactone–20% tricalcium phosphate (PCL–TCP) composite and immersed in PBS. Rai et al. detected a sustained release of IGF1 and PDGF over 21 days and related the difference between IGF-1 and PDGF levels to the molecular size and the amounts of both growth factors stored in platelets. The platelet content of IGF-1 was found to be much lower than that of PDGF (Weibrich et al., 2002). IGF-1 is a basic, single chain peptide with a molecular weight of 7.5 kDa (Schliephake et al, 2002). PDGF-AB is a basic, heterodimeric protein of 30 kDa molecular weight (Pfeilschifter et al., 1990). A larger size growth factor released in high amounts from platelets would mean reduced surface area of the substrate to volume ratio, which implies that fewer proteins could adhere onto the substrates, resulting in more release over time into the PBS. In previous studies, PDGF-AB was also detected in higher levels compared to IGF1 when released from calcium- activated PRP mixed with alginate beads and capsules and immersed in culture media (Lu et al., 2008) and when released from thrombin- activated PRP into culture medium (Schär et al., 2015).

In conclusion, these ELISA experiments demonstrated that the choice of platelet activator and the underlying substrate can influence the release kinetics of GFs from PRP. Thrombin used in association with FA may be a good choice for activation of PRP, as thrombin maximally promotes the release of PDGF-AB while FA alone ensures the release of IGF-1. However, there may be no need to use extraneous thrombin clinically, as non-activated PRP can be injected

directly into the injured tissue and will become activated on contact with collagen. Collagen is one of the most potent physiological activators of platelet activation and leads to slower and more sustained release of GFs compared to thrombin (Fufa et al., 2008; Harrison et al., 2011). Therefore, further studies are needed to determine whether collagen will have a significant effect on GFs release, specifically PDGF-AB from PRP loaded on FA coatings compared to thrombin.

6.3.2 Cumulative release of growth factors from PRP gel and PRP releasate when combined with uncoated SS and organised FA coatings

In the current study, the release of IGF-1 and PDGF-AB from platelet-containing PRP gel and platelet- free PRP releasate (obtained by extracting the soluble components released within 30 minutes of PRP activation) were compared when the gel and releasate were loaded on uncoated SS and organised FA coated surfaces for 3 days.

Results showed that IGF-1 release from PRP gel was lower than from PRP releasate on both SS and organised FA coated surfaces. In contrast, PDGF-AB release from PRP gel was higher than from PRP releasate on both SS and organised FA coated surfaces release.

To explain this result, it is important to realise that PDGF-AB originates from α-granules found within platelets (Kniess et al., 2003) while plasma IGF-1 is derived mainly from the liver (Schmidmaier et al., 2006) and its level in plasma does not correlate with plasma platelet count (Rubin and Baserga, 1995). Intracellular IGF-1 concentration in platelets is much lower than that of PDGF (Weibrich et al., 2002). Therefore, PRP gel will be expected to have a higher amount of PDGF-AB regardless of the underlying substrates. The platelets in PRP gel act as a reservoir of PDGF-AB and its release from PRP gel meant that PDGF-AB can accumulate in the PBS overtime. In contrast, PDGF-AB levels in PRP releasate are already fixed at their maximum value as PRP releasate contains no platelets. The fixed maximum value being the amount released within 30 minutes of platelet activation prior to removal of the platelets during preparation of the releasate. In agreement to the present study, higher concentrations of IGF-1 compared to PDGF-AB in PRP releasate was also

reported by Cho et al. (2011) who also found a positive correlation between PDGF-AB and PRP platelets count, supporting the contention that platelets in PRP gel are a reservoir of PDGF-AB.

6.3.3 Release of Ca^{2+} from disorganised FA and organised FA coatings when combined with PRP gel

FA is stable and has low dissolution rate. The dissolution studies related this stability to the high crystallinity of FA, orientation of the crystals and to the composition of FA (Bhadang and Gross, 2004, Kim et al., 2004). In this study, release of Ca^{2+} from disorganised and organised FA and FA/PRP gel combinations into PBS was monitored at different time points (see figure 53). This study showed that disorganised and organised FA had similarly low dissolution rate. A very low amount of Ca^{2+} ion was released into PBS by both types of FA coatings (~0.07 mg/L) at all the time points up to 14 days. However, adding PRP gel to FA coatings increased Ca^{2+} release over 24 hours (~0.1 mg/L – 1 mg/L) compared to FA alone. The rate of release level then dropped between 3 and 14 days similar to that recorded in FA alone. The high Ca^{2+} concentrations detected when PRP gel is added to FA compared to FA alone might be a result of the platelet activation process triggered by the coating in addition to thrombin, stimulating intracellular calcium release from platelet dense granules (in addition to GFs from the α-granules) (Zucker-Franklin et al., 1998). Ca^{2+} may also be associated with PRP gel as serum albumin is the major Ca^{2+} binding protein in the blood (Eatough et al., 1978). Interestingly, PRP gel showed higher Ca^{2+} release over the first 24 hours when combined with organised FA compared to disorganised FA. The reason for this is unclear but may be related to the larger specific area of the disorganised FA crystals (which as described previously exhibit a greater surface roughness) being able to bind and immobilise more Ca^{2+}.

6.3.4 Cytotoxicity of FA/PRP combinations

Biocompatibility is very important for dental implant materials. The present study has shown that FA synthesised via a hydrothermal method was not cytotoxic. Interestingly, the addition of PRP to FA improved the cell viability. This finding

suggests that the FA/PRP combination might play a critical role in influencing cell behaviour though the effect of GFs. The release of Ca^{2+} from the FA coatings and its role in inducing high and sustain GF release was explained earlier in this study (section 6.3.1).

6.3.5 Protein adsorption of PRP on FA coatings

The biological activity of a surface is determined by its surface properties (chemistry and topography), that influence protein adsorption and cell responses. In the current study, it was demonstrated that a wide range of proteins (15kDa to over 250KDa) adsorbed to FA substrates from PRP gel, PRP releasate and FBS control. In contrast, no detectable PRP proteins from donor 1 nor FBS proteins were recovered from the uncoated SS. However, significant proteins of PRP gel of donor 2 were recovered from uncoated SS which indicates the effect of donor variability on PRP composition and behaviour. The higher protein retention observed in FA samples compared to SS could be attributed to surface properties of the material including topography and heterogeneity, electrical potential, wettability and hydrophobicity. The crystals can interact with organic molecules (proteins) by electrostatic interaction between charged amino acid side chains and the negative and positive charges on the crystal surfaces. The uncoated SS samples might adsorb low amounts of proteins with low affinity that were readily removed while washing the discs. In addition, though phosphate buffer is well known for its ability to desorb proteins from apatite, its ability to desorb proteins from SS is not clear, it may be that the phosphate desorption was less effective in the case of desorbing donor 1 PRP protein from SS.

Interestingly, there was a very clear differential adsorption between the organised and disorganised FA coatings. Furthermore, organised FA adsorbed higher amounts of protein from PRP and FBS compared to the disorganised FA. It was reported in an early study that proteins are adsorbed onto different surfaces in different quantities, conformations and orientations depending on the chemical and physical properties of the surfaces (e.g. van der Waals forces and hydrophobic forces) (Roach et al., 2005).

6.3.6 Comparing cell morphology and attachment on disorganised FA and organised FA coatings in combination with PRP

The protein adsorption analysis of PRP on FA coatings was complimented by investigating the biologic activity of FA/PRP combination on cell adhesion and proliferation using osteoblast-like cells (G292). In the current study, PRP releasate had the same effect as FBS on cell morphology (see chapter 4, section 4.2.2.2) in which the cells formed isolated clusters attached to individual patches of disorganised FA crystals through cytoplasmic extensions. While on organised FA, the cells were more spindle-shaped and were spread on the surfaces via long, more prominent cytoplasmic extensions compared to disorganised FA. However, the cells of the organised coating combined with PRP releasate had less prominent cytoplasmic extensions compared to cells of FBS probably due to the presence of higher number of cells compared to FBS. The difference of cells morphology observed between organised and disorganised FA surfaces is related in part to the difference in the crystal organisation in both coatings. Indeed, it has been reported that the cell behaviour is highly influenced by topographically different microenvironments and the intrinsic characteristics of a substrate (e.g. chemical composition, charge and hydrophobicity) (Liu et al., 2010, 2011 and 2102). The capability of the cells in sensing the substrate geometry, rigidity and microstructure was also reported previously (Vogel and Sheetz, 2006). They stated that the cells transfer the geometrical and physical cues provides by the surface on which they are adsorbed into cellular biochemical signals that regulate various cellular events. Cell morphological changes to varied geometric microenvironments were also recorded (Poellmann et al., 2010). PRP gel seemed to provide a favourable extracellular environment for the cells as it was seen under the SEM and confocal microscopy as a sheet of protein matrix populated with a high number of cells but the gel prevented the recognition of cells' cytoskeleton.

6.3.7 Assessment of cell attachment and proliferation on FA/PRP combinations quantitatively

The synergistic effect of FA and PRP on improving cell attachment and growth was demonstrated quantitatively in the present study. Both FA coatings under standard cell culture conditions (FBS) induced no changes to the proliferation rate compared to uncoated SS discs. This was in agreement with a previous study, in which no significant difference was found between the number of dermal-derived human microvascular endothelial cells grown on SS and organised FA surfaces for 1, 7 and 14 day (Wang et al., 2013). In contrast, Liu et al. (2010 and 2012) reported that FA coatings showed low rates of cell proliferation of MG-63 osteoblast-like cells and adipose -derived stem cells compared to uncoated SS surfaces after 3 days in cell culture. This difference in cell proliferation results between different studies using the same FA coating could be attributed to differences in the adhesion abilities of the different cells grown on the two surfaces (SS and FA coated) which precede cell proliferation. It might also be related to cell harvesting technique utilised in the above studies which was trypsin-EDTA. The presence of Ca^{2+} associated with FA samples may inhibit trypsin enzyme activity used for detachment of the cells prior to cell counting. In addition, the 3D structure of the FA coating could prevent the complete exposure of the cells to trypsin and even when released, cells could be mechanically trapped in the forest of crystals that could compromise the collection of the cells compared to the flat surfaces of SS discs and lead to artefactual low cell counts for the FA surfaces. Further to the above, Liu et al. (2010, 2011 and 2012) and Czajka-Jakubowska et al. (2011) reported that initial cellular attachment in vitro was significantly higher on organised FA compared to disorganised FA surfaces, although both surfaces showed excellent biocompatibility. This was also evident in the present study at day 3 and 7 of cell culture presumably due to the difference in proteins adsorbed to both surfaces as shown and explained in the proteomic analysis (section 6.3.5). It is believed that proteins are adsorbed onto different surfaces depending on the chemical and physical properties of the surfaces (e.g. van der Waals forces and hydrophobic forces) and that the adsorbed proteins may act as mediators for cell adhesion if they have the correct geometry (Roach el al., 2005). Thus, the

composition and conformation of the protein adsorbed to FA might account for the enhanced cellular response on the organised FA surfaces.

As stated before, several advantages have been reported on the potential use of platelet-rich plasma (PRP) as a 3D gel scaffold for cell support. Among these advantages, the capacity of fibrin (one of the main components of PRP gel) to interact with the extracellular matrix and cellular components mediating cell attachment and the abundance of growth factors inducing cell proliferation (Anitua el al., 2012). G292 cell attachment and proliferation was increased in a constant manner upon the addition of PRP gel to both FA coatings compared to the addition of FBS or PRP-releasate. This synergistic effect might reasonably be expected due to the presence of the osteoconductive fibrin scaffold and osteoinductive growth factors released from PRP gel and the FA coatings which enhanced protein adsorption and sustained release of PRP growth factors (see section 6.3.5 and 6.3.1). It was thought that the major effect of PRP is derived from the effect of PDGF which has a key role in hard- and soft-tissue healing. PDGF has been shown to stimulate, in addition to chemotaxis and mitogenesis, the production of fibronectin which is an important extracellular cell adhesion protein (Yang et al., 2000). Fibronectin is known to mediate the specific interaction of the cells to underlying surfaces via cell integrin receptors, along with vitronectin, fibrinogen, collagens, laminin, osteopontin, and other trace proteins (Steele et al., 1995). The finding of the present study that PRP gel enhanced cell proliferation on FA coatings was supported by in vitro study of Kasten et al. (2008) who found that mesenchymal stem cells (MSCs) proliferation was significantly improved by adding PRP gel on calcium phosphate scaffolds. In another study, non- activated PRP significantly stimulated the cell growth of MSCs for 28 day on HA scaffolds when calcium element of HA induced platelets aggregation and growth factor release (Nair et al., 2009). Furthermore, the synergistic effect of PRP with calcium phosphates to promote cell proliferation of MSCs for more than 7 days was reported as well by other in vitro studies (Bi et al., 2010; Qi et al., 2015).

In addition to the above, the synergistic effect of FA and PRP on cell proliferation may be attributed to the combined effect of fluoride and PRP growth factors. Considerable fluoride release (2 - 3 mg/L) from organised FA

coatings was detected by Clark (2013) at pH 7.0 and 6.0 within 30 minutes and related this initial release to the loosely bound fluoride remaining from the synthesis process and/or to soluble fluoride containing non-apatitic phases generated as by product during FA synthesis. The possible molecular mechanism of the osteogenic action of fluoride ions was suggested in previous studies through the tyrosyl phosphorylation level of cellular proteins (Lau et al., 1989; Lau et al., 1998; Lau and Baylink, 1998). Protein phosphorylation serves to control the activity of the target protein and is a central feature of cell signalling pathways. The overall tyrosyl phosphorylation level of cellular proteins is determined by two important and opposing enzymatic reactions (Figure 71A), Tyrosyl phosphorylation which is catalyzed by protein tyrosine kinases (PTKs) and the tyrosyl dephosphorylation which is mediated by phosphotyrosine phosphatase enzymes (PTPs). It is believed that the binding of a growth factor to its corresponding cell surface receptor promotes the receptor's intrinsic PTKs activity (Figure 71B), and consequently triggers a cascade of tyrosine phosphorylation reactions targeting a number of cellular signalling proteins (Fantl et al., 1993). Signalling pathways are controlled by the action of PTPs which dephosphorylate the phosphorylated target proteins returning them to a resting state. However, some PTPs are inhibited by fluoride (Figure 71B). When fluoride enters the bone cells, it inhibits the activity of fluoride-sensitive PTPs and as a result signalling proteins remain phosphorylated for longer which potentiates the impact of the signalling pathway leading eventually to potential osteoblast cell proliferation and differentiation (Lau and Baylink, 1998).

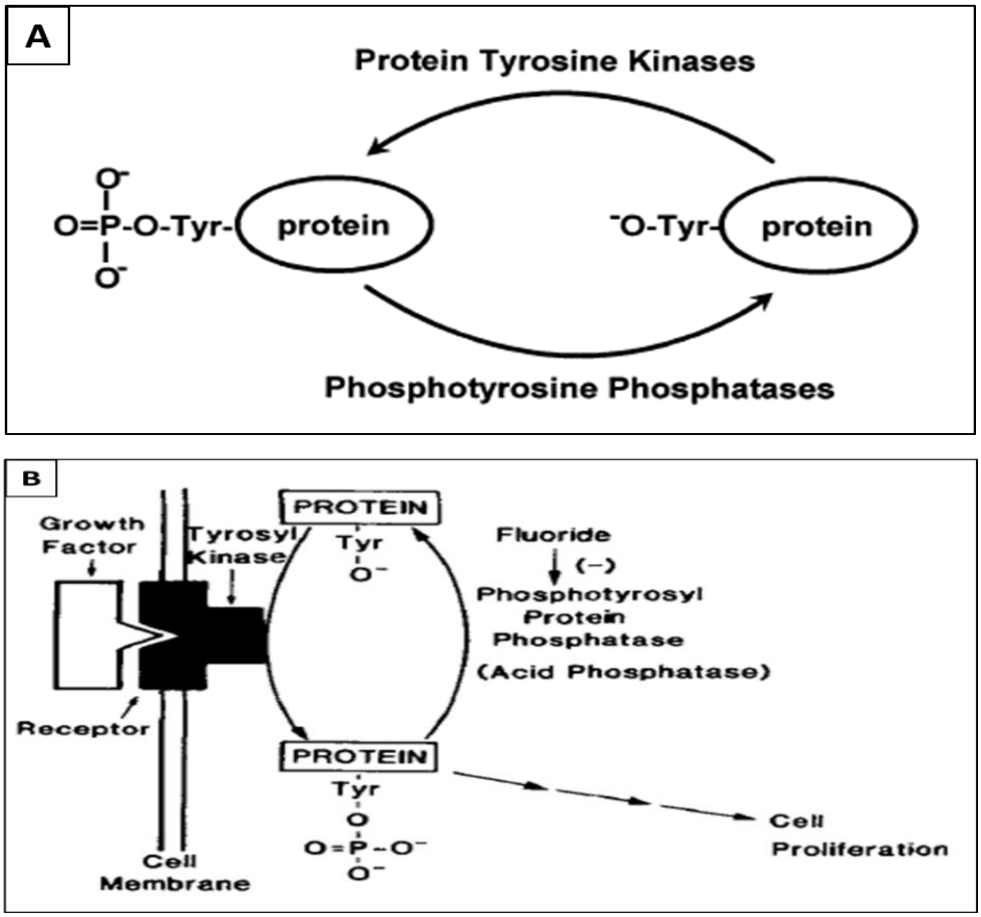

Figure 71: A, Schematic diagram showing the overall tyrosyl phosphorylation level of cellular proteins. It is controlled by 2 opposing enzymatic reaction: protein tyrosine kinases (PTKs) and phosphotyrosine phosphatase enzymes (PTPs). B, Schematic diagram showing the stimulation of PTKs activity by growth factors and inhibition of PTPs by fluoride leading eventually to an increase in the overall level of tyrosyl phosphorylation of cellular signalling proteins (https://onlinelibrary. wiley.com/doi/epdf/10.1359/ jbmr. 1998. 13. 11. 1660).

6.3.8 Osteogenic differentiation of human dental pulp stem cells (hDPSCs) on FA/PRP combinations

For tissue engineering purposes, in addition to its potential to promote cell attachment and proliferation, the ability of the implant surface to stimulate the osteogenic differentiation of mesenchymal stem cells is important for a successful osseointegration between the implant and the surrounding bone (Lavenus et al., 2011). Very few studies have investigated the osteogenic differentiation and mineralisation of stem cells on FA coatings (Liu et al., 2012;

Wang et al., 2012; Wang et al., 2013), and none have investigated their behaviour on FA/PRP combinations specifically. The present study was the first attempt to examine the osteogenic differentiation of human dental pulp stem cells (hDPSCs) cultured under osteogenic conditions on FA/PRP combinations. hDPSCs were chosen for this study because they are readily available and were proved to be a generic source of mesenchymal stem cells, showing characteristic stem cell features of high proliferative ability after prolonged culture (Papaccio et al., 2006, Govindasamy et al., 2010). Moreover, hDPSCs showed in earlier studies positive expression for mesenchymal stem cell markers including CD29, CD44, CD146, CD90, CD105, STRO-1, CD106, and OCT4 (Gronthos et al., 2002; Lindroos et al., 2008). Many previous studies have reported the ability of hDPSCs to differentiate into functional osteoblasts and produce mineralised matrix (Pisciotta et al., 2012, Riccio et al., 2010). Furthermore, the ability of hDPSCs to reconstruct bony structures were confirmed in some in vivo studies (d'Aquino et al., 2009, Giuliani et al., 2013, Sheth et al., 2017). hDPSCs were shown to have a comparable behaviour to human bone marrow stem cells (El-Gendy, 2010). However, DPSCs have higher osteogenic potential in vivo compared to BMSCs when implanted with platelet-rich plasma (PRP) into bone defects (Yamada et al., 2011) or in dental implant cavity (Ito et al., 2011).

In order to accelerate and promote mineralisation of hDPSCs in culture, osteogenic induction has been successfully achieved in earlier studies by adding the inducing agents dexamethasone and ascorbic acid to the culture media (El-Gendy et al., 2012; Alkharobi, 2016). Such osteogenic induction was also tested and confirmed in this study where alkaline phosphatase stain (early osteoblast marker) was more positive in hDPSCs cultured on monolayer under osteogenic conditions compared with basal culture (no osteogenic induction). It must be pointed out that the present study did not aim to examine the osteoinductive properties of FA/PRP combination but focused on the osteoconductive ability of this combination to support the differentiation of hDPSCs which were already induced toward osteogenic differentiation by dexamethasone and ascorbic acid. Therefore, the osteogenic differentiation of

hDPSCs (derived from single human donor) cultured for 3 days on FA/PRP was examined using quantitative and qualitative analyses.

6.3.8.1 Determination of expression of osteogenic marker genes by hDPSCs cultured on FA/PRP combinations using qRt-PCR

ALPL, RUNX-2, OCN and OPN are markers indicative of active osteogenic differentiation (d'Aquino et al., 2007; d'Aquino et al., 2008; Lindroos et al., 2008).

- **ALPL gene expression**

ALPL is considered an early osteoblast differentiation marker (Jaiswal et al., 1997) and is useful osteogenic marker for in vitro cell cultures (Gronthos et al., 2000). Several results were made during this study:

1) ALPL results obtained using PRP from 2 donors clearly demonstrated that when cells were grown on organised FA showed no increase in ALPL expression whether the coatings were used with standard culture (FBS) or in combination with PRP gel or releasate compared to the control (uncoated SS combined with FBS). This might indicate that the cells grown on organised FA were still in an active proliferation stage which could take longer time for the cells to reach confluency on 3-D surface before starting the differentiation stage compared to cells growing on 2-D flat surface of SS. Interestingly, PRP gel and releasate obtained from the 2 blood donors confirmed this hypothesis when they showed higher levels of ALPL gene expression when used on SS compared to when used in combination with organised FA. Cell proliferation and differentiation are both essential for bone regeneration. However, these two processes cannot happen in the cell at the same time. Cell proliferation is essential in the early phases of regenerative wound healing and must occur before differentiation is initiated (Graziani et al., 2006). Therefore, using hDPSCs at higher cell density would have been helpful in disentangling the data of this study. Li et al. (2013) observed an increase in cell proliferation and a reduction in the expression of lineage specific markers by PRP-expanded human muscle derived progenitor cells, suggesting that failure to exit the cell

cycle was responsible for preventing the cells from entering a differentiation phase.

2) It was reported in previous studies that increased dental pulp cell density and longer culture times of 3 or 4 weeks established higher levels of ALPL expression associated with lower proliferation of the cells as they reach confluency (Shiba et al., 1995; Tomlinson et al., 2015; Alkharobi, 2016). Therefore, it is worthwhile in the future to evaluate the gene expression using longer time durations than 3 days as used in the present study.

3) Data of ALPL expression obtained in PRP groups can depend heavily on the blood donor. ALPL results associated with one of the donors showed that loading PRP gel or releasate on uncoated SS and organised FA stimulated high ALPL expression of hDPSCs compared to FBS. This suggests that both PRP types supported the osteogenic differentiation of hDPSCs at higher levels compared to FBS regardless of the underlying substrate. This result was similar to that published recently in which the expression of ALPL by hDPSCs cultured on PRP gel combined with 3D-printed polycaprolactone scaffolds for 7 days and 14 days was significantly higher than those cultured on bare scaffolds (+FBS) (Li et al., 2017). Whereas, data of another blood donor used in the present study displayed no effect of PRP on ALPL expression compared to FBS when combined with uncoated SS or organised FA and this in agreement with an observation in which no significant difference was detected in ALPL expression of goat bone marrow stem cells between bare HA (+FBS) and PRP-coated HA at 7,14, 21 and 28 day in culture (Nair et al., 2008). The efficacy of PRP is based on the release of multiple growth factors (GFs) when platelets are activated. The GF concentrations varied among donors and the varying GF concentrations in turn may result in different biologic effects including cell proliferation and differentiation (Cho et al., 2011).

- **Runx-2 gene expression**

Runx-2 is a master transcription factor of the bone that is required in maintaining fully functional cells and is essential in early stages of the differentiation of pluripotent mesenchymal cells to osteoblasts (Ducy et al., 1997). Results of this study indicated the following:

1) RUNX-2 expression of hDPSCs was upregulated in cells grown on PRP gel and releasate of donor 1 when loaded on uncoated SS and when used in combination with organised FA compared to the control (uncoated SS loaded with FBS). This suggests that hDPSCs might be still in an active differentiation stage, as RUNX-2 expression is known to be up-regulated until complete maturation of functioning osteoblasts (Nakashima and de Crombrugghe, 2003). However, RUNX-2 findings demonstrated a clear donor variability where using PRP of second blood donor showed a decrease in RUNX-2 expression in SS and FA groups compared to the control (uncoated SS loaded with FBS). The difference in RUNX-2 expression between the 2 PRP donors might mean that the cells cultured on PRP samples from the two donors were at different stages of osteoblastic differentiation. PRP donors' variability is a possible reason for that when affects cell proliferation and the subsequent cell differentiation rate.
2) Interestingly, the upregulation of RUNX-2 by cells grown on PRP releasate and FBS of both donors was higher when loaded on uncoated SS compared to when combined with organised FA. A possible explanation for that is because the cells growing on a high specific surface area scaffold (organised FA), they theoretically take longer time to reach confluency compared to SS surface. Similarly, Kanno et al. (2005) observed that RUNX-2 was expressed only in the confluent samples of osteoblast-like cells cultured in 10% PRP. They found that when the cells underwent proliferation, cell differentiation was suppressed and once the cells had grown to confluence, PRP effectively enhanced ALP production and bone marker expression including RUNX-2 and OPN.
3) RUNX-2 expression of hDPSCs grown on organised FA groups showed variability of expression between the 2 blood donors when comparing PRP and FBS. RUNX-2 results of one blood donor showed that loading PRP gel or releasate on organised FA stimulated high RUNX-2 expression compared to FBS. This result was similar to that published recently by Li et al. (2017) in which the expression of RUNX-2 by hDPSCs cultured on a combination of PRP gel and 3D-printed polycaprolactone scaffolds for 7 days and 14 days was significantly higher than those cultured on bare scaffolds (+FBS) (Li et al., 2017). In contrast to donor 1, cells grown on PRP gel and releasate of donor 2 combined with organised FA expressed low RUNX-2 compared to FBS.

Therefore the results of FA were confusing and more PRP donors would have been helpful to draw a final conclusion.

4) Organised FA under standard conditions (FBS) inhibited RUNX-2 expression in both donors compared to the control (SS combined with FBS). This finding is different from that of Wang et al. (2012) who studied the osteogenesis gene profile of hDPSCs cultured on FA coatings for 4 weeks under standard osteogenic culture condition (FBS). They found that RUNX -2 was significantly upregulated in cells grown on organised FA surfaces relative to SS surfaces. This variation might be related to the difference in cell density and culture duration which might allow more time for the cells to stop proliferation on both substrates (SS and FA) and start the differentiation process.

- **OCN gene expression**

OCN is a convenient marker of fully differentiated osteoblasts and matrix mineralisation (Zur Nieden et al., 2003). OCN gene encodes osteocalcin protein which is a non-collagenous highly abundant bone matrix protein synthesised and secreted exclusively by osteoblasts in the late stage of maturation. It regulates bone mineralisation and the differentiation of osteoclast progenitors and hence promotes bone remodelling activity (Boskey et al., 1998).

The results of OCN expression herein showed similar levels of expression in FA coating groups to that of the controls in both donors. It seems that all the different construct were in active stage of differentiation but none consistently promoted OCN expression compared to the control. It was reported earlier that OCN expression is increased with time and this increase may be associated with elevated levels of matrix mineralisation and lower osteoblast proliferation (Candeliere et al., 2001). A time dependant rise of OCN expression has been previously observed in hDPSCs (Wei et al., 2007). This was also reported by Nair et al. (2008) who found no significant difference in OCN expression of goat bone marrow stem cells when grown on HA (+FBS) and PRP-coated HA after 7 days in culture but OCN expression increased significantly with PRP-coated HA after 14, 21 and 28 days in culture. Another study has recently reported high OCN gene expression in bone mesenchymal stem cells cultured with calcium phosphate particles and PRP gel after 7 days in culture compared to calcium

particles alone (Qi et al., 2015). The difference in OCN expression between the above studies and the present study might also reflect the controversial reports on the potential of PRP in stem cells osteogenic differentiation in vitro depending on donor variability and PRP preparation technique where each method generates a different PRP product with different biological properties and uses.

- **OPN gene expression**

OPN is a marker of mature osteoblast cells and is produced by osteoblastic cells at various stages of differentiation (Zohar et al., 1997).

1) In the current study, the results obtained using PRP from 2 donors showed that OPN expression of hDPSCs was promoted by organised FA when combined with FBS, PRP gel or PRP releasate compared to the control (SS/FBS), however, both PRP types induced a greater expression of OPN compared to FBS. This was in accordance with a previous report in which OPN expression of goat bone marrow stem cells was significantly better on PRP-coated HA than bare HA (+FBS) after 7, 14, 21 and 28 days in culture (Nair et al., 2008). Moreover, a recent study showed that OPN expressed by hDPSCs was significantly higher in cells cultured for 7 days and 14 days on scaffolds of PRP gel and 3D-printed polycaprolactone compared to cells cultured on scaffolds alone without PRP (+FBS) (Li et al., 2017).

2) In contrast to organised FA, uncoated SS when loaded with PRP gel and PRP releasate of one donor showed low OPN expression compared to the control and PRP of a second donor exhibited slightly higher degree of OPN expression. This could illustrate that PRP loaded on uncoated SS might upregulate early bone markers (ALP and RUNX-2) but organised FA might upregulate late bone marker OPN.

3) OPN expression by hDPSCs was stimulated by organised FA coated discs compared to uncoated SS discs under standard culture condition (FBS) for 3 days. This result was comparable to that of Liu et al. (2011) who have grown hDPSCs on FA surfaces for 3 days and investigated the expression of human pathway-focused matrix and adhesion molecules using PCR array. They reported an upregulation of OPN when hDPSCs were grown on organised FA

coatings under standard culture condition (FBS). Investigating the gene expression after 3 days in culture is important for studying gene regulation responsible for cell adhesion selectivity in cell-surface interactions and thus to obtain accurate cell adhesion information. Moreover, OPN is regarded as a cell-matrix adhesion molecule that has the potential to serve as a bridge between cells and hydroxyapatite through its RGD amino acid sequence (Oldberg et al., 1986). Therefore, OPN was highly upregulated on organised FA crystals compared to uncoated SS surfaces in the present study and this differential expression of OPN may play important role in enhancing the initial cellular response of hDPSCs to the coatings including cell adhesion. The surface characteristics was suggested to affect the first stage of cell-surface interaction (cell attachment, adhesion and spreading) which may in turn influence the second stage of the interaction involving proliferation and differentiation of the mesenchymal stem cells (Curran et al., 2006).

6.3.8.2 ALP activity in hDPSCs cultured on FA/PRP combinations

In the light of above cell culture conditions, alkaline phosphatase activity (ALP) was also evaluated quantitatively in hDPSCs after 2 weeks in culture under osteogenic conditions. ALP is the most widely recognized biochemical marker for osteogenic activity and hard tissue cell differentiation (Sharma et al., 2014). ALP is involved in skeletal mineralisation by acting both to increase the local concentration of inorganic phosphate and to decrease the concentration of extracellular pyrophosphate (an inhibitor of mineral formation) (Golub and Boesze-Battaglia, 2007).

In the present study, PRP gel and releasate when loaded on uncoated SS enhanced ALP activity of hDPSCs compared to the control (SS/FBS). In contrast, they inhibited ALP activity of hDPSCs when combined with organised FA compared to the control. Interestingly, Arpornmaeklong et al., (2004) reported that PRP gel increased cell proliferation but reduced ALP activity in a dose dependant manner in rat bone marrow stromal cells cultured on porous collagenous scaffold for 21 days. They found that high PRP concentrations containing 2.5×10^8 platelet/scaffold had the strongest inhibitory effect on ALP activity compared to lower PRP concentrations and related this effect to the

high concentrations of growth factors released from PRP and adsorbed on the collagenous scaffold fibres for slow release later (Arpornmaeklong et al., 2004). Taking this study into account, the influence of PRP when combined with organised FA should rather be correlated to the observations in the PRP groups loaded on uncoated SS as it is possible that the released growth factors of PRP gel and PRP releasate were rapidly adsorbed on the FA coating behaving as a carrier, and later slowly released into culture medium, resulting in high cell proliferation and low ALP activity. However, it was reported previously that thrombin- activated PRP decreased ALP activity compared to non-activated PRP in vivo (Han et al., 2009). Therefore, it is worthy to investigate FA/PRP combination in vivo without activating the PRP and will become activated on contact with collagen or in vitro with using collagen as an activator. Collagen is one of the most potent physiological activators of platelet activation and leads to slower and more sustained release of GFs compared to thrombin (Fufa et al., 2008; Harrison et al., 2011). Cho et al. (2011) also documented that using 10% PRP releasate in MSCs culture induced marked cell proliferation but reduced ALP activity compared to the control (10%FBS). Additionally, they noted that PRP releasate stimulated cell proliferation in a dose dependant manner and that this proliferation was positively correlated with TGF-β1 and PDGF concentrations while ALP activity was negatively correlated with PDGF-BB concentration. A previous report has also suggested that PDGF-BB induced bone formation in a dose dependant manner (Ranly et al., 2005). Therefore, these remarkable findings, coupled with the current study results, indicate that individual differences in growth factors should be taken into consideration in order to ensure standardised application of PRP. For example, PDGF which is a strong mitogen and responsible for the major effects of PRP (Ross et al., 1986), its content in PRP gel was very high according to the ELISA data and was enhanced by FA coatings (see section 6.3.1). PDGF has been found to increase DNA synthesis and decrease ALP activity in a dose dependent manner in cultured foetal rat calvaria osteoblasts (Graves et al., 1989; Hsieh and Graves, 1998). A similar effect was reported for PDGF growth factor impregnated in an inorganic bovine collagen matrix (Stephan et al., 2000), or a chitosan sponge (Park et al., 2000).

In the present study, hDPSCs showed low ALP activity when grown on organised FA when combined with either FBS or PRP compared to the control (SS/FBS) but with a higher ALP activity shown by PRP gel and PRP releasate compared to FBS. This result was in contrast to an earlier study which showed that ALP activity of MSCs was unaffected by the addition of PRP to tricalcium phosphate scaffold compared to the scaffold alone although PRP enhanced the cellular proliferation (Kasten et al., 2008). While ALP activity of goat bone marrow stem cells was much higher in tricalcium phosphate/chitosan and PRP gel combination than that of tricalcium phosphate/chitosan/FBS on days 7 and 14 of cell culture (Bi et al., 2010). Similarly, Qi et al. (2015) indicated a higher ALP activity, alizarin red stain and bone markers gene expression of bone MSCs treated with PRP gel and calcium phosphate (CaP) particles compared to CaP alone (+FBS). They related this potential to the growth factors of the PRP assuming that the release was enhanced by contact of PRP with CaP particles. Low ALP activity of cells grown on organised FA could also be detected because more cells were retained in the more densely deposited mineral nodules and matrix layers on the organised FA crystal surfaces; thus, less amount of cells was being retrieved leading consequently to low ALP activity. The biochemical finding of ALP activity of the present study was confirmed by histochemical stain (ALP stain) of hDPSCs after 2 weeks in culture under osteogenic conditions. It was previously demonstrated that ALP expression is detectable between days 12 and 18 in monolayer culture using the histochemical methods (Wessinger and Owens, 1990, Jaiswal et al., 1997). The finding of the present study showed that alkaline phosphatase was positive in all uncoated SS groups, however coating SS discs with organised FA coating seemed to reduce ALP expression when combined with FBS. This finding was in contrast to Wang et al. (2012) who found stronger ALP staining displayed by hDPSCs grown under standard conditions (FBS) on organised FA compared to cells grown on uncoated SS after 1 week in culture with and without osteogenic induction. They related this effect to the intrinsic properties and surface characteristics of the FA coating (chemical compositions, charge, hydrophobicities and the topographical features). The difference between ALP finding of the present study and Wang et al (2012) may be related to the

variability among the cells of different donors which was demonstrated earlier by El-Gendy (2010) who investigated the osteogenic potential of hDPSCS of 3 cell donors when seeded on 3D bioglass construct under osteogenic conditions for 2 weeks and 4 weeks. Alkharobi (2016) also found such cell donor variability in osteogenic differentiation of hDPSCs when cultured in monolayer for 1 and 3 weeks. Moreover, Kasten et al. (2008) detected large differences in ALP activity between individual donors' bone marrow stem cells. Therefore, using hDPSCs obtained from more than one donor would have been helpful in confirming the data.

In addition to the above, the substitution of FBS by PRP gel and releasate on SS and FA seemed to increase ALP deposition to a greater level. Interestingly, the ALP stain results were in keeping with ALP activity and ALPL gene expression results. This suggests that the combination of PRP and FA might have a strong proliferative effect on the cells but at the cost of cell differentiation which is clear evidence that PRP maintained the cells on FA in a less differentiated state. Whereas, PRP had a constant and a strong effect on cell proliferation and differentiation compared to FBS, irrespective of the underlying substrate (SS or FA).

6.3.8.3 Effect of FA/PRP combinations on mineralisation induced by hDPSCs

Mineralisation of hDPSCs cultured for 2 weeks on SS and organised FA coated discs under osteogenic conditions was also investigated to identify calcium deposits and nodules using alizarin red stain. In vitro mineralization was considered as a parameter of osteoblastic differentiation in the mature stage and calcium nodules are regarded as a marker for the late stage of mineralized tissue formation (Aubin, 1998a). In accordance with OCN gene expression which regulates bone mineralisation, all uncoated and organised FA coated discs showed positive alizarin stain when combined with FBS, PRP gel or PRP releasate. This result demonstrated an extensive osteogenic mineralisation potential of hDPSCs and suggested that hDPSCs grown on organised FA surfaces were capable of differentiating into mineralised tissue forming cells and promote subsequent mineralization.

The present finding of low ALP and high calcium deposition showed by FA/PRP combination was similar to that of Dolder et al. (2006) who investigated PRP gel as a coating for the tissue culture wells 75µL/cm^2 before rat bone marrow cells were cultured. They observed that PRP showed a downregulation in ALPL gene expression, a decrease in ALP activity and increased calcium content compared to standard culture (FBS) (Dolder et al., 2006) and they related this effect to the high growth factor content.

The ability of hDPSCs to produce mineralised nodules on FA coatings suggests the suitability of FA as a bone engineering material. This finding is supported by earlier studies which demonstrated that organised FA induced much stronger intensity alizarin stain compared to SS under standard conditions (FBS) when colonised by either adipose-derived stem cells (Liu et al., 2012), hDPSCs (Wang et al., 2012) or mesenchymal/endothelial co-cultures (Wang et al., 2014). Bi et al. (2010) found that PRP promoted the osteogenic mineralisation of MSCs on TCP/chitosan composite and showed high alizarin red positive nodules. Moreover, Qi et al (2015) showed that alizarin red stain and calcified nodes were increased in bone marrow stem cells co-cultured with CaP particles/PRP compared to CaP alone.

Summary

In summary, this study demonstrated that organised FA and PRP combinations provided a favourable extracellular environment for the cells in regards of high and sustained growth factor release (see section 6.3.1), protein adhesion (section 6.3.5) and osteoblast-like cell attachment and proliferation (see section 6.3.6 and 6.3.7). PRP induced and stimulated cell proliferation and differentiation regardless of the underlying substrates (see section 6.3.7). PRP gel had better effect than PRP releasate on osteoblast-like cell proliferation especially when combined with organised FA but showed almost similar effect to PRP releasate on the differentiation of hDPSCs into osteoblasts (See section 6.3.8). Furthermore, FA/PRP combination increased the mineralisation process and enhanced the osteogenic differentiation of hDPSCs but not in a constant manner as PRP derived from different blood donors gave differing results (see section 6.3.8).

Chapter 7: General Discussion

7.1 General Discussion

The use of dental implants for correction of tooth and tissue loss has increased exponentially around the world with high success rates. However, using implants to treat some conditions remains a challenge. For example, poor bone quality in the implantation site associated with systemic diseases such as osteoporosis and diabetes compromises the peri-implant healing process (Elsubeihi and Zarb, 2002). Another challenge is the strategy of immediate implant loading to reduce the patient anxiety and social inconvenience associated with the long waiting time required between implant placement and loading with dental prosthesis (Gapski et al., 2003). Such conditions justified the necessity for this research to investigate the factors that can improve and accelerate the integration of the dental implant with the surrounding bone (Albrektsson and Lekholm, 1989). In this study, a strategy combining fluorapatite coatings (FA) with platelet-rich plasma (PRP) was tested. Implant failure usually occurs at relatively early stages after implantation surgery according to clinical studies (Esposito et al., 1998), indicating the necessity to understand the initial response of the surrounding tissues to the implant surface. Therefore, the initial cellular response to FA/PRP combinations was investigated including cell viability and proliferation of osteoblast-like cells and differentiation of human dental pulp stem cells into an osteogenic lineage.
The present hypothesis was that FA/PRP combinations contain several components and qualities ideal for bone regeneration:
1) High quantities of calcium and phosphate important for bone mineralisation
2) Physiologically high concentrations of platelet derived growth factors important for bone healing and formation (osteoinductive properties)
3) Physiologically high concentrations of adhesive plasma proteins important for cell attachment and migration e.g. fibrin (osteoconductive property)
4) Providing a time-dependent and sustained release of growth factors.

For tissue regeneration purposes a biocompatible, bioactive scaffold with appropriate chemical, physical and mechanical properties is essential (Wang et

al., 2012). Fluorapatite was recently used as an osteoconductive implant coating due to its similarity to human bone and its favourable mechanical properties and high stability compared to other inorganic calcium phosphate materials (Bhadang and Gross, 2004; Kim et al., 2004). FA coatings have been applied to implants by plasma spraying, in which the implant surface is exposed to a stream of FA powder blown through a very high temperature plasma flame that melts the powder (Ranz et al., 1997). However, the rapid cooling process causes a change in the orientation of the FA crystals (Klein et al., 1994). In addition, all coating processes are likely to alter the composition of the coating materials, influence their microstructure and crystallinity as well as the biological responses (Yang et al., 1997, Sun et al., 2001). Therefore, Czajka-Jakubowska et al., (2009a) demonstrated a hydrothermal technique to grow a film of disorganised FA crystals on upper surfaces of metal plates and a film of compacted well-aligned FA crystals on under surfaces at 121^{o}C and 2 atm for 10 hours. They reported that the crystal structure was very similar in chemical composition and in structure to natural tooth enamel. In vitro studies have been conducted to investigate the initial cellular response to such FA coatings and have revealed that the well aligned FA crystals (organised) generated using the mild hydrothermal method appeared to promote the initial cellular attachment of the osteoblast-like cells and hDPSCs better than the disorganised crystals although both surfaces showed excellent biocompatibility (Liu et al., 2010; Czajka-Jakubowska et al., 2011). Moreover, Liu et al. (2011) found the same results when they succeeded in growing dental pulp stem cells (hDPSCs) on these FA coatings with an ambition to induce dentin and pulp formation in vitro with a view to creating an implantable tooth analogue.

In the present study (Chapter 4), SS discs (medical grade 316) were used as substrates to grow disorganised FA coatings on the upper surfaces and organised FA coatings on the under surfaces. Both coatings had the same chemical composition and had Ca/P and Ca/F ratios close to the theoretical values of FA (1.67 and 5 respectively). Both coatings were not cytotoxic and they appeared to induce cell adherence and growth by stimulating the cells to attach to underlying crystals through long, thin and dynamic filopodia, confirming the potential of the coatings to support cellular growth. However, the

cells grown on organised coatings were more spindle-like shaped and exhibited prominent cytoplasmic extensions which suggested good cell adhesion. Cell adhesion is usually preceded by protein adsorption which in turn determines cell–substrate contact and attachment and the consequent host response to the implant surface material. Therefore, correlations among surface properties, protein adsorption, and cell response have been of great interest to researchers. In the current study, cell proliferation was higher on organised FA compared to disorganised FA surfaces when FBS was used as growth supplement. The difference in cell morphology and proliferation rate between cells attached to and grown on disorganised and organised FA coatings was presumably due to the difference in the amount and type of proteins adsorbed onto both surfaces. Roach et al. (2005) believed that adsorbed proteins may act as mediators for cell adhesion if they have the correct geometry. The proteomic analysis in the present study showed a higher amount of FBS proteins adsorbed on organised FA compared to the disorganised coatings which could be attributed to surface properties of the coatings including topography and heterogeneity, electrical potential, wettability and hydrophobicity (Matsumoto et al., 2004). Proteins are charged molecules that change conformation (the protein's three-dimensional shape) depending on their electrochemical environment. The conformation of the protein determines the availability of certain bioactive peptide sequences located within the protein for specific cells (Ratner, 1993). For example, the arginine-glycine-aspartic acid (RGD) amino acid sequence is a bioactive peptide sequence that is responsible for mediating cell binding and integrin-mediated signalling for many different types of cells (e.g. endothelial cells, osteoclasts and osteoblasts). Proteins like fibronectin and vitronectin contain peptide sequences that are responsible for mediating cell adhesion for many different kinds of cells (Kieswetter et al., 1996). Fibrinogen, complement and IgG proteins are important for platelet activation, coagulation and inflammatory response (Kuzyk and Schemitsch, 2011).

The main aim of the present study was to improve the cell response to the FA coatings by introducing PRP. The biological function of fibrin provided by PRP is based on its capacity to interact with the surrounding tissue (extracellular matrix and cellular components) and mediate cell attachment, spreading and

proliferation forming a conductive scaffold (Anitua el al., 2012). The successful use of PRP gel to replace fibrin glues in oral and maxillofacial surgery was first described by Whitman et al., (1997). In addition to fibrin, PRP also contains many growth factors (GFs) that can influence cell chemotaxis, proliferation and differentiation, thereby enhancing bone-implant contact (Kasten et al., 2008). Previously, commercial GFs were used in combination with bone scaffolds to obtain a favourable outcome in regard to bone regeneration. However, it was found that the biological effect of a single GF is less than that of multiple GFs and might represent an inefficient method in terms of time needed for bone healing and the inappropriate (non-physiological) amounts of GF required (Babensee et al., 2000; Raiche and Puleo, 2004). PRP from autologous blood was identified as a rich source of multiple GFs that poses no risk of any immune response or transmissible diseases (Marx, 2001). PRP usage has increased over the past decades in dental and oral surgeries since the1990s (Kao et al., 2009). However, conflicting results were obtained on the use of PRP in combination with dental implants to improve osseointegration and bone formation. Some studies showed positive outcomes (Anitua, 2006; Gentile et al., 2010; Anand and Mehta, 2012) and others showed no significant results (Thor et al., 2005; Garcia et al., 2010). Such controversial results may be caused by biological variabilities between donors, the methods of PRP preparation and also the concentration of platelets used and the method by which they were activated. Early studies suggested that few folds of platelets (2-4 fold) above baseline levels in blood is enough to promote the proliferation and differentiation of primary osteoblast and fibroblasts (Anitua et al., 2009a, Graziani et al., 2006).

In the present study (Chapter 5), PRP was prepared manually from whole blood using a two-step centrifugation procedure resulting in a platelet count within the recommended range of about 5 - 8 times greater than the physiological average count in healthy human adult (200 $x10^3$ Plt/µL). By activating the PRP with an exogenous activator such as calcium chloride or thrombin, two key processes may be initiated; degranulation of platelets to release GFs from their α-granules and fibrinogen cleavage into insoluble fibrin (Wasterlain et al., 2012). In the present study, activated PRP and PRP releasate (obtained by extracting the

soluble components of activated PRP) used at 10% in culture medium showed better cell viability and proliferation compared to 10% FBS. The biological actions of GFs in cell proliferation and bone regeneration have been documented in many studies (Sporn and Roberts, 1993; Greenhalgh, 1996; Eppley et al., 2004). Cho et al. (2011) revealed that cell proliferation is positively correlated with transforming growth factor-beta1 (TGF-β1) and platelet-derived growth factors (PDGFs) concentrations. In addition, many studies have reported the successful culture of cells incorporated into PRP gels, suggesting that the gel environment enhances viability and proliferation of encapsulated cells (Ho et al., 2006; Kawasumi et al., 2008; Xie et al., 2012; Jalowiec et al., 2015). Thus, it was decided to focus on investigating and comparing PRP gel and PRP releasate on cell proliferation and differentiation when combined with FA coatings (Chapter 6).

Some investigators have used PRP in combination with other biomaterials to create a microenvironment favourable for tissue healing including induction of chemotaxis, cell proliferation and differentiation stimulated by platelet GFs (Okuda et al., 2005; Yamamiya et al., 2008; Bi et al., 2010). PRP gel contains proteins such as fibrin, fibronectin and vitronectin which act as cell adhesion molecules, thus favouring osteoconduction as well as being essential in forming bone matrix (Anitua et al., 2004; Gandhi et al., 2006). The biomaterial can induce better protein adhesion and therefore can improve subsequent cell adhesion. Growth factors from PRP theoretically adsorb to PRP fibrin network and to the underlying biomaterial surfaces. Thus, the biomaterial can act as a carrier for the GFs allowing for a sustained release over a long period of time after diffusion of the incorporated growth factors out of the combinations and with degradation of the PRP gel. Studies have shown that activation of platelets with thrombin can cause immediate activation with surge of GFs release where 70% of the GFs are released within 10 min of clotting and 100% are released within 1 hour (Foster et al., 2009). This rapid and high GFs release in addition to the fact that PRP has naturally a short half-life, limit the impact of the GFs on cell stimulation over time as most GFs are cleared before they can exert a therapeutic effect (Lu et al., 2008). Therefore, a controlled release strategy was suggested in many studies using several natural polymer delivery systems and

hydrogels to temporarily regulate GF bioavailability and enhance the clinical efficiency of PRP (Lin et al., 2006; Lu et al., 2008; Kurita et al., 2011; Kakudo et al., 2017; Jain et al., 2017). Several biomaterials have been employed to prolong the release of GFs from PRP preparations e.g. gelatin, alginate, collagen and calcium sulphate (Chen et al., 2010). However, the use of natural polymers (alginate) is shown to have some disadvantages such as batch-to-batch variability, non-specific polymer-protein interactions, immuno-toxicity and limited control over hydrogel properties (Malafaya et al., 2007). Thus, using synthetic scaffolds exhibiting well controlled and acceptable properties would be preferable. With this in mind, the release of 2 important osteogenic GFs (IGF-1 and PDGF-AB) from PRP gel combined with FA coatings was monitored over 7 days (Chapter 6). It was reported earlier that the combination of IGF-1 and PDGF-AB could increase bone formation on implant surfaces (Stefani, et al., 2000). According to the findings of the present study, the addition of PRP gel to organised FA induced an enhancement and a sustained release of both GFs from the gels (IGF-1 and PDGF-AB). This could form a good strategy to coordinate GF release and to maximise the clinical efficiency of PRP, creating osteo-inductive, osteo-conductive tissue engineered constructs for rapid bone healing. Interestingly, the findings of this study indicated that the loosely bound Ca^{2+} ions of organised FA coatings were capable, without addition of exogenous agent, to trigger a high and sustained release of IGF-1 over 7 days from PRP. Nair et al. (2008) showed similar results when coated HA scaffolds with non-activated PRP with agitation for 1 hour. They proposed that HA can activate platelets without the addition of any triggering factors like calcium chloride or thrombin and can induce platelet aggregation and activation. Nair et al. confirmed platelets activation by identifying the activation markers: P-selectin adhesion molecules (which are expressed on activated platelets) and plasma factor-4 (released by aggregated platelets).

The present study confirmed that the high Ca^{2+} content of the disorganised coatings triggered a burst release of IGF-1 over a short term while the organised coatings triggered a sustained release of IGF-1 over an extended period of time. This finding was supported by the proteomic analysis of the current study which showed that organised FA surfaces adsorbed bigger

amounts of PRP proteins compared to disorganised FA. This probably result in entrapping more GFs within the fibrin network of the PRP gel and creating a reservoir of GFs for a sustained release later. However, in the current study, thrombin was required to ensure high release of PDGF-AB from PRP. Some researchers questioned the necessity of using thrombin in vivo, as commercially available thrombin derived from bovine plasma has been associated some years ago with the development of antibodies to some clotting factors (V, XI and thrombin) and sporadically caused life-threatening coagulopathies (Zehnder and Leung, 1990). In the same time, non-activated PRP liquid was reported to enhance bone formation (Anitua 1999; Dugrillon et al. 2002) and to improve bone apposition to roughened titanium implants during the early post implantation healing phase (Nikolidakis et al. (2006). It was suggested that non-activated PRP can be injected directly into injured tissue to become activated by contact with collagen rather than by applying thrombin. Recently, collagen was demonstrated as one of the most potent activators of platelet activation leading to a slower and more sustained release of GFs compared to thrombin (Fufa et al., 2008; Harrison et al., 2011).

In addition to the above, PRP gel containing platelets showed higher concentrations of PDGF-AB compared to platelet-free PRP releasate regardless of the underlying substrate (uncoated or FA coated SS). While PRP releasate showed higher concentrations of IGF-1. Therefore, effect of both types of PRP was further investigated on cell proliferation. The major effect of PRP is derived from the effect of PDGF originating from the platelets which has a key role in hard- and soft-tissue healing (Rozman and Bolta, 2007). PDGF has been shown to stimulate cell chemotaxis and mitogenesis, and the production of fibronectin which is an important extracellular cell adhesion protein (Yang et al., 2000). IGF-1 is an important osteogenic factor that can enhance bone formation when bound to a specific receptor on the cell membrane of preosteoblasts and can stimulate their proliferation and differentiation and the subsequent osteogenesis (Hock et al., 1988). It was shown to enhance cell proliferation of osteoblast-like cells and osteogenic differentiation by increasing ALP activity (Schmid et al., 1984). It increased type I collagen synthesis as well in foetal rat calvarial cell culture and (Canalis et al., 1988).

There is little information on the effect of PRP acting in synergy with other biomaterials on osteoblast cell proliferation. In the present study, under standard cell culture condition (FBS), FA coatings induced cell attachment and proliferation at a comparable rate to that of uncoated SS discs. However, cell attachment and proliferation was increased upon the addition of PRP gel to organised FA coatings. Organised FA adsorbed higher amounts of PRP gel proteins and induced higher growth factor release and cell proliferation compared to uncoated SS and disorganised FA. Thus, the composition and conformation of the adsorbed protein layer might be responsible for the enhanced G292 cellular response on the organised FA surfaces. FA/PRP combinations induced higher cell proliferation compared to PRP loaded on SS surfaces. This emphasised that the combined effect of PRP and FA can sustain cell viability and proliferation. In addition, the present study suggested that fibrin provided by PRP gel adsorbed very well to FA coatings minimising cell loss and leading to enhanced cell growth compared to PRP releasate and FBS. The synergistic effect of PRP with calcium phosphate to promote cell proliferation of mesenchymal stem cells for more than 7 days was reported by several in vitro studies (Kasten et al., 2008; Nair et al., 2009; Bi et al., 2010; Qi et al., 2015). Recent advances in stem cell biology and tissue engineering offer an attractive prospect for hard tissues healing (Yen and Sharpe, 2008). For tissue engineering purposes, three key ingredients are required; biocompatible and bioactive scaffolds, mesenchymal cells and inductive growth factors. Ideally, it is desirable that a scaffold should not only support the growth of specific cells but also direct the differentiation of these cells toward the creation of functional tissues (Wang et al., 2012). The interactions between stem cell and biomaterial can provide valuable information of the relationship of material characteristics with cell phenotypic behaviour (adherence, proliferation and differentiation) which are fundamental to the future application of these biomedical materials in the orthopedic and dental fields (Liu et al., 2010). It was thus essential to investigate the synergistic effect of FA and PRP on stem cells differentiation and mineralisation using hDPSCs.

The findings of the current study concluded that FA and PRP supported hDPSCs differentiation into an osteogenic lineage. Interestingly, there was a

clear PRP donor variability in ALPL and RUNX-2 gene expression while neither FA nor PRP promoted OCN expression compared to the control. In accordance with OCN gene expression (which regulates bone mineralisation), all uncoated and organised FA coated discs showed positive calcium deposition (mineralisation) when combined with FBS, PRP gel or PRP releasate. This result demonstrated the osteogenic mineralisation potential of hDPSCs and suggested that hDPSCs grown on organised FA surfaces combined with PRP were capable of differentiating into mineralised tissue forming cells and promote ECM mineralisation. OPN expression (cell-matrix adhesion molecule and late osteoblast marker) was highly induced by organised FA when combined with either FBS, PRP gel or releasate which demonstrates that organised FA had a strong effect on cell-substrate contact and on the late stage of cell differentiation. It can be concluded that the combination FA/PRP might have a potential for bone regeneration but further studies using more blood donors are need to fully prove this hypothesis and elucidate the mechanisms involved.

Cell proliferation and differentiation are both essential for bone regeneration. However, these two processes cannot happen in the cell at the same time. Cell proliferation is essential in the early phases of regenerative wound healing and must occur before cell differentiation is initiated (Graziani et al., 2006). Therefore, using hDPSCs at higher cell density and over longer culture duration might allow more time for the cells to stop proliferation on both substrates (SS and FA) and start the differentiation process.

ALP activity was enhanced by both PRP types but suppressed by organised FA when combined with either FBS or PRP. This result was also confirmed by ALP stain images. It is possible that the GFs released from PRP gel and PRP releasate were rapidly adsorbed on the FA coatings and were slowly released into the cell culture medium which in turn promoted the cell proliferation and reduced ALP activity. However, thrombin- activated PRP decreased ALP activity compared to non-activated PRP in vivo (Han et al., 2009). Therefore, it is worthy to investigate FA/PRP combinations in vivo without activating the PRP or in vitro using collagen to activate the PRP samples.

The ability of PRP to enhance cell proliferation and reduce ALP activity has been proven earlier. Arpornmaeklong et al., (2004) reported that PRP gel

increased cell proliferation but reduced ALP activity in a dose dependant manner when cultured rat bone marrow stromal cells on porous collagenous scaffold for 21 days. Kasten et al. (2008) investigated the in vitro effect of PRP gel on MSCs seeded on calcium phosphate scaffolds and similar to the previous studies, they found that PRP improved cell proliferation on the scaffold but did not affect ALP activity compared to the scaffold alone and they related this result to inefficient preparation and storage of PRP. However, if their PRP was compromised in some way, it is questionable whether it could even enhance cell proliferation or affect ALP activity. Cho et al. (2011) documented that using 10% PRP releasate in MSCs culture induced marked cell proliferation but reduced ALP activity compared to the control (10%FBS). Further, Li et al. (2013) observed an increase in cell proliferation and a reduction in the expression of lineage specific markers by the PRP-expanded human muscle derived progenitor cells, suggesting that failure to exit the cell cycle was responsible for preventing the cells from entering differentiation phase. Organised FA in the present study inhibited ALP activity in standard culture (FBS) compared to uncoated SS. This finding might again be related to the fact that cells growing on 3-D constructs need longer time than cell growing on 2-D surface of SS to reach confluency, exit the cell proliferation cycle and start cell differentiation. In contrast, Wang et al. (2012) found higher ALP activity when hDPSCs were grown under standard conditions (FBS) on organised FA compared to cells grown on uncoated SS after 1 week in culture with and without osteogenic induction. They related this effect to the intrinsic properties and surface characteristics of the FA coating (chemical composition, charge, hydrophobicity and topographical features). The difference between ALP findings reported in the present study and Wang et al (2012) may be related to the variability among hDPSCs of different donors which was demonstrated earlier by El-Gendy (2010) and Alkharobi (2016). Therefore, using hDPSCs obtained from more than one donor would have been helpful in confirming this data. Variability of donated DPSCs response could be related to the patient's dental health which could have an effect on the biological behaviour of the residing stem cells. For example, dental pulp inflammation was associated with lower yield of DPSCs and a decreased mineralisation potential (Alongi et al.,

2010). Deep tooth caries (decay) also affects the proliferation rate and differentiation potential of DPSCs (Ma et al., 2012). Pressure and tension caused by previous orthodontic tooth movement can also induce differentiation of residing DPSCs (Zainal Ariffin et al., 2011). Smoking affects the mineralization potential of DPSCs (Yanagita et al., 2008) and donors' age decreases cell proliferation and differentiation of DPSCs (Ma et al., 2009). However, the expression of stem cell markers was observed in DPSCs from donors ranging from 14 to 60 years old (Atari et al., 2012). The age is not a crucial factor in the maximal division potential of DPSCs and cells derived from donors ranging from 12 to 30 years old are all suitable for stem cell banking (Kellner et al., 2014).

In general, as long as organised FA/PRP gel combinations promoted a higher proliferation rate, enhanced expression of late osteoblast markers (OPN) and mineralisation potential, they might be of significant use in bone tissue engineering. Using PRP in combination with biomaterials for tissue engineering purposes is a controversial and interesting area to discuss. Some investigators reported that using PRP in combination with HA/tricalcium phosphate (TCP) scaffolds may hold some promise for tissue engineering purposes by enhancing in vivo bone regeneration compared to the use of scaffolds alone (Okuda et al., 2005; Abhijit, 2006; Rai et al., 2007; Chevallier et al., 2010; Bi et al., 2010, Qi et al., 2015). Yamada et al. (2004), in an animal study, observed a well-formed mature bone in osseous defects when injected with PRP gel and MSCs compared to PRP alone or autogenous bone graft. They found a progressive and complete resorption of PRP gel and relatively mature remodelled bone. Another animal study showed that the bone regeneration around dental implants was promoted when the implants were placed simultaneously with a combination of MSCs, PRP and fibrin glue (a composite containing fibrinogen and thrombin) in areas with poor bone quality or low bone volume (Ito et al., 2006). Fibrin glue was used as osteoconductive scaffold for stem cells and as a carrier for PRP growth factors. Another study evaluated the effect of PRP in the treatment of periodontal intrabony defects (Yamamiya et al., 2008) and reported a more favourable clinical improvement in the periodontal defects when treated with a combination of HA, PRP and human periosteum sheet (containing

osteoprogenitor cells and extracellular matrix) compared to HA and PRP combination. The result was attributed to the additional benefit of the osteogenic cells found in the periosteum sheet. Another study introduced a calcium sulphate and PRP combination as a novel biomaterial that is able to induce bone formation in the bone defects. They assumed that the exothermic reaction generated by the mixture of calcium sulphate with PRP activated the platelets contained within the PRP and this combination behaved as time-controlled releasing matrix for all the platelet GFs (Intini et al., 2007).

In contrast to the above studies, it was concluded in previous animal studies that the use of PRP gel did not have any effect on the bone-implant contact of trabecular bone (Nikolidakis et al., 2006) and cortical bone (Nikolidakis et al., 2008) compared to calcium phosphate coated implants, while non-activated PRP in a liquid form induced an increase in bone apposition to roughened titanium implants. They related this difference to the mechanical trauma caused by the pressure of the PRP gel on the walls of the already tightly fitted implant leading consequently to bone resorption and necrosis of interfacial bone. They supported their hypothesis by indicating remnants of PRP gel around the implant surfaces which couldn't be seen around calcium phosphate coated implants, suggesting that calcium phosphate coating may enhance macrophage activation (Silva et al., 2003) and play a role in the faster degradation of PRP gel. Another recent animal study also suggested that treating bone defects with TCP/PRP did not have a significant effect compared to PRP alone (Sebben et al., 2012). The underlying reasons for these conflicting results are still unclear. However, as stated earlier, the major factors in PRP thought to be involved in the biological events are GFs. It was believed that the GFs have a complex synergistic effect that is not fully understood. Many different signalling pathways can be triggered from the synergistic interaction of GFs and can lead to either enhancement or inhibition of tissue healing depending on the mode of growth factor release, as well as the dynamics of the wound area (Border and Ruoslahti, 1992). Therefore, it is important in the future to correlate the effects of PRP derived GFs (acting singularly and together in concert) with cell proliferation and with the expression of specific osteogenic marker genes and any other characteristics that indicate the osteogenic differentiation of cells.

7.2 Conclusions

1. Within the limits of the current study, it can be concluded that combinations of FA coatings and PRP were biocompatible. The PRP prepared had a platelet count in the accepted therapeutic range. All PRP concentrations and configurations used herein were not cytotoxic. In cell monolayer culture, PRP-releasate (10% in culture medium) promoted the highest rate of cell growth compared to PRP gel and FBS. While on FA coatings, especially the organised form, PRP gel induced the highest growth of osteoblast-like cells.
2. FA stimulated high and sustained release of IGF-1 and PDGF-AB for up to 7 days. However, thrombin was required to induce the highest release of PDGF-AB. Furthermore, FA coatings, especially organised FA, promoted high protein adsorption and high cell attachment when combined with PRP gel.
3. There was a clear PRP donor variability in ALPL and RUNX-2 gene expression when combined with uncoated SS or FA while neither FA nor PRP promoted OCN expression compared to the control. Organised FA when used under standard culture conditions did not promote early bone markers ALPL and RUNX-2 and late marker OCN but increased late OPN bone marker expression and inhibited ALP activity compared to uncoated SS. PRP gel and releasate supported the osteogenic differentiation of hDPSCs on uncoated SS by inducing high ALP activity compared to when combined with organised FA. Organised FA/PRP combinations showed a high OPN osteoblast gene expression and mineralisation potential. Thus, such combinations might be of use in bone tissue engineering and may represent an effective approach to enhancing the osseointegration of dental implants but further investigations are necessary to confirm this.

7.3 Limitations

1. The variability between PRP results of 2 blood donors was considerable. Therefore, the effect of inter-donor variability could be averaged out by using PRP samples extracted from more blood donors.
2. Variability of stem cell behaviour and their response to stimuli may again be due to donor variation. Unfortunately, because of time limits, it was

impossible to isolate hDPSCs from different teeth and donors when studying the effect of FA/PRP on cell proliferation and osteogenic differentiation concurrently.

3. The hDPSCs were extracted from samples obtained from the tissue bank and came with very limited information about the medical and dental history of the patients donating the samples. This information would be useful for a better understanding of the behaviour of the cells and how their behaviour might correlate to their past history.
4. Another limitation of this study is that it did not investigate whether other platelet derived osteogenic GFs (e.g. TGF-B1) are secreted and affected by a specific activator when released from FA/PRP combinations. Platelets contain over 30 GFs and it would be preferable to investigate the effect of all these GFs on stem cell biology.
5. Finally, due to time limits and the short time course (3 days) associated with gene expression differentiation assays, it would be worth performing more extensive time course studies to better observe any time-dependent expression of genes involved in early and late osteoblast differentiation and function.

7.4 Future work

1. The work around PRP proteins and FA coatings and the effect they have on cell biology was the central theme of this thesis but further work is required to explore the molecular mechanisms involved in the cellular response to FA/and or PRP coated titanium samples.
2. Further research is needed to fully understand the release pattern and kinetics of the full cocktail of GFs present in platelets when used synergistically with FA coatings.
3. A key question remaining is how PRP/FA coatings would affect the osteogenic differentiation of stem cells in vitro and in vivo including, characterisation of osteoblastic cell phenotype using immunohistochemical staining/ Western Blotting against a range of bone markers such as alkaline phosphatase, collagen I, osteopontin, osteonectin, osteocalcin and bone

sialoprotein so as to confirm protein expression related to gene expression data.

4. The PRP and FBS proteins adsorbed to the coatings need to be better characterised and the role of specific components on cell attachment and behaviour need to be further investigated. This may involve testing the bioactive effects of purified components (or recombinant analogues) on stem cell differentiation and subsequent behaviour with regard to bone regeneration.
5. Well designed and properly controlled studies are needed to provide solid evidence of the capacity of PRP alone or combined with FA to enhance osseointegration of dental implants. For example, clinical trials should include a sufficient number of patients and a proper design (randomized, controlled, clinical trials). Future studies should assess the ideal concentration of the various growth factors, characterise other physiochemical factors that may be present in the platelet concentrate, and explain the potential beneficial effects of PRP treatment in bone regeneration.
6. Regarding the use of hDPSCs in in vitro studies, efforts should be made to restrict the variability of hDPSCs by extracting cells from only impacted wisdom teeth for example. However, donor variation would still be a concern. For example, age, gender and patient's history may still affect hDPSCs.
7. This study only used hDPSCs. Other dental tissues containing stem cells are readily accessible; e.g. periodontal ligament stem cells. It would be interesting to compare the behaviour of FA/PRP used in combination with hDPSCs, periodontal ligament stem cells and hBMSCs.
8. It was stated earlier in this thesis that PDGF release from PRP gel combined on FA coatings required thrombin. As it has been reported that the use of thrombin has some drawbacks, it would be worth investigating the potential of collagen as an alternative platelet activator in bone regeneration applications.

Chapter 8: References

1. Abhijit, V. 2006. A comparative study of hydroxyapatite and platelet rich plasma coated hydroxyapatite in extracted mandibular third molar tooth socket. Thesis, RGUHS.

2. Adell, R. et al. 1981. A 15-year study of osseointegrated implants in the treatment of the edentulous jaw. International journal of oral surgery. 10(6), pp.387-416.

3. Aiba-Kojima, E. et al. 2007. Characterization of wound drainage fluids as a source of soluble factors associated with wound healing: comparison with platelet-rich plasma and potential use in cell culture. Wound repair and regeneration. 15(4), pp.511-520.

4. Albanese, A. et al. 2013. Platelet-rich plasma (PRP) in dental and oral surgery: from the wound healing to bone regeneration. Immunity and Ageing. 10(1), pp.23.

5. Alberts, B. et al. 2002. The cytoskeleton and cell behaviour. Molecular Biology of the Cell. 4th edition.

6. Albrektsson, T. and Lekholm, U. 1989. Osseointegration: current state of the art. Dental Clinics of North America. 33(4), pp.537-554.

7. Albrektsson, T. and Wennerberg, A. 2004. Oral implant surfaces: Part 1--review focusing on topographic and chemical properties of different surfaces and in vivo responses to them. International Journal of Prosthodontics. 17(5), pp.536-543.

8. Albrektsson, T. et al. 1981. Osseointegrated titanium implants: requirements for ensuring a long-lasting, direct bone-to-implant anchorage in man. Acta Orthopaedica Scandinavica. 52(2), pp.155-170.

9. Alhilou, A. 2012. An in vitro study to assess the effect of fluoroapatite implant coatings on peri-implantitis. Ph.D. thesis. University of Leeds.United Kingdom.

10. Alhilou, A. et al. 2016. Physicochemical and antibacterial characterization of a novel fluorapatite coating. ACS omega. 1(2), pp.264-276.

11. Alkharobi, H.E. 2016. Characterisation of Dental Pulp Cells Derived from Carious Teeth. Thesis, University of Leeds.

12. Alongi, D.J. et al. 2010. Stem/progenitor cells from inflamed human dental pulp retain tissue regeneration potential. Regenerative medicine. 5(4), pp.617-631.

13. Anand, U. and Mehta, D. 2012. Evaluation of immediately loaded dental implants bioactivated with platelet-rich plasma placed in the mandibular posterior region: A clinico-radiographic study. Journal of Indian Society of Periodontology, 16, pp.89.
14. Andrae, J. et al. 2008. Role of platelet-derived growth factors in physiology and medicine. Genes & development. 22(10), pp.1276-1312.
15. Anil, S. et al. 2011. Dental implant surface enhancement and osseointegration. Implant Dentistry: A Rapidly Evolving Practice. New York: InTech. pp.83-108.
16. Anitua, E. 1999. Plasma rich in growth factors: preliminary results of use in the preparation of future sites for implants. International journal of Oral and maxillofacial Implants. 14(4), pp.529-535.
17. Anitua, E. A. 2006. Enhancement of osseointegration by generating a dynamic implant surface. Journal of Oral Implantology, 32, pp.72-76.
18. Anitua, E. et al. 2004. Autologous platelets as a source of proteins for healing and tissue regeneration. Thromb Haemost. 91, pp.4-15.
19. Anitua, E. et al. 2005. Autologous preparations rich in growth factors promote proliferation and induce VEGF and HGF production by human tendon cells in culture. Journal of Orthopaedic Research. 23(2), pp.281-286.
20. Anitua, E. et al. 2007. The potential impact of the preparation rich in growth factors (PRGF) in different medical fields. Biomaterials. 28(31), pp.4551-4560.
21. Anitua, E. et al. 2008. Clinical outcome of immediately loaded dental implants bioactivated with plasma rich in growth factors: a 5-year retrospective study. Journal of periodontology, 79, pp.1168-1176.
22. Anitua, E. et al. 2009a. Fibroblastic response to treatment with different preparations rich in growth factors. Cell proliferation. 42(2), pp.162-170.
23. Anitua, E. et al. 2009b. The effects of PRGF on bone regeneration and on titanium implant osseointegration in goats: a histologic and histomorphometric study. Journal of Biomedical Materials Research Part A, 91, pp.158-165.
24. Anitua, E. et al. 2009a. Fibroblastic response to treatment with different preparations rich in growth factors. Cell proliferation, 42, 162-170.

25. Anitua, E. et al. 2012. Perspectives and challenges in regenerative medicine using plasma rich in growth factors. Journal of Controlled Release. 157(1), pp.29-38.

26. Antoniades, H.N. 1981. Human platelet-derived growth factor (PDGF): purification of PDGF-I and PDGF-II and separation of their reduced subunits. Proceedings of the National Academy of Sciences. 78(12), pp.7314-7317.
27. Antoniades, H.N. et al. 1991. Injury induces in vivo expression of platelet-derived growth factor (PDGF) and PDGF receptor mRNAs in skin epithelial cells and PDGF mRNA in connective tissue fibroblasts. Proceedings of the National Academy of Sciences. 88(2), pp.565-569.

28. Appel, T.R. et al. 2002. Comparison of three different preparations of platelet concentrates for growth factor enrichment. Clinical Oral Implants Research. 13(5), pp.522-528.
29. Arpornmaeklong, P. et al. 2004. Influence of platelet-rich plasma (PRP) on osteogenic differentiation of rat bone marrow stromal cells. An in vitro study. International journal of oral and maxillofacial surgery. 33(1), pp.60-70.
30. Atari, M. et al. 2012. Dental pulp of the third molar: a new source of pluripotent-like stem cells. J Cell Sci. 125(14), pp.3343-3356.
31. Aubin, J.E. 1998a. Advances in the osteoblast lineage. Biochemistry and Cell Biology. 76(6), pp.899-910.
32. Aubin, J.E. 1998b. Bone stem cells. Journal of cellular biochemistry. 72(S30–31), pp.73-82.
33. Babensee, J.E. et al. 2000. Growth factor delivery for tissue engineering. Pharmaceutical research. 17(5), pp.497-504.
34. Bates, C. et al. 2013. Soft tissue attachment to titanium implants coated with growth factors. Clinical implant dentistry and related research, 15, pp.53-63.
35. Bayliss, P. et al. 1986. Mineral powder diffraction file. JCPDS, USA. 271.
36. Beck, L. S. et al.1993. One systemic administration of transforming growth factor-β1 reverses age- or glucocorticoid-impaired wound healing. Journal of Clinical Investigation. 92(6), pp. 2841–2849.
37. Behr, B. et al. 2011. Locally applied vascular endothelial growth factor A increases the osteogenic healing capacity of human adipose-derived stem cells by promoting osteogenic and endothelial differentiation. Stem Cells. 29(2), pp. 286–296.
38. Betoni-Junior, W. et al. 2013. Evaluation of the bone healing process utilizing platelet-rich plasma activated by thrombin and calcium chloride: a histologic study in rabbit calvaria. Journal of Oral Implantology. 39(1), pp.14-21.

39. Bhadang, K.A. and Gross, K.A. 2004. Influence of fluorapatite on the properties of thermally sprayed hydroxyapatite coatings. Biomaterials. 25(20), pp.4935-4945.
40. Bi, L. et al. 2010. Reconstruction of goat tibial defects using an injectable tricalcium phosphate/chitosan in combination with autologous platelet-rich plasma. Biomaterials. 31(12), pp.3201-3211.
41. Bijlani, M. and Lozada, J. 1996. Immediately loaded dental implants—influence of early functional contacts on implant stability, bone level integrity and soft tissue quality: a retrospective 3 and 6 year clinical analysis. Int J Oral Maxillofac Implants. 11(1), pp.126-127.
42. Boanini, E. et al. 2010. Ionic substitutions in calcium phosphates synthesized at low temperature. Acta biomaterialia. 6(6), pp.1882-1894.
43. Bonewald, L. and Mundy, G. 1990. Role of transforming growth factor-beta in bone remodeling. Clinical orthopaedics and related research. (250), pp.261-276.
44. Border, W.A. and Ruoslahti, E. 1992. Transforming growth factor-beta in disease: the dark side of tissue repair. The Journal of clinical investigation. 90(1), pp.1-7.
45. Boskey, A. et al. 1998. Fourier transform infrared microspectroscopic analysis of bones of osteocalcin-deficient mice provides insight into the function of osteocalcin. Bone, 23, pp.187-196.
46. Boyan, B. D. et al. 2001. The titanium-bone cell interface in vitro: the role of the surface in promoting osteointegration. Titanium in medicine. Springer.
47. Braceras, I. et al. 2009. In vivo low-density bone apposition on different implant surface materials. International journal of oral and maxillofacial surgery, 38, pp.274-278.
48. Brandl, F. et al. 2007. Rational design of hydrogels for tissue engineering: impact of physical factors on cell behavior. Biomaterials. 28(2), pp.134-146.
49. Brånemark, P.-I. 1983. Osseointegration and its experimental background. The Journal of prosthetic dentistry, 50, pp.399-410.
50. Brånemark, P.-I. et al. 1969. Intra-osseous anchorage of dental prostheses: I. Experimental studies. Scandinavian journal of plastic and reconstructive surgery. 3(2), pp.81-100.
51. Brecher, G. and Cronkite, E.P. 1950. Morphology and enumeration of human blood platelets. Journal of Applied Physiology. 3(6), pp.365-377.

52. Brett, P. et al. 2004. Roughness response genes in osteoblasts. Bone. 35(1), pp.124-133.

53. Brown, P.W. and Constantz, B. 1994. Hydroxyapatite and related materials. CRC press.
54. Brown, R. et al. 1994. PDGF and TGF-alpha act synergistically to improve wound healing in the genetically diabetic mouse. J SurgRes56. pp.562-570.
55. Byers, B. A. and GARCÍA, A. J. 2004. Exogenous Runx2 expression enhances in vitro osteoblastic differentiation and mineralization in primary bone marrow stromal cells. Tissue engineering. 10, pp.1623-1632.
56. Canalis, E. et al. 1988. Isolation and characterization of insulin-like growth factor I (somatomedin-C) from cultures of fetal rat calvariae. Endocrinology. 122(1), pp.22-27.
57. Canalis, E. et al. 1989. Effects of platelet-derived growth factor on bone formation in vitro. Journal of cellular physiology. 140(3), pp.530-537.

58. Canalis, E. et al. 1996. The divalent strontium salt S12911 enhances bone cell replication and bone formation in vitro. Bone. 18(6), pp.517-523.
59. Candeliere, G. et al. 2001. Individual osteoblasts in the developing calvaria express different gene repertoires. Bone. 28(4), pp.351-361.
60. Cao, M. et al. 2004. Preparation of ultrahigh-aspect-ratio hydroxyapatite nanofibers in reverse micelles under hydrothermal conditions. Langmuir. 20(11), pp.4784-4786.
61. Caplan, A. I. 1991. Mesenchymal stem cells. J Orthop Res. 9, pp.641-50.
62. Carlson, E. 2000. Bone grafting the jaws in the 21st century: the use of platelet-rich plasma and bone morphogenetic protein. The Alpha omegan. 93(3), pp.26-30.
63. Carmeliet, P. 2000. Mechanisms of angiogenesis and arteriogenesis. Nature medicine, 6, pp.389-396.
64. Castro-malaspina, H. et al. 1981. Human megakaryocyte stimulation of proliferation of bone marrow fibroblasts. Blood. 57, pp.781-7.
65. Celeste, A.J. et al. 1990. Identification of transforming growth factor beta family members present in bone-inductive protein purified from bovine bone. Proceedings of the National Academy of Sciences. 87(24), pp.9843-9847.
66. Chen, F.M. et al. 2010. A review on endogenous regenerative technology in periodontal regenertaive medicine. Biomaterials. 31(31), pp. 7892-7927.

67. Chen, H. et al. 2006a. Synthesis of fluorapatite nanorods and nanowires by direct precipitation from solution. Crystal growth and design. 6, 1504-1508.
68. Chen, H. et al. 2006b. Acellular Synthesis of a Human Enamel-like Microstructure. Advanced Materials. 18, pp.1846-1851.
69. Chevallier, N. et al. 2010. Osteoblastic differentiation of human mesenchymal stem cells with platelet lysate. Biomaterials. 31, pp.270-278.
70. Cho, H.S. et al. 2011. Individual variation in growth factor concentrations in platelet-rich plasma and its influence on human mesenchymal stem cells. The Korean journal of laboratory medicine. 31(3), pp.212-218.
71. Choi, B.-H. et al. 2005. Effect of platelet-rich plasma (PRP) concentration on the viability and proliferation of alveolar bone cells: an in vitro study. International journal of oral and maxillofacial surgery. 34(4), pp.420-424.
72. Chou, B.-Y. and Chang, E. 2002. Plasma-sprayed hydroxyapatite coating on titanium alloy with ZrO2 second phase and ZrO2 intermediate layer. Surface and Coatings Technology. 153(1), pp.84-92.
73. Choukroun, J. et al. 2006. Platelet-rich fibrin (PRF): a second-generation platelet concentrate. Part IV: clinical effects on tissue healing. Oral Surgery, Oral Medicine, Oral Pathology, Oral Radiology, and Endodontology. 101, pp.e56-e60.
74. Clark, D.R. 2013. In vitro anti-caries effect of fluoridated hydroxyapatite-coated preformed metal crowns. European Archives of Paediatric Dentistry. 14 (4), pp. 253-258.
75. Clark, R.A. 2001. Fibrin and wound healing. Annals of the New York Academy of Sciences. 936(1), pp.355-367.
76. Cochran, D. L. et al. 2002. The use of reduced healing times on ITI® implants with a sandblasted and acid-etched (SLA) surface. Clinical oral implants research. 13, pp.144-153.
77. Cognasse, F. et al. 2009. Donor platelets stored for at least 3 days can elicit activation marker expression by the recipient's blood mononuclear cells: an in vitro study. Transfusion. 49(1), pp.91-98.
78. Cooper, L. F. et al. 2006. Fluoride modification effects on osteoblast behavior and bone formation at TiO2 grit-blasted cp titanium endosseous implants. Biomaterials. 27, pp.926-936.
79. Cooper, L.F. 1998. Biologic determinants of bone formation for osseointegration: clues for future clinical improvements. The Journal of prosthetic dentistry. 80(4), pp.439-449.

80. Couble, M. L. et al. 2000. Odontoblast differentiation of human dental pulp cells in explant cultures. Calcif Tissue Int. 66, pp.129-38.
81. Curran, J. M. et al. 2006. The guidance of human mesenchymal stem cell differentiation in vitro by controlled modifications to the cell substrate. Biomaterials. 27, pp.4783-4793.
82. Czajka-jakubowska, A. et al. 2009a. The influence of Ti surface topography on producing FA coatings for implants. Dental forum. 1 (XXXVII), pp.11-14.
83. Czajka-jakubowska, A.E. et al. 2009b. The effect of the surface characteristics of various substrates on fluorapatite crystal growth, alignment, and spatial orientation. Medical Science Monitor. 15(6), pp. MT84-MT88.
84. Czajka-Jakubowska, A. et al. 2011. Initial cellular response of dental pulp stem cells to fluorapatite surfaces. Dental forum. 1 (XXXIX), pp.11-14.
85. d'Aquino, R. et al. 2007. Human postnatal dental pulp cells co-differentiate into osteoblasts and endotheliocytes: a pivotal synergy leading to adult bone tissue formation. Cell death and differentiation. 14(6), pp.1162.
86. d'Aquino, R. et al. 2008. Dental pulp stem cells: a promising tool for bone regeneration. Stem cell reviews. 4(1), pp.21-26.
87. d'Aquino, R. et al. 2009. Human mandible bone defect repair by the grafting of dental pulp stem/progenitor cells and collagen sponge biocomplexes. Eur Cell Mater. 18, pp.75-83.
88. Davies, J. E. 2003. Understanding peri-implant endosseous healing. Journal of dental education. 67, pp.932-949.

89. De Aza, P. et al. 2005. Crystalline bioceramic materials. Bol. Soc. Esp. Ceram. 44(3), pp.135-145.
90. De Maat, M.P. and Verschuur, M. 2005. Fibrinogen heterogeneity: inherited and noninherited. Current opinion in hematology. 12(5), pp.377-383.
91. De oliveira, P. T. et al. 2003. Early expression of bone matrix proteins in osteogenic cell cultures. J Histochem Cytochem. 51, pp.633-41.
92. Denhardt, D. T. et al. 2001. Osteopontin as a means to cope with environmental insults: regulation of inflammation, tissue remodeling, and cell survival. J Clin Invest. 107, pp.1055-61.
93. Dhert, W. et al. 1991. A mechanical investigation of fluorapatite, magnesiumwhitlockite, and hydroxylapatite plasma-sprayed coatings in goats. Journal of biomedical materials research. 25(10), pp.1183-1200.

94. Dhert, W. et al. 1993. A histological and histomorphometrical investigation of fluorapatite, magnesiumwhitlockite, and hydroxylapatite plasma-sprayed coatings in goats. Journal of Biomedical Materials Research Part A. 27(1), pp.127-138.
95. Din, E. 10993-5: 2009. Technical Committee ISO/TC. 194.
96. Doessing, S. et al. 2010. GH and IGF1 levels are positively associated with musculotendinous collagen expression: experiments in acromegalic and GH deficiency patients. European journal of endocrinology. 163(6), pp.853-862.
97. Dolder, J.V.D. et al. 2006. Platelet-rich plasma: quantification of growth factor levels and the effect on growth and differentiation of rat bone marrow cells. Tissue engineering. 12(11), pp.3067-3073.
98. Dominici, M. et al. 2006. Minimal criteria for defining multipotent mesenchymal stromal cells. The International Society for Cellular Therapy position statement. Cytotherapy. 8(4), pp.315-317.
99. Doucet, C. et al. 2005. Platelet lysates promote mesenchymal stem cell expansion: A safety substitute for animal serum in cell-based therapy applications. Journal of cellular physiology. 205, pp.228-236.
100. Duarte Campos, D.F. et al. 2014. The stiffness and structure of three-dimensional printed hydrogels direct the differentiation of mesenchymal stromal cells toward adipogenic and osteogenic lineages. Tissue Engineering Part A. 21(3-4), pp.740-756.
101. Dubey, V.K. et al. 2007. Papain-like proteases: Applications of their inhibitors. African Journal of Biotechnology. 6(9).
102. Ducy, P. et al. 1997. Osf2/Cbfa1: a transcriptional activator of osteoblast differentiation. Cell. 89(5), pp.747-754.
103. Dugrillon, A. et al. 2002. Autologous concentrated platelet-rich plasma (cPRP) for local application in bone regeneration. International journal of oral and maxillofacial surgery. 31(6), pp.615-619.
104. Dunn, M.K. et al. 1995. Cyclopamine, a steroidal alkaloid, disrupts development of cranial neural crest cells in Xenopus. Developmental dynamics. 202(3), pp.255-270.
105. Eatough, D.J. et al. 1978. The binding of Ca^{2+} and Mg^{2+} to human serium albumin: A calorimetric study. Thermochimica Acta. 25(3), pp.289-297.

106. Ehrenfest, D.M.D. et al. 2009. Classification of platelet concentrates: from pure platelet-rich plasma (P-PRP) to leucocyte-and platelet-rich fibrin (L-PRF). Trends in biotechnology. 27(3), pp.158-167.
107. Ekman, S. et al. 1999. Increased mitogenicity of an αβ heterodimeric PDGF receptor complex correlates with lack of RasGAP binding. Oncogene. 18(15), p2481.
108. El-Gendy, R. et al. 2012. Osteogenic differentiation of human dental pulp stromal cells on 45S5 Bioglass® based scaffolds in vitro and in vivo. Tissue Engineering Part A. 19(5-6), pp.707-715.
109. El-Gendy, R. O. O. M. 2010. Bone tissue engineering using dental pulp stem cells. University of Leeds.
110. Elsubeihi, E.S. and Zarb, G.A. 2002. Implant prosthodontics in medically challenged patients: the University of Toronto experience. Journal-Canadian Dental Association. 68(2), pp.103-109.
111. Eppley, B.L. et al. 2004. Platelet quantification and growth factor analysis from platelet-rich plasma: implications for wound healing. Plastic and reconstructive surgery. 114(6), pp.1502-1508.
112. Esposito, M. et al. 1998. Biological factors contributing to failures of osseointegrated oral implants,(I). Success criteria and epidemiology. European journal of oral sciences. 106(1), pp.527-551.
113. Evans, M.J. and Kaufman, M.H. 1981. Establishment in culture of pluripotential cells from mouse embryos. Nature. 292(5819), pp.154.
114. Fallouh, L. et al. 2010. Effects of autologous platelet-rich plasma on cell viability and collagen synthesis in injured human anterior cruciate ligament. JBJS. 92(18), pp.2909-2916.
115. Fantl, W.J. et al. 1993. Signalling by receptor tyrosine kinases. Annual review of biochemistry. 62(1), pp.453-481.
116. Farndale, R.W. et al. 2003. Collagen-platelet interactions: recognition and signalling. In: Biochemical Society Symposia: London; Portland on behalf of The Biochemical Society; 1999, pp.81-94.
117. Fathi, M. and Zahrani, E.M. 2009. Fabrication and characterization of fluoridated hydroxyapatite nanopowders via mechanical alloying. Journal of Alloys and Compounds. 475(1), pp.408-414.
118. Fazan, F. and Marquis, P.M. 2000. Dissolution behavior of plasma-sprayed hydroxyapatite coatings. Journal of materials science: Materials in Medicine. 11(12), pp.787-792.

119. Forghani, A. et al. 2013. Novel Fluorapatite-Forsterite Nanocomposite Powder for Oral Bone Defects. International Journal of Applied Ceramic Technology. 10(s1), pp.E282-E289.
120. Foster, T.E. et al. 2009. Platelet-rich plasma: from basic science to clinical applications. The American journal of sports medicine. 37(11), pp.2259-2272.
121. Frenkel, B. et al. 1997. Activity of the osteocalcin promoter in skeletal sites of transgenic mice and during osteoblast differentiation in bone marrow-derived stromal cell cultures: effects of age and sex. Endocrinology. 138(5), pp.2109-2116.
122. Freshney, R.I. 2006. Basic principles of cell culture. Culture of cells for tissue engineering. pp.11-14.
123. Freymiller, E.G. and Aghaloo, T.L. 2004. Platelet-rich plasma: ready or not? Journal of Oral and Maxillofacial Surgery. 62(4), pp.484-488.
124. Fu, D.-l. et al. 2012. Fluorescence microscopic analysis of bone osseointegration of strontium-substituted hydroxyapatite implants. Journal of Zhejiang University Science B. 13(5), pp.364-371.
125. Fufa, D. et al. 2008. Activation of platelet-rich plasma using soluble type I collagen. Journal of Oral and Maxillofacial Surgery. 66(4), pp.684-690.
126. Gan, S.D. and Patel, K.R. 2013. Enzyme immunoassay and enzyme-linked immunosorbent assay. J Invest Dermatol. 133(9), pe12.
127. Gapski, R. et al. 2003. Critical review of immediate implant loading. Clinical oral implants research. 14(5), pp.515-527.
128. Gandhi, A. et al. 2006. The effects of local platelet rich plasma delivery on diabetic fracture healing. Bone. 38(4), pp.540-546.
129. Garcia, R.V. et al. 2010. Effect of platelet-rich plasma on peri-implant bone repair: a histologic study in dogs. Journal of Oral Implantology. 36(4), pp.281-290.
130. Garg, A.K. 2000. The use of platelet-rich plasma to enhance the success of bone grafts around dental implants. Dental implantology update. 11(3), pp.17.
131. Gassling, V. et al. 2010. Platelet-rich fibrin membranes as scaffolds for periosteal tissue engineering. Clinical oral implants research. 21, pp.543-549.
132. Gaßling, V.L. et al. 2009. Platelet-rich plasma and platelet-rich fibrin in human cell culture. Oral Surgery, Oral Medicine, Oral Pathology, Oral Radiology, and Endodontology. 108(1), pp. 48-55.
133. Gentile, P. et al. 2010. Application of platelet-rich plasma in maxillofacial surgery: clinical evaluation. Journal of Craniofacial Surgery. 21(3), pp.900-904.

134. Giannoudis, P.V. et al. 2007. Fracture healing: the diamond concept. Injury. 38, pp.S3-S6.
135. Gibble, J. and Ness, P. 1990. Fibrin glue: the perfect operative sealant? Transfusion. 30(8), pp.741-747.
136. Gineset, L. et al. 1999. Degradation of hydroxyapatite, fluoroapatite and fluorhydroxyapatite coatings of dental implants in dogs. Journal of Biomedical material research. 48, pp.224-234.
137. Giovanini, A. et al. 2010. Platelet-rich plasma diminishes calvarial bone repair associated with alterations in collagen matrix composition and elevated CD34+ cell prevalence. Bone. 46(6), pp.1597–1603.
138. Giuliani, A. et al. 2013. Three Years After Transplants in Human Mandibles, Histological and In-Line Holotomography Revealed That Stem Cells Regenerated a Compact Rather Than a Spongy Bone: Biological and Clinical Implications. Stem Cells Translational Medicine. 2(4), pp.316-324.
139. Goldstein, J.I. et al. 2017. Scanning electron microscopy and X-ray microanalysis. Springer.
140. Golub, E.E. and Boesze-Battaglia, K. 2007. The role of alkaline phosphatase in mineralization. Current Opinion in Orthopaedics. 18(5), pp.444-448.
141. Govindasamy, V. et al. 2010. Inherent differential propensity of dental pulp stem cells derived from human deciduous and permanent teeth. Journal of Endodontics. 36, pp.1504-1515.
142. Govoni K. E. et al. 2005. Themulti-functional role of insulin-like growth factor binding proteins in bone. Pediatric Nephrology. 20(3), pp. 261–268.
143. Grageda, E. 2004. Platelet-rich plasma and bone graft materials: a review and a standardized research protocol. Implant dentistry. 13(4), pp.301-309.
144. Grassi, S. et al. 2006. Histologic evaluation of early human bone response to different implant surfaces. Journal of periodontology. 77, pp.1736-1743.
145. Graves, D.T. et al. 1989. The potential role of platelet-derived growth factor as an autocrine or paracrine factor for human bone cells. Connective tissue research. 23(2-3), pp.209-218.
146. Graziani, F. et al. 2006. The in vitro effect of different PRP concentrations on osteoblasts and fibroblasts. Clinical oral implants research. 17(2), pp.212-219.
147. Greenhalgh, D.G. 1996. The role of growth factors in wound healing. Journal of Trauma and Acute Care Surgery. 41(1), pp.159-167.

148. Gronthos, S. et al. 2000. Postnatal human dental pulp stem cells (DPSCs) in vitro and in vivo. Proceedings of the National Academy of Sciences. 97(25), pp.13625-13630.
149. Gronthos, S. et al. 2002. Stem cell properties of human dental pulp stem cells. Journal of dental research. 81(8), pp.531-535.
150. Groot, K.d. et al. 1987. Plasma sprayed coatings of hydroxyapatite. J Biomed Mater Res. 21(12), pp.1375-1381.
151. Gruber, R. et al. 2004. Platelet-released supernatants increase migration and proliferation, and decrease osteogenic differentiation of bone marrow-derived mesenchymal progenitor cells under in vitro conditions. Platelets. 15(1), pp.29-35.
152. Gruia, I. 2017. Micro-tomography and x-ray analysis of geological samples. Proceedings of the romanian academy series a-mathematics physics technical sciences information science. 18(1), pp.42-49.
153. Gupta V. et al. 2011.Regenerative Potential of Platelet Rich Fibrin in Dentistry: Literature Review. Asian journal of oral health and Allied sciences. 1(1), pp. 22-28.
154. Hakimi, M. et al. 2010. Combined use of platelet-richplasma andautologous bone grafts in the treatment of long bone defects in mini-pigs. Injury. 41(7), pp. 717–723.
155. Han, B. et al. 2009. The effect of thrombin activation of platelet-rich plasma on demineralized bone matrix osteoinductivity. JBJS. 91(6), pp.1459-1470.
156. Hänseler, E. et al. 1996. Estimation of the lower limits of manual and automated platelet counting. American journal of clinical pathology. 105(6), pp.782-787.
157. Hansson, H. et al. 1983. Structural aspects of the interface between tissue and titanium implants. Journal of Prosthetic Dentistry. 50(1), pp.108-113.
158. Harrison, P. and Briggs, C. 2013. Platelet counting. Platelets (Third Edition). Elsevier, pp.547-557.
159. Harrison, S. et al. 2011. Platelet activation by collagen provides sustained release of anabolic cytokines. The American journal of sports medicine. 39(4), pp.729-734.
160. Hashikawa, T. et al. 2003. Involvement of CD73 (ecto-5□-nucleotidase) in adenosine generation by human gingival fibroblasts. Journal of Dental Research. 82 (11). pp. 888–892.

161. Hauschka, P. et al. 1986. Growth factors in bone matrix. Isolation of multiple types by affinity chromatography on heparin-Sepharose. Journal of Biological Chemistry. 261(27), pp.12665-12674.
162. Hayakawa, T. et al. 2000. Effect of surface roughness and calcium phosphate coating on the implant/bone response. Clinical Oral Implants Research. 11, pp.296-304.
163. He, L. et al. 2009. A comparative study of platelet-rich fibrin (PRF) and platelet-rich plasma (PRP) on the effect of proliferation and differentiation of rat osteoblasts in vitro. Oral Surgery, Oral Medicine, Oral Pathology, Oral Radiology and Endodontology. 108, pp.707-713.
164. Heldin, C.-H. and Westermark, B. 1999. Mechanism of action and in vivo role of platelet-derived growth factor. Physiological reviews. 79(4), pp.1283-1316.

165. Hinsbergh, V.W. et al. 2001. Role of fibrin matrix in angiogenesis. Annals of the New York Academy of Sciences. 936(1), pp.426-437.
166. Ho, W. et al. 2006. The behavior of human mesenchymal stem cells in 3D fibrin clots: dependence on fibrinogen concentration and clot structure. Tissue engineering. 12(6), pp.1587-1595.
167. Hobo, S. et al. 1989. Osseointegration and occlusal rehabilitation. Quintessence Pub Co.
168. Hock, J.M. et al. 1988. Insulin-like growth factor I has independent effects on bone matrix formation and cell replication. Endocrinology. 122(1), pp.254-260.
169. Hoemann, C.D. et al. 2002. A multivalent assay to detect glycosaminoglycan, protein, collagen, RNA, and DNA content in milligram samples of cartilage or hydrogel-based repair cartilage. Analytical biochemistry. 300(1), pp.1-10.
170. Horwitz, E. et al. 2005. Clarification of the nomenclature for MSC: The International Society for Cellular Therapy position statement. Cytotherapy. 7(5), pp.393-395.
171. Hsiao S. T. et al. 2012. Comparative analysis of paracrine factor expression in human adult mesenchymal stem cells derived from bone marrow, adipose, and dermal tissue. Stem Cells and Development. 21(12), pp. 2189–2203.

172. Hsieh, S.C. and Graves, D.T. 1998. Pulse application of platelet-derived growth factor enhances formation of a mineralizing matrix while continuous application is inhibitory. Journal of cellular biochemistry. 69(2), pp.169-180.
173. Hsu, C.-W. et al. 2009. The negative effect of platelet-rich plasma on the growth of human cells is associated with secreted thrombospondin-1. Oral Surgery, Oral Medicine, Oral Pathology, Oral Radiology, and Endodontology. 107(2), pp.185-192.
174. Huang, G. T. et al. 2006. In vitro characterization of human dental pulp cells: various isolation methods and culturing environments. Cell Tissue Res, 324, pp.225-36.
175. Huang, G.-J. et al. 2009. Mesenchymal stem cells derived from dental tissues vs. those from other sources: their biology and role in regenerative medicine. Journal of dental research. 88(9), pp.792-806.
176. Intini, G. et al. 2007. Calcium sulfate and platelet-rich plasma make a novel osteoinductive biomaterial for bone regeneration. J Transl Med. 5, pp.13.
177. ISO 10993-5, I. 2009. Biological evaluation of medical devices–Part 5: Tests for in vitro cytotoxicity. International Organization for Standardization Geneve, Switzerland.
178. Ito, K. et al. 2006. Simultaneous implant placement and bone regeneration around dental implants using tissue-engineered bone with fibrin glue, mesenchymal stem cells and platelet-rich plasma. Clinical oral implants research. 17(5), pp.579-586.
179. Jain, E. et al. 2017. Sustained release of multicomponent platelet-rich plasma proteins from hydrolytically degradable PEG hydrogels. Journal of Biomedical Materials Research Part A. 105(12), pp.3304-3314.
180. Jaiswal, N. et al. 1997. Osteogenic differentiation of purified, culture-expanded human mesenchymal stem cells in vitro. Journal of cellular biochemistry. 64(2), pp.295-312.
181. Jakse, N. et al. 2003. Influence of PRP on autogenous sinus grafts. Clinical Oral Implants Research. 14(5), pp.578-583.
182. Jalowiec, J.M. et al. 2015. An in vitro investigation of PRP-gel as a cell and growth factor delivery vehicle for tissue engineering. Tissue Engineering. Part C: Methods. 22(1), pp.49-58.

183. James, M.J. et al. 2006. Different roles of runx2 during early neural crest–derived bone and tooth development. Journal of Bone and Mineral Research. 21(7), pp.1034-1044.
184. Jivraj, S. and Chee, W.W. 2007. Treatment planning in Implant Dentistry. London: British Dental Association.
185. Johnsson, A. et al. 1982. Platelet-derived growth factor: identification of constituent polypeptide chains. Biochemical and biophysical research communications. 104(1), pp.66-74.
186. Johnson, L. et al. 2011. Cryopreservation of buffy-coat-derived platelet concentrates in dimethyl sulfoxide and platelet additive solution. Cryobiology. 62(2), pp.100-106.
187. Jokstad, A. et al. 2003. Quality of dental implants. International dental journal. 53(S6P2), pp.409-443.
188. Joseph B. K. et al. 1996. In situ hybridization evidence for a paracrine/autocrine rolefor insulin-like growth factor-I in tooth development. Growth Factors. 13(1-2), pp.11–17.
189. Junker, R. et al. 2009. Effects of implant surface coatings and composition on bone integration: a systematic review. Clinical oral implants research. 20, pp.185-206.
190. Kakudo, N. et al. 2008. Proliferation-promoting effect of platelet-rich plasma on human adipose–derived stem cells and human dermal fibroblasts. Plastic and reconstructive surgery. 122(5), pp.1352-1360.
191. Kakudo, N. et al. 2017. Angiogenic effect of platelet-rich plasma combined with gelatin hydrogel granules injected into murine subcutis. Journal of tissue engineering and regenerative medicine. 11(7), pp.1941-1948.
192. Kamoda H. et al. 2012. Platelet-rich plasma combined with hydroxyapatite for lumbar interbody fusion promoted bone formation and decreased an inflammatory pain neuropeptide in rats. Spine.37 (20), pp.1727–1733.
193. Kanagaraja, S. et al. 1996. Platelet binding and protein adsorption to titanium and gold after short time exposure to heparinized plasma and whole blood. Biomaterials. 17, pp.2225-2232.
194. Kanno, T. et al. 2005. Platelet-rich plasma enhances human osteoblast-like cell proliferation and differentiation. Journal of Oral and Maxillofacial Surgery. 63(3), pp.362-369.

195. Kanthan, S. R. et al. 2011. Platelet-rich plasma (PRP) enhances bone healing in non-united critical-sized defects: a preliminary study involving rabbit models. Injury. 42(8), pp.782–789.
196. Kao, R.T. et al. 2009. The use of biologic mediators and tissue engineering in dentistry. Periodontology 2000. 50(1), pp.127-153.
197. Karp J.M. et al. 2005. Thrombin mediated migration of osteogenic cells. Bone. 37 (3), pp.337–348.
198. Karsenty, G. 1999. The genetic transformation of bone biology. Genes & development. 13(23), pp.3037-3051.
199. Kasten, P. et al. 2008. Effect of platelet-rich plasma on the in vitro proliferation and osteogenic differentiation of human mesenchymal stem cells on distinct calcium phosphate scaffolds: the specific surface area makes a difference. Journal of biomaterials applications.
200. Kawase, T. et al. 2003. Platelet-rich plasma-derived fibrin clot formation stimulates collagen synthesis in periodontal ligament and osteoblastic cells in vitro. Journal of periodontology. 74(6), pp.858-864.
201. Kawasumi, M. et al. 2008. The effect of the platelet concentration in platelet-rich plasma gel on the regeneration of bone. Bone and Joint Journal. 90(7), pp.966-972.
202. Kellner, M. et al. 2014. Differences of isolated dental stem cells dependent on donor age and consequences for autologous tooth replacement. Archives of oral biology. 59(6), pp.559-567.
203. Kells, A.F. et al. 1995. TGF-β and PDGF act synergistically in affecting the growth of human osteoblast-enriched cultures. Connective tissue research. 31(2), pp.117-124.
204. Khursheed, A. 2007. Scanning electron microscope. Google Patents.
205. Kieswetter, K. et al. 1996. The role of implant surface characteristics in the healing of bone. Crit Rev Oral Biol Med. 7, pp.329-45.
206. Kilian, O. et al. 2004. Effects of platelet growth factors on human mesenchymal stem cells and human endothelial cells in vitro. European journal of medical research. 9(7), pp.337-344.
207. Kim, H.-W. et al. 2004. Fluor-hydroxyapatite sol–gel coating on titanium substrate for hard tissue implants. Biomaterials. 25(17), pp.3351-3358.
208. Kim, S.-G. et al. 2002. Use of Particulate Dentin--Plaster of Paris Combination with/without Platelet-Rich Plasma in the Treatment of Bone

Defects Around Implants. International Journal of Oral and Maxillofacial Implants. 17(1).
209. Kim, T. et al. 1998. Highly adhesive hydroxyapatite coatings on alumina substrates prepared by ion-beam assisted deposition. Surface and Coatings Technology. 99(1-2), pp.20-23.
210. Kim, Y.-J. et al. 1988. Fluorometric assay of DNA in cartilage explants using Hoechst 33258. Analytical biochemistry. 174(1), pp.168-176.
211. Klein, C. 1990. Study of solubility and surface features of different calcium phosphate coatings in vitro and in vivo: a pilot study.
212. Klein, C. et al. 1994. Calcium phosphate plasma-sprayed coatings and their stability: An in vivo study. Journal of Biomedical Materials Research Part A. 28(8), pp.909-917.
213. Klein, C.P. et al. 1991. Plasma-sprayed coatings of tetracalciumphosphate, hydroxyl-apatite, and α-TCP on titanium alloy: An interface study. Journal of Biomedical Materials Research Part A. 25(1), pp.53-65.
214. Klein, M. et al. 2010. Modulation of platelet activation and initial cytokine release by alloplastic bone substitute materials. Clinical oral implants research. 21(3), pp.336-345.
215. Kniess, A. et al. 2003. Potential parameters for the detection of hGH doping. Analytical and bioanalytical chemistry. 376, pp.696-700.
216. Kocaoemer, A. et al. 2007. Human AB serum and thrombin-activated platelet-rich plasma are suitable alternatives to fetal calf serum for the expansion of mesenchymal stem cells from adipose tissue. Stem cells. 25(5), pp.1270-1278.
217. Koellensperger, E. et al. 2006. Human Serum from Platelet-Poor Plasma for the Culture of Primary Human Preadipocytes. Stem cells. 24(5), pp.1218-1225.
218. Komori, T. et al. 1997. Targeted disruption of Cbfa1 results in a complete lack of bone formation owing to maturational arrest of osteoblasts. cell. 89(5), pp.755-764.
219. Komori, T. 2009. Regulation of osteoblast differentiation by Runx2. Osteoimmunology. Springer, pp.43-49.
220. Korzyńska, A. and Zychowicz, M. 2008. A method of estimation of the cell doubling time on basis of the cell culture monitoring data. Biocybernetics and Biomedical Engineering. 28, pp.75-82.

221. Kovács, K. et al. 2003. Comparative study of β-tricalcium phosphate mixed with platelet-rich plasma versus β-tricalcium phosphate, a bone substitute material in dentistry. Acta Veterinaria Hungarica. 51(4), pp.475-484.
222. Koyama, N. et al. 2009. Evaluation of pluripotency in human dental pulp cells. Journal of Oral and Maxillofacial Surgery. 67, pp.501-506.
223. Kreja, L. et al. 2010. Non-resorbing osteoclasts induce migration and osteogenic differentiation of mesenchymal stem cells. Journal of Cellular Biochemistry. 109(2), pp. 347–355.
224. Kurita, J. et al. 2011. Enhanced vascularization by controlled release of platelet-rich plasma impregnated in biodegradable gelatin hydrogel. The Annals of thoracic surgery. 92(3), pp.837-844.
225. Kuroda, S. et al. 2005. Patterns and localization of gene expression during intramembranous bone regeneration in the rat femoral marrow ablation model. Calcified tissue international. 77(4), pp.212-225.
226. Kuzyk, P. R. and Schemitsch, E. H. 2011. The basic science of peri-implant bone healing. Indian journal of orthopaedics. 45, pp.108.
227. Lacoste, E. et al. 2003. Platelet Concentrates: Effects of Calcium and Thrombin on Endothelial Cell Proliferation and Growth Factor Release. Journal of Periodontology. 74(10), pp.1498-1507.
228. Landesberg, R. et al. 2000. Quantification of growth factor levels using a simplified method of platelet-rich plasma gel preparation. Journal of Oral and Maxillofacial Surgery. 58(3), pp.297-300.
229. Langenbach, F. and Handschel, J. 2013. Effects of dexamethasone, ascorbic acid and β-glycerophosphate on the osteogenic differentiation of stem cells in vitro. Stem cell research and therapy. 4(5), pp.117.
230. LaRochelle, W.J. et al. 2001. PDGF-D, a new protease-activated growth factor. Nature cell biology. 3(5), p517.
231. Larsson, C. et al. 2001. The titanium-bone interface in vivo. Titanium in medicine. Springer, pp.587-648.
232. Lau, K.-H.W. et al. 1998. Osteogenic actions of fluoride: its therapeutic use for established osteoporosis. Anabolic treatments for osteoporosis. CRC Press Boca Raton, FL, pp.207.
233. Lau, K.W. and Baylink, D.J. 1998. Molecular mechanism of action of fluoride on bone cells. Journal of bone and mineral research. 13 (11), pp.1660-1667.

234. Lau, K.W. et al. 1989. A proposed mechanism of the mitogenic action of fluoride on bone cells: inhibition of the activity of an osteoblastic acid phosphatase. Metabolism-Clinical and Experimental. 38(9), pp.858-868.
235. Laurens, N. et al. 2006. Fibrin structure and wound healing. Journal of Thrombosis and Haemostasis. 4(5), pp.932-939.
236. Lavenus, S. et al. 2011. Adhesion and osteogenic differentiation of human mesenchymal stem cells on titanium nanopores. Eur Cell Mater. 22(1), pp.84-96.
237. Le guéhennec, L. et al. 2007. Surface treatments of titanium dental implants for rapid osseointegration. Dental materials. 23, pp.844-854.
238. Leitner, G. et al. 2006. Platelet content and growth factor release in platelet-rich plasma: a comparison of four different systems. Vox sanguinis. 91(2), pp.135-139.
239. Li, H. et al. 2013. Platelet-rich plasma promotes the proliferation of human muscle derived progenitor cells and maintains their stemness. PloS one. 8(6), pe64923.
240. Li, J. et al. 2017. Evaluation of 3D-printed polycaprolactone scaffolds coated with freeze-dried platelet-rich plasma for bone regeneration. Materials. 10(7), pp.831.
241. Li, X. et al. 2000. PDGF-C is a new protease-activated ligand for the PDGF α-receptor. Nature cell biology. 2(5), p302.
242. Lin, S.S. et al. 2006. Controlled release of PRP-derived growth factors promotes osteogenic differentiation of human mesenchymal stem cells. In: Engineering in Medicine and Biology Society, 2006. EMBS'06. 28th Annual International Conference of the IEEE: IEEE, pp.4358-4361.
243. Lindroos, B. et al. 2008. Characterisation of human dental stem cells and buccal mucosa fibroblasts. Biochemical and biophysical research communications. 368(2), pp.329-335.
244. Liu, J. et al. 2004. Self-assembly of hydroxyapatite nanostructures by microwave irradiation. Nanotechnology. 16(1), pp.82.
245. Liu, J. et al. 2010. The effect of novel fluorapatite surfaces on osteoblast-like cell adhesion, growth, and mineralization. Tissue Engineering Part A. 16(9), pp. 2977-2986.
246. Liu, J. et al. 2011. Adhesion and growth of dental pulp stem cells on enamel-like fluorapatite surfaces. Journal of Biomedical Materials Research Part A. 96(3), pp. 528-534.

247. Liu, J. et al. 2012. The stimulation of adipose-derived stem cell differentiation and mineralization by ordered rod-like fluorapatite coatings. Biomaterials. 33(20), pp.5036-5046.
248. Liu, P. et al. 2005. Interpretation of protein adsorption: surface-induced conformational changes.Journal of the American Chemical Society. 127(22), pp. 8168-8173.
249. Liu, Y. et al. 2002. Fibroblast proliferation due to exposure to a platelet concentrate in vitro is pH dependent. Wound Repair and regeneration. 10(5), pp.336-340.
250. Liu, Y. et al. 2007. The influence of BMP-2 and its mode of delivery on the osteoconductivity of implant surfaces during the early phase of osseointegration. Biomaterials, 28, 2677-2686.
251. Long, M.W. 2001. Osteogenesis and bone-marrow-derived cells. Blood Cells, Molecules, and Diseases. 27(3), pp.677-690.
252. Lu, H.H. et al. 2008. Controlled delivery of platelet-rich plasma-derived growth factors for bone formation. Journal of biomedical materials research Part A. 86(4), pp.1128-1136.
253. Lucarelli, E. et al. 2003. Platelet-derived growth factors enhance proliferation of human stromal stem cells. Biomaterials. 24(18), pp.3095-3100.
254. Ma, D. et al. 2009. Effect of age and extrinsic microenvironment on the proliferation and osteogenic differentiation of rat dental pulp stem cells in vitro. Journal of endodontics. 35(11), pp.1546-1553.
255. Ma, D. et al. 2012. Changes in proliferation and osteogenic differentiation of stem cells from deep caries in vitro. Journal of endodontics. 38(6), pp.796-802.
256. Malafaya, P.B. et al. 2007. Natural–origin polymers as carriers and scaffolds for biomolecules and cell delivery in tissue engineering applications. Advanced drug delivery reviews. 59(4-5), pp.207-233.
257. Malhotra, A. et al. 2014. Platelet-rich plasma and bone defect healing. Tissue Engineering Part A. 20(19-20), pp.2614-2633.
258. Marco, F. et al. 2005. Peri-implant osteogenesis in health and osteoporosis. Micron. 36, pp.630-644.
259. Marks Jr, S.C. and Popoff, S.N. 1988. Bone cell biology: the regulation of development, structure, and function in the skeleton. American Journal of Anatomy. 183(1), pp.1-44.

260. Marks, S.C. and Odgren, P.R. 2002. Structure and development of the skeleton. Principles of Bone Biology (Second Edition). Elsevier, pp.3-15.

261. Martin, P. and Leibovich, S.J. 2005. Inflammatory cells during wound repair: the good, the bad and the ugly. Trends in cell biology. 15(11), pp.599-607.
262. Marx, R.E. et al. 1998. Platelet-rich plasma: growth factor enhancement for bone grafts. Oral Surgery, Oral Medicine, Oral Pathology, Oral Radiology, and Endodontology. 85(6), pp.638-646.
263. Marx, R.E. 2001. Platelet-rich plasma (PRP): what is PRP and what is not PRP? Implant dentistry. 10(4), pp.225-228.
264. Marx, R.E. 2004. Platelet-rich plasma: evidence to support its use. Journal of Oral Maxillofacial Surgery. 62(4), pp. 489-496.

265. Matsuda, N. et al. 1992. Mitogenic, chemotactic, and synthetic responses of rat periodontal ligament fibroblastic cells to polypeptide growth factors in vitro. Journal of periodontology. 63(6), pp.515-525.
266. Matsumoto, T. et al. 2004. Hydroxyapatite particles as a controlled release carrier of protein. Biomaterials. 25, pp.3807-3812.
267. Mavrogenis, A. et al. 2009. Biology of implant osseointegration. J Musculoskelet Neuronal Interact, 9, pp.61-71.
268. Mazzucco, L. et al. 2009. Not every PRP-gel is born equal Evaluation of growth factor availability for tissues through four PRP-gel preparations: Fibrinet®, RegenPRP-Kit®, Plateltex® and one manual procedure. Vox sanguinis. 97(2), pp.110-118.
269. Mccracken, M. S. 2006. Bone associated with implants in diabetic and insulin-treated rats. Clinical oral implants research. 17, pp.495-500.
270. McManus L. M. and Pinckard R. N. 2000. PAF, a putative mediator of oral inflammation," Critical Reviews in Oral Biology and Medicine.11 (2). pp. 240–258.
271. McPherson, E.J. et al. 1995. Hydroxyapatite-coated proximal ingrowth femoral stems. Clin Orthop. 315, pp.223-230.

272. Mehta, S. and Watson, J.T. 2008. Platelet rich concentrate: basic science and current clinical applications. Journal of orthopaedic trauma. 22(6), pp.432-438.

273. Misch, C.E. 2014. Rationale for dental implants. Text book on Dental Implant Prosthetics (Carl E Misch, Elsevier Publ). 3, pp.1-17.
274. Mishra, A. et al. 2009. Buffered platelet-rich plasma enhances mesenchymal stem cell proliferation and chondrogenic differentiation. Tissue Engineering Part C: Methods. 15(3), pp.431-435.
275. Miura, M. et al. 2003. SHED: stem cells from human exfoliated deciduous teeth. *Proceedings of the National Academy of Sciences.* 100(10), pp.5807-5812.
276. Miyazono K. and Takaku F.1989. Platelet-derived growth factors. Blood Reviews. 3(4), pp. 269–276.
277. Mohan, S. and Baylink, D.J. 1991. Bone growth factors. Clinical orthopaedics and related research. (263), pp.30-48.
278. Mohan S. and Baylink D. J. 2002. IGF-binding proteins are multifunctional and act via IGF-dependent and –independent mechanisms. Journal of Endocrinology. 175(1), pp.19–31.

279. Montesinos, M.C. et al. 2002. Adenosine promotes wound healing and mediates angiogenesis in response to tissue injury via occupancy of A2A receptors. The American journal of pathology. 160(6), pp.2009-2018.
280. Mori, K. et al. 2006. Modulation of mouse RANKL gene expression by Runx2 and PKA pathway. Journal of cellular biochemistry. 98(6), pp.1629-1644.

281. Morito, T. et al. 2008. Synovial fluid-derived mesenchymal stem cells increase after intra-articular ligament injury in humans. Rheumatology. 47(8), pp.1137-1143.
282. Mosby, C. 2009. Mosby’s medical dictionary. Elsevier Atlanta, GA.
283. Moy, P.K. et al. 2004. Dental implant failure rates and associated risk factors. The International journal of oral and maxillofacial implants. 20(4), pp.569-577.
284. Mrozik, K.M. et al. 2010. Proteomic characterization of mesenchymal stem cell-like populations derived from ovine periodontal ligament, dental pulp, and bone marrow: analysis of differentially expressed proteins. Stem cells and development. 19(10), pp.1485-1499.
285. Muddugangadhar, B. et al. 2011. Biomaterials for dental implants: An overview. International Journal of Oral Implantology and Clinical Research. 2, pp.13-24.

286. Mupparapu, M. and Beideman, R. 2000. Imaging for maxillofacial reconstruction and implantology. Oral and maxillofacial surgery: reconstructive and implant surgery. Philadelphia: WB Saunders. pp.17-34.
287. Nair, M.B. et al. 2008. Platelet-Rich plasma and fibrin glue–coated bioactive ceramics enhance growth and differentiation of goat bone marrow–derived stem cells. Tissue Engineering Part A. 15(7), pp.1619-1631.
288. Nakashima, K. and de Crombrugghe, B. 2003. Transcriptional mechanisms in osteoblast differentiation and bone formation. TRENDS in Genetics. 19(8), pp.458-466.
289. Ng F. et al. 2008. PDGF, tgf-2.AndFGFsignaling is important for differentiation and growth of mesenchymal stem cells (mscs): transcriptional profiling can identifymarkers and signaling pathways important in differentiation of MSCs into adipogenic, chondrogenic, and osteogenic lineages. Blood. 112(2), pp. 295–307.
290. Nikolidakis, D. and Jansen, J.A. 2008. The biology of platelet-rich plasma and its application in oral surgery: literature review. Tissue Engineering Part B: Reviews. 14(3), pp.249-258.
291. Nikolidakis, D. et al. 2006. The effect of platelet-rich plasma on the bone healing around calcium phosphate-coated and non-coated oral implants in trabecular bone. Tissue engineering. 12(9), pp.2555-2563.
292. Nikolidakis, D. et al. 2008. Effect of platelet-rich plasma on the early bone formation around Ca-P-coated and non-coated oral implants in cortical bone. Clinical oral implants research. 19(2), pp.207-213.
293. Ninomiya, J.T. et al. 1990. Heterogeneity of human bone. Journal of Bone and Mineral Research. 5(9), pp.933-938.
294. Nordquist, W. D. 2011. Part II: Crystalline fluorapatite-coated hydroxyapatite implant material: a dog study with histologic comparison of osteogenesis seen with FA-coated HA grafting material versus HA controls: potential bacteriostatic effect of fluoridated HA. Journal of Oral Implantology, 37, pp.35-42.
295. Novaes, Jr, A.B. et al. 2002. Histomorphometric analysis of the bone-implant contact obtained with 4 different implant surface treatments placed side by side in the dog mandible. International journal of oral and maxillofacial implants. 17(3), pp.377-383.
296. Okazaki, M. et al. 1981. Solubility behavior of CO_3 apatites in relation to crystallinity. Caries research. 15(6), pp.477-483.

297. Okuda, K. et al. 2003. Platelet-rich plasma contains high levels of platelet-derived growth factor and transforming growth factor-β and modulates the proliferation of periodontally related cells in vitro. Journal of Periodontology. 74(6), pp.849-857.
298. Okuda, K. et al. 2005. Platelet-rich plasma combined with a porous hydroxyapatite graft for the treatment of intrabony periodontal defects in humans: a comparative controlled clinical study. Journal of periodontology. 76(6), pp. 890-898.
299. Okuda, K. et al. 2005. Platelet-rich plasma combined with a porous hydroxyapatite graft for the treatment of intrabony periodontal defects in humans: a comparative controlled clinical study. Journal of periodontology. 76, pp.890-898.
300. Oldberg, A. et al. 1986. Cloning and sequence analysis of rat bone sialoprotein (osteopontin) cDNA reveals an arg-gly-asp cell-binding sequence. Proc Natl Acad Sci USA. 83, pp.8819-8823.
301. Olson, E. N. Proto-oncogenes in the regulatory circuit for myogenesis. Seminars in cell biology. 1992. Elsevier, pp.127-136.
302. Otaki, S. et al. 2007. Mesenchymal progenitor cells in adult human dental pulp and their ability to form bone when transplanted into immunocompromised mice. Cell biology international. 31, pp.1191-1197.
303. Overgaard, S. et al. 1997. Resorption of hydroxyapatite and fluorapatite coatings in man. J Bone Joint Surg Br. 79(4), pp.654-659.
304. Owen, T.A. et al. 1990. Progressive development of the rat osteoblast phenotype in vitro: reciprocal relationships in expression of genes associated with osteoblast proliferation and differentiation during formation of the bone extracellular matrix. Journal of cellular physiology. 143(3), pp.420-430.
305. Paddock, S.W. 2000. Principles and practices of laser scanning confocal microscopy. Molecular biotechnology. 16(2), pp.127-149.
306. Papaccio, G. et al. 2006. Long-term cryopreservation of dental pulp stem cells (SBP-DPSCs) and their differentiated osteoblasts: A cell source for tissue repair. Journal of cellular physiology. 208(2), pp.319-325.
307. Park, Y.J. et al. 2000. Platelet derived growth factor releasing chitosan sponge for periodontal bone regeneration. Biomaterials. 21(2), pp.153-159.
308. Pfeilschifter, J. et al. 1990. Stimulation of bone matrix apposition in vitro by local growth factors: a comparison between insulinlike growth factor I, platelet

derived growth factor, and transforming growth factor h, Endocrinology. 127, pp.69–75.
309. Phelan, K. and May, K.M. 2007. Basic techniques in mammalian cell tissue culture. Current protocols in cell biology. pp.1.1.1-1.1. 22.
310. Piattelli, A. et al. 1997. Immediate loading of titanium plasma-sprayed screw-shaped implants in man: a clinical and histological report of two cases. Journal of periodontology. 68(6), pp.591-597.
311. Pietrzak, W. S. and Eppley, B. L. 2005. Platelet rich plasma: biology and new technology. Journal of Craniofacial Surgery. 16 (6). pp.1043–1054.

312. Pisciotta, A. et al. 2012. Human serum promotes osteogenic differentiation of human dental pulp stem cells in vitro and in vivo. PloS one. 7, e50542.
313. Pittenger, M.F. et al. 1999. Multilineage potential of adult human mesenchymal stem cells. Science. 284(5411), pp.143-147.
314. Plachokova, A.S. et al. 2008. Effect of platelet-rich plasma on bone regeneration in dentistry: a systematic review. Clinical oral implants research. 19(6), pp.539-545.
315. Poellmann, M.J. et al. 2010. Geometric microenvironment directs cell morphology on topographically patterned hydrogel substrates. Acta biomaterialia. 6(9), pp.3514-3523.
316. Pullen B., Gross M. Materials in medicine. 2005. J. of Mater. Sci. 16, pp. 399-404.
317. Qi, Y. et al. 2015. Combining mesenchymal stem cell sheets with platelet-rich plasma gel/calcium phosphate particles: a novel strategy to promote bone regeneration. Stem cell research and therapy. 6(1), pp. 1-16.
318. Radonić, A. et al. 2004. Guideline to reference gene selection for quantitative real-time PCR. Biochemical and biophysical research communications. 313(4), pp.856-862.
319. Rai, B. et al. 2005. An in vitro evaluation of PCL–TCP composites as delivery systems for platelet-rich plasma. Journal of controlled release. 107 (2), pp. 330-342.
320. Rai, B. et al. 2007. Combination of platelet-rich plasma with polycaprolactone-tricalcium phosphate scaffolds for segmental bone defect repair. Journal of Biomedical Materials Research Part A. 81(4), pp.888-899.

321. Raiche, A. and Puleo, D. 2004. Cell responses to BMP-2 and IGF-I released with different time-dependent profiles. Journal of Biomedical Materials Research Part A. 69(2), pp.342-350.
322. Raines, E. et al. 1990. Platelet-derived growth factor. Peptide growth factors and their receptors I. Springer, pp.173-262.
323. Ranly, D.M. et al. 2005. Platelet-derived growth factor inhibits demineralized bone matrix-induced intramuscular cartilage and bone formation: a study of immunocompromised mice. JBJS. 87(9), pp.2052-2064.
324. Ranz, X. et al. 1997. Properties of plasma sprayed bioactive fluorhydroxyapatite coatings. Bioceramics. Paris: Elsevier Science Ltd. p10.
325. Rappolee, D.A. et al. 1988. Wound macrophages express TGF-alpha and other growth factors in vivo: analysis by mRNA phenotyping. Science. 241(4866), pp.708-712.
326. Ratner, B.D. 1993. New ideas in biomaterials science—a path to engineered biomaterials. Journal of Biomedical Materials Research Part A. 27(7), pp.837-850.
327. Raynaud, C. et al. 2012. Comprehensive characterization of mesenchymal stem cells from human placenta and fetal membrane and their response to osteoactivin stimulation. Stem cells international. 2012.
328. Rey, C. et al. 2009. Bone mineral: update on chemical composition and structure. Osteoporos International, 20(6), pp.1013-1021.
329. Riccio, M. et al. 2010. Human dental pulp stem cells produce mineralized matrix in 2D and 3D cultures. European journal of histochemistry: EJH. 54(4).
330. Roach, P. et al. 2005. Interpretation of protein adsorption: surface-induced conformational changes. Journal of the American Chemical Society. 127(22), pp.8168-8173.
331. Roberts, D.E. et al. 2004. Mechanism of collagen activation in human platelets. Journal of Biological Chemistry. 279(19), pp.19421-19430.
332. Robinson, C. et al. 2004. The effect of fluoride on the developing tooth. Caries research. 38(3), pp.268-276.
333. Robinson, C. et al. 2017. Dental enamel formation to destruction. CRC press.
334. Rodan, G. A. 1992. Introduction to bone biology. Bone. 13, pp.S3-S6.
335. Ross, R. et al. 1986. The biology of platelet-derived growth factor. Cell. 46(2), pp.155-169.

336. Rotter, N. et al. 2008. Isolation and characterization of adult stem cells from human salivary glands. Stem cells and development. 17(3), pp.509-518.
337. Rottmar, M. et al. 2010. Stem cell plasticity, osteogenic differentiation and the third dimension. Journal of Materials Science: Materials in Medicine. 21(3), pp.999-1004.
338. Rowan, R. et al. 1972. Evaluation of an automatic platelet counting system utilizing whole blood. Journal of clinical pathology. 25(3), pp.218-226.
339. Rozman, P. and Bolta, Z. 2007. Use of platelet growth factors in treating wounds and soft-tissue injuries. Acta Dermatovenerologica Alpina Panonica et Adriatica. 16(4), pp.156.
340. Rubin, R. and Baserga, R. 1995. Insulin-like growth factor-I receptor. Its role in cell proliferation, apoptosis, and tumorigenicity. Laboratory investigation; a journal of technical methods and pathology. 73(3), pp.311-331.
341. Sakae, T. et al. 2000. In vitro interactions of bone marrow cells with carbonate and fluoride containing apatites. Key Engineering Materials. 192, pp.347-350.
342. Salama, H. et al. 1995. Immediate loading of bilaterally splinted titanium root-form implants in fixed prosthodontics--a technique reexamined: two case reports. International Journal of Periodontics and Restorative Dentistry. 15(4).
343. Salgado, A. J. et al. 2004. Bone Tissue Engineering: state of the art and future trends. Macromol Biosci. 4, pp.743-765.
344. Sammartino, G. et al. 2009. Platelet-rich plasma and resorbable membrane for prevention of periodontal defects after deeply impacted lower third molar extraction. Journal of Oral and Maxillofacial Surgery. 67(11), pp.2369-2373.
345. Sánchez, A.R. et al. 2003. Is platelet-rich plasma the perfect enhancement factor? A current review. International Journal of Oral and Maxillofacial Implants. 18(1).
346. Saraswathy, N. and Ramalingam, P. 2011. Concepts and Techniques in Genomics and Proteomics. Elsevier.
347. Sato, M. et al. 2006. Increased osteoblast functions on undoped and yttrium-doped nanocrystalline hydroxyapatite coatings on titanium. Biomaterials. 27(11), pp.2358-2369.
348. Schallmoser, K. et al. 2007. Human platelet lysate can replace fetal bovine serum for clinical-scale expansion of functional mesenchymal stromal cells. Transfusion. 47(8), pp.1436-1446.

349. Schär, M.O. et al. 2015. Platelet-rich concentrates differentially release growth factors and induce cell migration in vitro. Clinical Orthopaedics and Related Research®. 473(5), pp.1635-1643.
350. Scherjon, S.A. et al. 2003. Amniotic fluid as a novel source of mesenchymal stem cells for therapeutic transplantation. Blood. 102(4), pp.1548-1549.

351. Schliephake, H. 2002. Bone growth factors in maxillofacial skeletal reconstruction. International journal of oral and maxillofacial surgery. 31(5), pp.469-484.
352. Schliephake, H. et al. 2005. Functionalization of dental implant surfaces using adhesion molecules. Journal of Biomedical Materials Research Part B: Applied Biomaterials. 73, pp.88-96.
353. Schmid, C. et al. 1984. Insulin-like growth factor I supports differentiation of cultured osteoblast-like cells. FEBS letters. 173(1), pp.48-52.
354. Schmidmaier, G. et al. 2006. Quantitative assessment of growth factors in reaming aspirate, iliac crest, and platelet preparation. Bone. 39(5), pp.1156-1163.
355. Searson, L.J. et al. 2005. Implantology in General Dental Practice.London: Quintessence publishing Co.Ltd.
356. Sebben, A.D. 2012. Comparative study on use of platelet-rich plasma alone and in combination with alpha-tricalcium phosphate cement for bone repair in rats. Revista Brasileira de Ortopedia. 47(4), pp. 505-512.
357. Sell, S.A. et al. 2012. The incorporation and controlled release of platelet-rich plasma-derived biomolecules from polymeric tissue engineering scaffolds. Polymer International. 61(12), pp.1703-1709.
358. Sennerby, L. et al. 1993. Early tissue response to titanium implants inserted in rabbit cortical bone. Journal of Materials Science: Materials in Medicine. 4(3), pp.240-250.
359. Shalabi, M. et al. 2006. Implant surface roughness and bone healing: a systematic review. Journal of dental research. 85(6), pp.496-500.
360. Shalhoub, V. 1992. Glucocorticoids promote development of the osteoblast phenotype by selectively modulating expression of cell growth and differentiation associated genes. J Cell Biochem, 50, pp.425-40.
361. Sharma, U. et al. 2014. Alkaline phosphatase: an overview. Indian Journal of Clinical Biochemistry. 29(3), pp.269-278.

362. Sheth, N. et al. 2017. Human mandible bone defect repair by the grafting of dental pulp stem/progenitor cells—a pilot study. International Journal of Oral and Maxillofacial Surgery. 46, pp.215.
363. Shi, S. et al. 2005. The efficacy of mesenchymal stem cells to regenerate and repair dental structures. *Orthodontics & craniofacial research.* **8**(3), pp.191-199.
364. Shiba, H. et al. 1995. Effects of basic fibroblast growth factor on proliferation, the expression of osteonectin (SPARC) and alkaline phosphatase, and calcification in cultures of human pulp cells. Developmental biology. 170(2), pp.457-466.
365. Silva, S. et al. 2003. Effect of biphasic calcium phosphate on human macrophage functions in vitro. Journal of Biomedical Materials Research Part A. 65(4), pp.475-481.
366. Soffer, E. et al. 2004. Effects of platelet lysates on select bone cell functions. Clinical oral implants research. 15(5), pp.581-588.
367. Soskolne, W. A. et al. 2002. The effect of titanium surface roughness on the adhesion of monocytes and their secretion of TNF-α and PGE2. Clinical oral implants research. 13, pp.86-93.
368. Sporn, M.B. and Roberts, A.B. 1993. A major advance in the use of growth factors to enhance wound healing. Journal of Clinical Investigation. 92(6), pp.2565.
369. Steele, J. G. et al. 1995. Adsorption of fibronectin and vitronectin onto Primaria™ and tissue culture polystyrene and relationship to the mechanism of initial attachment of human vein endothelial cells and BHK-21 fibroblasts. Biomaterials. 16, pp.1057-1067.
370. Stefani, C. et al. 2000. Platelet-derived growth factor/insulin-like growth factor-1 combination and bone regeneration around implants placed into extraction sockets: a histometric study in dogs. Implant dentistry. 9(2), pp.126-131.
371. Stephan, E.B. et al. 2000. Platelet-derived growth factor enhancement of a mineral-collagen bone substitute. Journal of periodontology. 71(12), pp.1887-1892.
372. Strnad, Z. et al. 2000. Effect of plasma-sprayed hydroxyapatite coating on the osteoconductivity of commercially pure titanium implants. International Journal of Oral and Maxillofacial Implants. 15(4), pp.483-490.

373. Stvrtecky, R. et al. 2003. A histologic study of bone response to bioactive glass particles used before implant placement: a clinical report. The Journal of prosthetic dentistry. 90(5), pp.424-428.
374. Sun, L. et al. 2001. Material fundamentals and clinical performance of plasma-sprayed hydroxyapatite coatings: A review. Journal of biomedical materials research. 58, pp.570-592.

375. Tamimi, F.M. et al. 2007. A comparative study of 2 methods for obtaining platelet-rich plasma. Journal of oral and maxillofacial surgery. 65(6), pp.1084-1093.
376. Tavassoli-Hojjati, S. et al. 2016. Effect of platelet-rich plasma concentrations on the proliferation of periodontal cells: An in vitro study. European journal of dentistry. 10(4), pp.469.
377. Tecles, O. 2005. Activation of human dental pulp progenitor/stem cells in response to odontoblast injury. Arch Oral Biol. 50, pp.103-8.
378. Teplyuk, N.M. et al. 2008. Runx2 regulates G protein-coupled signaling pathways to control growth of osteoblast progenitors. Journal of Biological Chemistry. 283(41), pp.27585-27597.
379. Textor, J.A. and Tablin, F. 2012. Activation of Equine Platelet-Rich Plasma: Comparison of Methods and Characterization of Equine Autologous Thrombin, Veterinary Surgery. 41(7), pp.784-794.
380. Thomson, J.A. et al. 1998. Embryonic stem cell lines derived from human blastocysts. Science. 282(5391), pp.1145-1147.
381. Thor, A. et al. 2005. Reconstruction of the Severely Resorbed Maxilla with Autogenous Bone, Platelet-Rich Plasma, and Implants: 1-Year Results of a Controlled Prospective 5-Year Study. Clinical implant dentistry and related research. 7(4), pp.209-220.
382. Thornton, J.A. and Bunshah, R.F. 1982. Deposition technologies for films and coatings. Noyes Pub. pp.170-237.
383. Tomlinson, M.J. et al. 2015. Tissue non-specific alkaline phosphatase production by human dental pulp stromal cells is enhanced by high density cell culture. Cell and tissue research. 361(2), pp.529-540.
384. Tozum, T. and Demiralp, B. 2003. Platelet-rich plasma: a promising innovation in dentistry. Journal-Canadian Dental Association. 69(10), pp.664-665.

385. Tsukamoto, Y. et al. 1992. Mineralized nodule formation by cultures of human dental pulp-derived fibroblasts. Arch Oral Biol. 37, pp.1045-55.
386. Vehof, J.W. et al. 2001. Ectopic bone formation in titanium mesh loaded with bone morphogenetic protein and coated with calcium phosphate. Plastic and reconstructive surgery. 108(2), pp.434-443.
387. Vehof, J.W. et al. 2002. Bone formation in Transforming Growth Factor beta-1-loaded titanium fiber mesh implants. Clinical oral implants research. 13(1), pp.94-102.
388. Vercaigne, S. et al. 2000. A histological evaluation of TiO2-gritblasted and Ca-P magnetron sputter coated implants placed into the trabecular bone of the goat: part 2. Clinical oral implants research. 11, pp.314-324.
389. Voet, D. 1995. JG Voet in Biochemistry. John Wiley & Sons, New York.
390. Vogel, V. and Sheetz, M. 2006. Local force and geometry sensing regulate cell functions. Nature reviews Molecular cell biology. 7(4), pp.265.
391. Volponi, A. A. et al. 2010. Stem cell-based biological tooth repair and regeneration. Trends in cell biology. 20, pp.715-722.
392. Wagner, W. et al. 2005. Comparative characteristics of mesenchymal stem cells from human bone marrow, adipose tissue, and umbilical cord blood. Experimental hematology. 33(11), pp.1402-1416.
393. Walker, B. R. and Colledge, N. R. 2013. Davidson's Principles and Practice of Medicine E-Book, Elsevier Health Sciences.
394. Wang, X. et al. 2012. In vitro differentiation and mineralization of dental pulp stem cells on enamel-like fluorapatite surfaces. Tissue Engineering Part C: Methods. 18(11), pp.821-830.
395. Wang, X. et al. 2013. Fluorapatite enhances mineralization of mesenchymal/endothelial cocultures. Tissue Engineering Part A. 20(1-2), pp.12-22.
396. Wasterlain, A.S. et al. 2012. Contents and formulations of platelet-rich plasma. Operative Techniques in Orthopaedics. 22(1), pp.33-42.
397. Watson, R.M. et al. 2003. Introducing dental implants. Churchill Livingstone.
398. Wei, J. et al. 2011. Development of fluorapatite cement for dental enamel defects repair. Journal of Materials Science: Materials in Medicine. 22(6), pp.1607-1614.
399. Wei, X. et al. 2007. Expression of mineralization markers in dental pulp cells. Journal of endodontics. 33, 703-708.

400. Weibrich, G. and Kleis, W.K. 2002. Curasan PRP kit vs. PCCS PRP system. Clinical oral implants research. 13(4), pp.437-443.
401. Weibrich, G. et al. 2002. Growth factor levels in platelet-rich plasma and correlations with donor age, sex, and platelet count. Journal of Cranio-Maxillofacial Surgery. 30(2), pp.97-102.
402. Weibrich, G. et al. 2003. Comparison of platelet, leukocyte, and growth factor levels in point-of-care platelet-enriched plasma, prepared using a modified Curasan kit, with preparations received from a local blood bank. Clinical oral implants research. 14(3), pp.357-362.
403. Weibrich, G. et al. 2004. Effect of platelet concentration in platelet-rich plasma on peri-implant bone regeneration. Bone. 34(4), pp.665-671.
404. Weibrich, G. et al. 2005. Comparison of the platelet concentrate collection system with the plasma-rich-in-growth-factors kit to produce platelet-rich plasma: a technical report. International Journal of Oral and Maxillofacial Implants. 20(1).
405. Weiner, S. and Traub, W. 1992. Bone structure: from angstroms to microns. FASEB Journal, 6(3), pp.879-85.
406. Wennerberg, A. et al. 1996. Bone tissue response to commercially pure titanium implants blasted with fine and coarse particles of aluminum oxide. International Journal of Oral & Maxillofacial Implants. 11(1).
407. Wennerberg, A. and Albrektsson, T. 2000. Suggested guidelines for the topographic evaluation of implant surfaces. International journal of oral and maxillofacial implants. 15(3), 331-344.
408. Wessinger, W. D. and Owens, S. M. 1990. Influence of phencyclidine (PCP) pharmacokinetics on PCP dependence after i.v. and s.c. routes of administration. NIDA Res Monogr. 105, 431-2.
409. Whitman, D.H. et al. 1997. Platelet gel: an autologous alternative to fibrin glue with applications in oral and maxillofacial surgery. Journal of oral and maxillofacial surgery. 55(11), pp.1294-1299.
410. Wikesjö, U. M. et al. 2008. Alveolar ridge augmentation using implants coated with recombinant human bone morphogenetic protein-2: histologic observations. Journal of clinical periodontology. 35, pp.1001-1010.
411. Woodell-May, J.E. et al. 2005. Producing accurate platelet counts for platelet rich plasma: validation of a hematology analyzer and preparation techniques for counting. Journal of Craniofacial Surgery. 16(5), pp.749-756.

412. Worthington, P. et al. 2003. Osseointegration in Dentistry. Second Edition. Canada: Quintessence publishing Co,Inc.
413. Xia, Y. et al. 2003. One-dimensional nanostructures: synthesis, characterization, and applications. Advanced materials. 15(5), pp.353-389.
414. Xie, X. et al. 2012. Comparative evaluation of MSCs from bone marrow and adipose tissue seeded in PRP-derived scaffold for cartilage regeneration. Biomaterials. 33(29), pp.7008-7018.
415. Xue, W. et al. 2008. Synthesis and characterization of tricalcium phosphate with Zn and Mg based dopants. Journal of Materials Science: Materials in Medicine. 19(7), pp.2669-2677.
416. Yamada, Y. et al. 2004. Autogenous injectable bone for regeneration with mesenchymal stem cells and platelet-rich plasma: tissue engineered bone regeneration. Tissue Engineering. 10(5-6), pp. 955–964.
417. Yamaguchi, A. et al. 2000. Regulation of osteoblast differentiation mediated by bone morphogenetic proteins, hedgehogs, and Cbfa1. Endocrine reviews. 21(4), pp.393-411.
418. Yamaguchi, R. et al. 2012. Effects of platelet-rich plasma on intestinal anastomotic healing in rats: PRP concentration is a key factor. Journal of surgical research. 173(2), pp.258-266.
419. Yamamiya, K. et al. 2008. Tissue-engineered cultured periosteum used with platelet-rich plasma and hydroxyapatite in treating human osseous defects. Journal of periodontology. 79(5), pp.811-818.
420. Yanagita, M. et al. 2008. Nicotine inhibits mineralization of human dental pulp cells. Journal of endodontics. 34(9), pp.1061-1065.
421. Yang, C. et al. 1997. In vitro and in vivo mechanical evaluations of plasma-sprayed hydroxyapatite coatings on titanium implants: The effect of coating characteristics. Journal of biomedical materials research. 37, pp.335-345.
422. Yang, C.-Y. et al. 2010. The influence of plasma-spraying parameters on the characteristics of fluorapatite coatings. Journal of Medical and Biological Engineering. 30, pp.91-98.
423. Yang, D. et al. 2000. Platelet-derived growth factor (PDGF)-AA: a self-imposed cytokine in the proliferation of human fetal osteoblasts. Cytokine. 12(8), pp.1271-1274.
424. Yang, F. et al. 2012a. Osteoblast response to porous titanium surfaces coated with zinc-substituted hydroxyapatite. Oral surgery, oral medicine, oral pathology and oral radiology. 113(3), pp.313-318.

425. Yang, G.-l. et al. 2012b. Effect of strontium-substituted nanohydroxyapatite coating of porous implant surfaces on implant osseointegration in a rabbit model. International Journal of Oral and Maxillofacial Implants. 27(6).
426. Yang, L. et al. 2010. The effects of inorganic additives to calcium phosphate on in vitro behavior of osteoblasts and osteoclasts. Biomaterials. 31(11), pp.2976-2989.
427. Yen, A.H.-H. and Sharpe, P.T. 2008. Stem cells and tooth tissue engineering. Cell and tissue research. 331(1), pp.359-372.
428. Yin, T. and Li, L. 2006. The stem cell niches in bone. The Journal of clinical investigation. 116(5), pp.1195-1201.
429. Ying, Q. L. 2002. Changing potency by spontaneous fusion. Nature, 416, pp.545-8.
430. Yoshida, C.A. et al. 2004. Runx2 and Runx3 are essential for chondrocyte maturation, and Runx2 regulates limb growth through induction of Indian hedgehog. Genes and development. 18(8), pp.952-963.
431. Zainal Ariffin, S.H. et al. 2011. Cellular and molecular changes in orthodontic tooth movement. The Scientific World Journal. 11, pp.1788-1803.
432. Zechner, W. et al. 2002. Influence of platelet-rich plasma on osseous healing of dental implants: a histologic and histomorphometric study in minipigs. The International journal of oral and maxillofacial implants. 18, pp.15-22.
433. Zehnder, J.L. and Leung, L.L.K. 1990. Development of antibodies to thrombin and factor V with recurrent bleeding in a patient exposed to topical bovine thrombin. Blood. 76, pp.2011–6.
434. Zhang, N. 2013. Research progress in the mechanism of effect of PRP in bone defficiency healing. The scientific world journal. 2013, pp.1-7.
435. Zhang, Q. et al. 1990. Characterization of fetal porcine bone sialoproteins: secreted phosphoprotein I (SPPI, osteopontin), bone sialoprotein, and a 23 kDa glycoprotein. Demonstration that the 23 kDa glycoprotein is derived from the carboxy-terminus of SPPl. Biol Chem 265, pp.7583-7589.
436. Zhang, W. et al. 2008. Hard tissue formation in a porous HA/TCP ceramic scaffold loaded with stromal cells derived from dental pulp and bone marrow. Tissue Engineering Part A. 14, pp.285-294.
437. Zimmermann, R. et al. 2001. Different preparation methods to obtain platelet components as a source of growth factors for local application. Transfusion. 41(10), pp.1217-1224.

438. Zohar, R. et al. 1997a. Single cell analysis of intracellular osteopontin in osteogenic cultures of fetal rat calvarial cells. I Cell Physiol 170, pp.88-98.
439. Zucker-Franklin, D. 1988. Megakaryocyte and platelet. Atlas of blood cells.
440. Zur Nieden, N.I. et al. 2003. In vitro differentiation of embryonic stem cells into mineralized osteoblasts. Differentiation. 71(1), pp.18-27.

Chapter 9: Appendices

Appendix 1: Growth of G292 cells seeded on PRP gel, encapsulated in PRP gel and PRP releasate supplemented medium for 7 days using 2 PRP samples donors. Cells were successfully cultured in all experimental groups compared to the controls. PRP releasate enhanced the cell proliferation as compared with the others. The maximum increase in DNA content was observed when cells where cultured with PRP releasate reaching 3423 ng ± 96 after 7 days and 4015 ng ± 41 for donors 1 and 2 respectively, followed by when cells were encapsulated in PRP gel (2902ng ± 634 and 2856ng ± 475 for donors 1 and 2

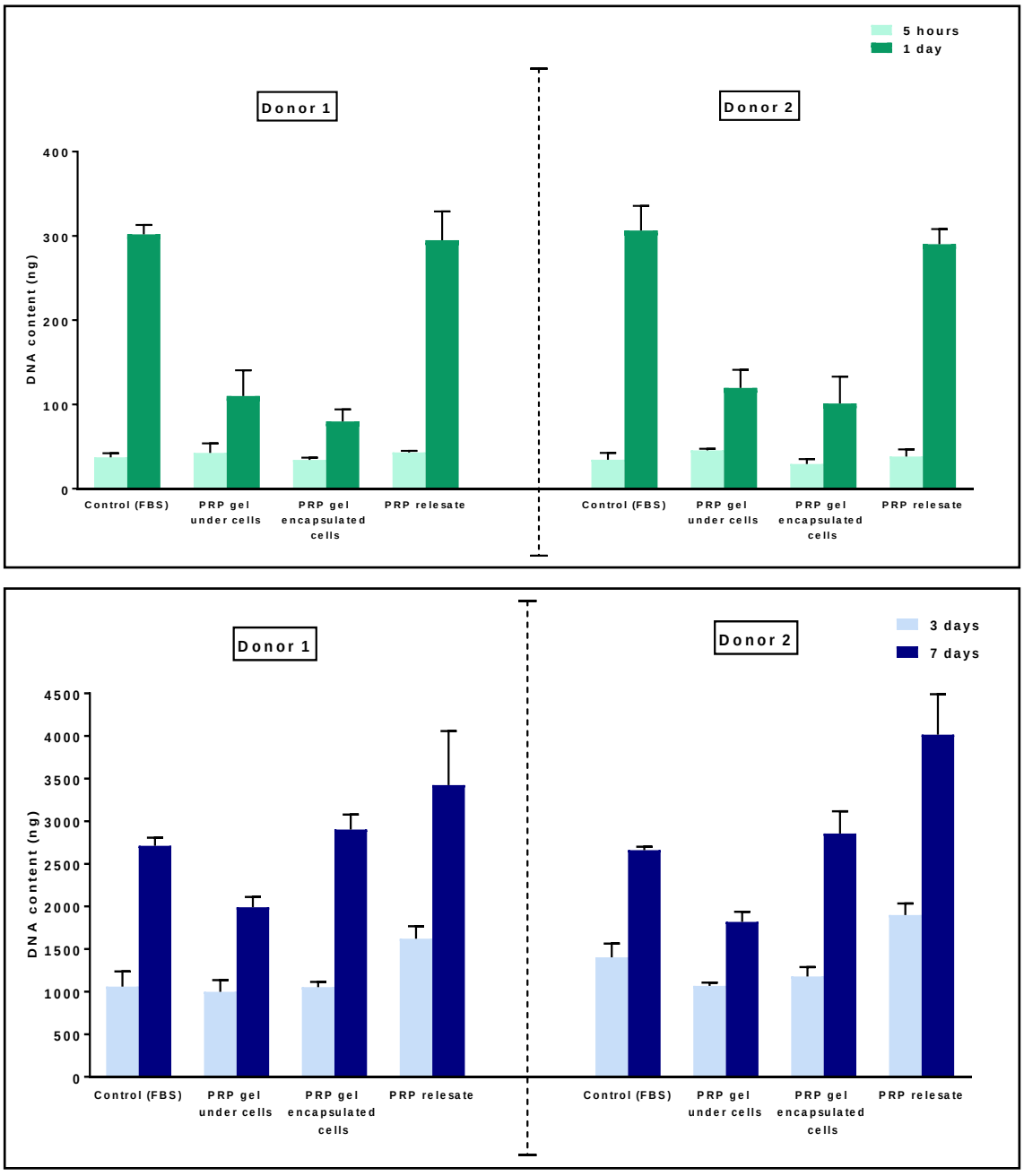

Appendix 2: Cell attachment and proliferation of G292 osteoblast-like cells on combinations of FA coatings and PRP extracted from blood donor 1 assessed by DNA quantification at 5 hours and 1, 3 and 7 days of cell culture. A gradual increase in DNA content was seen in all groups with a higher cell growth rates recorded for SS substrate compared to FA coatings. PRP gel induced the highest DNA content in all the substrate groups, followed by PRP releasate and FBS.

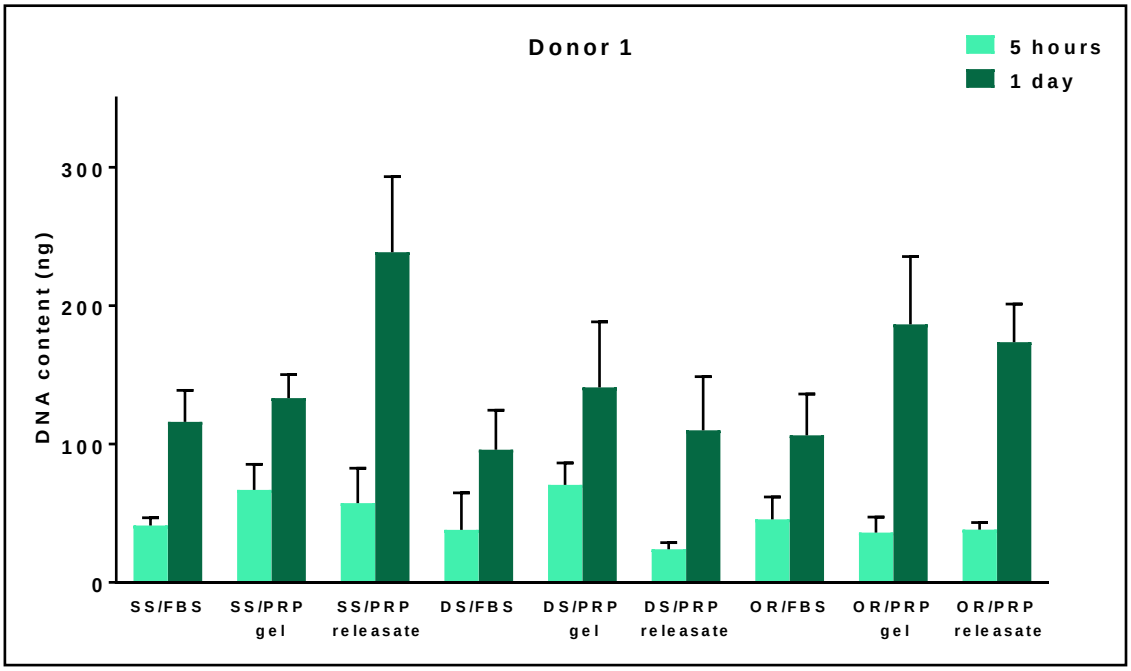

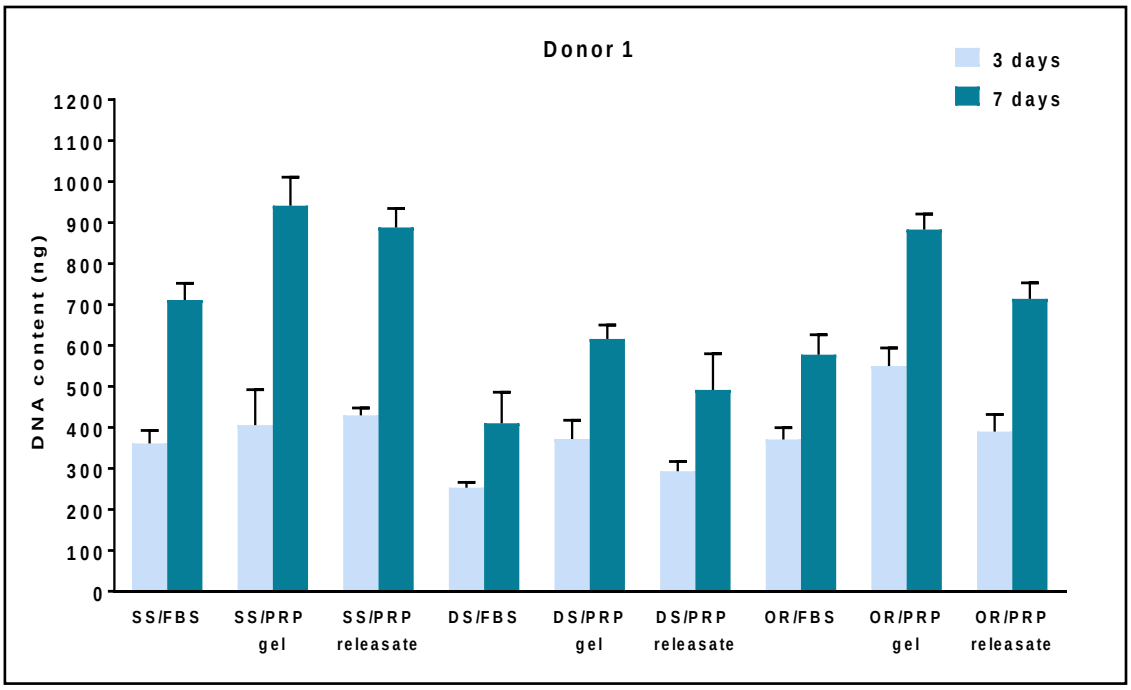

Appendix 3: Proliferation of G292 osteoblast-like cells on combinations of FA coatings and PRP extracted from blood donor 2 assessed by DNA quantification at 5 hours and 1, 3 and 7 days of cell culture. PRP of donor 2 showed a boost in cell proliferation at day 3 and a comparative growth rates for all substrate groups. Overall, PRP gel induced the highest DNA content in all the substrate groups, followed by PRP releasate and FBS.